Meghnad Saha Memorial International Conference On Frontiers of Physics (MSMICFP-2023)

"The Centenary Celebration of the Department of Physics"

November 22 - 24, 2023

Department of Physics, University of Allahabad, Prayagraj-211 002, India

in association with

The National Academy of Sciences, India

The Centenary Celebration of the Department of Physics, University of Allahabad

ABSTRACT BOOK

Department of Physics
University of Allahabad
Prayagraj-211002, U.P. India

Cover page designed by Dr. Triranjita Srivastava

“Science is not only a disciple of reason but, also, one of romance and passion."

- Stephen Hawking

Editorial

Welcome to the intellectual mosaic – *The Abstract Book*, of the "**Meghnad Saha Memorial International Conference on Frontiers of Physics (MSMICFP-2023)**".

The conference aims to provide a well-organized international forum to cater the exchange of ideas amongst the experimental and theoretical researchers and stimulate progress in both academia and industry, covering the frontiers of research in major streams of Physics and interdisciplinary areas.

We have oral and poster presentations besides Plenary and Invited talks in the fields of Theoretical & Experimental Condensed Matter Physics, Astronomy & Astrophysics, Soft & Active Matter Systems, Quantum Optics, Quantum Information & Quantum Computation, Advanced Functional Materials, Energy, Photovoltaics & Green Materials, Saha's endeavors for the Science & Society, Nuclear & High Energy Physics, Nano Photonics, Optical Fibers, Optical Sensors & Optoelectronics, Nano-electronics & Nano Technology, Statistical Mechanics & Critical Phenomena, Computational Physics & Simulations, Bio Materials & Implant Materials, Laser & Plasma Physics, Materials Characterization Techniques and Other cutting-edge research areas of Physics.

We have organized the received abstracts in five major sessions namely:

A. CMP, PT and CP: Condensed Matter Physics, Phase Transition and Critical Phenomenon
B. NHP and QGP: Nuclear and High Energy Physics, Quark-Gluon Plasma
C. LSLPI, FO and Photonics: Lasers, Spectroscopy, LIBS, Laser Plasma Interaction, Fiber Optics and Photonics
D. Astro., QO and QC: Astrophysics, Quantum Optics and Quantum Computation
E. Other CER and Nano: Other Cutting Edge Research Areas of Physics and Nanotechnology

This booklet reflects the diverse ideas and shared knowledge of the "**Meghnad Saha Memorial International Conference on Frontiers of Physics (MSMICFP-2023)**".

As we finish this journey, let's take what we have gained here to inspire more discussions and push our understanding even further.

INDEX

Understanding High Density Quark and Gluonic Matter: Past Present and Future

Larry D. McLerran

The various forms of matter at energy densities greater than nuclear matter are qualitatively discussed. The Quark Gluon Plasma (QGP) has been the object of study at high energy heavy ion accelerators and plays a role in early universe cosmology. The very earliest stages of heavy ion collisions is described by new forms of matter, the Color Glass Condensate (CGC) and the Glasma. The (CGC) may also be studied in electron-ion collisions Such matter has interesting topological excitations which play analogous roles in the theory of fluids and condensed matter systems. Recent neutron star measurements have given good determinations of cold matter at high baryon number density, Quarkyonic Matter, and suggest that quark degrees of freedom are essential.

Development of Science & Technology in India: A Brief Historical Perspective

Ajoy Ghatak
Formerly Professor of Physics at Indian Institute of Technology Delhi
Email:ajoykghatak@gmail.com

In this talk we will discuss the transition to the formal university education in the 19th century which was followed by high quality scientific research in India by scientists like C V Raman, Meghnad Saha, Satyendra Nath Bose, Jagadish Chandra Bose, Prasanta Mahalanabis and many others. And then we had great visionaries like Homi Bhabha, Meghnad Saha, S. S. Bhatnagar, Vikram Sarabhai, Abdul Kalam and many others; our recent achievements have been because of them. But about 25% of our population (implying more than 300 million people) is still very poor! How to eradicate that poverty? The answer is: we have to learn from the past, eradicate corruption and have greater emphasis on education, science and technology.

Structure of the Universe

A. M. Srivastava

We honor the legacy of Meghnad Saha, the scientist who did not remain in his “Ivory Tower”, but engaged deeply in addressing the problems of society at large, and in national reconstruction. Among his invaluable scientific contributions is the famous “Saha Ionization equation”, used widely from stellar spectra to many different areas. Saha himself may not have anticipated how crucial this equation will be for our understanding of the evolution of the Universe where it determines the stage of decoupling of the Cosmic Microwave Background Radiation from the early hot cosmic plasma. We will discuss the early stages of the Universe and its evolution using the space-time picture of Einstein's General Theory of Relativity. Research in this area has brought out a startling revelation, that it is not possible to study the extremely large structure of the universe without understanding the properties of the smallest constituents of matter, the elementary particles, and their interactions. This talk will explain the physical basis for this surprising interconnection. Issues of matter-antimatter asymmetry, dark matter, dark energy etc. will also be discussed.

ब्रहमांड की संरचना

आज मेघनाद साहा को याद करना अत्यंत समयानुकूल है। वैज्ञानिकों के लिए अक्सर कहा जाता है कि वे अपने “आइवरी टावर “ में रहते हैं, आम जनता से दूर । मेघनाद साहा निश्चित रूप से इसके अपवाद थे। उन्होंने, हमेशा राष्ट्र की समस्याओं से निपटने के लिए, और राष्ट्र के निर्माण के लिए, अथक प्रयास किये । विज्ञान की क्षेत्र में उनके बहुमूल्य योगदानों में है “साहा आयनीकरण समीकरण (साहा आयनाइज़ेशन इक्वेशन)”। तारों के स्पेक्ट्रम से लेकर, विभिन्न क्षेत्रों में समझ बनाने में इसकी अत्यंत महत्वपूर्ण भूमिका रही है। साहा ने स्वयं यह नहीं सोचा होगा कि यह समीकरण ब्रहमांड की प्रारंभिक अवस्था को समझने में एक बहुमूल्य भूमिका निभाएगा। ब्रहमांडीय सूक्ष्म तरंग विकिरण (कॉस्मिक माइक्रोवेव बैकग्राउंड रेडिएशन) के प्रारंभिक अतितप्त प्लाज्मा से अलग होने की प्रक्रिया इसी समीकरण से समझी जाती है। हम ब्रहमांड की उत्पत्ति और उसके विकास को आइन्स्टाइन के आधुनिक गुरुत्वाकर्षण सिद्धांत (अपेक्षक्षकता के व्यापीकृत सिद्धांत) की समय काल की अवधारणा से समझेंगे। इस विषय पर शोध से एक महत्वपूर्ण निष्कर्ष निकलता है, कि इस अत्यंत विशाल ब्रहमांड को समझने के लिए यह आवश्यक है कि हम अतिसूक्ष्म मूल कणों के गुण धर्म, और उनके पारस्परिक बलों को समझें। हम अतिविशाल से अतिसूक्ष्म के बीच के इस आश्चर्यजनक संबंध को समझेंगे। हम अन्य सम्बंधित विषयों पर चर्चा भी करेंगे, जैसे, द्रव्य प्रति-द्रव्य (मैटर-एंटी-मैटर) की असमानता , श्याम द्रव्य (डार्क मैटर) , श्याम ऊर्जा (डार्क एनर्जी), इत्यादि ।

Magnetism in two-dimensional van der Waals materials

Subhasis Ghosh
School of Physical Sciences, Jawaharlal Nehru University, New Delhi, India

The van der Waals ferromagnets, such as CrI_3, $CrTe_2$, $Cr_2X_2Te_6$ (X = Si and Ge) and Fe_3GeTe_2 provide an excellent platform to investigate ferromagnetism in two dimensional (2D) systems which are being considered as the potential material for future spintronic devices. In particular, Fe_3GeTe_2 and Fe_5GeTe_2 are being investigated vigorously due to exceptional tunability of their magnetic properties and high Curie temperature which is near or above room temperature [1]. Ferromagnetism in 2D is forbidden according to Hohenberg-Mermin-Wagner (HMW) theorem [2,3]. Short ranged exchange interaction, such as 2D Ising and 2D XY driven phase transition have been observed in $Cr_2X_2Te_6$ and CrI_3 respectively. However, 2D-Heisenberg ferromagnet has not yet been observed in accordance with HMW theorem. The presence of long range (LR) interaction changes the scenario completely [4]. Though it is realized that LR driven ferromagnetism is essential for circumventing HMW theorem in 2D, but experimental realization remains elusive in magnetic materials. Here, we show that Fe_3GeTe_2 is a 2D Heisenberg ferromagnet by overridingthe limit of HMW theorem. This has been possible due to the presence of both itinerant and local-moment magnetism in Fe_3GeTe_2 [5]. Temperature dependence of magnetization with signature of 2D magnons, Rhodes-Wohlfarth (RW) and generalized RW based analysis [6] established that Fe_3GeTe_2 is a 2d ferromagnet with itinerant magnetism which can be tuned by magnetic field. So far critical phenomena and second order phase transition have been dealt with renormalization group theory. However, the same in the presence of long range interaction is nontrivial [4,7]. Here we present an improvised method to deal with phase transition and critical phenomena mediated by long Heisenberg interaction in 2D in the presence of long range Ruderman-Kittel-Kasuya-Yusida (RKKY). We show that critical exponents in this case can vary with external parameter. The critical exponents crossfrom mean field universality class to 2d Heisenberg universality class as field increases [8]. We argue that variable critical exponents is the key signature for 2d Heisenberg ferromagnetism, as emphasizedby recent theoretical calculations [9]. Fe in Fe_3GeTe_2 has two inequivalent charge states i.e., Fe^{2+} and Fe^{3+} which lead to multi-orbital path for different spin-spin interactions. In case of a hexagonal crystal field, as in Fe_3GeTe_2, the five 3d orbitals of the Fe atom split into a three group of orbitals with differing localization which is responsible for long range ordering forboth itinerant and local-moment ferromagnetism.

References

[1] Y. Deng, Y. Yu, Y. Song, J. Zhang et al., Nature 563, 94 (2018).
[2] N. D. Mermin and H. Wagner, Phys. Rev. Lett. 17, 1133 (1966).
[3] P. C. Hohenberg, Phys. Rev. 158, 383 (1967).
[4] N. Defenu, T. Donner, T. Macri, G. Pagano, S. Ruffo, and A. Trombettoni, [Rev. Mod. Phys (to be published)] 10.48550/arXiv.2109.01063.
[5] Z. Fei, B. Huang, P. Malinowski, W. Wang, T. Song,J. Sanchez, W. Yao, D. Xiao, X. Zhu, and A. F. May et al., Nat. Mater 17, 778 (2018).
[6] Y. Takahashi, Spin fluctuation theory of itinerant electron magnetism, Vol. 9 (Springer, 2013).
[7] H. C. Chauhan, B. Kumar, A. Tiwari, J. Tiwari, and S. Ghosh, Phys. Rev. Lett. 128, 015703 (2022).
[8] A. Tiwari, H. Ahn, B. Kumar, J. Saini, P. K. Srivastava, B. Singh, C. Lee and Subhasis Ghosh, Phys. Rev. Lett (under review)
[9] J. Zhao, M. Song, Y. Qi, J. Rong, and Z. Y. Meng, 10.48550/arXiv.2306.01044.

Integrated Quantum Photonics

K Thyagarajan
Former Professor of Physics, IIT Delhi, New Delhi 110016
Email: ktrajan@gmail.com

Quantum science and technology have assumed great importance in view of their applications in quantum computing, quantum key distribution, quantum sensing, quantum teleportation and quantum information sciences. Integrated quantum photonics (IQP) deals with integration of photonic components operating at the quantum level on a single chip, much like integrated electronic circuits. This enables all the advantages of integration in the form of small size and weight, novel functionalities, lower power consumption, and ease in practical implementation of quantum devices. Photons are one of the key elements in quantum information transmission and processing. The talk will introduce the concept of photon followed by different important quantum states of light such as squeezed states and entangled states. A few integrated optic devices that find applications in quantum circuits and nonlinear optical effects which provide us with a very efficient means to create non classical states of light will also be presented.

Quantum biology as a new paradigm to explore low dose biological phenomena

D. K. Aswal
Director, Health, Safety and Environment Group, Bhabha Atomic Research Center, Mumbai 400085
Email: dkaswal@barc.gov.in

The field of radiobiology has long relied on the Linear No-Threshold (LNT) model and "target theory" to assess the effects of low-dose radiation exposure. However, recent observations of non-linear phenomena such as adaptive responses, radiation-induced bystander effects, low-dose radio-hypersensitivity, and genomic instability challenge these established theories. Despite their significance, these phenomena lack widely accepted explanations. This talk explores the emerging field of quantum biology as a potential framework to shed light on these alternative low-dose radiation effects. Quantum biology delves into the nano and sub-nanoscale world of biological systems, where ions, atoms, and molecules exhibit quantum mechanical behaviour. By introducing quantum physical explanations, we may uncover a more fundamental scientific basis for these phenomena, complementing existing in-vitro, in-vivo, and epidemiological evidence. In my discussion, I will provide a historical context of quantum biology and present illustrative examples of its application in understanding intermolecular dynamics in photosynthesis, olfaction, DNA point mutation etc. By bridging the gap between quantum mechanics and biology, one can strengthen the recognition of non-linear radiation effects and challenge the conventional LNT hypothesis. This talk invites you to explore the exciting possibilities that quantum biology offers in unravelling the mysteries of cellular responses to low-dose radiation exposure.

Quark Gluon Plasma: the perfect and most vortical fluid

Bedangadas Mohanty
NISER and CERN

The fundamental constituents of visible matter are quarks, gluons, and leptons. The quarks and gluons are not found to exist in a free state in nature. They are confined inside particles called hadrons. However, they were believed to be in a free state in the micro-second old Universe. We will discuss the formation of such a primordial matter of de-confined quarks and gluons in the laboratory and some of its interesting properties.

Complex Strontium Titanate Materials for Solid Oxide Fuel Cells

Anand K Tyagi
Vice Chancellor, Mahatma Gandhi Kashi Vidyapeeth, Varanasi

The complex strontium titanates ($SrTiO_{3-\delta}$) ceramics of perovskite (ABO_3) family have promising features; like high stability in oxygen, carbon and sulfur containing atmospheres, remarkable activity for methane (CH_4) oxidation at high temperature, high conductivity (mainly in doped forms), dimensional and chemical stability upon redox cycling etc for fabrication of various components of SOFC; a reliable, fuel flexible, environment friendly and highly efficient power generating technique. By close inspection and critical analysis of the results of substitutional studies performed on various compounds of Strontium Titanate family, gadolinium and thulium have been chosen as dopants on strontium and titanium sites respectively as their addition to strontium titanates ($SrTiO_3$) leads to enhancement in electrical properties with minimal impact on the crystallographic chemistry of these compounds. We have employed low temperature Sol gel Technique for the synthesis of samples in the present work as this technique is easy and produces contamination free, highly pure, nano size, mechanically stable and homogeneous powders at relatively low temperatures.

The main objective of the present work was to synthesize application grade cubic perovskite samples of ($SrTiO_{3-\delta}$) family with best suited properties to be used in fabrication of various components of SOFCs. We had successfully synthesized these materials using a low temperature novel synthesis route of Sol gel, both in pure and derived forms i.e. $SrTiO_{3-\delta}$, $Sr_{1-x}Gd_xTi_{1-y}Tm_yO_{3-\delta}$ ($0\leq x\leq 0.30$, $0\leq y\leq 0.05$) and $Sr_{1-x}Gd_xTiO_{3-\delta}$ ($0\leq x\leq 0.15$) samples. Thermal analysis, XRD investigations and FESEM/EDX studies have proved that pure $SrTiO_{3-\delta}$, $Sr_{1-x}Gd_xTi_{1-y}Tm_yO_{3-\delta}$ ($0\leq x\leq 0.30$, $0\leq y\leq 0.05$) and $Sr_{1-x}Gd_xTiO_{3-\delta}$ ($0\leq x\leq 0.15$) samples have been produced with required cubic perovskite structure at sintering temperature of 1250^oC. The dense, phase pure and homogeneous samples having nano scale dimensions, synthesized here, are potential candidates for SOFC applications as they meet all the essential prerequisites and technical requirements to be used as SOFC components.

Nanopatterning of Surfaces: For Sensor, Device and Bio-applications

Shikha Varma
Institute of Physics, Bhubaneswar
Email: shikha@iopb.res.in

Ion Irradiation can produce an array of wonder materials. Low energy ion irradiation is especially suitable in fabricating a variety of nanostructures on the surfaces which show many important properties. We will present some results related to the development of Resistive memory Devices based on Oxide materials, Bio-applications with DNA and Photo-absorption of Graphene Quantum Dots.

Intriguing Aspects of Particle-Octupole Phonon Coupling in Nuclear Structure Studies

Rudrajyoti Palit
Department of Nuclear and Atomic Physics,
Tata Institute of Fundamental Research, Mumbai-400005, India

The collective excitation and its coupling with the single-particle excitation mode in nuclei remains a fundamental issue in modern nuclear structure physics [1]. In particular, the interplay between single-particle and octupole collective vibrational mode is of immense interest [2,3] due to various possibilities. The odd-mass nuclei with an even-even core having large B(E3) strength are ideal testing grounds for these investigations. A series of measurements have been carried out on nuclei around A~90 and 140 regions using a hybrid array of clover HPGe and $LaBr_3$(Ce) detectors at BARC-TIFR Pelletron Linac Facility (PLF) at TIFR, Mumbai, to study the evolution of neutron or proton coupling to octupole phonon through lifetime measurements [4,5]. Some of these results on Zr and La isotopes will be presented in this talk. Future investigation possibilities of this coupling in neutron-rich heavy nuclei at radioactive ion beam facilities like FAIR and RIBF will be discussed.

References:

[1] T. Otsuka et al., EPJ Web of Conferences 178, 02003 (2018).
[2] S. Leoni, A. Bracco, G. Coló, and B. Fornal, Eur. Phys. J. A 55, 247 (2019).
[3] P. Van Isacker and M. Rejmund, Phys. Rev. Res. 4, L022031 (2022).
[4] Md. S. R. Laskar et al., Phys. Rev. C**104**, L011301 (2021).
[5] P. Dey *et al*., *manuscript in preparation*.

Recent progress in the studies with weakly bound nuclei

V. V. Parkar
Nuclear Physics Division, Bhabha Atomic Research Centre, Mumbai - 400085 Homi Bhabha National Institute, Anushaktinagar, Mumbai - 400088

Weakly bound nuclei are characterized by predominant cluster structures and low separation energies. These nuclei can break very easily in the field of another nucleus and hence alter the reaction mechanism. Study of nuclear reactions involving weakly bound projectiles is very interesting because of the observation of several unusual features compared to the case of strongly bound projectiles. Various reaction mechanisms like elastic scattering, transfer/ breakup and fusion around Coulomb barrier energies with stable weakly bound ^{6,7}Li and ^{9}Be projectiles on several targets have been studied. Major accomplishments in these studies will be highlighted. These studies help in building the foundation for similar studies with unstable weakly bound nuclei to be available with upcoming radioactive ion beam facilities.

References:

[1] V. V. Parkar, Physics News - Bulletin of IPA 50(3), 31 (2020)
[2] V. Jha, V. V. Parkar, S. Kailas, Physics Reports 845, 1 (2020)
[3] V.V. Parkar *et al.*, Eur. Phys. Jour. A (Letters) 59, 88 (2023)
[4] V.V. Parkar *et al.*, Phys. Rev. C 107, 024602 (2023), *ibid* 104, 054603 (2021)
[5] V.V. Parkar *et al.*, Phys. Rev. C 97, 014607 (2018), *ibid* 98, 014601 (2018), *ibid* 82, 054601 (2010)
[6] V.V. Parkar *et al.*, Phys. Rev. C 87, 034602 (2013), *ibid* 78, 021601(Rapid Comm.) (2008)

Guided Wave Photonics: Computational and Modelling Methods

Anurag Sharma
Optics and Photonics Centre and Physics Department,
Indian Institute of Technology Delhi, New Delhi 110016

Modelling and simulation of wave propagation through optical waveguides and devices based on them has been a central theme in the theory of guided wave photonics. It basically entails solving the wave equation (obtained from Maxwell's equations) for the boundary conditions represented by the waveguide/device. In some cases, for example step-index planar or cylindrical (optical fiber) waveguides, the solutions can be obtained analytically. However, in most cases of practical importance, the solutions cannot be obtained analytically and such problems have to be dealt with either by resorting to some approximations or by using numerical methods. Both approaches have been used extensively in the literature each approach has some advantages and some limitations. We have developed methods in both these categories, and in this paper, we will discuss both approaches and include some examples.

Wave propagation problem can be approached in two ways. In the modal approach, the modes of the waveguide are solved and the incident field is propagated in terms for these modes. This works well for uniform waveguides or for slowly varying waveguides in which coupling among modes is considered. However, most practical waveguides are single mode and hence obtaining the fundamental mod becomes a central issue in all such cases. We have developed closed form approximations for such waveguides [1-4]. We will discuss some of these.

The second approach is the beam propagation approach in which the incident field is propagated directly by solving the wave equation. These methods are more rigorous, but are evidently more intensive computationally, particularly when actual 3-D wave propagation in involved. We have developed beam propagations methods [5-10] and some of these will be discussed.

References:

[1] Anurag Sharma and Hansa Chauhan, "A new analytical model for the field of microstructure optical fibers" *Optical and Quantum Electronics* **41** 235-242 (2009).
[2] Dinesh Kumar Sharma and Anurag Sharma, "On the mode field diameter of microstructured optical fibers",
[3] Dinesh Kumar Sharma and Anurag Sharma, "Improved analytical model for the field of index-guiding microstructured optical fibers", *Optics Communications* **366**, 127-135 (2016).
[4] Kanchan Gehlot and Anurag Sharma, "Optimization of Si slot waveguide using approximate semi-analytical method", *Opt. Express* **24**, 4722-4729 (2016).
[5] Anurag Sharma and Arti Agrawal, "A new finite-difference based method for wide-angle beam propagation", *IEEE Photon. Technol. Lett.* **18**, 944-946 (2006).
[6] Debjani Bhattacharya and Anurag Sharma, "Finite difference split step method for non-paraxial semivectorial beam propagation in 3D", *Optical and Quantum Electronics* **40**, 933-942 (2008).
[7] Debjani Bhattacharya and Anurag Sharma, "Simulation of multiple reflecting structures using a nonparaxial bidirectional split-step finite difference method", *Journal of Lightwave Technology* **31**, 2106-2112 (2013).
[8] Pratiksha Choudhary and Anurag Sharma, "Vector mode propagation in graded index ring core fibers", *XXVII International Workshop on Optical Wave & Waveguide Theory and Numerical Modelling (OWTNM-2023)*, Marseille, France, May 4-5, 2023.
[9] Ramesh Kumar and Anurag Sharma, "A new method to analyze fiber Bragg gratings", *Optical* Fiber *Technology* **53**, 102017 (pp. 1-5) (2019).
[10] Ajay Kumar and Anurag Sharma, "A propagation method for higher order modes in fiber structures", *XXVII International Workshop on Optical Wave & Waveguide Theory and Numerical Modelling (OWTNM-2023)*, Marseille, France, May 4-5, 2023.

Characterization of Raman instability in laser-plasma interaction

Alireza Paknezhad
Physics department, Shabestar Branch, Islamic Azad University, Shabestar, Iran
Email: alireza.pak1359@gmail.com

Stimulated Raman scattering (SRS) instability has long been a topic of interest in theory and experiment, especially, in inertial confinement fusion (ICF), particle acceleration or radiation. SRS is characterized as a parametric instability in which an incident light wave decays resonantly into an electron plasma wave and a scattered sideband wave at a shifted frequency. The scattered-light wavelength ranges from 1 to 2 times that of the incident light, depending on the plasma density and temperature. It produces a plasma wave with large phase velocity near the speed of light that could accelerate charged particles to high energies.SRS occurs below the quarter-critical density which may cause significant laser energy loss and hot electron production, where the latter can preheat the fusion targets. In this presentation, we discuss some features of Raman instability in the interaction of high intensity laser beam with a preformed plasma channel. We use the wave equation and the nonlinear momentum equation of electrons to find the dispersion relation. The nonlinearity arises from the ponderomotive force exerted by the wave on plasma electrons, which modifies the densities. Considering the coupling between the sideband wave and the excited plasma wave, an expression of growth rate of this instability is obtained. The effect of plasma density as well as the effect of external magnetic field on the growth rate of instability has been discussed.

Keywords: Stimulated Raman scattering, scattered sideband, quarter-critical density, ponderomotive force, growth rate.

Nanostructures and Ferroelectric Nanocomposites for Clean Energy Harvesting

Neeraj Khare
Physics Department, Indian Institute of Technology Delhi
Hauz Khas, New Delhi-110016, India
Email : nkhare@physics.iitd.ernet.in

With the ever-increasing demand for energy and also due to an increase in environmental pollution, there has been a lot of interest to develop novel materials for clean energy generation. Harvesting vibration energy through piezo/tribogenerator [1-4], and hydrogen generation through photoelectrochemical water splitting and thermoelectric generators are among the promising environmentally friendly approach to providing solutions to the present problem. We have designed several nanocomposite/nanostructures and explored its potential application for efficient piezo/tribo generators, thermoelectric generator and as photoanodes for PEC water splitting.

Triboelectric effect based nanogenerator have the edge over other mechanical energy harvesters because of its robustness, cost-effectiveness and higher energy. In the solid-solid interface based tribo-nanogenerator both the material used for contact are solid [1,2] whereas in the solid-liquid interface based tribo-nanogenerator liquid (water drop) comes in contact with a solid material [3]. The performance of these tribo-nanogenerator depends upon the number of induced charges during the contact and the retentively of these charges which can be captured for generating electricity. In the Photoelectrochemical water splitting device use of ferroelectric nanocomposite/heterostructures enabled to tune of the band edge position and thus results in much-improved efficiency [5].

The present talk will review the progress made so far in our group at IIT Delhi in the above-mentioned area [2-6] and will also present the main challenges.

Reference:

[1] H. H. Singh and N. Khare, Nano Energy, 52, 216-222 (2018).
[2] H. H. Singh and N. Khare, Energy, 178, 765-771 (2019).
[3] H. H. Singh and N. Khare, Advanced Materials Interfaces, 8, 2170068 (2021).
[4] A. Mondal, M. Faraz, N. Khare, Applied Physics Letters, 121, 103901 (2022).
[5] D. Kumar, S. Sharma, N. Khare, Renewable Energy, 163, 1569-1579 (2021).
[6] AK Gautam, HH Singh, N Khare, Nano Energy 107, 108125 (2023).

Non-equilibrium dynamics in correlated quantum systems

Pinaki Majumdar
HRI, Prayagraj

Correlated quantum systems define a frontier in many body physics, where there is often no convincing theory even for equilibrium properties. Experiments however have moved on to probing the non-equilibrium properties of such systems, for example the voltage bias driven breakdown of a Mott insulator, or the pump-probe dynamics of charge density waves in a strong coupling electron-phonon system. I will discuss a couple of phenomena in this category.

New Insights into the Properties of Matter at High Baryon Number Density

Larry Mclerran

I discuss Quarkyonic matter. I present an explicit theory whose assumptions are that quarks are confined inside of nucleons and the occupation probability for both nucleons and quarks is less than 1. Such
a theory has two phases: an ordinary free nucleon gas at low density and a Quarkyonic phase at high density. The high density phase has a hard equation of state. In this phase, the quark Fermi Sea is filled except for a finite surface thickness, while the nucleon distribution has a peak at the Fermi surface, surrounding an under-filled density of nucleons.

Fluctuations as a zooming tool to study the QCD critical point

Rajiv V. Gavai
Physics Department, Infinity Building
Indian Institute of Science Education & Research Bhopal Bypass Road, Bhauri, Bhopal 462066
Email: gavaitifr.res.in

The theory of strong interactions, called Quantum Chromo Dynamics (QCD), predicts new phases at high temperatures as well as high baryon densities. The QCD phase diagram in the temperature-density plane is expected to have a critical point. Higher order fluctuations of baryon number have been advocated to be suitable to look for the critical point. An ordering of the ratios of baryon number fluctuations i.e., $\frac{\chi_6}{\chi_2} < \frac{\chi_5}{\chi_1} < \frac{\chi_4}{\chi_2} < \frac{\chi_3}{\chi_1}$, where χ_n is the nth order cumulant of baryon number fluctuation, has been suggested. Using simulations of two-dimensional Potts models, we investigated such fluctuations of the corresponding order parameters to investigate how general such inequalities may be. We draw valuable lessons from our work for the case of QCD.

Societal Application of HEP detector elements and related technologies

M. Naimuddin
Raja Ramana Fellow

In the pursuit of understanding the basic building blocks of the universe and its working, high energy physicist develops large accelerators and big & complex detector systems. The detector systems are the state of art and pushes the boundaries of technologies and our current capabilities. The detector system consists of development and employment of new detector technologies, enhanced electronics and readout systems and the next level of computing and algorithm developments. India has a rich history of contributing to the high energy physics in house and internationally. We have made major contributions to the high energy physics experiments in terms of development of detector system, development of readout and electronics as well as in the software and algorithm development. Much of these can be put to the direct use of immediate societal applications as a spin-off of the HEP research. I will provide a glimpse of the detector technologies that are being currently developed within the country and the efforts that has been made to utilise them for societal applications. I will particularly focus on the development of Gas Electron Multiplier (GEM) detectors and their applications in the imaging which has potential use in cargo scanning, defence sector, etc.

Optical Tweezers Combined with Holographic Microscopy for Tracing the Motion of Waveguide Trapped RBCs and Spermatozoa Cells and their Quantitative Analysis

Dalip Singh Mehta
Bio-photonics and Green-photonics Laboratory, Department of Physics, Indian Institute of Technology Delhi, Hauz Khas, New Delhi, India.
Email: mehtads@physics.iitd.ac.in

In optical tweezers tightly focused laser beams are used for trapping and manipulation of tiny particles, atoms, micro-particles, biological cells and organellesby means of utilizing the forces of radiationpressure and gradient force. These are the forces arising from the momentum of the lightitself and the momentum imparted to an object from the light is called radiation pressure. Optical tweezers are non-contact and non-invasive and hence delicate biological cells can be trapped and manipulated and forces of sub-Pico Newton range can be measured. There are a variety of optical trapping schemes, i.e., by means of balancing radiation pressure forces using counter propagating laser beams, single beam trap using gradient forces and multiple beam holographic optical tweezers. These schemes have been used for many applications in physical and biological sciences and have proven unique techniques for these applications.

More recently optical tweezers have also been realized using wave guide trapping scheme using evanescent field. In this talk we will be presenting an overview of optical tweezers and some of its important applications. We have established optical waveguide trapping combined with holographic microscopy for quantitative measurement of various parameters. First waveguide trapping of human red blood cells (RBCs) along with holographic microscopy will be discussed. Experimental results phase map, refractive index, cell dry mass, cell motility and live cell trajectory will be presented. Effect of trapping forceson RBCs with be presented. Further, the tracing the motion of waveguide trapped polystyrene beads and spermatozoa cells will be presented. The effect of partial spatial coherence on the holographic phase microscopy will also be presented. WE report an order of magnitude higher accuracy in phase measurement of trapped RBCs and sperm cells will be discussed. Prospects related to holographic phase-nanos copy of wave guide trapped cells will be discussed.

Femtosecond stimulated Raman scattering microscopy: Home-built realization and a case study of biological imaging

Rajeev Ranjan
Aix Marseille Univ, CNRS, Centrale Marseille, Institut Fresnel, F-13013 Marseille, France

Stimulated Raman Scattering (SRS) microscopy has emerged as a valuable tool for studying molecular vibrations in samples, enabling the generation of chemical images. Its applications in biomedical research, particularly in examining living cells, tissues, and biomolecules, have proven significant. SRS microscopy offers non-invasive, label-free imaging capabilities, facilitating studying molecular processes in various physiological and pathological conditions.

This technique operates through a dissipative process, transferring energy from input photons to molecular vibrations. From a quantum mechanical perspective, SRS involves a two-photon stimulated process: one pump photon at frequency ω_p is annihilated (stimulated Raman loss, SRL), while one Stokes photon at frequency ω_s is emitted (stimulated Raman gain, SRG) as illustrated in figure 1. Concurrently, the material transitions from the electronic ground state to a vibrationally excited state. SRS finds application in diverse fields such as nanophotonics [1-2], bio photonics [3], and materials science [1]. SRS microscopy provides label-free imaging with high spatial and spectral resolution, sensitivity, 3D sectioning, and rapid image acquisition (few seconds) across various Raman spectra regions: C-H region (>2800 cm^{-1}), silent region (1800-2800 cm^{-1}), and fingerprint region (<1800 cm^{-1}). However, similar chemical bonds among biomolecular species can compromise detection specificity. A bio-orthogonal chemical imaging platform has been explored to address this limitation, combining SRS microscopy with small, Raman-active vibrational probes.

The optical design and implementation of stimulated Raman microscopy leverage three femtosecond laser sources: a Titanium-sapphire (740 nm – 880 nm), an optical parametric oscillator (1000 nm – 1600 nm), and a second harmonic generator (500 nm – 800 nm) integrated into a laser scanning microscope [4,5]. This system covers the full Raman spectra, offering high sensitivity across C-H, silent, and fingerprint regions. Its primary focus lies in investigating living cells to elucidate the functionalities of lipids and protein and their implications in cancer.

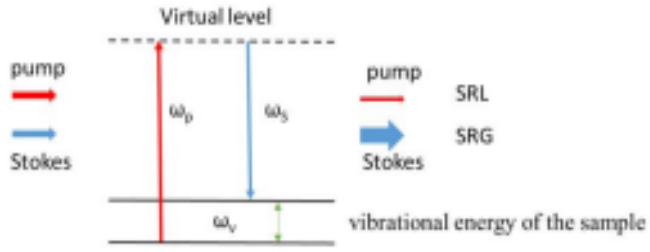

Figure 1. Schematic representation of Stimulated Raman Scattering

References:

[1] Sirleto, L.; Ferrara, M.A.; Nikitin, T.; Novikov, S.; Khriachtchev, L. Giant Raman gain in silicon nanocrystals. Nat. Commun. 2012, 3, 1–6. doi: 10.1038/ncomms2188.

[2] R. Ranjan, A. D'arco, M. A. Ferrara, M. Indolfi, M. Larobina, and L. Sirleto, "Integration of stimulated Raman gain and stimulated Raman losses detection modes in a single nonlinear microscope," Opt. Express, vol. 26, no. 20, p. 26317, Oct. 2018.

[3] Ferrara MA, Filograna A, Ranjan. R, Corda D, Valente C, Sirleto L (2019) Three-dimensional label-free imaging throughout adipocyte differentiation by stimulated Raman microscopy. PLoS ONE 14(5): e0216811.

[4] R. Ranjan, M. A. Ferrara, A. Filograna, C. Valente and L. Sirleto, "Femtosecond Stimulated Raman Microscopy: Home-built realization and a case study of Biological imaging," JINST 14 P09008 (2019).

[5] Ranjan, R., Costa, G., Ferrara, M. A., Sansone, M., Sirleto, L., J. Biophotonics (2022), e202100379.

Rare earths activated materials as frequency upconvertor and temperature sensor

Vineet Kumar Rai
Laser and Spectroscopy Laboratory, Department of Physics, IIT(ISM), Dhanbad-826004, Jharkhand, India
Email: vineetkrrai@iitism.ac.in; vineetkrrai@yahoo.co.in

Solid materials containing rare earth ions as dopants have been studied to investigate the effect of host materials on the spectroscopic properties of the rare earth ions. Hosts having low phonon frequencies play vital role in improving the spectroscopic properties, especially the photoluminescence properties, because of the reduced energy loss due to multiphoton emissions followed by the non-radiative relaxations. The fluoride-based materials are the lowest phonon frequency materials, but their hygroscopic nature limit the practical applications. The up conversion (UC) luminescence means the conversion of low energy photons into high energy photons. This optical characteristic makes the UC materials very demanding in the field of optical technology for varieties of applications. To make the optical devices such as optical switches, sensors, upconverters, optical limiters, sensors, etc. with optimized characteristics, solid hosts have attracted much due to the fascinating optical properties. Along with the hosts phonon frequency, the concentration of dopants plays significant role. The energy transfer between the rare earth ions increases the fluorescence intensity up to certain level. The concentration of rare earth ions needs to be low to minimize the luminescence quenching. The alternative way to compensate the harmful effect caused by the quenching is to alter the dopants environment by introducing some heavy materials or nanoparticles or sensitizers. The frequency up conversion and optical thermometric behavior of the rare earth ions doped materials under certain suitable excitation conditions along with the various involved processes will be discussed [1-5].

References:

[1] Upconverting nanoparticles- From fundamentals to applications, Vineet Kumar Rai (Ed.), Published by WILEY- VCH, ISBN: 978-3-527-83487-7 (e-book); ISBN 978-3-527-34965-4 (Print); ISBN: 978-3-527-83488-4 (O-book), First published published 11 May 2022. DOI:10.1002/9783527834884.

[2] Manisha Mondal; Rai, V. K.; Chandan Srivastava (2017): Influence of silica surface coating on optical properties of Er^{3+}-Yb^{3+}: $YMoO_4$ upconverting nanoparticles, Chemical Engineering Journal, 327, 838–848.

[3] H. Zhang, H. Zhang, A. Pan, B. Yang, L. He, Y. Wu (2021): Rare earth-free luminescent materials for WLEDs: recent progress and perspectives, Advanced Materials Technologies, 6, 2000648.

[4] Vineet Kumar Rai (2012). Frequency Upconversion in Rare-Earth Ions, Solid-State Laser, Amin H. Al-Khursan (Ed.), ISBN: 978-953-51-0086-7, InTech, Available from: http://www.intechopen.com/books/solid-state-laser/frequency-upconversion-in-rare-earth-ions.

[5] M.D. Mehare, C.M. Mehare, H.C. Swart, S.J. Dhoble (2022): Recent development in color tunable phosphors: a review, Prog. Mater. Sci., 133,101067.

Fundamental Physics of Semiconductor Quantum Structures and Devices

T. K. Sharma[1,2]
[1]Materials Science Section, Raja Ramanna Centre for Advanced Technology, Indore-452013
[2]Homi Bhabha National Institute, Training School Complex, Anushakti Nagar, Mumbai-400094
Email: tarun@rrcat.gov.in

Semiconductor quantum structures are the heart of numerous advanced photonic devices. Understanding the fundamental physics of such quantum structures is critical to optimize the operating characteristics of photonic devices that are made based on them. In our lab, we have been synthesizing quantum structures based on GaAs and GaN semiconductor materials. Advanced photonic devices like high power laser diode arrays and radiation tolerant photodetectors operating over a broad wavelength range are developed by using the grown heterostructures. Prior to the fabrication of devices, an in-depth characterization of the quantum structures is carried out by using optical, electrical and x-ray probes. It provides key parameters of the associated quantum structures which play a pivotal role in fine tuning the operating characteristics of indigenously made photonic devices. During this talk, selected examples will be presented with an emphasis on understanding the fundamental physics of semiconductor quantum structures grown by MOVPE and MBE techniques.

Metal Halide Perovskite Nanocrystals as Building Blocks for Efficient and Stable Optoelectronic Devices

Zishan Husain Khan
*Organic Electronics and Nanotechnology Research Laboratory, Department of Applied Sciences and Humanities, Jamia Millia Islamia, New Delhi 110025
Email: zishanhk@jmi.ac.in

Metal halide perovskite nanocrystals are defined by their distinctive perovskite crystal structure, denoted as ABX_3 (single perovskite structure) and $A_2B'B''X_6$ (for double perovskite). In these structure, A and B (B', B") represent cations, while X stands for halide anions. It is this unique structural arrangement that endows them with their extraordinary optical properties. Perhaps one of the most captivating features of metal halide perovskite nanocrystals is their tunable bandgap. Through careful manipulation of the A, B, and X components, it is possible to precisely control the absorption and emission properties of nanocrystals. This tunability is invaluable, allowing engineers and researchers to fine-tune the optical characteristics of these nanocrystals to match specific requirements in diverse optoelectronic applications. Metal halide perovskite nanocrystals excel in this aspect by frequently exhibiting high photoluminescence quantum yields (PLQY). Another noteworthy attribute of these nanocrystals is their solution-processability. This feature enables their cost-effective and scalable production using techniques such as spin-coating, inkjet printing, and solution casting. The ease of integration into existing device fabrication processes positions them as highly desirable components for next-generation optoelectronics. In addition to their optical properties, metal halide perovskite nanocrystals boast high charge carrier mobility, facilitating efficient charge transport within optoelectronic devices. This high mobility is especially significant for applications like solar cells and photodetectors, where rapid and efficient charge transfer is crucial for device performance. While the potential of metal halide perovskite nanocrystals is undeniable, their long-term stability has raised concerns. These materials can be sensitive to environmental factors, including moisture and heat, which can lead to degradation over time. Addressing these stability challenges is a critical research focus, as it is key to unlocking the full potential of these nanocrystals. The present talk focuses on the improvement the phase stability and the photo-photophysical properties of Cesium based metal halideperovskite nanocrystals using mixed halide and B-site doping approaches achieved via facile one pot synthesis protocols. Highly stable Mixed halide $CsPbI_2Br$ nanocrystals doped with Zn^{2+} and Sn^{2+} ions are synthesized using ultrafast thermodynamic control assisted ultrasound and studied for their photophysical properties. Singnificant improvements in the photophysical properties of Zn^{2+} and Sn^{2+} doped $CsPbBrI_2$nanocrystals are observed.

Indias' contributions to the CERN-LHC Program: An Overview

Brajesh Choudhary
Department of Physics, University of Delhi

In this talk, I will discuss what we want to understand about our universe using the Large Hadron Collider (LHC) at the European Organization for Nuclear Research (CERN), what are the main challenges and how have we overcome it and what have we leant till now. I will also talk about India's main contributions to the LHC accelerator, CMS and ALICE detectors and important physics that we have learnt.

Hawking radiation from acoustic black holes in relativistic heavy ion collisions and in hydrodynamical flow of electrons

Ajit Mohan Srivastava
Institute of Physics, Bhubaneswar

Acoustic black holes are formed when a fluid flowing with subsonic velocities accelerates and becomes supersonic. When the flow is directed from the subsonic to supersonic region, the surface on which the normal component of fluid velocity equals the local speed of sound acts as an acoustic horizon. This is because no acoustic perturbation from the supersonic region can cross it to reach the subsonic part of the fluid. One can show that if the fluid velocity is locally irrotational, the field equations for acoustic perturbations of the velocity potential are identical to that of a massless scalar field propagating in a black hole background. One, therefore, expects Hawking radiation in the form of a thermal spectrum of phonons. We discuss this possibility for the case of relativistic heavy-ion collisions where this Hawking radiation may be observable in terms of a thermal component in the rapidity dependence of the transverse momentum distribution of detected particles. We also discuss the case of hydrodynamic flow of electrons in condensed matter systems where the resulting Hawking radiation may appear in terms of current fluctuations.

Matter and Molecules in Astrophysics

Shantanu Rastogi
Department of Physics, DDU Gorakhpur University, Gorakhpur – 273 009
shantanu_r@hotmail.com

The visible astrophysical objects in the sky are usually too hot to allow molecules to exist. Yet there is seemingly invisible matter between the stars that not only dims the light of background stars but also plays a major role in the formation, evolution andfate of stars. This interstellar medium (ISM) is dust and gas. The ISM is rich in molecules that play an important role in star formation and may also have pre-biotic significance. Observational detection of the ISM and the discovery of first diatomic molecules began in early nineteenth century. Today there aremore than 200 molecules confirmed in the interstellar and circumstellar medium. A majority of these molecules are carbonaceous. Dust or solid matter plays and important role in molecule formation and its chemical evolution. The physical and chemical complexity of any astrophysical environment can be interpreted by the molecules detected in the region. There is also a whole group of polycyclic aromatic hydrocarbon molecule that are spectroscopically indicated in the interstellar space. Understanding the processes that induce growth of such largemolecules lead to a better understanding of the physical and chemical state of the astrophysical environment. Molecules are also important in the study of atmospheres of exoplanets that may lead us to trace evidence of life and its evolution. The current status in the study of ISM pertaining to all these aspects will be reviewed and discussed.

Heavy Ion Fusion Cross-sections: Understanding Fusion Hindrance from Astrophysical S-Factor

B. P. Singh
Department of Physics, Aligarh Muslim University, Aligarh-202002 (U.P.), India
Email: bpsinghamu@gmail.com

Study of nuclear reactions induced by heavy ions is important for unravelling the mysteries of the cosmos, particularly in astrophysical scenarios where these processes play a pivotal role. In the present work a thorough investigation of the S-factor in heavy ion induced reactions has been made. A systematic analysis of experimental data across a spectrum of heavy ion fusion reaction channels, involving various target and projectile combinations has been made. The experiments to measure the fusion cross-sections have been carried out using both the α-clustered as well as non-α-cluster beams viz., ^{12}C,^{13}C,^{14}N,^{16}O,^{18}O, ^{19}F etc., on the same targets, at the Pelletron facility of the Inter University Accelerator Centre (IUAC), New Delhi, India. The stacked foil activation technique has been employed for irradiations of the target samples. The bombarded samples were counted with the help of HPGe gamma ray spectrometer. Both the fusion as well as break-up fusion residues have been identified with their characteristic gamma radiations and well as measured half-life. The intensity of characteristic gamma lines has been used to determine the cross-sections for particular reaction channels. Statistical model codes have been rigorously employed to analyse experimental data on fusion cross-sections. Further, the experimental data has also been used to extract the astrophysical S-factor information. The S-factor quantifies the probability of a nuclear reaction at a given energy. It is crucial for calculating reaction rates in astrophysical environments, influencing processes like stellar nucleosynthesis. In heavy-ions induced reactions, fusion cross-sections are found to decrease rapidly as the incident energy decreases, eventually reaching to a point where fusion becomes prohibited. At a specific energy, the S-factor is expected to reach its maximum value, and below this energy, fusion cross-sections exhibit a significant decrease, in general. This decrease in fusion cross-sections is considered as an indication of fusion hindrance. Exploring the astrophysical relevance of the S-factor in heavy ion induced reactions, contributes to the broader effort of deciphering the fundamental processes shaping our universe. Further details regarding measurements and analysis will be presented.

Complexity and entropy crisis in the amorphous glassy state

Shankar P. Das
School of Physical Sciences, Jawaharlal Nehru University, New Delhi 110067, India

In this talk, I will discuss the transformations in a liquid as its density increases. We focus on freezing an isotropic liquid to a crystalline state and beyond in the supercooled state. The relaxation behaviour of supercooled liquids approaching amorphous solid-like states differs over different temperature ranges. It has been modelled using microscopic descriptions based on the statistical mechanics of many particle systems. After a broad review of the basic models, we will discuss extending the usual thermodynamic approach. In the latter, the metastable supercooled liquid is studied in terms of the free energy landscape (FEL) for a suitable free energy functional $F[\psi]$. The field $\psi(x)$ models a continuum field theoretic description of the many-particle system. In the deeply supercooled state, distinct basins form in the FEL, corresponding to different local minima of the free energy. This transformation of the FEL for the supercooled liquid has been termed a spontaneous breakdown of ergodicity. In the case of structural glasses, this fragmentation of the FEL occurs without the presence of any quenched disorder. Calculating the corresponding partition function is facilitated using a composite system of m identical Replicas of the original system. We will discuss a calculation of the so-called Complexity or the configurational entropy of the supercooled liquid using this description regarding the continuum or coarse-grained field theoretic models.

Emerging trends in self-healable nanomaterials for triboelectric nanogenerators relevant to self-powered sensor applications

Prof. B. C. Yadav
Nanomaterials and Sensor Research Laboratory,
Department of Physics, Babasaheb Bhimrao Ambedkar University,
Lucknow-226025, U.P., India
Email:balchandra_yadav@rediffmail.com

The present talk will include a thorough analysis of triboelectric nanogenerators (TENGs) that make use of self-healable nanomaterials. These TENGs have shown promise as independent energy sources that do not require an external power source to function. TENGs are developing into a viable choice for powering numerous applications as low-power electronics technology advances. Despite having less power than conventional energy sources, TENGs do not directly compete with these. On the other hand, they provide unique opportunities for future self-powered systems and might encourage advancements in energy and sensor technologies. The discussion of life cycle evaluations of TENGs provides details on how well they perform in terms of the environment and identifies potential improvement areas. Additionally, the cost-effectiveness, social acceptability, and regulatory implications of self-healing TENGs are examined. We have successfully incorporated self-healing and self-powered functionalities in different types of sensors e.g. Photo sensor, LPG, Moisture and Fluoride sensors. TENG was used in powering these different kinds of sensors. We have incorporated different types of polymeric materials (2-D and spherical) and metal oxide nanomaterials in TENG for enhanced output performance.

Keywords : self-healable nanomaterials, triboelectric nanogenerator, self-powered sensors

Structures in a 2D colloids interacting via modified inverse-power potentials with tunable softening of inner core

Dr. Pankaj Mishra
Department of Physics, Indian Institute of Technology (Indian School of Mines) Dhanbad, Dhanbad, India
Email: pankaj@iitism.ac.in

We have used classical density functional theory, HNC integral equation theory (IET) and NVT Monte-Carlo Simulation to investigated the effects of gradual softening of inverse-power repulsive interaction on the pair structure and phase transition properties of the two-dimensional system of colloidal dispersion. We aim to understand the anomalous behaviours and structure formation in a one-component 2D colloidal system using DFT by carefully examining the crossover from one length to two-length scale characteristics of purely repulsive interaction potential. The particles are assumed to interact via modified inverse-power (MIP) potentials whose strength of the repulsion is softened in a range of distances with an interparticle separation dependent exponent. The radial distribution curves of IET are found to exhibit a non-monotonous nature with an emergence of new peak at a shorter distance. It points to the existence of two competing length scales of nearestneighbor distance, i.e., a larger soft length fading out with increasing density in favour of the smaller hard length. At higher densities, in-contrast to the HNC IET, the RDF, obtained by MC simulation for high-softness parameter case, display a splitting of the second peak. Using DFT with structural inputs obtained by HNC IET we propose a fluid-triangular solid phase diagram in the temperature-density plane for various softness of the interparticle interaction. Comparison of the virial pressure obtained by HNC and MC simulations has been found to reveal an interesting feature. Whereas the pressure versus density curve given by HNC increases monotonically, the same due to MC simulation, on the other hand, shows a discontinuity. Interestingly the line emerging at the discontinuity is found to have greater slope than the line corresponding to fluid. This suggests the possibility of the formation of amorphous glassy phase in 2D system at hand. In order to verify it further, Wendt-Abraham parameter which is a simple and yet useful empirical criterion that has been employed from both the Monte Carlo (MC) and molecular-dynamics (MD) simulations to investigate the liquid-glass transition, has been calculated. We have also calculated the bond orientational order parameter which reaffirms the presence of amorphous solid phase for the case of high softening parameter.

Understanding Star Formation in Merging Galaxies using the ASTROSAT Ultraviolet Imaging Telescope (UVIT)

Mousumi Das
Indian Institute of Astrophysics, Bangalore

The interaction and mergers of gas rich galaxies are known to produce large amounts of star formation and nuclear activity in galaxies. Most of the luminosity arises from massive star formation which results in large amounts of UV emission. In this study we present far-UV and near-UV observations of star formation in merging and interacting galaxies in our nearby universe using the Ultraviolet Imaging telescope (UVIT) which is mounted on the Indian space telescope ASTROSAT. We show that merging galaxies often have dual nuclei, whose nature varies from accreting supermassive black hole (AGN) pairs to starburst pairs. The UV emission is associated with the tidal arms, star forming nuclei, resonance rings, nuclear spirals as well as accretion activity associated with massive black hole(s) in the centers of the galaxies. We show that radio emission is often closely associated with the UV emission, arising from both star formation as well as black hole accretion activity. We find that the comparison of optical imaging with UV emission can reveal unique systems such as dual and triple AGN systems, where the UV emission traces the interaction between the galaxies. The longer lifetime of UV emission compared to optical line emission can also lead to the surprising detection of diffuse galaxies, such as UVIT2022, which was previously thought to be the tidal tail of an interacting pair. We also show that UV emission is a good tracer of star formation in metal poor dwarf galaxies, where interactions are surprisingly common and star formation patterns are different compared to massive galaxies. Thus, UV is a powerful tool to study star formation in all types of galaxy mergers - massive galaxy mergers as well as interacting pairs of dwarf galaxies.

Searching for the galaxies that reionized the universe

Kanak Saha
IUCAA, Ganeshkhind,
Pune, Maharashtra, India

One of the outstanding problems of current observational cosmology is to understand the nature of sources that produced the bulk of the ionizing radiation after the Cosmic Dark Age. Direct detection of these reionization sources is practically infeasible at high redshift due to the steep decline of the intergalactic medium transmission. Not surprisingly, only a handful of ionizing sources are discovered to date. In this talk, the speaker will report the recent success in detecting faint, distant galaxies with AstroSat and discuss the nature of those ionizing sources.

The 3.6-meter Devasthal Optical Telescope for observations of faint celestial sources

A. Omar
Space, Planetary and Astronomical Sciences & Engineering (SPASE)

The Devasthal Optical Telescope with a 3.6-meter diameter mirror is presently India's largest optical telescope with a fully steerable mount situated in Himalayas at an altitude of ~2500 meter. The telescope is equipped with a state-of-the-art control system and an active optics mechanism to obtain sharp images of the celestial sky and related phenomena. This telescope fulfills scientific needs of both national and international astronomers with a fleet of high sensitivity instruments capable of carrying out imaging and spectroscopy observations in visible and near infrared bands. This talk will present an overview of the telescope and its instruments along with a brief description of their journey from inception to realization. Some of the important science results obtained with this telescope will also be highlighted.

Sputtered Deposited Semiconducting Nanostructures for Gas Sensing and Optoelectronic Applications

Beer Pal Singh
Department of Physics, Chaudhary Charan Singh University, Meerut – 250004 (UP), India
Email: drbeerpal@gmail.com

Abstract

Semiconducting nanostructures are used in state-of-arts applications due to their heightened physical properties. Semiconducting metal oxides and sulfides nanostructures are a growing asset in current semiconductor technology due to their extraordinary physical, chemical, and electronic properties and their outstanding applications indifferent sensing and optoelectronic devices. This talk covers the introduction of nanomaterials with different state-of-arts applications of different doped and undoped metal oxides and sulfides nanostructures as CuO, ZnO and MoS_2. The gas sensing capability of semiconducting nanostructures is a recent research interest of many researchers. Sputtered grown Pd-capped CuO thin films were found highly sensitive and selective hydrogen gas sensing. The MoS_2 thin films were grown using reactive sputteringand the sensing performance of pure MoS_2 and Cu-MoS_2 thin films was studied towards nitrogen dioxide (NO_2) gas concentrations (2-200 ppm) at the optimum working temperature of 100℃. The Cu-MoS_2 sensor provides a high sensing response as compared to the pure MoS_2 thin-film sensor towards 20 ppm of NO_2 gas with a fast response and recovery time. A high response/recovery and self-powered undoped ZnO (UZO) and Cu-doped ZnO (CZO) thin film-based visible light photodetector fabricated on a cost-effective Si substrate using reactive co-sputtering. The CZO/n-Si exhibits a higher on/off ratio, responsivity and detectivity than UZO/n-Si. A relative study of CZO/n-Si and UZO/n-Si-based photodetector reveals the enhanced performance of CZO/n-Si photodetector with a high on/off ratio of ~300 with high specific detectivity 2.8×10^{10}Jones for 75 mW visible light. The prepared self-powered CZO/n-Si/Ag thin films-based visible-light photodetector paves the way for the development of high-performance photodetector designs.

Enhanced photocatalytic activity of metal ion loaded metal oxide nanostructures for environmental remediation

Sushil Kumar
Department of Physics, Chaudhary Devi Lal University, Sirsa-125055, Haryana, India
Email: sushil.phys@gmail.com

During the past few decades, materials research at nanoscale has been observed as the most studied field of Science and Technology due to its tremendous applications in different areas. Nanostructured materials have the potential employability in a variety of optical, electronic, biomedical and environmentalsectors. In recent years, the photocatalytic degradation of organic pollutants(dyes)through semiconductor metal oxides nanostructures has created keen interest among researchers for textile effluentsorwaste-water treatment in order to prevent hazardous environmental contamination meaning conservation of natural resources. The structural, microstructural, optical and photocatalytic properties of undoped and transition metal ions doped semiconductor metal oxides nanostructures have been studied through different complementary analytical tools such as XRD, XPS, FTIR, SEM, EDX, TEM, UV-Vis, PL and photocatalytic measurements. XRD data analysis revealed the nano-crystalline structure/symmetry of samples with crystallite size in nm range. XPS results confirmed that the transition metal ions exist in the particular oxidation states and successfully incorporated into the metal oxide matrix. The morphology observed by SEM, TEM, HRTEM exhibited shape and size of nanoparticles. The energy bandgap of metal ions loaded metal oxide nanostructures had a reduction in band gap due to incorporation of transition metal ions as estimated by the optical absorption data. The doped/loadednanostructures exhibited reduction in intensity ofluminescence emission peaks in PL spectra. Enhancement in photocatalytic activity was observed for metal ions incorporated metal oxidesnanostructures attributed to the enhanced light absorption, reduced band gap and lowering of charge carriersrecombination rate. The results of present study depicted that hydrothermally synthesized metal ion loaded metal oxides nanostructurescan be employed efficiently as environmentally convenient photocatalyst for industrial effluent or waste-water treatment.

Enhanced Physical and Mechanical Properties of ZrO_2 and AlOOH Reinforced Resin Nano Composites for Dental Applications

Chandkiram Gautam* and Savita Kumari
Department of Physics, University of Lucknow, Lucknow - 226007, Uttar Pradesh, India
Email: gautam_ceramic@yahoo.com

Resin has limited applications however, its composites with metal oxides exhibited improved characteristics for numerous applications such as dental restoration, dentures etc. [1]. Herein, various compositions were fabricated by substituted$ZrO_2$and AlOOH into resin via a scalable heat cure process. For phase identification and structural analysis, XRD and FT-IR techniques were employed. Further, a detailed study of its composites was characterized using numerous techniques such as UV-Vis spectroscopy, SEM with EDAX, and universal testing machine (UTM). The bandgap energy of the PMMA and its oxide composites were evaluated and lies in the range of 5.43±0.01 - 5.39±0.01 eV, 5.31±0.005 -5.35±0.005 eV respectively. Mechanical performances have been carried out for the determination of several parameters such as compressive strength, compressive strain, Young's modulus, fracture toughness etc. The 5 wt. % of ZrO_2 in PMMA (RZ5) and 15 wt. % of AlOOH (PZA15) shows the maximum strength, 76.6 MPa and 85.2 MPa.As increasing ZrO_2content, improves the mechanical performance of the composites upto a certain level and thereafter it starts to deteriorate the strength of the resin composites. So, to overcome this decay occurring due to substituted ZrO_2, we incorporated AlOOH into the resin material [2]. Further, to check the biocompatibility of these resin-based composites the MTT assay was carried out. The synthesized compositeswere found to be highly biocompatible with enhanced mechanical performances. Therefore, the lower and the upper part of the final base-denture were successfully fabricated using investigated (RZ5 and PZA15) composites (Figure1).

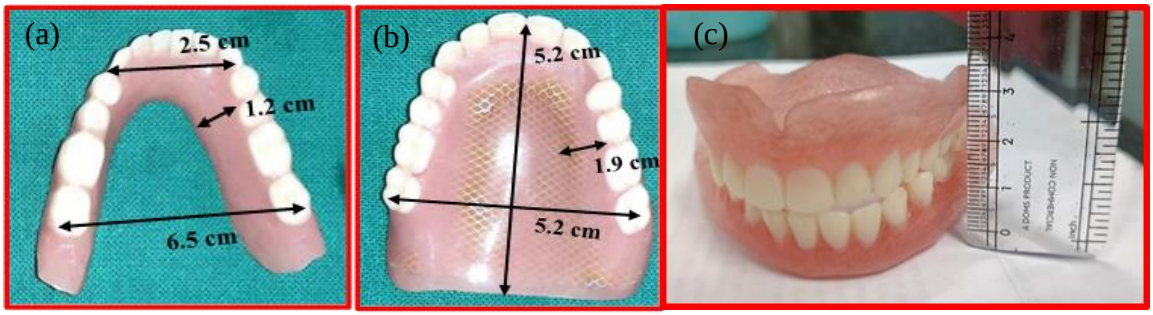

Figure 1 *(a,b, and c) Lower and upper part of fabricated5 wt. % of ZrO_2(RZ5) and 15 wt. % of AlOOH (PZA15) composites dentures*

Keywords: Acrylicresin: PMMA; Denture based nanocomposites; mechanical; MTT Assay.

References:

[1] Chęcińska, K., Chęciński, M., Sikora, M., Nowak, Z., Karwan, S., &Chlubek, D. (2022). The effect of zirconium dioxide (ZrO_2) nanoparticles addition on the mechanical parameters of polymethyl methacrylate (PMMA): A systematic review and meta-analysis of experimental studies. *Polymers*, *14*(5), 1047.

[2] Kumari, S., Hussain, A., Rao, J., Singh, K., Avinashi, S. K., & Gautam, C. (2023). Structural, mechanical and biological properties of PMMA-ZrO_2 nanocomposites for denture applications. *Materials Chemistry and Physics*, *295*, 127089.

Characterization of GaN based advanced Device Structures

Dr. Brajesh S. Yadav
Solid State Physics Laboratory, Lucknow Road, Timarpur Delhi-110054, India

Group–III nitride semiconductors are considered to have a great potential in optoelectronic and microelectronic applications. This is due to III-nitrides having properties such as large direct band gap, high saturation electron velocity, high thermal and chemical stability. AlGaN/GaN HEMT (high electron mobility transistors) as a device thus has excellent properties such as high breakdown fields for high voltage and frequencies handling capabilities, hence enabling them to be used in a wide range of applications. The performance of HEMT device critically depends on the epitaxial layer's material parameters such as uniformity of epitaxial layers, composition, thickness, interface quality, relaxation state, and crystalline perfection. The Group–III nitride epitaxial semiconducting films usually contain a high density of structural defects due to large and lattice and thermal mismatch with the foreign substrates. Thus, accurate determination of the above parameters become more important for the multilayered epitaxial HEMT device structure. The impact of point defects manifests themselves as shallow or deep level states are responsible for device degradation and can be created at different locations in the stack during the material growth. Present study focuses on the investigation of various component layers of metal organic chemical vapor deposition (MOCVD) grown AlGaN/GaN HEMT structures using high resolution X-ray diffraction (HRXRD), secondary ion mass spectrometry (SIMS), angle resolved X-ray photoelectron spectroscopy (ARXPS), photoluminescence (PL) and cathodoluminescence (CL). The ARXPS experimental result show that Al/Ga intensity ratio varies with the emission angles in the presence of cap layer otherwise remains constant. Also, the modeling of this intensity ratio gives its thickness which is also substantiated by SIMS depth profiling and CL studies. Low electron beams accelerating voltages (below 1 KV) CL spectra of samples with good quality GaN cap layer showed surface quantum well (SQW) transition in the CL spectrum. The cap layer thickness and its quality can be determined from the SQW emission energy and its integrated intensity. The investigation of radiative defects in various component layers in an AlGaN/GaN HEMT structure by measuring CL spectrum as a function of accelerating voltages show that the low intensity electron beam provides information about the defects in the cap layer as well as barrier layer through the intensity and energy of the yellow luminescence peak. SIMS analysis showed that intrinsic carbon incorporation around two orders can be controlled effectively in GaN layer by varying the growth parameters. The effect of incorporation of the intrinsic carbon concentration on the yellow luminescence (YL) and blue luminescence (BL) band intensities was investigated by cross-sectional cathodoluminescence (X-CL) shall be presented.

Graphene and its Derivative-based Materials: Synthesis, Properties and Applications to Energy Storage/ Conversion

Rajesh Kumar
Department of Mechanical Engineering, Indian Institute of Technology (IIT), Kanpur-208016
Email: rajeshk@iitk.ac.in; rajeshbhu1@gmail.com

Graphene, a two-dimensional (2D) monolayer and atomically thin carbon material with remarkable properties, has emerged as a promising candidate for use as electrode in electrochemical energy storage/ conversion. This carbon-based 2D layered material contains exceptional mechanical strength, high surface area, unique electronic/ thermal and enhanced electrochemical properties makes desirable for advanced electrode materials in supercapacitors and batteries. Graphene-based composites including various functional components are the subject of extensive study due to their unusual characteristics. Epitaxial growth, liquid phase chemical/electrochemical exfoliation, mechanical exfoliation, chemical vapor deposition, and laser-assisted synthesis are some of the most widely used processing techniques to synthesize graphene. Graphene has been prepared from graphene oxide/graphite oxide using chemical, thermal, microwave, and laser reduction techniques. Different chemical and physical methods have been developed to produce graphene-based materials. Recent studies conducted by researchers demonstrated that hybrids/ composites of graphene-derivatives with metal oxides and metal sulfides can significantly improve the efficiency of electrode materials applied in energy storage devices. In order to develop high-performance electrodes for electrochemical energy storage, researchers have incorporated heteroatoms doping and other vacancies into graphene-based materials. The electrochemical properties of graphene-based composite can be significantly altered by vacancy defects, leading to improved charge-transfer processes and reactions. In addition to facilitating ion diffusion as electrodes, atomic-scale defects can act as additional host sites for inserted protons or tiny cations.

Keywords: Graphene based materials, Reduction/ exfoliation, Electrode materials, Electrochemical performance, Energy storage/ conversion

References:

[1] Kumar R. *et al.* (2023) Graphene-metal oxide hybrid materials with 2D and 3D morphologies for advanced supercapacitor electrodes: Status, challenges and prospects. Materials Today Nano, 24, 100399.
[2] Kumar R. *et al.* (2022) Laser processing of graphene and related materials for energy storage: State of the art and future prospects. Progress inEnergyandCombustionScience91, 100981.
[3] Kumar R. *et al.* (2020) Heteroatom doped graphene engineeringfor energy storage and conversion. Materials Today, 39, 47-65.
[4] Kumar R. *et al.* (2019) Recent progress in the synthesis of graphene and derived materials fornext generation electrodes of high-performance lithium-ion batteries. Progress in Energy and Combustion Science, 75, 100786.

Photocathodes: Past performance and Recent advances

Bhartendu K. Singh
Physics Department, Banaras Hindu University (BHU), Varanasi 221 005, India
&
PDPM Indian Institute of Information Technology, Design and Manufacturing, Jabalpur 852 005, India
Email id: bksingh@bhu.ac.in; director@iiitdmj.ac.in

Light detection and imaging at very low intensities, down to individual photon detection, has been made available by the development of various photon detectors and imaging tubes. One of the photon detectors is vacuum-based Photomultiplier tubes which have two main components: a photocathode and an electron multiplication part. However, their performance has been limited by the response of the photocathodes. I will discuss the underlying science of photocathode preparation which indicates that they are still performing well below their full potential. The reasons for this are discussed and some indications of how improvements could be made are suggested.

Stitching the patches between fusion and fission dynamics

Ajay Tyagi
Department of Physics, Banaras Hindu University, Varanasi

Angular momentum variation and entrance channel effects have been explored experimentally during the fusion and fission process by several research group at international level, but still there is no unique explanation which could resolve the anomalies in the above-mentioned processes. A new approach to resolve the issue of angular momentum hindrance and entrance channel effects will be discussed in detail.

Semiconducting Quantum Dots: Synthesis for Device Applications

Kedar Singh
School of Physical Sciences, Jawaharlal Nehru University, New Delhi-110067
Email: kedar@mail.jnu.ac.in

Semiconducting quantum dots (QDs) are typically semiconductor crystals in the size range of 2-10 nm. Due to the quantum confinement effects arising from their small size, they exhibit composition, shape and size-dependent electrical and optical properties. These highly tunable properties have driven the research for several decades into their understanding and subsequent commercial application in several fields especially for the optoelectronic devices and photovoltaics. II-VI QDs have shown great promise as tunable light absorbing and/or emitting layers in LED devices and displays, in photovoltaics and imaging. Semiconducting quantum dot are important materials for fundamental and technological viewpoints. Quantum confinement effects are known to enhance exchange interactions and induce magnetic properties that were previously not observed in bulk materials. The growth kinetics of the CdSe core and CdSe/V_2O_5 core/ shell QDs studied by using Ultrafast transient absorption (TA) spectroscopy and exhibited slow electron cooling in core/shell QDs because of the de-coupling of the electronic wave functions with their hole counterpart. These exciting properties reveal a new paradigm shift from CdSe QDs to CdSe/V_2O_5 core/shell QDs for highly suitable applications in photovoltaics (PV) and optoelectronic devices.

$CsPbBr_3$ Perovskite semiconducting quantum dots (PSQDs) were synthesized by hot injection method. It is report that temperature- and field-induced magnetic states in $CsPbBr_3$ PSQDs attributed to Br defects and found that temperature dependent structural distortion is the main source of various temperature-induced magnetic states in Br-defect host CsPbBr3 PQDs. Comprehensively examined magnetization data through Arrott plots, Langevin and Brillouin function fitting, and structural analysis reveal the presence of various oxidation states (i.e., Pb^0, Pb^+, $Pb2^+$, and Pb^{3+}) yielding different magnetic states, such as diamagnetic states above 90 K, paramagnetic states below ≈90 K, and perhaps locally ordered states between 58 and 90 K. It is realized from theoretical fits that paramagnetic ions exist (i.e., superparamagnetic behavior) due to Br defects causing Pb+ (and/ or Pb3+ ions) in the diamagnetic region. We anticipate that our findings will spur future research of the development of spin-optoelectronics, such as spin light-emitting diodes, and spintronics devices based on $CsPbBr_3$ PSQDs.

Solution processed ion conducting metal oxide and its application as gate dielectric of a low operating voltage thin film transistor

Bhola Nath Pal[1*], Anand Sharma[1], Nila Pal[1], Utkarsh Pandey[1] and Nitesh Churasia[1]
[1]School of Materials Science and Technology, Indian Institute of Technology (BHU), Varanasi-221005, India
Corresponding Author's e-mail: bnpal.mst@iitbhu.ac.in

A thin film of ion-conducting metal oxide (ICMO) contains mobile light ions like Li^+, Na^+, K^+ which makes it possible to fabricate a high areal capacitance of the film due to their ionic polarization. An insulating ICMO has low DC conductivity with high AC conductivity which is suitable for using it as a gate dielectric of a low operating voltage thin film transistor (TFT). In the last decade a significant achievement has been made on solution processed ICMO based metal oxide TFT which can attain a carrier mobility > 20 cm^2/Vs with an on/off ratio $>10^5$ under 2 V operating voltage [1-5]. The key difficulty of this ICMO based dielectric is its high processing temperature. However, gradually reducing this processing temperature it is possible to make it compatible for printable thin film transistors. This presentation will focus on the development of these solution processed ICMOs for low operating voltage metal oxide TFT fabrication and its various applications including phototransistor [2,6], memory transistor [5] and synaptic transistor.

References:

[1] B. N. Pal, B. M. Dhar,K. See, and H. E. Katz, "Solution-deposited sodium beta-alumina gate dielectrics for low-voltage and transparent field-effect transistors", *Nature Materials*,**8**, 898-903, 2009.

[2] Anand Sharma, Nitesh k.Chourasia, Yogesh Kumar, SatyabrataJit, Shun-Wei Liu, SajalBiring and Bhola N. Pal Solution processed Li_5AlO_4 dielectric for low voltage transistor and its application for low power consumption quantum dot phototransistor,*J. Mater. Chem. C, 2018, 6, 790-798*

[3] N K Chourasia, A Sharma, V Acharya, N Pal, S Biring, Bhola N Pal, Solution processed low band gap ion-conducting gate dielectric for low voltage metal oxide transistor**,** *J Alloys Compd.* 2019, 777, 1124-1132

[4] Nila Pal, Baishali Thakurta, Rajarshi Chakraborty, Utkarsh Pandey, Vishwas Acharya, Sajal Biring, Monalisa Pal, Bhola N Pal, Application of a microwave synthesized ultra-smooth aC thin film for the reduction of dielectric/semiconductor interface trap states of an oxide thin film transistor, *J. Mater. Chem. C, 2022, 10, 14905-14914*

[5] Rajarshi Chakraborty, Nila Pal, and Bhola Nath Pal, Fabrication of non-volatile memory transistor by charge compensation of interfacial ionic polarization of a ferroelectric gate dielectric, *Appl. Mater. Today*, 2023, 33, 101862

[6] Utkarsh Pandey, Akhilesh Kumar Yadav, Nila Pal, Pijush Kanti Aich and Bhola N. Pal; Enhanced sub-band gap photosensitivity by an asymmetric source-drain electrode low operating voltage oxide transistor, *J. Mater. Chem. C*, 2023, 11 (43), 15276-15287

Forecasting Maximum Amplitude and Timing of Solar Cycle 25 using Geomagnetic Precursor Technique

Kavita Sharma*, Anushree Rajwanshi, and Gulfam Ansari
Department of Physics, C.C.S. University, Meerut
**Corresponding author email id: Sharmak29@gmail.com*

The Sun goes through cycles of magnetic activity that last 11 years on average, during which the swap of its magnetic poles takes place. Scientific community attempts to understand this variability and the associated causes. Solar activity variations cause changes in interplanetary and near-Earth space environment. This may deteriorate the operation of space-borne and ground based technological systems (space flights, navigation, radars, high-frequency radio communications, ground power lines, etc.). Scientists predict the exact duration and intensity of each solar cycle based on a variety of methods from purely statistical models using observations of previous cycles to complex simulations of solar physics. The present study is based on the prediction of solar cycle 25 using geomagnetic precursor technique. In this technique starting from solar cycles 17 up to 24, linear correlations are obtained between 12-month moving averages of the number of disturbed days when Ap is greater than or equal to 25, called the disturbance index, DI, at thirteen selected times (called variates blocks 1, 2, etc.) during the declining portion of the ongoing sunspot cycle and the maximum amplitude of the following sunspot cycle. In particular, variate block 9, which occur just prior to subsequent cycle minimum, give the best correlations (0.91) with minimum standard error of estimation (±13), and hindcasting shows agreement between predicted and observed maximum amplitudes to about 10 percent. A multivariate fit using the two best DI indexes in variate block 9 also gives the similar correlation to about 0.94 with standard error of estimation (±14). As applied to cycle 25, the modified precursor technique yields a maximum amplitude of about 111 ± 14, occurring about 48 ± 0.9 months after its minimum amplitude occurrence, probably in September 2024.

Keywords: Solar cycle, Geomagnetic precursors, Sunspots, Geomagnetic index

Observational Search of PAHs Footprints using SUBARU/COMICS Telescope

Mridusmita Buragohain[1*], Takashi Onaka[2], Itsuki Sakon[3], and Amit Pathak[4]
[1]School of Physics, University of Hyderabad, Hyderabad 500046, India
[2]Department of Physics, Faculty of Science and Engineering, Meisei University, Tokyo 191-8506, Japan
[3]Department of Astronomy, Graduate School of Science, The University of Tokyo, Tokyo 113-0033, Japan
[4]Department of Physics, Banaras Hindu University, Varanasi 221 005, India
**Corresponding author email id: ms.mridusmita@uohyd.ac.in*

Polycyclic Aromatic Hydrocarbons (PAHs) have found a noteworthy place in the family of possible interstellar organics as revealed by their spectral footprints, particularly observed in the mid-infrared wavelength range starting from 3 to 20 μm (Allamandola et al., 1989; Tielens, 2008; Li, 2020). The observed emission bands in these wavelengths are popularly known as "Aromatic Infrared Bands (AIBs)" as suggested by nature of the carriers. PAHs are mostly apolar or weakly polar, hence rotational spectroscopy, which is the usual method of identification of a molecule, is rather difficult. The nearest comparable confirmed species to PAH is benzonitrile (c−C6H5CN), which was detected through rotational transitions, and may be considered as a precursor for PAH formation in the ISM (McGuire et al., 2018). A recent detection of two isomers of small PAHs (naphthalene) with a CN group by McGuire et al. (2021) have encouraged the community to search for more varieties of PAHs and their characteristic features. PAH features may vary in terms of width, intensity and profile from one astronomical source to another. In this work, I am discussing PAH features observed towards MWC1080 (A Herbig Ae/Be star) obtained using SUBARU/COMICS that operates in the wavelength range of ∼7−25 μm. Spatially resolved features extracted from different sections of the target have been discussed here and any variations in PAH features have been looked for. These kinds of observations help to prioritize goals for the very powerful James Webb Space Telescope (JWST) that offers higher sensitivity as well as resolution and could be used to make powerful observations, which are unattainable by previous observations.

References:

[1] Allamandola L. J., Tielens A. G. G. M., Barker J. R., 1989, ApJS, 71, 733
[2] Li A., 2020, Nature Astronomy, 4, 339
[3] McGuire B. A., et al., 2018, Science, 359, 202
[4] McGuire B. A., et al., 2021, Science, 371, 1265
[5] Tielens A. G. G. M., 2008, ARA&A, 46, 289

Exchange of Orbital Angular Momentum of a Higher-order Bessel-Gauss Beam via Four-wave Mixing in Atomic Vapor

Onkar N. Verma*, and Niti Kant,
Department of Physics, University of Allahabad, Prayagraj-211002, Uttar Pradesh, India
**Corresponding author email id: onkarnath15verma@gmail.com*

We propose a scheme to demonstrate the exchange of orbital angular momentum of a higher-order Bessel-Gauss beam between Stokes field and anti-Stokes field generated via four-wave mixing (FWM) process in a four-level double-Λ type atomic system. We found that the intensity profile of both transmitted beams are identical, whereas the phase profile are conjugate to each other. The transverse phase distributions of both transmitted beams are explored by superimposing them on a co-propagating reference plane wave.

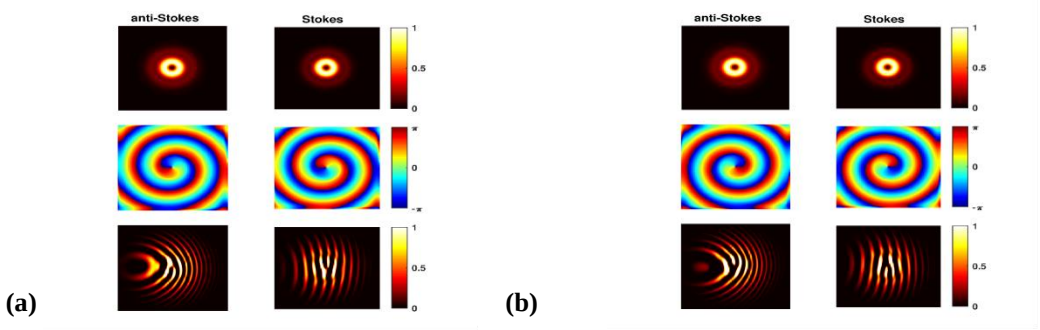

Fig. 1: 2DIntensity profiles (I-row), phase profiles (II-row), and fork fringes (III-row) of transmitted anti-Stokes and Stokes beam when input vortex is seeded into (a) anti-Stokes beam with OAM = 1; (b) Stokes beam with OAM = 1.

We exploit higher-order Bessel-Gauss (BG) modes to transfer its spiral phase profile between anti-Stokes and Stokes beams generated in FWM process. The higher-order BG beams have a vortex at the center as shown in Fig. 1. An optical vortex is basically a phase structured beam. Such light beams have an azimuthal phase dependence of form of $e^{il\varphi}$, where φ is azimuthal angle and l is referred as topological charge having integer values [1]. The phase in the field rotates about the propagation axis of the beam resulting in a helical wavefront. This twisting of transverse phase is responsible for the origin of orbital angular momentum (OAM) of vortex beam. First, we launch seed signal into anti-Stokes beam with OAM=1, then generated FWM Stokes beam is transmitted with OAM=-1 as depicted in Fig. 1(a). Next, we put seed signal into Stokes beam with OAM=1, then generated anti-Stokes beam is transmitted with OAM=-1 as depicted in Fig. 1(b). Thus, the higher-order BG modes manifest a quantized OAM of $lh/2\pi$ per photon. The interaction of such BG beams with material media has potential applications in optical tweezing, optical trapping, and storage of phase information in optical media [2].

Keywords: Orbital angular momentum, Four-wave mixing, Vortex beam, Bessel-Gauss beam

References:

[1] Allen *et al.*, "Orbital angular momentum of light and the transformation of Laguerre-Gaussian laser modes," Phys. Rev. A 45, 8185 (1992).
[2] Verma *et al.*, "Efficient transfer of spatial intensity and phase information of arbitrary modes via four-wave mixing in an atomic vapor," Phys. Rev. A 106, 053713 (2022).

Early Thermal Evolution of the Proto-Earth Accreting in the Presence of Primordial Solar Nebula

Gurpreet Kaur Bhatia*,[1] and Kamlesh Yadav[2]
[1]Department of Physics, MM Engineering College, Maharishi Markandeshwar (Deemed to be University), Mullana-Ambala, Haryana, India 133207
[2] Department of Physics, University of Allahabad, Prayagraj, Uttar Pradesh, India -211001
*Corresponding author email id: gurpreetkaur@pu.ac.in

The recent isotopic analyses recommend the rapid accretion of (proto-Earth during the lifetime of solar nebula [1]. The discovery of low-density extrasolar planets with extensive gaseous envelopes suggest that the proto-Earth may have gravitationally acquired primordial atmosphere from the solar nebula around it [2]. We report the preliminary findings of the numerical simulations carried out for the early thermal evolution and differentiation of the proto-Earth during the lifespan of solar nebula. The heat conduction partial differential equation has been numerically solved to understand the early thermal evolution of the proto-Earth. The heat sources for the heating and melting of proto-Earth's interior are the decay energy of short-lived radionuclide ^{26}Al [3] and blanketing effect of the captured proto atmosphere of solar composition during accretion [4]. The parameters *tonset* (start of accretion after the formation of CAIs), *tacc.* (timescale for the complete accretion of proto-Earth), and various melting curves for iron and silicates were taken into consideration. The left panel in Figure 1 displays the heat profiles inside the proto-Earth at chosen timescales throughout the first 5 Ma (million years) of the solar system's formation, while the rights panels display the iron-silicate differentiation at interior due to ^{26}Al and at surface. The primordial atmosphere's blanketing effect during the latter stages of accretion melted the surface silicates, creating a magma ocean at the surface. The findings of the current study have consequences for how volatiles are distributed inside the proto-Earth [5].

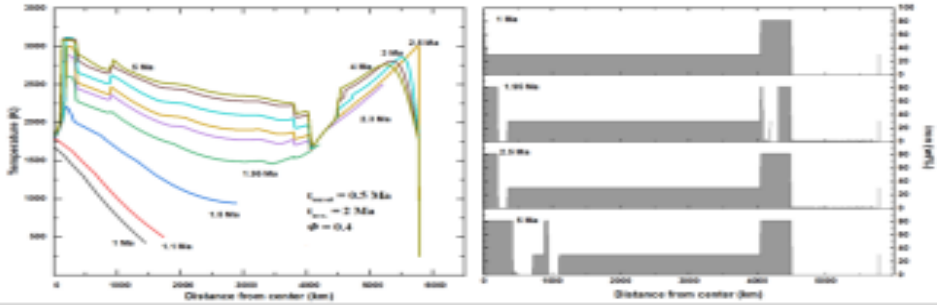

Figure 1 The thermal evolution (left panel) and iron-silicate differentiation (right panels) of proto-Earth

Keywords: Proto-Earth, Thermal evolution, Iron-silicate differentiation

References:

[1] Schiller, M., Bizzarro, M., & Siebert, J. (2020). Iron isotope evidence for very rapid accretion and differentiation of the proto-Earth. Science Advances, 6(7). https://doi.org/10.1126/sciadv.aay7604
[2] Masuda, K. (2014). Very low-density planets around kepler-51 revealed with transit timing variations and an anomaly similar to a planet-planet eclipse event. The Astrophysical Journal, 783(1), 53. https://doi.org/10.1088/0004-637x/783/1/53
[3] Bhatia, G. (2021). Early thermal evolution of the embryos of Earth: Role of 26Al and impact-generated steam atmosphere. Planetary and Space Science, 207, 105335. https://doi.org/10.1016/j.pss.2021.105335
[4] Hayashi, C., Nakazawa, K., & Mizuno, H. (1979). Earth's melting due to the blanketing effect of the primordial dense atmosphere. Earth and Planetary Science Letters, 43(1), 22–28. https://doi.org/10.1016/0012-821x(79)90152-3.
[5] Young, E., Shahar, A., & Schlichting, H. E. (2023). Earth shaped by primordial H2 atmospheres. Nature, 616(7956), 306– 311. https://doi.org/10.1038/s41586-023-05823-0.

Detection of an Extremely High-ionization Emission Line [Fe X] λ6374 in a Lyman-α Emitter at z ∼ 0.047

Abhishek Paswan
Department of Physics, University of Allahabad, Prayagraj - 211002, U.P., India

We report the first detection of an extreme high-ionization potential (262.1 eV) emission line [Fe X] λ6374 in the spectrum of a Lyman-α emitter (LAE), SHOC 579 at z ∼ 0.047. This detection is subsequently followed by the presence of optical nebular He II λ4686 emission line, X-ray (0.5 − 8 key) and 1.4-GHz radio continuum emissions. We diagnose the origin of all these emissions using the standard characteristic relation of star-forming galaxies such as radio-far-infrared correlation and X-ray luminosity relative to star formation rate and gas-phase metallicity. These relations do not exhibit any evidence of active galactic nuclei activity, and support the fact that the above detected emissions are most likely originated due to recent starburst event in the LAE. Our result strengthens the conclusions obtained from previous studies in the literature, indicating the importance of hard ionizing radiation in supporting the escape of ionizing photons from a compact starburst galaxy.

Keywords: Galaxy evolution, Starburst galaxies, HII regions, Interstellar medium, Radiative transfer, Reionization

Combined Density Functional Theory and Insilico Molecular Docking Studies for Understanding of Mechanism of Action of Cathinone Derivative 1 (4 methylphenyl) 2 (ethylamino)pentan 1 one

Akansha Tyagi, Anuj Kumar*
Department of Physics, Chaudhary Charan Singh University Meerut, India, 250004
Corresponding author email: dranujkumarccsu@gmail.com

Often known as synthetic Cathinone or "bath salts," Cathinone derivatives are a class of synthetic stimulant substances that have a euphoric effect. The primary way that cathinone derivatives work in the brain is through interacting with different neurotransmitter systems to produce stimulant and euphoric effects. In the central nervous system, catehinone derivatives mainly influence the release and absorption of neurotransmitters like serotonin, norepinephrine, and dopamine.

Density functional theory (DFT) is a popular computational technique for understanding and forecasting a variety of molecular and electrical properties of chemical systems. Additionally, it can be used to compute molecular properties and descriptors including polarizabilities, electrostatic potentials, and lipophilicity that are pertinent to biological activity. These characteristics can be utilised in QSAR models to forecast a compound's biological action.

In order to comprehend the pharmacological effects and related mechanisms of action of cathinone derivatives, docking is used to predict the binding interactions between these chemicals and particular target proteins, such as receptors or enzymes. In the present work, we have provided combined density functional theory and molecular docking studies to understand the mechanism of action of newly synthesized Cathinone derivative 1(4 methylphenyl)2 (ethylamino)pentan1one (4-MEAP). Molecular electrostatic potential (MEP), HOMO–LUMO, NBO, and Hirshfeld surface analysis are presented for the title molecule. Docking studies of 4-MEAP with Dopamine, Norepinephrine and Serotonin transporters, 6MOZ, 6MOF and 6M2R respectively, revealed that 4-MEAP could favourably interact with 6MOZ, 6MOF and 6M2R as can be concluded with low binding energies -7.3kcal/mol, -7.3kcal/mol and -7.0kcal/mol.

Keywords: DFT, HOMO-LUMO, NBO, Hirshfeld surface analysis, Molecular docking

Effect of Anisotropy on Phase Coexistence Diagrams: GEMC Simulation and Barker-Henderson Perturbation Theory

Bina Kumari
Brahmanand College, Chhatrapati Sahuji Maharaj University, Kanpur, Uttar Pradesh, India
**Corresponding author email: kumaribina7@gmail.com*

Studies of phase coexistence often have to deal with the fact that the interactions among the constituent particles are not isotropic. Here we introduce a minimal model of anisotropic pair potential without fore-aft symmetry to describe interaction of macromolecules. We find that Gibbs Ensemble Monte Carlo [1] (GEMC) simulations of our minimal model capture some essential aspects of the experimental phase coexistence diagrams of many simple fluids as well as some globular proteins. These include: (i) Agreement with the non-universal amplitude parameter in the scaled phase coexistence diagrams of many fluids and (ii) the demonstration that the flatness of these scaled phase diagrams at the critical point can be enhanced by raising the value of the anisotropy parameter of our model. Quantitative predictions regarding the latter are compared with the experimental data for the protein's lysozyme [3] and γ-IIIa crystalline [4]. We also test the accuracy of the predictions of generalized Barker-Henderson theory [2] for the fluid-fluid phase coexistence diagram of our minimal model via comparison with the results of an extensive set of high statistics GEMC simulations. We find that the agreement is less close than in the previous instances. We carefully analyse the reasons for this.

Keywords: Phase coexistence, Barker-Henderson theory, lysozyme, γ-IIIa crystalline.

References:

[1] Panagiotopoulos AZ (1987). Direct determination of phase coexistence properties of fluids by Monte Carlo simulation in a new ensemble.Mol Phys., 61, 813-826.
[2] Barker J A and Henderson D (1967), Perturbation theory and equation of state for fluids. A Successful Theory of Liquids. J. Chem. Phys.,47, 4714–4721.
[3] Petsev D N, et al. (2003), Thermodynamic Functions of Concentrated Protein Solutions from Phase Equilibria. J. Phys. Chem. B, 107, 3921−3926.
[4] Broide M L, Berland C R, Pande J, Ogun O O and Benedek G B (1991), Binary-liquid phase separation of lens protein solutions. PNAS, 88, 5660-5664.

Performance of an Active Brownian Particle in a Ratchet Potential Driven by Time-dependent Self-propulsion Velocity

Ronald Benjamin[a,*]
Department of Physics, Cochin University of Science and Technology (CUSAT), Kochi, India- 682022.

In this work, we study the energetics and transport coherence of an active Brownian particle [1,2,3] driven by a time-dependent self-propulsion force in a piece-wise linear ratchet potential subjected to a load as characterized by the thermodynamic efficiency and transport coherence of the motor. There are optimal values of various parameters such as the self-propelled velocity, temperature, asymmetry of the potential, at which the performance characteristics attain a maximum.

Keywords: Active Brownian Particle, Brownian Motion, Transport, Stochastic Energetics

References:

[1] Active Engines: Thermodynamics moves forward, Etienne Fodor and Michael E Cates, Europhysics Letters 134, 10003 (2021).
[2] Simulation of the active Brownian motion of a microswimmer, Volpe, Gigan and Volpe, American Journal of Physics 82, 659 (2014).
[3] Performance Characteristics of Brownian Motors, Linke, Downton and Zuckermann, Chaos 15, 026111 (2005).

Crystallization Dynamics of Metal/semiconductor Bilayer System Under Ion Irradiations

Shiv P. Patel*,[1] Topeswar Meher,[1] G. Maity[1], S. Ojha,[2] and D. Kanjilal[2]
[1]Department of Pure & Applied Physics, Guru GhasidasVishwavidyalaya (A Central University), Bilaspur 495009, India
[2]Inter University Accelerator Centre, ArunaAsaf Ali Marg, New Delhi 110067, India
Corresponding author email id: shivpoojanbhola@gmail.com

The polycrystalline Si has become an important material for large-area, low-cost semiconductor applications, such as solar cells and thin-film transistors. Methods such as solid-phase crystallization (SPC) [1-2] and laser crystallization [1-2] are employed most often to produce polycrystalline materials from amorphous solids. Crystallization by SPC method usually takes place by annealing the amorphous-Si (*a*-Si) at a temperature of approximately 600 °C over a period of 24 h or more [4]. On the other hand, *a*-Si films and *a*-Ge in contact with some metals (Al, Au and Ni etc.) have been observed to crystallize to poly-Si films at a significantly lower temperature (below eutectic) [1-4], by a process known as metal induced crystallization (MIC).

In the present article, the crystallization behaviour of amorphous (*a)*-Si and *a*-Ge under thermal annealing and swift heavy ion irradiation are presented. The *c*-Al (50nm)/*a*-Si (150) thin films have been prepared on thermally oxidized Si-substrates. A set of samples have been annealed at temperature ranges from 100 ºC to 500 ºC to achieve crystallization. Another set of similar samples have been irradiated at an elevated temperature of 100 ºC using 100 MeV Ni^{+7} ions at fluences of 1×10^{12} ions-cm^{-2}, 5×10^{12} ions-cm^{-2}, 1×10^{13} ions-cm^{-2}, and 5×10^{13} ions-cm^{-2}. The crystallization of *a*-Si is observed at annealing temperature of 200 °C and the crystallinity increases with increasing temperature. On the other hand, irradiation using swift heavy ion leads to crystallization of *a*-Si at a significantly lower temperature of 100 ºC. In case of Ge, the 50 nm *a*-Ge and 50 nm crystalline Au bilayer films (i.e. *a*-Ge/Au) have been prepared on ultrasonically cleaned quartz substrate using e-beam evaporation and thermal evaporation techniques, respectively. The as-prepared (i.e., pristine) samples (i.e. a-Ge/Au/quartz) have been irradiated with 100 MeV Ni^{+7} ions at different fluences of 1×10^{12} ions-cm^{-2}, 5×10^{12} ions-cm^{-2}, 1×10^{13} ions-cm^{-2}, and 5×10^{13} ions-cm^{-2} at room temperature (RT) followed by thermal annealing at 300 ºC leads to the crystallization Ge. In another case, the crystallization behaviour of Si in Al/a-Si and Ni/c-Si bilayer systems is also investigated under low energy ion irradiation. İn case of low energy ion irradiation, the crystallization is achieved at room temperature.

References:

[1] G. Maity, R. Singhal, S. Dubey, S. Ojha, P.K. Kulriya, S. Dhar, T. Som, D. Kanjilal, Shiv P. Patel, Journal of Non-Crystalline Solids, 523 (2019) 119628.

[2] G. Maity, S. Dubey, Anter El-Azab, R. Singhal, S. Ojha, P. K. Kulriya, S. Dhar, T. Som, D. Kanjilale and Shiv P. Patel, *"*An assessment on crystallization phenomena of Si in Al/a-Si thin films via thermal annealing and ion irradiation*"*,RSC Advances, 10 (2020) 4414-4426.

[3] G. Maity, S. Ojha, S. Dubey, P. K. Kulriya, I. Sulania, S. Dhar, T. Som, D. Kanjilal and Shiv P. Patel, "Crystallization of Ge in ion-irradiated amorphous-Ge/Au thin films*"*,CrystEngComm 22 (2020) 666.

[4] G Maity, R Singhal, S Ojha, A Mishra, UB Singh, T Som, S Dhar, D Kanjilal, Shiv P. Patel, "Room temperature fabrication of poly-crystalline Si thin films via Al-induced crystallization under 500 keV Xe^{+} ion irradiation", J. Appl. Phys. 132 (9), (2022) 09.

Zero Field Splitting Parameters of Mn^{2+} Doped BCCD Single Crystal

Maroj Bharati[a*], Vikram Singh[a,] Ram Kripal[b]
[a] Department of Physics, Nehru Gram Bharti (DU), Jamunipur, Prayagraj, India
[b] EPR Laboratory, Department of Physics, University of Allahabad, Prayagraj-211002, India
** Corresponding author email id: marojbharati99@gmail.com*

The superposition model (SPM) has been used to find crystal field (CF) parameters of Mn^{2+} doped betaine calcium chloride dihydrate (BCCD) single crystals. The zero-field splitting (ZFS) parameters D and E are then estimated using perturbation theory. These parameters show good matching with the experimental values indicating thereby that the Mn^{2+} ion substitutes at Ca^{2+} site in BCCD single crystal. The CF energy levels of the Mn^{2+} ion determined by diagonalizing the complete Hamiltonian are in reasonable agreement with the experimental ones. The process used may be applied for the modelling of other ion-host systems to explore the applications of crystals in technology and industry.

Keywords: A. Inorganic compounds; A. Single Crystal; C. Crystal structure and symmetry; D. Crystal and ligand fields; D. Optical properties; E. Electron paramagnetic resonance.

References:

[1] Weil J A & Bolton J R (2007). Electron Paramagnetic Resonance: Elementary Theory and Practical Applications, 2nd ed., Wiley, New York.
[2] Kripal R, Misra M G, Yadav A K, Gnutek P, Açıkgöz M & Rudowicz C (2023). Theoretical Analysis of Crystal field Parameters and Zero field Splitting Parameters for Mn^{2+} ions in Tetramethylammonium Tetrachlorozincate, Polyhedron, 235,116341
[3] Rudowicz C& Misra S K (2001). Spin-Hamiltonian formalisms in electron magnetic resonance (EMR) and related spectroscopies. Appl. Spectrosc. Rev. 36,11–63.
[4] Rudowicz C (1987). Concept of spin Hamiltonian, forms of zero field splitting and electronic Zeeman Hamiltonians and relations between parameters used in EPR. A critical review. Magn. Reson. Rev. 13,1-89.

Analysis of Binary Mixture of Poly (Ethylene Glycol) 200 with Ethanolamine, m-Cresol and Aniline through Excess Parameters

Maimoona Yasmin[1], Abhishek Mishra[2], Laxmi Kumari[3], Ajaz Hussain[4] and Manisha Gupta[2]*
[1]Department of Physics, National PG College, Lucknow, 226001 India
[2]Department of Physics, University of Lucknow, Lucknow-226007 India
[3]Department of Physics, School of management sciences, Lucknow, India
[4]Department of Physics, Ewing Christian College, University of Allahabad, India
* *Corresponding author email id: guptagm@rediffmail.com, myasmin908@gmail.com*

Poly (ethylene glycols) are polymeric materials whose chain are composed of polymeric materials whose chain are composed of oxyethylene units and terminated by hydroxyl group at both ends. these are of industrial importance. The experimentally evaluated data of densities and ultrasonic velocities for the binary mixtures of PEG with ethanolamine, m-cresol and aniline has been used to calculate excess intermolecular free length, excess molar enthalpy and deviations in isentropic compressibility at 298.15 K. The variation of these parameters with respect to the change in concentration of polymer have been explained in terms of specific intermolecular and intramolecular interactions present in the mixture. The excess values of thermodynamic parameters are found to explain the interactions in each mixture.
Various models and mixing rules have been applied to evaluate the ultrasonic velocity data of the liquid mixtures under investigation and have been compared with the experimental results to test their applicability.

Keywords: Poly (ethylene glycol) 200, Ultrasonic velocity, Excess parameter, Hydrogen bonding

Thickness Dependent Evolution of Structural and Magnetic Properties of CoFeB Interfaced with Ru

Gagan Sharma[1, *], Mukul Gupta[2], V. R. Reddy[2], Ajay Gupta[3], Kavita Sharma[4], Harsh Vardhan[4], Yasmeen Jafri[4], Shubham Kumar[4]

[1] Department of Physics, University of Allahabad, Prayagraj, Utter Pradesh, 211002, India

[2] UGC-DAE Consortium for Scientific Research, University Campus, Khandwa Road, Indore-452001, India

3Department of Physics, University of Petroleum and Energy Studies, Dehradun-248007, India

[4] Amity Center for Spintronic Materials, Amity Institute of Applied Sciences, Amity University UP, Sector-125, Noida-201313, India

**Corresponding author email.id: gagansharma@allduniv.ac.in*

Viability of CoFeB as a magnetic material interfaced with 4d / 5d heavy metals gained considerable interest because of potential applications in spintronic devices accredited to modified functional properties [1, 2]. In this direction, CoFeB interfaced with Ru finds its key role in development of synthetic antiferromagnets in spin valve structures which reduces the critical current density [3]. However, the strength of interlayer coupling in such structures varies with the thickness of layer. Moreover, the presence of any interfacial dead layer at CoFeB / Ru interface would affect the strength of coupling and hence the performance of applicable device. This necessitates a detailed exploration of the evolution of properties of CoFeB i.e., magnetic and structural, while interfaced with Ru. In the present work, Ru / CoFeB (t) / Ru system has been studied for different thicknesses (t) of CoFeB. While the structural properties were investigated using X-ray measurements viz. X-ray reflectivity and Grazing incidence X ray Diffraction; the magnetic properties with increasing CoFeB thickness were studied using Magneto-Optical Kerr effect. Measurements were done at different points of the wedge structure at sub-nanometer thickness interval. Such evolution studies are also helpful to calculate the thickness of interfacial magnetic dead layer at CoFeB / Ru interface.

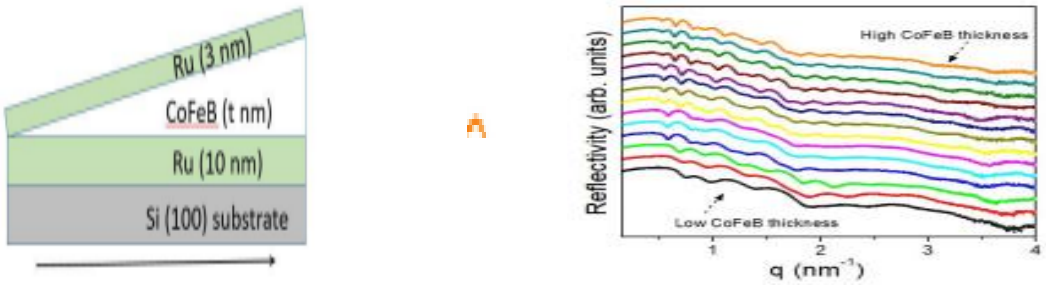

(a) **(b)**

Figure 1: (a) Schematic of wedge structure deposited using ion beam sputtering and (b) X-ray reflectivity data at different points of wedge structure

Keywords: Interface, XRR, MOKE, Dead layer

Reference:

[1] Hait S et al., (2021), Impact of ferromagnetic layer thickness on the spin pumping in Co60Fe20B20/Ta bilayer thin films, J. Mater. Sci. Mater. Electron. 32 12453–12465

[2] Herrera Diez L. et al., (2019), Enhancement of the Dzyaloshinskii-Moriya interaction and domain wall velocity through interface intermixing in Ta/CoFeB/MgO, Phys. Rev. B 99 054431

[3] Mouhoub A et al., (2023), Exchange energies in CoFeB/Ru/CoFeB synthetic antiferromagnets, Phys. Rev. Materials 07 044404

Tuning Electron Optics with Dirac Fermions in Presence of Magnetic Barriers in 2D Materials

*Neetu Agrawal and Triranjita Srivastava
Department of Physics, University of Allahabad, Prayagraj, Uttar Pradesh - 211002
**Corresponding author email id: neetu@allduniv.ac.in*

Dirac fermions arising from relativistic like behaviour of electrons in 2D materials viz. graphene, phosphorene, topological insulators exhibit remarkable characteristics including exhibiting the chiral dispersion. We investigate the ballistic transport for Dirac fermions in the presence of highly inhomogeneous magnetic field in combination with gate voltage induced electrostatic potential. The presence of electric and magnetic barriers substantially modifies the band structure near the Dirac point affecting the transport near the Dirac point significantly [1-3]. We emphasize particularly in understanding the analogy of such transport with propagation of light wave through medium with varying dielectric constant. We believe that our investigations provide insight with potential implications for future nano-electronic devices.

Keywords: 2D Materials, Electron Optics, Graphene, Phosphorene, Topological Insulators

References:

[1] S. Ghosh and M. Sharma, J. Phys. Cond. Matt. 21, 292204 (2009).
[2] M. Sharma and S. Ghosh, J. Phys. Cond. Matt. 23, 055501 (2011).
[3] N. Agrawal (Garg), S. Ghosh and M. Sharma, Int. Journal of Modern Physics B, 27, 1341003 (2013)

Modelling of 2-T Monolithic $MAPbI_3$-on-$CuInSe_2$ Tandem Solar Cells using SCAPS-1D

Vineet Kumar Singh[*1], Ajeet Kumar Singh[1], Shiv P. Patel[2], Madan Singh Chauhan[1]
[1]Department of Physics, DDU Gorakhpur University, Gorakhpur 273009, India
[2]Department of Pure & Applied Physics, Guru Ghasidas Vishwavidyalaya (A Central University), Bilaspur 495009, India
Corresponding author email id: vineetkumarsingh@gmail.com

Copper indium diselenide ($CuInSe_2$) is a promising candidate for photovoltaic applications because of its narrow bandgap of ~1.04 eV, higher absorption coefficient in the visible region, and non-toxic nature [1-3]. The narrow bandgap $CuInSe_2$ has the potential to produce a power conversion efficiency (PCE) of ~30% with the combination of the wide bandgap of methyl ammonium lead tri-iodide ($MAPbI_3$) in two-terminal (2-T) tandem solar cells (TSCs) [4]. The performance of the independent top and bottom sub-cells is explored by considering the physical parameters such as interface defects density, bulk defects density, and absorber layer thickness. In 2-T TSCs, both the sub-cells, the top sub-cell of wide bandgap and the bottom sub-cell of narrow bandgap, are integrated in series. Due to the series connection, an equal current generation by both the sub-cells are astringent criterion. The filtered spectra have been used to investigate the performance of 2-Tmonolithically integrated TSCs.

Keywords: $CuInSe_2$, $MAPbI_3$, Recombination, Tandem Solar Cell, Interface Defects

References:

[1] Regmi, G., Velumani, S., 2022. Impact of selenization temperature on the performance ofsequentially evaporated $CuInSe_2$thin film solar cells. Mater. Sci. Semicond. Process.137, 106215
[2] Feurer, T., Bissig, B., Weiss, T.P., Carron, R., Avancini, E., Lockinger, J., Buecheler, S.,Tiwari, A.N., 2018. Single-graded CIGS with narrow bandgap for tandem solar cells.Sci. Technol. Adv. Mater. 19, 263-270.
[3] Feurer, T., Carron, R., Torres Sevilla, G., Fu, F., Pisoni, S., Romanyuk, Y.E., Buecheler, S., Tiwari, A.N., 2019a. Efficiency Improvement of Near-Stoichiometric $CuInSe_2$ Solar Cells for Application in Tandem Devices. Adv. Energy Mater. 9, 1901428.
[4] Singh, A.K., Chauhan, M.S., Patel, S.P., Singh, R.S. and Singh, V.K., 2023. MAPbI3-on-CuInSe2 two-terminal monolithically integrated and four-terminal mechanically stacked tandem solar cells: A Theoretical Investigation Using SCAPS-1D. *Results in Optics*, *10*, p.100358.

Ab-initio Quantum Mechanical Determination of Photovoltaic Properties of AlSb and GaSb *p-n* Junction Solar Cell Structures

Ramesh Mamindla, and Manish K. Niranjan*
Department of Physics; Indian Institute of Technology, Hyderabad, TS, 502285, India
*Corresponding author email id: manish@phy.iith.ac.in

The semiconductors AlSb and GaSb have emerged, in recent years, as important candidates for photovoltaic applications due to their strong absorption coefficient and other photovoltaic properties. In this study, AlSb (GaSb) *p-n* junction based solar cell device parameters and properties are studied using density functional theory [1] and non-equilibrium Green function approach [2]. The effect of temperature on various solar cell parameters such as open-circuit voltage, and power conversion efficiency, photocurrent density, short-circuit current etc. is investigated using the special-thermal-displacement approach along with GGA-1/2 exchange correlation functional. As temperature increases, the phonons are found to significantly influence the charge carrier transport in the solar cell. The computed power conversion efficiency for AlSb is estimated as 12.31 % and 10.21 % at 0 K and 400 K, respectively. The obtained results strongly indicate that the electron-phonon coupling and resulting phonon-assisted photon absorption is necessary for accurate description and prediction of solar cell properties. The estimates obtained in this study may serve as first-principles parameters with possible use in continuum model based multiscale simulations of AlSb (GaSb) *p-n* homo-junction solar cells [3].

Keywords: Non-Equilibrium Green Function method, Density Functional Theory, Electron Phonon coupling, *p-n* junction solar cell, Photovoltaic properties

References:

[1] W. Kohn et al., Phys. Rev., 140, 4A, A1133 (1965)
[2] M. Brandbyge et al., Phys. Rev. B, 65, 16,165401, (2002)
[3] M. Ramesh et al., Physical Chemistry Chemical Physics, 24 (39), 24181 (2022)

Ab-initioStudy of Optical Properties of the Most Stable Zn_xTe_y(x + y = 2 to 4)Nanoclusters

Dheeraj Kumar Pandey[1], Anilesh[2] and P. S. Yadav[3]
[1]Department of Physics, R. B. College (A Constituent College of Lalit Narayan Mithila University, Darbhanga), Dalsingsarai, Samastipur, Bihar - 848114, India
[2]Department of Physics, R. N. A. R. College (A Constituent College of Lalit Narayan Mithila University, Darbhanga), Samastipur, Bihar - 848101, India
[3]Department of Physics, University of Allahabad, Prayagraj, Uttar Pradesh – 211002, India
Corresponding author email id: dheerajgkp85@mail.com

An ab initio study has been performed for the optical properties of the most stable Zn_xTe_y (x + y = 2 to 4) nanoclusters. A B3LYP-DFT/LANL2DZ methodis employed to optimize the geometries of ZnTe nanoclusters and a TDDFT method is used for the study of optical properties of the most stable structures of each configuration. The zero-point energy correction is also considered in this study. The structure having minimum energy in comparison to other structures for same values of "x" and "y" is considered as most stable. Some of the nanoclusters show at least one imaginary vibrational frequency, which results to their instability. The optical absorption is weak in visible region but is strong for the ultraviolet region in most of the nanoclusters except few. These investigations reveal that in most of the nanoclusters, the absorption is obtained in lower energy side in Zn-rich nanoclusters and in higher energy side in Te-rich nanocluster. The growth of most stable nanoclusters may be possible in the experiments.

Keywords: Nanoclusters, Zero Point Energy, Optical properties, TDDFT study.

Critical Behaviour of Magnetic Polymers on the three dimensional Sierpiński Gasket

Sumitra Rudra[1], Damien Paul Foster[2], Sanjay Kumar[1]*
[1]Department of Physics, Banaras Hindu University, Varanasi 221 005, India
[2]School of Computer Science and Digital Technologies, College of Engineering and Physical Sciences, Aston University, Birmingham BE4 7ET, UK
**Corresponding author email id: ksanjay@bhu.ac.in*

We present the exact phase diagram of a magnetic polymer on the Sierpińsky gasket embedded in three dimensions using the renormalization group method. We report distinct phases of the magnetic polymer, including paramagnetic swollen, ferromagnetic swollen, paramagnetic collapsed, and ferromagnetic collapsed states. By evaluating critical exponents associated with phase transitions, we located the phase boundaries between different phases. If the model is extended to include a four-site interaction which disfavors configurations with a single spin of a given type, we find a rich variety of critical behaviors. Notably, we uncovered a phenomenon of reentrance, where the system transitions from a paramagnetic collapsed state to a paramagnetic swollen state followed by another paramagnetic collapse state and ultimately reaching a ferromagnetic collapsed state. These findings shed new light on the complex behavior of (lattice) magnetic polymers.

References:

[1] D. P. Foster and D. Majumdar (2021). Critical behavior of magnetic polymers in two and three dimensions. Phys. Rev. E 104, 024122.
[2] T. A. Larsson (1985). Ising model on a 3d Sierpinski gasket with a non-trivial phase transition. J. Phys. A:Math. Gen. 18, L149-L152.

Brillouin Spectroscopy of Structural Phase Transition in Relaxor Ferroelectric $Pb(Sc_{0.5}Nb_{0.25}Ta_{0.25})O_3$

Venkatasubramanian Sivasubramanian
Condensed Matter Physics Division, Indira Gandhi Centre for Atomic Research, Kalpakkam-603102
Corresponding author e-mail id: shiva@igcar.gov.in

The cubic-rhombohedral structural phase transition in the relaxor ferroelectric $Pb(Sc_{0.5}Nb_{0.25}Ta_{0.25})O_3$single crystal have been studied by Brillouin spectroscopy. Brillouin light scattering measurements have been carried out in the back-scattering geometry in the temperature range 873 – 200 K. The frequency and the width of longitudinal acoustic (LA)phonon exhibits a pronounced anomaly in the vicinity of phase transition temperature T_{cr} = 283 K. The width of the LA phonon shows a typical λ type behaviour near T_{cr}. The observed anomalus behaviour of LA phonon near the phase transition region is discussed in terms of the coupling between strain and local polarization. The temperature dependence of the relaxation time calculated using the Landau-Khalatnikov relaxation mechanism reveals a critical slowing down towards the transition temperature T_{cr}.

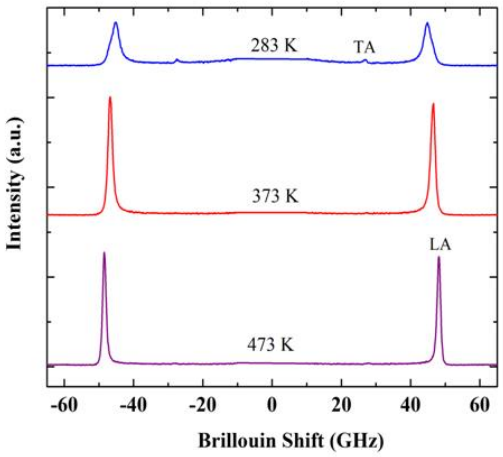

Brillouin spectra measured at various temperatures

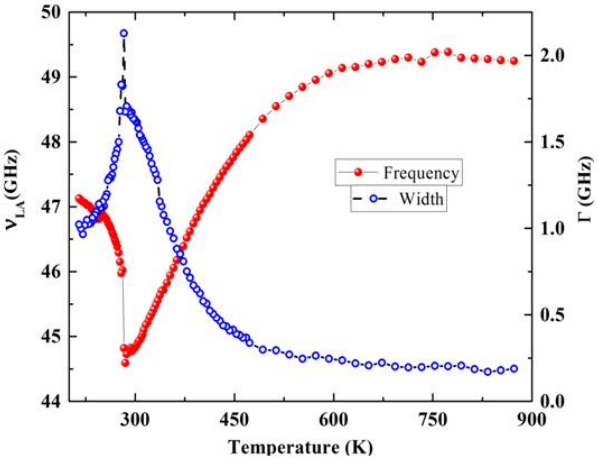

Temperature dependence of frequency and width of LA phonon

Keywords: Relaxor ferroelectrics, Brillouin scattering, Acoustic phonon, Relaxation

References:

[1] Ko J.-H. Kim D.H. and Kojima S. (2008) Central peak, acoustic modes, and the dynamics of polar nanoregions in $Pb[(Zn_{1/3}Nb_{2/3})_{1-x}Ti_x]O_3$ single crystals studied by Brillouin spectroscopy. *Phys. Rev. B* 77 104110.

[2] Ahart M. Hushur A. Ping Y. Ye Z.-G. Hemley R.J. and Kojima S. (2009) Critical slowing down of relaxation dynamics near the Curie temperature in the relaxor $Pb(Sc_{0.5}Nb_{0.5})O_3$. *Appl. Phys. Lett*. 94 142906.

Highly Sensitive Surface Plasmon Resonance Refractive Index Sensor Employing Photonic Crystal Fiber

Monika Goyal[1], Mohit Sharma[2]
[1]Department of Physics, Dronacharya Degree College, Kurukshetra - 136119, India
[2]Department of Physics, SLAS, Mody University of Science and Technology, Lakshmangarh, Rajasthan, India

This article presents a novel concept of surface plasmon resonance refractive index sensor utilizing a photonic crystal fiber and investigation fits optical properties. Gold (Au) is employed as the plasmonic material to generate excitation between the core and plasmonic mode. The aim of carrying out a sensitivity analysis is to examine the effects on loss depth and amplitude sensitivity. The influence of altering structural parameters, including pitch distance, air hole diameter, gold layer thickness, analyte layer thickness, and geometrical shapes of air hole, on sensing performance are investigated. The finite element method is used to facilitate the design and investigation of the influence of different geometric characteristics on the sensing performance of the sensor. The reported results yield to exhibit the high sensitivity with feasible fabrication process. This work exhibits potential as a viable option for swift, cost-effective detection and analysis of various biochemical, biological, chemical substances, and thorough optimization of structural parameters to ensure high levels of accuracy.

Keywords: Photonic crystal fiber, Surface plasmon resonance, Refractive index, Wavelength sensitivity, Amplitude sensitivity.

References:

[1] Kretchmann E, et al (1968). Radiative decay of non-radiative surface plasmon excited by light. Z. Naturforsch.A. Phys. Sci. 23, 2135–2136.
[2] Md. Islam S, et al (2018). Dual-polarized highly sensitive plasmonic sensor in the visible to near-IR spectrum. Optics Express 26(23), 30347.
[3] Momota M R and Md. Hasan R (2018). Hollow-core silver coated photonic crystal fiber plasmonic sensor. Optical Materials 76, 287-294.

Spectroscopic Study of ^{107}Sn

D. Sudip[1*], B. Bhardwaj[2*], M. Kumar Raju[1#], D. Negi[2#], T. Trivedi[3], A. Dhal[4], S. Kumar[5], V. Kumar[5], S. Roy[6], S. Appannababu[7], G. Mohanto[8], J. Kaur[9], R. K. Sinha[10], R. Kumar[11], R. P. Singh[11], S. Muralithar[11], A. K. Bhati[9], S. C. Pancholi[5,11], and R. K. Bhowmik[11]

[1]Department of Physics, GITAM School of Science, GITAM University, Visakhapatnam-530045, India
[2]Department of Physics, Manipal Institute of Technology,
Manipal Academy of Higher Education, Manipal 576104, India
[3]Department of Physics, University of Allahabad, Allahabad 211002
[4]Extreme Light Infrastructure (ELI-NP), Bucharest, Romania
[5]Department of Physics and Astrophysics, University of Delhi, Delhi 110007
[6]S.N. Bose National Centre for Basic Sciences, Block JD, Sector III, Kolkata 700098
[7]Department of Nuclear Physics, Andhra University, Visakhapatnam 530003
[8]Nuclear Physics Division, Bhabha Atomic Research Center (BARC), Mumbai
[9]Department of Physics, Punjab University, Chandigarh 160014
[10]Department of Physics, Banaras Hindu University, Varanasi 221005 and
[11]Inter University Accelerator Centre, Aruna Asaf Ali Marg, New Delhi – 110067
[#]*Corresponding author email id:kmukhi@gitam.edu, dinphysics@gmail.com*

The spectroscopic study of nuclei near N=Z=50 shell closures shed light on nuclear shell structures near the proton drip line. Nuclei with a limited number of valance nucleons compared to a ^{100}Sn core, offer a unique opportunity to investigate various structural phenomena, such as magnetic and anti-magnetic rotation, band termination, and the transition between collective and non-collective structures [1-4]. In the present work, we have investigated the level structure of odd-A ^{107}Sn (*Z=50, N=57*) through in-beam gamma-ray spectroscopy employing the fusion evaporation reaction ^{94}Mo(^{16}O, 3n)^{107}Sn at a beam energy of 70 MeV delivered by the 15UD Pelletron Accelerator at Inter-University Accelerator Centre (IUAC), New Delhi. The de-excited γ-rays from the reaction products were detected utilizing the Indian National Gamma Array (INGA) [5], equipped with seventeen Compton-suppressed Ge clover detectors at various angles relative to the beam axis. The γ-γcoincidence data were analyzed offline and constructed the level scheme of ^{107}Sn, aligning our findings with prior research. The known band structures have been reconfigured and expanded to encompass higher spin states by introducing over twenty new γ-ray transitions. Further analysis of DCO and polarization information is in progress to confirm the spins and parities of the observed gamma transitions, and complete level scheme information will be presented during the conference.

Acknowledgments
The authors gratefully acknowledge the financial support by DST for the INGA project (No.IR/S2/PF-03/2003-1). One of the authors (M. K. R) like to thank the financial support of SERB-SRG Grant (SRG/2022/001959) from DST. We also thank the IUAC pelletroncrewand INGA collaboration for making this experiment possible.

References:

[1] A. Gadea et al., Phys. Rev. C 55, 1 (1997).
[2] L. Kaubler et al., Z. Phys. A 356, 235-237(1996).
[3] M. Wolinska-Cichocka et al., Eur. Phys. J.A 24, 259{274 (2005)
[4] T. Ishii et al., Z. Phys. A 347, 4147 (1993).
[5] S. Muralithar et al., Nucl. Instrum. Methods. A 622, 1, 281-287 (2010)

Emission Properties of NSs Under the effect of Magnetic Field

Shubham Yadav, M. Mishra*, and Tapomoy Guha Sarkar
Department of Physics, Birla Institute of Technology & Science, Pilani, Pilani Campus
**Corresponding author email id: madhukar@pilani.bits-pilani.ac.in*

Astrophysical objects such as Neutron Stars, White Dwarfs, Black Hole etc. have long been considered as Laboratories for Physicists, especially those who are working in the area of Astrophysics, Astronomy and Cosmology. Question about the existence and properties of dark matter has been studied very extensively for the last a few years. The most of the work pertaining to this area of research lies under the Physics beyond Standard Model. The possibility of the dark matter to be made of several dark matter candidates have been explored in the past a few years, yet no firm statement cab be given regarding properties and nature of its constituents. The axion is considered an excellent cold dark matter candidate, originally proposed to solve the strong CP problem in strong interactions. A novel method to detect galactic/astrophysical axions was proposed a few years ago using their conversion to electromagnetic waves from boundaries between materials of different dielectric constants under a strong magnetic field. In this work, by assuming axions as a dark matter candidate, we attempt to find the impact of the magnetic field on its possible emission from the core and crust of the NSs by employing the modified TOV system of equations. We will also try to explore the possibility of explaining various observations related to the above-mentioned objects under the assumption of neutrino, photons and axion emission from the NSs.

Keywords: Neutron stars, Axions

References:

[1] Yadav S, Mishra M, Sarkar TG, and Singh CR. Thermal Evolution and Emission Properties of Strongly Magnetized Neutron Star. 2022. arXiv: 2212.11652.

Efficient THz Generation by Obliquely Incident Laser in Magnetized Plasma

Niti Kant*
Department of Physics,
University of Allahabad,
Prayagraj-211002, U.P., India.
**Corresponding author e-mail id: nitikant@yahoo.com*

Efficient Terahertz (THz) radiation generation by using two short pulse lasers of slightly different frequencies propagating in plasma with density ripple in the presence of static magnetic field has been studied. The p-polarized lasers propagating in x-z plane and incident obliquely to density ripple and exert ponderomotive force on electrons so that the plasma electrons start oscillating. This oscillatory velocity contributes with the density ripple to produce nonlinear current density which drives the THz generation in plasma. Efficiency of THz radiation can be enhanced by optimizing the magnetic field strength and laser parameters.

Key Words: Terahertz radiation, Plasma, Density ripple, obliquely incident lasers, Magnetic field

Amplification of Laser Pulses by the Stimulated Brillouin Back Scattering Mechanism in Plasma Channel

Updesh Verma[1,2],
[1]M.K.R Govt. Degree College, Ghaziabad, U.P., India.
[2]Princeton Plasma Physics Laboratory, Princeton University, Princeton, New Jersey, USA
Corresponding author e-mail: updeshiitd@gmail.com

A Theoretical model is developed to study the laser pulse amplification and compression by stimulated Brillouin scattering (SBS) in laser produces plasma channel. When a short pulse laser of pulse duration shorter than the ion response time impinges on a pre-ionized plasma it exerts a ponderomotive force on the electrons and expels them from the axial region of higher intensity to marginal regions. This forms a low-density region near the axis leaving behind an unbalanced space charge. The space charge electrostatic field $\vec{E}_s = -\vec{\nabla}\phi_s$, pulls the electrons back to the axis. In a time of the order of ω_p^{-1}, where $\omega_p^2 = n_0 e^2 / m\varepsilon_0$, a quasi-steady state is realized, when the ponderomotive potential balances the space charge potential and a steady state plasma channel with electron density minimum on the axis is formed. The amplification of laser pulses by plasmas is based on a coupling of three waves: two transverse electromagnetic waves and a longitudinal plasma response. The plasma response via ion-acoustic wave called Brillouin amplification. This process requires that the resonance condition for energy (frequency, ω) and momentum (wave-vector, k) is fulfilled. The laser pulse interacts with counter propagating seed laser pulse via stimulated Brillouin scattering. Exchange of energy takes places between the two lasers via stimulated Brillouin scattering process. The long pump gives energy to the short seed and seed amplified as well as compressed whereas the pump gets depleted after losing its energy. We observed the amplified laser pulses as the plasma waves become localized in the channel, hence increased the amplification. We have used parabolic profile of plasma to create the channel. SBS mechanism is preferred than Raman scattering mechanism as nearly all the energy is transferred from pump to seed, also pump and seed can be at the same frequency as interaction of the two laser takes places via ion acoustic wave, which have very low frequency. The theoretical results are compared with simulation results which are in good agreements.

References:

[1] V.M. Malkin, G. Shvets and N.J. Fisch, "Fast compression of laser beams to highly overcritical powers", Phys. Rev. Lett. 82, 4448 (1999). V.M. Malkin, Yu. A. Tsidulko, and N.J. Fisch, "Stimulated Raman Scattering of Rapidly Amplified Short Laser Pulses", Phys. Rev. Lett. 85, 4068 (2000).

[2] Y. Ping et al., "Amplification of ultrashort laser pulses by a resonant Raman scheme in a gas-jet plasma" Phys. Rev. Lett. 92, 175007 (2004).

[3] A.A. Andreev et al., "Short light pulse amplification and compression by stimulated Brillouin scattering in plasmas in the strong coupling regime" Phys.Plasmas 13, 053110 (2006).

[4] Ren, J., Cheng, W., Li, S. & Suckewer, S. "A new method for generating ultraintense and ultrashort laser pulses" Nature Physics 3, 732-736 (2007).

[5] P. Mardahl, H. J. Lee, G. Penn, J S Wurtele and N J Fisch, "Intense laser pulse amplification using Raman backscatter in plasma channels", Phys. Lett. A, 296, 109-116 (2002).

[6] C.-H. Pai, M.-W. Lin, L.-C. Ha, S.-T. Huang, Y.-C. Tsou, H.-H. Chu, J.-Y. Lin, J. Wang, and S.-Y. Chen, "Backward Raman Amplification in a Plasma Waveguide". Physical Review Letters 101 065005 (2008).

[7] A. Dunaevsky, A. Goltsov, J. Greenberg, E. Valeo, and N. J. Fisch, "Formation of laser plasma channels in a stationary gas". Physics of Plasmas 13 043106 (2006).

[8] V. B. Pathak and V. K. Triapthi, Phys. Plasmas 13, 082105 (2006) and N. Kumar, and V.K. Tripathi, Eur. Phys. J. D 32, 63 (2005).

Photonic Spin Hall Effect in Hybrid Plasmonic System

Triranjita Srivastava[1], Subrat Sahu[2], Rajan Jha[2] and Neetu Agrawal[1]
[1]Department of Physics, University of Allahabad, Prayagraj, 211002, India
[2]Nanophotonics and Plasmonics Laboratory, School of Basic Sciences, IIT Bhubaneswar, Khurda, 752050, India
Corresponding author email id: triranjita@allduniv.ac.in

The Photonic Spin Hall Effect (PSHE) of light attributes to the splitting of opposite spin photons perpendicular to the plane of incidence of the light beam, thereby giving rise to the Imbert–Fedorov (*IF*) shift [1]. It is spin-dependent transverse splitting of linearly polarized light into circular polarization, which has been considered as a promising candidate for high-precision measurement when combined with a weak measurement technique [2].The PSHE has been intensively studied and widely applied, especially in spin photonics in diverse nanophotonic structures such as metamaterials, multilayer dielectric films, and metal film-based plasmonic nanostructures.

Here, we propose hybrid plasmonic system, also known as Plexcitonic system comprising of metal (silver; Ag) and organic J-aggregate (TDBC). The proposed system takes the advantage of the combined effect of plasmons present in Ag and excitons present in J-aggregate. By the aforementioned effect, enhanced spin-orbit interaction takes place, which results in high *IF* shift ~ 73 μm. We believe that our investigations will provides an alternative method for the enhancement of PSHE, thus opening up opportunities for the design of various photonic devices based on PSHE.

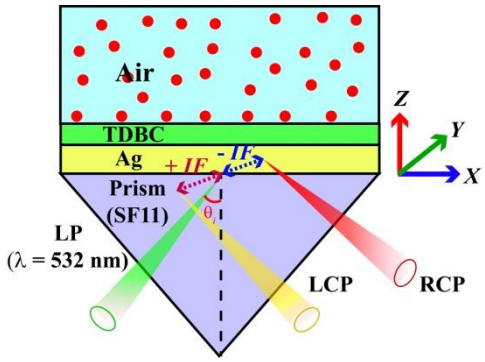

Fig. 1 Schematic of an optical structure with four layers as a Plexciton system with PSHE, where + *IF* and + *IF* are the transverse displacements of LCP and RCP components of light, respectively.

Keywords: PSHE, Weak Measurement, Imbert–Fedorov shift, Sensing

References:

[1] Q. Yue, X. Zhou, and D. Deng,(2023) "Goos–Hänchen and Imbert–Fedorov shifts of the Airy beam in dirac metamaterials," *New J. Phys.*, vol. 25, no. 1, p. 18001.
[2] T. Srivastava, S. Chitriv, S. Sahu, P. Gorai, and R. Jha,(2022) "Photonic spin Hall effect using hybrid Tamm plasmon polariton," *J. Appl. Phys.*, vol. 132, no. 20, p. 203103.

Role of PS Model to Understand the N-N Collision at Relativistic Energy with Emulsion Technology

U. Rawat[1], M. K. Singh*[1], M. Goyal[1], V. Singh[2]
[1]Department of Physics, IAH, GLA University, Mathura-281406, India
[2]Department of Physics, School of Physical and Chemical Sciences, Central University of South, Bihar, Gaya-824236, India
**Corresponding author email id:* manoj.singh@gla.ac.in

Using a modified version of the participant's spectator (PS) model, we will explained the idea of two regions with hot and cold temperatures and varying alpha projectile fragment emission probabilities in the manuscript [1,2]. We will explain and drive the mathematical expression of the total transverse momentum distribution. We will also cover the development of emulsion detector technology, classification of the numerous types of fragments that result from the interactivity of ^{84}Kr with emulsion at relativistic energy, and present automatic event scanning technologies [2-4]. This manuscript will cover the highlights on how emulsion technology is used to look for neutrinos in unusual instances [5]**.**

Keywords: RHIC, PS model, NED.

References:

[1] Singh M. K. et al., (2010). Characteristics of alpha projectile fragments emission in interaction of nuclei with emulsion. Indian J. Phys. 84, 1257-1273.

[2] Singh M. K. et al., (2020). Emission Characteristics of the grey particles produced in the interaction of the $^{84}_{36}$Kr with nuclear emulsion detector at 1 A GeV. Eur. Phys. J. Plus. 135, 740(1-8).

[3] Marimuthu N. et al., (2017). Analysis of Various Projectile Interactions with Nuclear Emulsion Detector Nuclei at ~1 GeV per Nucleon Using Coulomb Modified Glauber Model. Adv. High Energy Phys. 2017. 7907858(1-16).[4] Singh M. K. et al., (2009). Photographic Nuclear Emulsion Detector: Past, Present and Future. Jour. PAS.15, 166-175.[5] Andronic A. et al., (2005). Excitation function of elliptic flow in Au + Au collisions and the nuclear matter equation of state. Phys. Lett. B. 612, 173-180.

Two – Proton Radioactivity: A New Decay Mode of Exotic Nuclei

Shweta Prakash, Niti Maheshwari, Vimlesh Mishra
Ajay Kumar Garg Engineering College, 27thKm Stone, Delhi-Meerut Expressway,
Ghaziabad, Uttar Pradesh-201009, India
Email id: prakashshwet@akgec.ac.in, maheswariniti@akgec.ac.in, mishravimlesh@akgec.ac.in

The advancement in the experimental techniques has opened the path for the discovery of various exotic nuclei. These are found to lie beyond the stability line. If they lie more towards the proton number, they are proton-rich and if they lie more towards neutron number, they are neutron-rich exotic nuclei. The proton rich nuclei have been studied under various decay modes both experimentally and theoretically. Amongst them are alpha decay and proton emission decay modes. In the recent times, a new decay mode of proton rich nuclei has been detected. It is the two-proton radioactivity. In this paper, we have discussed about this decay mode of proton rich nuclei. We have studied the experimental techniques which have been used to discover these nuclei. We have also gone through various theoretical potential models and approaches which have been formed to study the two-proton radioactivity. It is found that the two-proton radioactivity gives very useful information about the low-lying proton energy states. It is expected that these decay modes would provide a better tool to test the existing potential models. The part which makes this decay mode different, is that two protons are being emitted. This pairing of protons can bring some concepts regarding the structure of the nucleus. It is therefore desirable that more and more of these exotic nuclei must be discovered, so that more theoretical studies can be done regarding the structure of the nucleus. Also, the study of two proton radioactivity would open new insights for dripline nuclei.

Keywords: Exotic, Decay modes, Proton-rich, Nucleus, Radioactivity

References:

[1] A. J. Leggett, “Nobel lecture: Superfluid 3He: the early days as seen by a theorist,” Rev. Mod. Phys. 76, 999–1011 (2004).
[2] B. Blank, M.J.G. Borge, Prog. Nucl. Part. Phys. 4560, 403 (2008) 190
[3] B.A. Brown, F.C. Barker, Phys. Rev. C 67, 041,304 (2003) 187, 188

Mini-review of direct detection of Dark matter

Venktesh Singh*
Department of Physics, Central University of South Bihar, Gaya
**Corresponding author email id: venktesh@cusb.ac.in*

Dark matter, an essential but enigmatic constituent of the universe, constitutes a significant portion of its mass-energy content. Unlike ordinary matter, it lacks electromagnetic interaction, rendering it optically invisible. Its existence is inferred from gravitational effects on visible matter and cosmic microwave background radiation. In the realm of modern astrophysics and particle physics, direct detection of dark matter is pivotal. This abstract presents mini review of experimental methodologies and recent advancements in direct dark matter detection. Techniques involving cryogenic, noble liquid, and scintillation detectors are scrutinized, elucidating their underlying principles and sensitivities. The challenges inherent in these experiments, including signal-background discrimination and characterization of potential dark matter candidates, are discussed. Recent experimental outcomes, encompassing null results and intriguing anomalies, are analyzed, illuminating the evolving landscape of direct dark matter detection. The abstract also underscores ongoing experimental initiatives and theoretical progress aimed at unraveling the mysteries of dark matter, emphasizing its critical role in advancing cosmic understanding and addressing profound inquiries in particle physics and cosmology.

Keywords: Dark Matter, Direct detection, Detector physics.

Investigation of Triaxiality in Nuclei form A~130 Mass Region

H. P. Sharma*, M. Anser, A. K. Rana, I. Sharma, A. K. Gupta, S. S. Tiwari†, S Chakraborty†, C. Majumdar†,
Banaras Hindu University, Varanasi 221005, INDIA
**Corresponding author email id: hpsharma_07@yahoo.com, †Current affiliation changed*

The phenomena of shape evolution are of major interest in nuclei and requires a proper understanding of the involvement of collective and single degree of freedoms. The in-beam γ-ray investigations are considered to be a tool to provide information on shapes in nuclei. The studies of properties of excited states leads to identification of shapes in nuclei. The orbitals near the Fermi surface play very important role in polarizing the core of the nuclei. Particularly, in the A~ 130 mass region, the presence of low-Ω unique parity $h_{11/2}$ orbitals near the proton Fermi surface and high-Ω $h_{11/2}$ orbitals near the neutron Fermi surface leads to prolate and oblate shape driving effects, respectively. This leads to tri-axial shape, measured with γ-deformation [1].

Transitional nuclei from the A~130 mass region, provide suitable ground for experimental and theoretical investigations for better understanding of the γ-degree of freedom (triaxiality). Further the role of single degree of freedom arises due to presence of the N~74 subshell closure makes the structure more complicated in these nuclei [1]. This gives rise to rich variety of structural phenomena, such as, unexpected signature splitting, signature inversion [2], wobbling motion [3], chirality [4], γ-vibration [5] and many more [6].

The observation of wobbling at low spin in ^{135}Pr and ^{187}Au was questioned by Bingfeng Lv and C. M. Petrache [7], which raises doubts regarding the nature of low spin wobbling and the effect of triaxiality at low spin. So, the investigation of band structures in this mass region is of utmost importance to understand the evolution of shapes.

Our group at BHU has been involved in the investigation of band structures of neutron rich isotopes of Iodine, Tellurium and Xenon nuclei from the A~130 mass region. The excited states of these nuclei were populated using fusion evaporation reactions with a suitable beam-target combinations. These investigations were carried out using the 15 UD Pelletron accelerator facility at the Inter-University Accelerator Centre (IUAC), New Delhi. The γ-rays from the excited nucleus were detected using the Indian National Gamma Array (INGA) which has most sophisticated clover detectors. The γ-γ-coincidence events were recorded by CAMAC-based data acquisition system [8]. Offline data analysis was carried out using INGASORT and RADWARE computer programmers [9].

Experiment 1: ^{7}Li was bombarded on ^{124}Sn target with E_{Beam} = 33MeV.

Experiment 2: ^{9}Be was bombarded on ^{122}Sn target with E_{Beam} = 48 MeV.

In the first experiment, high spin states of ^{127}I were populated [10]. In the second experiment, excited states of ^{124}Te [11], and ^{127}Xe [12, Signature splitting). In all these nuclei the signature of triaxiality were identified. The results of these experiments will be presented during the conference.

Keywords: Triaxiality, A~130, Fusion Evaporation Reaction, High Spin

References:

[1] I. Ragnarsson, et. al., Nucl. Phys. A233, 329 (1974); S. Frauendorf, et. al., Phys. Lett. B 125, 245 (1983)
[2] Li H J et al 2015 Phys. Rev. C 91 054314; Chen Y S et al 1983 Phys. Rev. C 28 2437; Bengtsson R et al 1984 Nucl. Phys. A 415 189
[3] Ødegård S W et al 2001 Phys. Rev. Lett. 86 5866; Frauendorf S and Dönau F 2014 Phys. Rev. C 89 014322; Matta J T et al 2015 Phys. Rev. Lett. 114 082501; Sensharma N et al 2019 Phys. Lett. B 792 170; Timár J et al 2019 Phys. Rev. Lett. 122 062501; Sensharma N et al 2020 Phys. Rev. Lett. 124 052501; Biswas S et al 2019 Eur. Phys. J. A 55 159; A. Mukherjee et al 2023 Phys. Rev C 107, 054310

[4] Grodner E et al 2006 Phys. Rev. Lett. 97 172501; Peng J et al 2003 Phys. Rev. C 68 044324;

[5] Wilets L and Jean M 1956 Phys. Rev. 102 788; Zamfir N V and Casten R F 1991 Phys. Lett. B 260 265

[6] Hayashi A et al 1984 Phys. Rev. Lett. 53 337

[7] Lv, B.; Petrache, C.M. 2023 Symmetry, 15, 1075

[8] Kumar B P A et al., DAE SNP 44B (2001)390.

[9] R Bhowmik et al., DAE SNP44B (2001)422; Radford D 1995 Nucl. Instru. and Methods in Physics Research Section 361 297–305. [10] S. Chakraborty, et al., (2020) JPG, 47, 095104; S. Chakraborty, et al., Eur. Phys. J. A (2018) 54: 112. [11] S.S. Tiwary et al., Eur. Phys. J. A (2019) 55: 163

[12] S. Chakraborty, et al., (2020), Physics Letters B, 811, 135854; S. Chakraborty, et al., (2018), Phys. Rev. C 97, 054311; S. Chakraborty, et al., (2020), Eur. Phys. J. A 56:50

Higher Flow Harmonics and Nuclear Modification Factor in pPb collisions (R_{pPb}) using Boltzmann Transport Equation at LHC Energies

Aviral Akhil, Aditya Kumar Singh, and Swatantra Kumar Tiwari∗
Department of Physics, University of Allahabad, Prayagraj- 211002, U.P

This paper presents an analysis of higher flow harmonics (v_3, v_4) in Pb-Pb collisions and the nuclear modification factor in p-Pb collisions (R_{pPb}) at the Large Hadron Collider (LHC) energies. We employ the Boltzmann transport equation in the relaxation time approximation, initializing our analysis with the Tsallis statistics for the initial distribution. We incorporate the Tsallis Blastwave (TBW) model to describe the evolution of the equilibrium distribution function governing particle production in the Boltzmann transport equation (BTE). Our study includes fitting of v_3, v_4 for identified hadrons, including pions, kaons, and protons, in Pb-Pb collisions at$\sqrt{s_{NN}} = 5.02TeV$, spanning various centrality categories. Additionally, we extend our analysis to fit the nuclear modification factor measured in p-Pb collisions, which includes $\pi^{\pm}, K^{\pm}, \ p + \overline{p}$ at an LHC energy of$\sqrt{s_{NN}} = 5.02TeV$, covering central to peripheral collision events. Our comprehensive approach successfully fits experimental data for higher flow harmonics up to p_T= 10 GeV/c. We have generated the R_{ppb} dataset by employing experimental data concerning the yields of $\pi^{\pm}, K^{\pm}, \ p + \overline{p}$ in p-Pb and p-p collisions [1]. Our analysis involved fitting the generated data up to p_T= 8 GeV/c, and the derived parameters are in strong alignment with hydrodynamic behaviour. The average transverse flow velocity exhibits a decline as we move from the most central to the peripheral collisions. The Tsallis parameters q_{AA} and q_{pp} increase as we transition from central to peripheral collisions, while the Tsallis temperature t_{ts} follows an opposing trend. These results indicate that the system approaches a state of closer equilibrium in central collisions compared to peripheral ones. Furthermore, we note a rising trend in azimuthal modulation amplitudes (ρ_a) for v_3, v_4as one transitions from central to peripheral collisions [2].

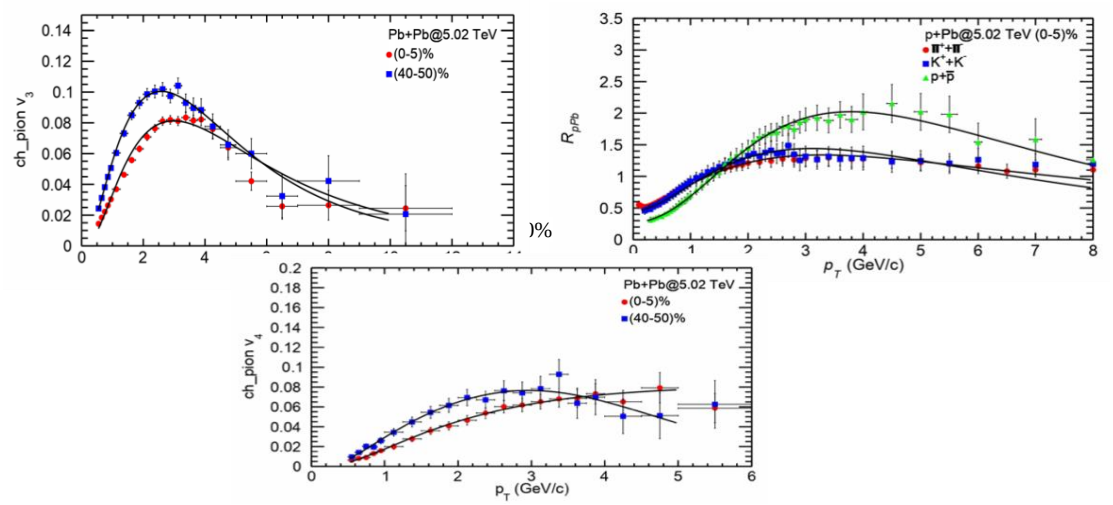

V_4 for pions at Pb-Pb collisions for the 0-5% and 40-50%

References

[1] A.~K.~Singh, A.~Akhil, S.~K.~Tiwari and P.~Pareek, arXiv:2309.17071 [nucl-th].
[2] A.~Akhil and S.~K.~Tiwari,arXiv:2309.06128 [hep-ph].

Exploration of Nuclear shape related phenomenon through gamma ray spectroscopy

T Trivedi[1*], S. Tiwari[1], A. Mukherjee[2], S, Bhattacharya[3]
[1]Department of Physics, University of Allahabad, Prayagraj-2110021
[2]Department of Pure and Applied Physics, Guru Ghasidas Vishwavidyalaya, Bilaspur-495009
[3]Amity Institute of Nuclear Science and Technology, Amity University UP, Noida-201313
*ttrivedi1@gmail.com

Nuclear shape and its associated phenomenon are distinctive aspects of nuclear structure studies. Nearly all the shape related phenomena such as shape coexistence, shape evolution, octupole correlations, etc are influenced by a favorable shell structure and the unique parity intruder orbitals near the Fermi energy. In particular, the nuclei lying mid-way between the closed shells at N or Z = 28 and 50 display various structural features due to the presence of competing shell gaps and unique parity $g_{9/2}$ intruder orbital. The availability of valence nucleons in the corresponding orbitals causes the interplay of single-particle and collective degrees of freedom leading to various interesting phenomena. Recently, we have studied the exotic structural properties like shape coexistence and octupole correlation in ^{72}Se and ^{73}Br using the Indian National Gamma Array Facility at New Delhi.

The aim of these studies is to have a better understanding of underlying phenomena by measuring the properties of quantum systems having a combination of protons and neutrons, by performing the detailed gamma ray spectroscopy of these nuclei. In this presentation, some of these interesting structural features will be discussed.

References:

[1] Mukherjee et al., (2022) Shape coexistence and octupole correlations in ^{72}Se, Phys Rev C. 105, 014322.
[2] S. Bhattacharya et al., (2022) Evidence for prolate-oblate shape coexistence in the odd-*A* ^{73}Br nucleus, Phys Rev C 106, 044312.

Optical Properties of N^+implanted TiO_2 Thin Films Synthesized by DC magnetron sputtering

Prashant Yadav[1, *], Beer Pal Singh[2]
[1]Janta Vedic College, Baraut (Baghpat)
[2] Department of Physics, Chaudhary Charan Singh University Meerut, Meerut, U. P., India. E-mail:
Corresponding author email id: prashantphy90@gmail.com

Titanium dioxide (TiO2) thin films were deposited onto highly cleaned soda lime glass substrates by DC magnetron sputtering system. Ti target, with purity of 99.99% was sputtered by argon gas in the sputtering chamber. Oxygen gas was introduced during the deposition process into the sputtering chamber for the formation of titanium dioxide. The structural, optical and chemical properties of thin films were characterized by X-ray diffraction (XRD), UV-Visible, Raman spectroscopy and FTIR spectroscopy. The optical properties of TiO2 thin films were studied with the effect of substrate temperature, sputtering power and nitrogen ion (N^+) implantation. The low energy ions beam (LEIB) was used for N^+-ions implantation in TiO2 thin films. The dose, 0.5×10^{15}, 1.0×10^{15} and 1.5×10^{15} ions/cm^{2}of N^+-ions were used respectively. The structural and optical properties of TiO2 thin films are the function of substrate temperature, sputtering power and N^+-ions dose. The optical bandgap (3.137-3.120 eV) shifted towards the higher wavelength. Functional studies showed Ti-O-Ti bond was observed between the band 750-900 cm^{-1}in both pristine and N^+-ions implanted TiO2 thin films.

Key words: TiO2 thin films, N^+-ions implantation, XRD, Raman and UV–Vis Spectroscopy, FTIR

References:

[1] M. Kalisz, M. Grobelny, M. Swiniarski, M. Mazur, D. Wojcieszak, M. Zdrojek, J. Judek, J. Domaradzki, Comparison of structural, mechanical and corrosion properties of thin TiO2/graphene hybrid systems formed on Ti-Al-V alloys in biomedical applications, Surf. Coat. Technol. 290 (2016) 124-134.

[2] Ayse V. Keskin, MetinGencten, SinemBozar, Melih B. Arvas, SerapGunes, YucelSahin, Preparation of anatase form of TiO2 thin film at room temperature byelectrochemical method as an alternative electron transport layer forinverted type organic solar cells, Thin Solid Films 706 (2020) 138093.

[3] Lijiang Tian, Liang Xing, Xiaoling Shen, Qinghui Li, Sijie Ge, Bingkun Liu, Li Jie,Visible lightenhanced Fe–I–TiO2 photocatalysts for the degradation ofgaseous benzene, Atmospheric Pollution Research 11 (2020) 179–185.

[4] Daniel Fabian Rodriguez, Patricia Maria Perillo, Marcela Patricia Barrera, High performance TiO2 nanotubes antireflection coating, Materials Science in Semiconductor Processing 71 (2017) 427–432.

[5] Prateek Bindra, Arnab Hazra, Selective detection of organic vapors using TiO2 nanotubes based singlesensor at room temperature, Sensors & Actuators: B. Chemical 290 (2019) 684–690.

[6] Hannelore Peeters, Maarten Keulemans, Gert Nuyts, Frederik Vanmeert, Chen Lic,Matthias Minjauw, Christophe Detavernier, Sara Bals, Silvia Lenaerts,Sammy W. Verbruggen, Plasmonic gold-embedded TiO2 thin films as photocatalytic self-cleaningcoatings, Applied Catalysis B: Environmental 267 (2020) 118654

Modifications in Structural and Optical properties of Zirconia-ceria Nanocomposites through Composition

Saruchi Rani, Sushil Kumar*
Department of Physics, Chaudhary Devi Lal University, Sirsa-125 055, Haryana, India.
**Corresponding author email.id: Presenting author E-mail: sushil.phys@gmail.com*

A series of $Zr_xCe_{1-x}O_2$ nanocomposites powders/thin films with different compositions (x=0.00, 0.25, 0.50 and 0.75) were synthesized by sol-gel protocol followed by spin coating technique using ammonium cerium nitrate $(NH_4)_2Ce(NO_3)_6$and zirconium oxychloride $ZrOCl_2 \cdot 8H_2O$ (procured from Merck) as precursors. Further, as prepared nano powders were annealed at 800^oC for 3h in a programmable furnace. Structural properties of $Zr_xCe_{1-x}O_2$ nanocomposites were investigated by X-ray diffraction (XRD) and Fourier transform infrared spectroscopy (FTIR). XRD and FTIR studies indicated that the prepared nanocomposites possessed a cubic CeO_2 phase. Optical properties of $Zr_xCe_{1-x}O_2$ nanocomposites were examined through UV-visible absorption spectroscopy and photoluminescence spectroscopy. Absorption spectra showed the blue shifting of absorption peaks on increasing concentration of Zr^{4+} ions into Ce^{4+} lattice. PL spectra exhibited the suppression of blue emission on increasing zirconia content in the nanocomposites. CIE and CCT coordinates indicated that the prepared nanocomposites have potential for applications in display devices.

Keywords: Zirconia-ceria nanocomposites, Sol-gel protocol, Structural parameters, Optical band gap, Chromaticity.

Study of Laser-induced Heterogeneous Colliding Titanium and Copper plasmas for the Formation of $CuTiO_2$ Nano-composites.

Pramod Kumar Pandey[1]and Ravi Pratap Singh[2]and John T Costello[3]
[1]Symbiosis Institute of Technology, Nagpur Campus, Symbiosis International (Deemed University), Pune, India
[2] Applied Science Department, Rajkiya Engineering College Subhadra
[3]School of Physical Sciences and National Centre for Plasma Science and Technology, Dublin City University, Dublin 9, Ireland
Corresponding author email id: anditpkp@gmail.com,ravipratap.physics@gmail.com

Present work shows the effectiveness of the colliding plasma deposition technique in producing nano-crystalline copper-titanium dioxide (Cu-TiO_2) nanocomposites. This material has garnered considerable attention due to its wide-ranging applications, including light-to electrical energy conversion, energy storage, and photo-catalysis. The colliding plasma deposition technique offers a multitude of advantages. It is a straightforward and versatile method that can be utilized not only for Cu-TiO_2 but also for various other nanocomposites. One of its key benefits is the elimination of the need for material preparation before deposition, making it a more convenient choice. Our study involved creating interactions among plasma species containing copper and titanium. Through this process, we gained valuable insights into the formation and characteristics of Cu-TiO_2 nanoparticles.

The structural morphology of the resulting nano-composites is notably influenced by the dynamics of plasma plume expansion and the interactions of plasma species with the surrounding gas. These interactions encompass not only collisions with the ambient gas but also collisions with other plasma plumes, which have been observed to play a pivotal role in the formation of nano-crystalline materials.

Keywords: Nano-composites, Colliding plasma, Spectroscopy, Laser ablated plasma

Reference:

[1] P.K. Pandey, R.K. Thareja, R.P. Singh, J.T. Costello, Deposition of nanocomposite Cu–TiO2 using heterogeneous colliding plasmas, Appl. Phys. B. 124 (2018) 50.
[2]. P.K. Pandey, R.K. Thareja, J.T. Costello, Heterogeneous (Cu-Ti) colliding plasma dynamics. *Phys. Plasmas* 23, 103516 (2016)

Nanomaterials: Recent Advances for Hydrogen Production and Hydrogen Storage

Thakur Prasad Yadav*
Department of Physics, Faculty of Science,
University of Allahabad, Prayagraj- 211 002, India
**Corresponding author email id: tpyadav@allduniv.ac.in*

The world is undergoing an energy crisis as a result of the limitation of fossil resources. It necessitates prompt attention in terms of availability and resolving energy demand by utilizing more efficient or clean alternative energy sources. Because of their astonishing properties and simplicity of production, nanomaterials such as nanopartials, nanotubes, and 2D materials are among the most important materials today and may be used as a catalyst for energy generation and storage. Hydrogen energy has been identified as the most energy dense clean and sustainable energy source. Now, the transport sector accounts for 25% of total energy demand, whereas it accounts for 20% of world greenhouse gas emissions. In automobiles, hydrogen can be used as a fuel for fuel cell vehicles or as a hydrogen system in internal combustion engine vehicles. In both scenarios, hydrogen storage is a critical factor. Temperature, hydrogen plateau pressure, and hydrogen storage capacity, as well as other key hydrogenation properties, vary widely among different types of hydrogen storage materials. Now, there is no one hydrogen storage material that can meet all the requirements of hydrogen storage for vehicle applications. Because quasicrystals are complex materials with distinct properties, they can be employed as a catalyst for hydrogen production. [1-3]. We developed a basic model of a catalyst with a two-dimensional layer of nanoparticles on quasicrystalline surfaces using leaching approaches. The high symmetry surfaces of single grain icosahedral (i)-Al-Cu-Fe and decagonal (d) Al-Ni-Co, (d)Al-Cu-Co quasicrystals and a polygrain (i)-Al-Pd-Re, (i)-Al-Cu-Fe, and (i)-Al-Pd-Mn quasicrystal with random surface orientation were leached with NaOH solution at varying times and the resulting surfaces were characterized by scanning electron microscopy, energy dispersive x-ray analysis and x-ray photoelectron spectroscopy. The leaching methods removed Al preferentially while producing nano-particles of transition metals and their oxides. The nano-particles were precipitated on the leached fivefold surface of i-Al-Cu-Fe, which had micron-sized dodecahedral voids. On the tenfold surface of d-Al-Ni-Co and the polygraini-Al-Pd-Re, no distinctive microstructure was detected. After polishing the leached layer, the quasicrystalline surface was restored, showing that leaching occurred only at a shallow depth from the surface. The leached as-grown and mechanically activated Al-Cu-Fe layer material was used as a catalyst in MgH_2 hydrogen storage materials [4]. The leached alloy's catalytic effect on de/rehydrogenenation properties will be discussed. The utilization of 2D nanomaterials for hydrogen generation will be thoroughly examined, with emphasis on how their extraordinary features can improve the efficiency of hydrogen production and storage.

Keywords: Physics of Materials; Nanomaterials; Quasicrystalline materials; 2D nanomaterials

References:

[1] Yadav et al., *Advanced Functional Materials* 28 (26) (2018)1801181.
[2] Yadav et al., *ACS Nano* 14 (6) (2020) 7435-7443.
[3] Mishra et al., International Journal of Hydrogen Energy 45 (2020) 24491-24501
[4] Verma et al., International Journal of Hydrogen Energy 48 (2023) 9762-9775.

Palladium Doped Zinc Oxide Nanorods for Nitrogen Dioxide Gas Detection

Yogendra K. Gautam* Durvesh Gautam
Smart Materials and Sensor Laboratory, Department of Physics, CCS University Campus
Meerut, Uttar Pradesh, 250004, India
Corresponding author Email: ykg.iitr@gmail.com

The high concentration of nitrogen dioxide (NO_2) makes it one of the most popular and harmful air pollutants. Therefore, it is required to monitor air quality precisely by using efficient and selective NO_2 gas sensors. In this work, Palladium-doped zinc oxide (Pd-ZnO) nanorods were synthesized with different Pd doping concentrations (0-1wt%) via a chemical hydrothermal method. The Pd-ZnO nanorods were characterized by XRD, FESEM, and XPS for their structural, morphological properties and chemical composition of the samples, respectively. The Pd (1wt%)-ZnO nanorods-based sensor shows good response with fast response/recovery time of 67s/118s for 100 ppm $NO_2$and 80s/145s for 1 ppm NO_2, at 200 °C. The sensor is found very selective towards NO_2 gas in comparison to carbon monoxide (CO), ammonia (NH_3), and hydrogen (H_2). The sensor presents strong stability for a longer time in a dry and humid environment.

Keywords: ZnO Nanorods, Gas sensor, NO_2 Gas, Palladium.

Advanced Lightweight and Flexible Nanocomposites for High-Performance Electromagnetic Interference Shielding and Microwave Absorption Application

Anju, Vanamoorthy Mariappan, Nithiya Hanna Wilson, Milan Masař, Michal Machovský, Michal Urbánek, Pavol Šuly, Barbora Hanulíková, Jarmila Vilčáková, Ivo Kuřitkaand Raghvendra Singh Yadav*
Centre of Polymer Systems, University Institute, Tomas Bata University in Zlín, Trida Tomase Bati 5678, 76001 Zlín, Czech Republic
**Correspondence: yadav@utb.cz; raghvendra.zlin@gmail.com; Tel.: +420576031725*

High-performance electromagnetic interference (EMI) shielding and microwave absorption materials are being investigated for mitigating significant radiation pollution as wearable electronics and wireless communications become more widespread [1]. A material for a microwave absorber and EMI shield should be able to attenuate and absorb incident EM waves by having balanced impedance matching and dielectric and magnetic loss properties. Researchers have paid a lot of attention to lightweight and flexible polymer nanocomposites as EMI shielding materials because of their many additional benefits, including corrosion protection, large-area manufacturing, low cost, etc. The development of high-performance shielding materials can produce amazing outcomes using polymer nanocomposites with dielectric and magnetic fillers [2]. The magnetic-dielectric properties of the spinel ferrite nanoparticles and the graphite/graphene/MXene based nanocomposite work in concert to produce remarkable EMI shielding and microwave absorption capabilities [3]. A number of factors, including dipole and interfacial polarization, conduction loss, multiple scattering, the eddy current effect, natural resonance, a high attenuation constant, and impedance matching, contribute to the high-performance electromagnetic interference shielding properties of developed nanocomposites [4]. This research offers a useful method for creating materials that are high-performance, lightweight, and flexible for EMI shielding and microwave absorption. The thin, lightweight, and flexible nanocomposite is a perfect contender for real-world uses in satellites, telecommunications, airplanes, and radar stealth.

Keywords: Nanocomposite, Electromagnetic Interference Shielding, Microwave Absorption, Two-dimensional Nanostructures, Spinel Ferrite

References:

[1] Yadav R S, Kuřitka I, Vilčáková J, (2021) Advanced Spinel Ferrite Nanocomposites for Electromagnetic Interference Shielding Applications, Elsevier Publishing, ISBN978-0-12-821290-5.
[2] YadavR S, KuřitkaI, VilcakovaJ, SkodaD, UrbánekP, MachovskyM, MasařM, Kalian, HavlicaJ, (2019). Lightweight $NiFe_2O_4$-Reduced Graphene Oxide-Elastomer Nanocomposite flexible sheet for electromagnetic interference shielding application, Composites Part B 166, 95–11.
[3] Anju, YadavR S, PötschkeP, PionteckJ, KrauseB, KuritkaI, VilcakovaJ, SkodaD, UrbánekP, MachovskyM, MasarM, Urbane, JurcaM, Kalina, HavlicaJ, (2021). High-Performance, Lightweight, and Flexible Thermoplastic Polyurethane Nanocomposites with Zn^{2+}-Substituted $CoFe_2O_4$Nanoparticles and Reduced Graphene Oxide as Shielding Materials against Electromagnetic Pollution, ACS Omega 6, 28098−28118.
[4] Skoda, VilcakovaJ, YadavR S, HanulikovaB, CapkovaT, JurcaM, UrbanekM, MachacP, SimonikovaL, AntosJ, KuritkaI, (2023). Nickel nanoparticle–decorated reduced graphene oxide via one-step microwave-assisted synthesis and its lightweight and flexible composite with Polystyrene-block-poly(ethylene-ran-butylene) -block-polystyrene polymer for electromagnetic wave shielding application, Advanced Composites and Hybrid Materials 6, 113.

Effect of Dispersion on Electrical Properties of Carbon Nanotubes-Polymer Composites

Kalpana Awasthi*
Department of Physics, K.N. Govt. P.G. College, Gyanpur, Bhadohi (UP), INDIA
**Corresponding author email.id: awasthi.k@gmail.com*

The carbon nanotubes (CNTs) have excellent mechanical, thermal, chemical and electrical properties, and are used as highly functional fillers in nanocomposites based on polymer [1-2]. Due to these superior properties, CNTs-polymer composites represent advanced materials and have variety of applications in electromagnetic shielding, antistatic coatings, lightweight energy storage etc. In the polymer nanocomposites, CNTs are dispersed in the polymeric matrix. The dispersion of CNTs in polymer influence the conductivity and mechanical properties of nanocomposites [3-4]. However, use of CNTs reinforcements in polymer composites has been a challenge because of the difficulties in the processing conditions to achieve good dispersion. The CNTs tends to form clusters and bundles due to strong van der Waals' forces of attraction and affect the properties of nanocomposite. In order to optimally utilize the CNTs as are inforcing component in the polymer matrix, some special treatments of CNTs, such as physical or chemical treatments are used to achieve better CNT dispersion and good interface between CNTs and polymer matrix. In the present study, the multiwalled CNTs (MWCNTs) - polyethylene oxide (PEO) composite films were prepared by solution cast technique. The as prepared composite samples were characterized by X-ray diffraction (XRD), scanning and transmission electron microscopy techniques. A comparative study has been made on the electrical property of these MWCNTs-PEO composites with different MWNTs loadings and results will be presented. It has been found that the ball milling of MWCNTs improves the dispersion of MWNTs into the polymer matrix.

Keywords: Carbon nanotube, Polyethylene oxide, Nanocomposite, Dispersion, Electrical conductivity

References:

[1] AjayanPM (1999). Nanotubes from carbon. Chem. Rev., 99,1787-1800.

[2] Onartuzumab M and Winey KI (2006). Review Polymer Nanocomposites Containing Carbon Nanotubes. Macromolecules, 39, 5194-5205.

[3] Mi D, Zhao Z and Bai H (2023). Effects of Orientation and Dispersion on Electrical Conductivity and Mechanical Properties of Carbon Nanotube/Polypropylene Composite. Polymers, 15, 2370.

[4] Awasthi S, Awasthi K, Kumar Rand Srivastava ON (2009). Functionalization Effects on the Electrical Properties of Multi-Walled Carbon Nanotube-Polyacrylamide Composites. J. Nanosci. Nanotechnol. 9, 5455-5460.

Highly Efficient Co and Zn Doped SnO Hybrid Nanocatalyst for Hydrogen Evaluation Reaction

Bishnu K Pandey*
Shyama Prashad Mukherjee Government PG College, University of Allahabad
**Corresponding author email id: bishnu.pandey750@gmail.com*

Highly efficient and Pt-free electrocatalysts for hydrogen evaluation reactions (HER) are considered a great challenge for carbon dioxide-free energy as well as sustainable development. Platinum-based catalysts are not appropriate for commercialization for hydrogen evaluation technologies due to their high cast. In this work, we have developed highly active and stable nano-electrocatalysts based on cobalt and zinc-doped tin oxide using hydrothermal techniques. X-ray diffraction and Raman spectroscopy were performed for the characterization of the synthesized nanocatalyst. Scanning electron microscopic studies were performed for particle size measurement. Further, electrochemical measurements were performed for hydrogen and oxygen evaluation reactions.

Key word: Nanocatalyst, HER, OER, Hydrogen energy, Hybrid catalyst

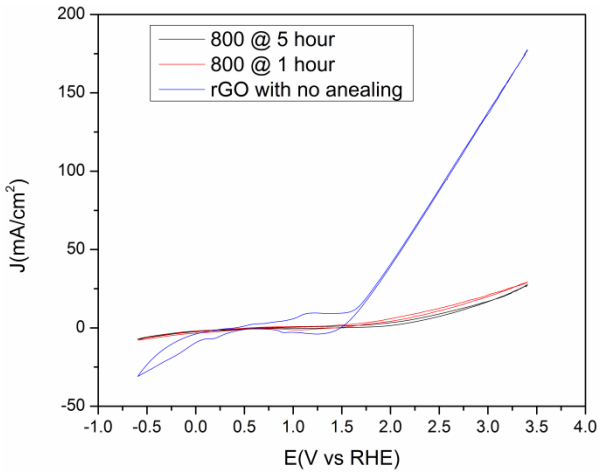

Fig. 1: HER and OER at different annealing temperature.

One-pot Synthesis of Binary Nickel ferrite -reduced Graphene Oxide Nanocomposite as Stable and High-performance Supercapacitor Electrode Material

G K Gupta, and Amit Srivastava
Department of Physics, TDPG College, VBS Purvanchal University, Jaunpur-222001, India

In the present study, we have successfully used an integrative approach to fabricate a three-dimensional hierarchical electrode material constructed by $NiFe_2O_4$/rGO nanostructure via a facile hydrothermal method and subsequently studied its electrocapacitive performances. The structural and morphological characteristics of as-synthesized $NiFe_2O_4$/rGO nanostructure have been characterized by X-ray diffraction (XRD), Raman spectroscopy, Transmission electron microscopy (TEM), Scanning electron microscopy (SEM) and X-ray photospectrometer (XPS). The electrocapacitive performances of the as-synthesized sample have been evaluated by galvanostatic charge-discharge (GCD), cyclic voltammetry (CV) and electrochemical impedance spectroscopy (EIS) using a three-electrode system with 3 M KOH electrolyte solution. As-prepared hierarchical electrode material exhibits specific capacity ~ 362.46 Fg^{-1} at a current density of 0.65 Ag^{-1}, suggesting good rate capability. $NiFe_2O_4$/rGO nanostructure electrode material exhibits a significant high energy…. and power density as…, respectively. Furthermore, the as-synthesized nanocomposite harvests a superior cycling stability over 2000 cycles without obvious capacitance attenuation. The $NiFe_2O_4$/rGO provides rapid pathways for electron transfer and diminish the ion diffusion routes due to $NiFe_2O_4$ over rGO sheets, which ultimately results in exceptional electrochemical properties. Henceforth, the unique morphological features, outstanding conductivity & favourable cyclic stability render $NiFe_2O_4$/rGO nanocomposite as a promising and prospective advanced electrode material for supercapacitor in the field of energy storage-conversion application.

EIS and Electrochemical Analysis of Plasticized Bio-polymer Electrolyte Membranes for EDLC Applications

A. L. Saroj*
Department Physics, Institute of Science, Banaras Hindu University, Varanasi (U.P.), India
Corresponding author email id: saroj@bhu.ac.in

Potential applications of bio-polymer based solid electrolytes in electrochemical devices have attracted considerable attention worldwide in the past few years. A super capacitor, formerly referred to as an electrochemical double layer capacitor (EDLC), is one of the most important devices, along with fuel cells and secondary batteries. Electrochemical impedance spectroscopic (EIS) technique is very versatile tool to understand the dielectric relaxation and capacitive behavior of the polymeric system. The potential applications of solid electrolytes based on biopolymers have attracted a lot of attention recently on a global scale. Polymers that possess a high degree of film-forming ability and the ability to build a stable network for the transportation of charge carriers are polymers like polyvinyl alcohol (PVA) and chitosan (CS), a polysaccharide having glucosamine and N-acetyl glucosamine units and many polar functional groups, including NH2, O-H, and C-O-C. This work investigates the effects of NaI on the ion transport mechanism and dielectric properties of plasticized bio-polymer electrolyte (BPE) films based on polyvinyl alcohol (PVA) and/or chitosan (CS) and ionic liquid (IL). The films that are based on CS/ and/or PVA-PEG/IL-NaI were made using the solution cast technique. Investigations into AC conductivity, dielectric properties, electric modulus analysis, and scaling have been carried out in order to comprehend the ion transport mechanism for developed IL-based BPBE films. The interactions between metal ions (Na+) and the functional groups of CS and/or PVA in the presence of plasticizers (IL/PEG) make the materials under research extremely desirable from the standpoint of device application. Measurements of CV and LSV were conducted in order to establish the electrochemical stability window. The properties of the ion species involved in conduction have also been studied by measurements of the ionic transference number. For the creation of the EDLC, an optimized sample with high conductivity was utilized. With the use of a CH instrument, the performance of the created EDLC was examined in terms of power density, specific capacitance, and Galvanostatic charge-discharge.

Keywords: Bio-polymer, EDLC, AC conductivity, XRD, FTIR, GCD, LSV and CV

Study of Anisotropy Superconducting properties of FeT_xSe (T: Fe, Cr) and $FeSe_{0.5}Te_{0.5}$ single Crystals via Electrical Transport Measurements

Anil K. Yadav[a,b*], Veg Singh Bhatt[a], Ajay D. Thakur[c], C. V. Tomy[b]
[a]Department of Physics, Ch. Charan Singh University Meerut, UP 250004, India
[b]Department of Physics, Indian Institute of Technology Bombay, Mumbai 400076, India
[c]School of Basic Sciences, Indian Institute of Technology Patna, Patna 800013, India
**Corresponding author email id: anilphy@ccsuniversity.ac.in*

Among all discovered Fe-based superconducting compounds, the Fe-11 system has drawn much attention of the research community due to its simple composition and crystal structure [1,2]. Anisotropy is important parameter of layered superconductors that exhibit in direction dependent superconducting properties. We report anisotropy of FeT_xSe (T: Fe, Cr) and optimal superconductor, $FeSe_{0.5}Te_{0.5}$single crystals of Fe-11 system via angle dependent resistivity measurements in superconducting state. Both doped single crystals consist two symmetric dips in resistivity in contrast to single dip in optimal superconductor. Quantitative Anisotropy, quantitative determined from angle dependent resistivity measurements as well from conventional method. Both measurements confirm isotropic nature of doped single crystals as compare to optimal superconductor which shows anisotropy.

Keywords: Fe-superconductor, Single crystals, Angular measurements, Anisotropy

References:

[1] S. Margadonna, Y. Takabayashi, M. T. McDonald, K. Kasperkiewicz, Y. Mizuguchi, Y. Takano, A. N. Fitch, E. Suarde and K. Prassides, "Crystal structure of the new $FeSe_{1-x}$ superconductor" Chem. Commun. issue 43 (2008) 5607. DOI: https://doi.org/10.1039/B813076K.

[2] A. Subedi, L. Zhang, D. J. Singh, and M. H. Du, "Density functional study of FeS, FeSe, and FeTe: Electronic structure, magnetism, phonons, and superconductivity", Phys. Rev. B 78 (2008)134514. DOI: https://doi.org/10.1103/PhysRevB.78.134514.

Z- scheme Based Photoactive$ZnO:TiO_2:CdO:g\text{-}C_3N_4$ Nanocomposites for Advance Oxidation Process

Gaurav K. Upadhyay[a, b, c*], Himani Sharma[b], Virpal Singh[d], Pramendra Kumar[e], Rudraman[f], L.P. Purohit[a*]

[a]Semiconductor Research Lab, Department of Physics, Gurukula Kangri (Deemed to be University), Haridwar, India

[b]Department of Physics, Doon University (A State University), Dehradun, India

[c]Department of Physics, Constituent Government Degree College, Bhadpura, Nawabganj Bareilly, MJPRU, Bareilly, India

[d]Department of Chemistry, Constituent Government Degree College, Bhadpura, Nawabganj Bareilly, MJPRU, Bareilly, India

[e]Department of Chemistry, Mahatma Jyotiba Phule Rohilkhand University, Bareilly

[f]Department of Mathematics, Constituent Government Degree College, Bhadpura, Nawabganj Bareilly, MJPRU, Bareilly, India

**Corresponding author E-mail: gauravphd123@gmail.com, proflppurohitphys@gmail.com*

In the present work, metal oxides [$(ZnO_{0.40}:_{0.60}TiO_2):CdO_{1.00}$] and z-scheme-based non-metal $g\text{-}C_3N_4$ nanocomposites were synthesized by sol-gel precipitation method and thermal polycondensation method, respectively. The synthesized quandary [$(ZnO_{0.40}:_{0.60}TiO_2):CdO_{1.00}$]:[$g\text{-}C_3N_4$] nanocomposites were used for the advanced oxidation process under visible illumination. The surface morphology was confirmed by FE-SEM, and morphology varied from compact crystal-like structure to mesoporous to compact sheet-type structure for samples ZTCG0 to ZTCG4. XRD patterns revealed that polycrystallinity was observed for all samples except $g\text{-}C_3N_4$. Moreover, $g\text{-}C_3N_4$ interacts with Zn^{+2} and Cd^{+2} extensively while not for Ti^{+4} resulting in significant changes observed in the lattice site of ZnO, $ZnTiO_3$, and CdO only. The optical bandgap was increased from 2.11 eV to 2.25 eV by adding $g\text{-}C_3N_4$ in samples ZTCG0 up to ZTCG4. Such z- scheme based [$(ZnO_{0.40}:_{0.60}TiO_2):CdO_{1.00}$]:[$g\text{-}C_3N_4$] nanocomposites show excellent catalytic activity. Sample ZTCG4 shows the maximum degradation efficiency of 99.7%, 99.8 %, and 99.9 % for methyle blue (MB), methyle green (MG), and methyle orange (MO), respectively in visible illumination. In spite of this, $g\text{-}C_3N_4$ embroiled with [$(ZnO_{0.40}:_{0.60}TiO_2):CdO_{1.00}$] resulting in a more active area would be obtained for the catalytic reaction by breaking aromatic ring from their central. The mineralized factors chemical oxygen demand (COD) and biological oxygen demand (BOD) were examined, in fact, maximum removal COD and BOD efficiencies were found at 89.4% and 88.9% for sample $g\text{-}C_3N_4$. In this way, organic contaminant-free water can be achieved by using our promising catalysts under visible illumination.

Keywords: Sol-gel precipitation method, Thermal polycondensation method, FE-SEM, XRD COD, BOD

Tri-directional Controlled Quantum-Teleportation in a Quantum Network

Nikhita Singh*, Ravi S. Singh†
Photonic Quantum-Information and Quantum Optics Laboratory, Department of Physics
Deen Dayal Upadhyaya Gorakhpur University, Gorakhpur (U.P.), 273009, Bharat (India).
**Corresponding author email id: singhnikhitabhi6@gmail.com; †yosora27@gmail.com*

Quantum network may bring novel capabilities to prevalent classical communication system. Quantum physical effect may be exploited to detect eavesdropping, to improve the shared sensitivity of separated astronomical instruments or to create distributed states that will enable quantum computation over a distance using teleportation, i.e., tele-computation.

Quantum Teleportation (QT) is a technique of transmitting arbitrary (unknown) quantum information caried by a quantum system living either in infinite-dimensional Hilbert space (CV regime) or in finite-dimensional Hilbert space (DV-regime) from Alice (sender) stationed at one place to Bob (receiver) located at any distant place with the assistance of a shared quantum channel, local unitary operations, and classical communications [1]. The first theoretical idea of QT in DV regime has been put forth by Bennett et al [2], nowadays termed as Standard QT. Multi-directional controlled QT schemes are indispensable in any quantum network to increase the security of transmitted quantum information. A scheme of tripartite-controlled QT is proposed by Li et. al [3] in which 'to be transmitted states' are arbitrary single qubits and controlled QT of three unknown Bell-pairs qubit-states is given by Choudhury and Samanta [4].

We worked out a tri-directional controlled QT protocol generalizing 'to be transmitted states' having prepared at multi-qubit states by employing a seven-qubit entangled state as a quantum channel, C-NOT gate operations, local unitary operations, and classical communications. In our scheme, three senders (Alice, Bob and Charlie) having unknown quantum information states like k-qubits, l-qubits and m-qubits, respectively are attempting to send their states to three different receivers, David, Edison, and Ford, respectively under the supervision of Eve. Furthermore, we analyzed and compared our protocol on the basis of intrinsic efficiency with similar protocols that appeared recently in the literature.

Keywords: Multi-directional controlled quantum-teleportation, Multi-qubit quantum states, Seven-qubit entangled channel, C-NOT Quantum Gate, Unitary Operation and Classical Communication.

References:

[1] Meter, Rodeny, N., (2014). Quantum Networking, *John Wiley & Sons, Inc*., USA.

[2] Bennett, C.H., Brassard, G., Crepeau, C., Josza, R., Peres, A., Wotters, W.K. (1993). Teleporting an unknown quantum quantum state via dual classical and Einstein-Podolsky-Rosen channels. *Phys. Rev. Lett*., **70**, 1895–1899.

[3] Li, W., Zha, X. W., Qi, J. X. (2016), Tripartite quantum-controlled teleportation via seven qubit cluster state. *Int. J. Theor. Phys*., **55**, 3927–3933.

[4] Choudhury, B.S., Samanta, S. (2017), Simultaneous perfect teleportation of three two qubit states. *Quantum Inf. Process.* **16**(9), 230.

Quantum Teleportation via noisy partially entangled states

Nidhi Singh*, Ravi S. Singh#
Photonic Quantum-Information and Quantum Optics Laboratory, Department of Physics,
Deen Dayal Upadhyaya Gorakhpur University, Gorakhpur (U.P.), 273009, Bharat.
**Corresponding author email id: singh.nidhi3927@gmail.com; #yesora27@gmail.com*

Quantum Teleportation (QT) is a fundamentally nonclassical scheme of quantum communication as it demonstrates the ability to transfer states of a quantum system living in finite /infinite dimensional Hilbert space to a quantum system nonlocally stationed at any distance, in principle. The theoretical discovery of QTisdone by Bennet et. al. in 1993 [1] although, physical implementation faces myriad challenges because of different kinds of noises presented by the prevalent environment, which interacts with quantum systems, carriers of quantum information.

We revisit a protocol proposed by Liang et al [2]wherein they analyzed various Pauli noises in a channel by solving the Lindblad master equation. We have noticed that the analysis of Liang et al [2], in our opinion, is not accurate. We looked upon the same protocol using the insights of Nakazatoet. al. [3] and Fortes et. al.[4] findings for solutions of the Lindblad equation in Kraus representation. To assess the effects of various noises on QT, we have evaluated fidelity and analyzed the same.

Keywords: Noisy Quantum Teleportation, Pauli noises, Kraus representation and Fidelity.

References:

[1] Bennett, C. H., Brassard, G., Crépeau, C., Jozsa, R., Peres, A., and Wootters, W. K.(1993), Teleporting an unknown quantum state via dual classical and Einstein-Podolsky-Rosen channels, Phys. Rev. Lett.70, 1895-1899.

[2] Liang, H.Q., Liu, J.M., Feng, S.S, Chen, J.G., (2013), Quantum teleportation with partially entangled states vianoisy channel, Quantum Inf. Process. 12, 2671-2687.

[3] Nakazato, H, Hida.Y, Yuasa.K, Militello,B, Napoli, A and Messina, A(2006), Solution of Lindblad equation In the Kraus representations, Phys.Rev.A 74, 062113.

[4] Fortes.R. & Rigolin. G, Fighting noise with noise in realistic quantum teleportation (2015),Phys. Rev. A 92,012338.

Enormously large nonlinear optical properties analysis of $Li_2F@Si_{60}$-LiF_2 by using First principal

Vijay Singh[b], Deen Dayal Dubey[a], Ashutosh Tiwari [a], Gaurav Mishra[a], Anoop Kumar Pandey[a*]
[a*] K. S. Saket Post Graduate College, Ram Manohar Lohia University, Ayodhya (India)
[b]Department of Physics, College of Natural and Mathematical Sciences, University of Dodoma, PO Box 259, Dodoma (Tanzania)
**Corresponding author email id: anooppandeyias@gmail.com*

Nonlinear optical (NLO) crystals have piqued the interest of researchers in recent decades due to their multiple applications in communication, LCDs, optical applications, organic electronics, and blue-green lasers, among others. In this paper, we propose a new class of NLO active complexes based on encapsulated superalkali Li_2F interactions with superhalogen LiF_2 utilizing a combination of the DFT/B3LYP technique and the 6-311G(d,p) basis set. The optimized Si_{60}structure is compared to $Li_2F@Si_{60}$-LiF_2. Encapsulated superalkali Li_2F interaction with superhalogen $LiF_2$with Si_{60} reactivity index is compared using frontier molecular orbitals. NLO active complexes are formed through charge transfer from donor to acceptor species. The electron transfer index (ECT) demonstrates that charge transfer from $Si_{60}@Li_2F$ to superhalogen alkali (LiF_2) occurs during the creation of $Li_2F@Si_{60}$-LiF_2 complexes. The DOS figure reveals that the HOMO and LUMO energy levels have shifted to the upper side as a result of the additional unoccupied energy level that arises in $Li_2F@Si_{60}$-LiF_2, resulting in a reduced energy gap in $Li_2F@Si_{60}$-LiF_2 when compared to Si_{60}. More polarization occurs as the frontier orbital energy gap narrows. The nonlinear optical behavior of $Li_2F@Si_{60}$-LiF_2 is computed using dipole moment, polarizability, and hyperpolarizability and compared to the equivalent Si_{60} cage parameters. The moment of electron causes a massive increase in hyperpolarizability (4377.16589 a.u.) in the interaction of superhalogen LiF_2 and encapsulated Si_{60} with Li_2F. The nonlinear-optical properties of $Li_2F@Si_{60}$-LiF_2have been analyzed on a single molecule in the gas phase, ignoring all other solvent effects.

Keywords: NLO, Superhalogen, Superalkali, DOS plot

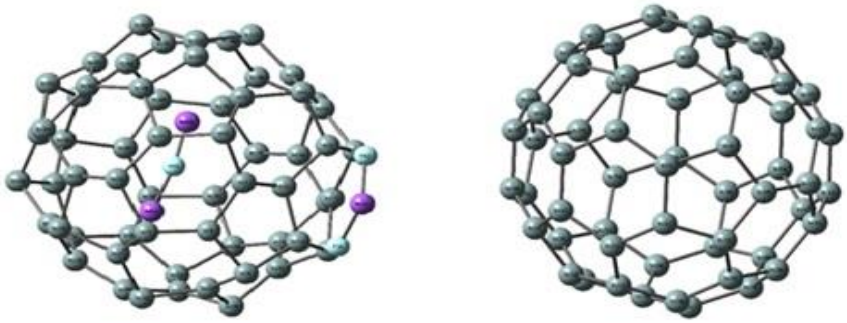

$Li_2F@Si_{60}$-LiF_2 Si_{60}

Fig-1*Optimized geometry of $Li_2F@Si_{60}$-LiF_2(left)and Si_{60}(right)*

Efficient Median Computation for Large FITS Datasets Using the Median of Medians Algorithm

Vinamra Roy Chowdhury
Barrackpore Rastraguru Surendranath College, West Bengal
**Corresponding author email id: vinamra@gmail.com*

Analyzing diffuse astronomical data, often stored in the FITS (Flexible Image Transport System) format, presents a substantial computational challenge in modern astronomy. Calculating intervals from such data can be computationally intensive and time-consuming. In response to this challenge, I propose employing the Median of Medians algorithm as an efficient strategy.

The Median of Medians algorithm, known for its robustness, offers a proven approach to reduce computational costs while accurately determining the median of a dataset. This method utilizes a divide-and-conquer procedure, enabling precise median estimation even for large and complex datasets.

This paper introduces MY adaptation of the Median of Medians algorithm tailored to the specific requirements of astronomical data stored in FITS files. Through customization of the algorithm to the characteristics of FITS datasets, I have achieved significant speed improvements in mean computation without sacrificing accuracy.

I conducted a series of experiments and compared various astronomical datasets obtained from telescopes to demonstrate the superiority of the Median of Medians algorithm over traditional methods. Our findings suggest that applying the Median of Medians algorithm to observational data of celestial objects holds the promise of accelerating research, facilitating quicker discoveries, and enabling deeper insights into the universe.

Keywords: Median of Medians Algorithm, Astronomical Data, Computational Efficiency, FITS Format, Speed Improvements.

References:

[1] Eberl, M. (2017b). The Median-of-Medians Selection Algorithm. Arch. Formal Proofs.
[2] Haslbeck, M. P. L., & Lammich, P. (2019). Refinement with Time—Refining the Run-Time of Algorithms in Isabelle /HOL. ITP. https://doi.org/10.4230/LIPICS.ITP.2019.20
[3] Kurosawa, N. (2016a). Quicksort with median of medians is considered practical (arXiv:1608.04852). arXiv. http://arxiv.org/abs/1608.04852

Investigating open clusters NGC 6604 and NGC 6793 using GAIA DR3 data

Ranjana Jaiswal*, Apara Tripathi, Shantanu Rastogi
DDU Gorakhpur University, Gorakhpur, 273009, India
**Corresponding author email id: jaiswalranjana926@gmail.com*

Stars in Galaxies form within star clusters. Star clusters are a group of gravitationally bound stars which form from the same molecular clouds. Open clusters are the ideal sites for star formation. We have selected two poorly studied young open clusters (i.e. NGC 6604 and NGC 6793) for detailed studies. The kinematic analysis of young open clusters NGC 6604 and NGC 6793 have been reported in this study. Gaia Data Release 3 (DR3) has been used for kinematic analysis to separate cluster member stars from the field stars and obtain precise structural and astrophysical parameters, such as cluster center and cluster extent. The refined cluster's center and radius of both clusters have been estimated in arcmin. Taking into account Gaia DR3 proper motion components and parallaxes of member stars, we found the mean proper motion of cluster in mas yr^{-1} in (RA, DEC). We also found the most probable (Pu>70%) cluster members with mean parallax. These two target fields contain several massive stars of O and B type. These massive stars might help a new generation of stars to form within the cluster, which means there might be triggered star formation.

Keywords: Open cluster, NGC 6604, NGC 6793, Gaia DR3 data.

References:

[1] Allison M. (2006). Star Clusters and How to Observe Them,Springer.
[2] Barbon R., Carraro G., Munari U., Zwitter T. (2000). Spectroscopy and BVI photometry of young open cluster NGC 6604, Astronomy and Astrophysics Supplement Series, 144, 451-456.

The variation in the indoor-outdoor natural gamma dose and annual effective dose around the Coal based Power Generation Facility in West U. P., India.

Pankaj Kumar*[1], Mukesh Kumar[1],
[1]Department of Physics, S.V. College, Aligarh-202001, U.P., India
**Corresponding author email id: pankaj198911@gmail.com*

The human beings have the continuously exposed to natural radiation due to radionuclides since primordial age both inside and outside the houses. In the present study, an effort has been made for measure of the natural gamma dose rate in the indoor and outdoor environment in the villages, around the National Thermal Power Corporation (NTPC), Dadri, Gautam Buddh Nagar, (U.P.) India. The variation in the indoor and outdoor annual effective doses as 0.93 to 1.87 mSv/y and 0.17 to 0.33 mSv/y with the mean values 1.41 ± 0.02 and 0.24 ± 0.003 mSv/y respectively. The ratio of indoor to outdoor gamma dose rates ranged from 1.00 to 2.12. The mean values of annual effective dose rate have been found higher than the prescribed limits by UNSCEAR (United Nations Scientific Committee on the Effects of Atomic Radiation)[1] and ICRP (International Commission on Radiological Protection) [2]. The mean excess lifetime cancer risk, lifetime dose rates and dose received by different organs have been calculated for the further analysis.

Keywords: Gamma radiation, annual effective dose, Excess Lifetime Cancer Risk, Organ dose, thermal power station.

References:

[1] United Nations Scientific Committee on the Effects of Atomic Radiation, & Annex, B. (2000). Exposures from natural radiation sources. *Cosmic rays*, *9*(11).

[2] InternationalCommissiononRadiologicalProtection.(2007).RecommendationsoftheICRP:AnnalsoftheICRP, *3 7*(2-4), 49-79.

Recent developments in the theory of granular matter

Manjeet Seth* and Awadhesh Kumar Dubey
Department of Pure and Applied Physics, Guru Ghasidas Vishwavidyalaya, Bilaspur
**Corresponding author email id: manjeetseth28@gmail.com*

Granular materials consist of a large collection of macroscopic particles and are able to show solid, liquid, gas, or glass-like behaviors. Though, they have been a greatly discussed topic for decades in physics and engineering but still lack a continuum theory like the kinetic theory of molecular gases. In the present article, we provide a comprehensive review of the progress so far and describe the research developments till date in above mentioned direction.

Keywords: Granular materials, Continuum Theory, Kinetic Theory, Granular glass.

References:

[1] Barker, G. C., and A. Mehta, 1991 Phys. Rev. Lett. 67, 394.
[2] Savage, S. B., 1997a, Disorder and Granular Media (North Holland, Amsterdam).
[3] Aoki, K. M., T. Akiyama, Y. Maki, and T. Watanabe, 1996, Phys. Rev. E 54, 874.
[4] Bagnold, R. A., 1966, Proc. R. Soc. London A 295, 219.
[5] Ackerson, B., and P. Pusey, 1988, Phys. Rev. Lett. 61, 1033.

Cosmological Parameters, Black Hole Dynamics, and Metric f(R) Gravity

*Suraj Kumar Pati, Bibekananda Nayak
P.G. Department of Physics, Fakir Mohan University, Vyasa Vihar, Balasore-756019, Odisha
**Corresponding author email id: surajkumarpati@gmail.com*

In this work, we investigated the fact that the presently observed accelerated expansion of the universe can be explained because of modification of gravity. From this, we found that the late-time accelerated expansion of the universe could be achieved by assuming the theory of gravity as Starobinsky type metric f(R) gravity without introducing the concept of dark energy. We, here, focused on evolution of the universe by studying different cosmological parameters like Hubble parameter, deceleration parameter, and jerk parameter, etc. Again, from our analysis, we conclude that the universe is undergoing an accelerated phase of expansion from$0.711t_0$, where t_0 is the present age of the universe and this accelerated phase of expansion will continue forever.We also use power-law cosmology to investigate the evolution of black holes within the context of metric f(R) gravity satisfying the conditions provided by Starobinsky model. Where we found that the mass of a black hole decreases by absorbing surrounding energy-matter due to modification of gravity and more the accretion rate more is the mass loss. Particularly the black holes, whose formation mass is nearly 10^{20}gm and above are evaporated at a particular time irrespective of their formation mass. Again, our analysis reveals that the maximum mass of a black hole supported by metric f(R) gravity is $10^{12}M_{\odot}$, where $M_{\odot}$ represents the solar mass.

Keywords: Metric f(R) Gravity, Starobinsky Model, Power-law Cosmology, Cosmological parameters, Black hole Evaporation

References:

[1] Riess, A. G., et al. "Observational evidence from supernovae for an accelerating universe and a cosmological constant." The astronomical journal 116.3 (1998): 1009.
[2] Perlmutter, S., et al. "Measurements of Ω and Λ from 42 high-redshift supernovae." The Astrophysical Journal 517.2 (1999): 565.
[3] Caldwell, R. R., Dave R., and Paul J. Steinhardt. "Cosmological imprint of an energy component with general equation of state." Physical Review Letters 80.8 (1998): 1582.
[4] Pati, S.K., Nayak, B., Singh, L.P., Black hole dynamics in power-law based metric f (R) gravity. Gen.Relativ. Gravit. 2020, 52, 78.
[5] Chakrabarti, S., Said, J. L., & Bamba, K. (2019). On reconstruction of extended teleparallel gravity from the cosmological jerk parameter. The European Physical Journal C, 79, 1-17.
[6] Popławski, N. J. (2006). The cosmic jerk parameter in f (R) gravity. Physics Letters B, 640(4), 135-137.
[7] Nojiri, S. & Odintsov, S. (2003). Modified gravity with negative and positive powers of curvature: Unification of inflation and cosmic acceleration. Physical Review D. 68. 10.1103
[8] Visser, M. (2005). Cosmography: Cosmology without the Einstein equations. General Relativity and Gravitation, 37, 1541-1548.
[9] Hawking, S. W.Particle creation by Blackhole. Commun. Math. Phys. 43 (1975) 199.
[10] J. D. Barrow, E. J. Copeland, E. W. Kolb and A. R. Liddle, Baryogenesis in extended inflation. Phys. Rev. D 43 (1991) 977.
[11] Myung, Y. S., Moon, T., & Son, E. J. (2011). Stability of f (R) black holes. Physical Review D, 83(12), 124009.
[12] Starobinsky, A. A. Variations on Starobinsky inflationary Model.J. Expt. Theor. Phys. Lett. 34 (1981) 460.
[13] Starobinsky, A. A. A new type of isotropic Cosmological Models without Singularity. Phys. Lett. B 91 (1980) 99.

Manipulation of coherent optical phenomena and the generation of orbital angular momentum (OAM)-based FWM signal using structured light

Samim Akhtar*, Aparajita Das, Rejjak Laskar, Jayanta K. Saha, Md. Mabud Hossain
Department of Physics, Aliah University, Action Area IIA/27, Newtown, Kolkata-160, India
**Corresponding author email id: samimakhtar1910@gmail.com*

Structured light with a helical phase-front [1] has received an immense amount of research interest over the last decades due to its variety of applications in optical communications, manipulation of optical phenomena, high-resolution imaging, and so on. The interaction of structured light with an atomic medium triggers two significant features of quantum coherence phenomena: the narrowing of spectral line shape and the generation of new structured light. In this work, we study various coherent optical properties, *e.g.*, two-photon electromagnetically induced transparency (EIT) [2] and three-photon EIT (TPEIT), in a four-level ladder (Ξ)-type system of ^{87}Rb atom, where the probe and control fields are Gaussian beams and the pump field is structured light. Additionally, the generated four-wave mixing (FWM) signal [3]has been studied. We adopt the semi-classical density matrix formalism to derive the required optical Bloch equations (OBEs), which are solved analytically using an iterative perturbative technique to obtain the optical coherence terms related to the probe and FWM signals. Interestingly, it is found that the generated FWM signal is spatially structured along with the azimuthal phase, which carries the orbital angular momentum (OAM) [1]. Our study has also illustrated that the coherent optical responses(EIT, TPEIT, FWM signals)can be manipulated by controlling the OAM number of the structured pump beam.

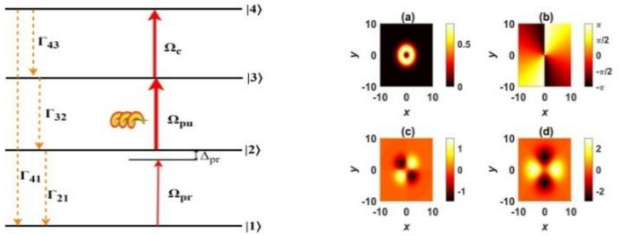

Figure: (Left side) Schematic diagram of a four-level ladder (Ξ)-typeatom-laser coupled system. (Right side) Different spatial profiles [(a) intensity, (b) phase, (c) Im(Ω_{pu}), and (d) Re(Ω_{pu})] of the structured pump beam (Ω_{pu}) for the OAM number l=2. The Laguerre-Gaussian (LG) beam is treated as a structured (vortex) light.

Keywords: Electromagnetically induced transparency (EIT), structured light, Laguerre-Gaussian (LG) beam, orbital angular momentum (OAM), four-wave mixing (FWM).

References:

[1] Allen, L., Beijersbergen, M. W., Spreeuw, R. J. C., & Woerdman, J. P. (1992). Orbital angular momentum of light and the transformation of Laguerre-Gaussian laser modes. *Physical Review A, 45*(11), 8185.
[2] Boller, K. J., Imamoğlu, A., & Harris, S. E. (1991). Observation of electromagnetically induced transparency. *Physical Review Letters*, *66*(20), 2593.
[3] Walker, G., Arnold, A. S., & Franke-Arnold, S. (2012). Trans-spectral orbital angular momentum transfer via four-wave mixing in Rb vapor. *Physical Review Letters*, *108*(24), 243601.

Quantum LiDAR: Super-resolution and super-sensitivity with multi-photonic state and photon number resolving detectors

Priyanka Sharma[1], Manoj K Mishra[2], and Devendra Kumar Mishra[1*]
[1]Deptartment of Physics, Banaras Hindu University, Varanasi-221005, India
[2]Space Applications Centre, Indian Space Research Organization (ISRO), Ahmedabad, Gujarat, India
**Corresponding author email id: kndmishra@gmail.com*

We investigate the enhancement in phase sensitivity and resolution of Mach-Zehnder interferometer (MZI) based quantum LiDAR [1] by using multi-photonic state (MPS) [2], (superposition of four coherent states) as the input. We use parity photon counting measurement, and zero-nonzero photon counting measurement as the detection schemes. We thoroughly investigate the results in lossless as well as lossy conditions. We found enhancement in resolution and phase sensitivity with this state in comparison to the coherent state and even coherent superposition state (ECSS) based quantum LiDAR. Our analysis shows that MPS may be an alternative nonclassical resource in the field of quantum imaging and quantum sensing technologies. This work is based on our work (arXiv:2309.12076 **[quant-ph]**) [3].

Keywords: Quantum Lidar, Mach-Zehnder interferometer, binary outcome photon counting measurement.

References:

[1] J. Dowling, Quantum lidar-remote sensing at the ultimate limit, in Louisiana State University Baton Rouge, Air Force Research Laboratory Information Directorate Rome Research Site Rome (Tech. Rep., 2009).
[2] M. K. Mishra, H. Prakash, and V. B. Jha, Ququats as a superposition of coherent states and their application in quantum information processing, International Journal of Quantum Information 19, 2150013 (2021).
[3] P. Sharma, M. K. Mishra & D. K. Mishra (2023). Super-resolution and super-sensitivity of quantum LiDAR with multi-photonic state and binary outcome photon counting measurement. ArXiv. /abs/2309.12076

Quantum sub-shot noise sensitivity of a Mach-Zehnder interferometer with the superposition of Schrödinger's cat-like state with vacuum state as an input under product detection scheme

Gaurav Shukla[1], Dhiraj Yadav[1], Priyanka Sharma[1], Anand Kumar[1]and Devendra Kumar Mishra[1*]
[1]Department of Physics, Institute of Science, Banaras Hindu University, Varanasi -221005, India
**Corresponding author email id: kndmishra@gmail.com*

We have studied the phase sensitivity of a Mach-Zehnder interferometer (MZI) using product detection (PD) scheme [1] by using the superposition of Schrödinger's cat-like state with the vacuum state (SCVS) as input in one arm and the coherent state as the input in the other arm of the MZI. We have compared our results, obtained from PD, with that of the parity detection scheme [2]. We found that in the higher energy range, PD performs better as compared to parity detection while in the lower energy range parity does better. But we found that in terms of working phase range, the PD scheme gives a broader phase range than the parity detection scheme approximately in all the cases. As a result, to perform detection in a wide-range PD scheme gives much better results than the parity detection scheme. We also found that in some cases PD beats the SNL by a significant amount and approaches the single parameter quantum Cramér-Rao bound (QCRB) in some cases. Therefore, we expect that the SCVS may be used as an alternative quantum resource with PD for the enhancement of phase measurement sensitivity of an MZI which might find potential application in quantum metrology and quantum sensing
technology.

Keywords: Mach-Zehnder interferometer, Product Detection, Schrödinger's cat-like state.

References:

[1] Steuernagel O and Scheel S 2004 Journal of Optics B: Quantum and Semiclassical Optics 6 S66.
[2] Shukla G, Mishra K M, Pandey A K, Kumar T, Pandey H and Mishra D K 2023 Optical and Quantum Electronics 55(5).

Enhancing the Phase Sensitivity of a Mach-Zehnder Interferometer by Introducing Schrödinger's Cat-Like State Superposition with Vacuum State using Parity Measurement

Gaurav Shukla[1], Krishna Mohan Mishra[1], Aviral K. Pandey[1], Taj Kumar[1], Hemendra Pandey[2], Devendra Kumar Mishra[1]*

1. Department of Physics, Institute of Science, Banaras Hindu University, Varanasi 221005, India
2. Variable Energy Cyclotron Centre, Kolkata, West Bengal, India

**Corresponding author email id: kndmishra@gmail.com*

We investigated the enhancement in the phase sensitivity of a Mach–Zehnder interferometer (MZI) by using the superposition of 'Schrödinger's cat-like state with the vacuum state (SCVS)' and the vacuum state as inputs of MZI using parity detection. Also, to find the ultimate precision bound on the estimation of unknown parameter we calculated the Quantum Fisher Information (QFI) and quantum Cramer-Rao bound [1]. With this setup, we observed the effect on the phase sensitivity of the interferometer using a parity detection scheme. We get better phase sensitivity under some conditions for this setup having potential application in the field of quantum sensing. This work is based on our work [2].

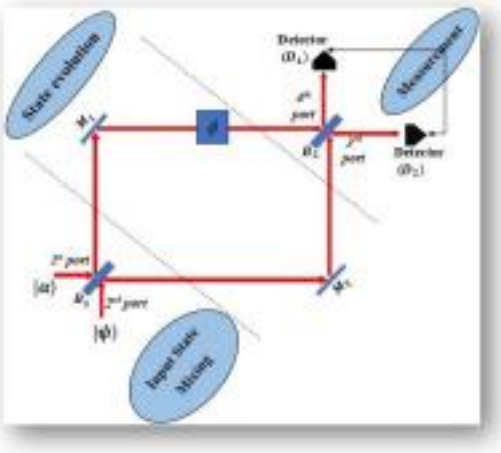

Schematic diagram of Mach-Zehnder interferometer

Keywords: Mach Zehnder interferometer, Schrodinger-cat state, quantum Cramer-Rao bound.

References:

[1] Helstrom, C. W. (1969). Quantum detection and estimation theory. *Journal of Statistical Physics*, *1*, 231-252.

[2] Shukla G., Mishra K. M., Pandey A. K., Kumar T., Pandey H., & Mishra D. K. (2023). Improvement in phase sensitivity of a Mach–Zehnder interferometer with the superposition of Schrödinger's cat-like state with vacuum state as an input under parity measurement. *Optical and Quantum Electronics*, *55*(5), 460.

Enhancement of nonlinear optical properties by spontaneously generated coherence (SGC) in a microwave mediated five-level Ξ-type atomic system

Aparajita Das[*,1], Rejjak Laskar[1], Samim Akhtar[1], Jayanta K. Saha[1], Md. Mabud Hossain[1]
[1]Department of Physics, Aliah University, Action Area IIA/27, Newtown, Kolkata-160, India
[*]Department of Physics, Surendranath College, M. G. Road, Kolkata-9, India
**Corresponding author email id: aparajita1223@gmail.com*

The enhancement of nonlinearity based on the laser-induced atomic coherence in multilevel atoms under the electromagnetically induced transparency (EIT) condition [1] has received ample theoretical as well as experimental contemplation over decades. The atomic coherence causing nonlinearity can further be modified by the spontaneously generated coherence (SGC) [2] effect and microwave (MW) field driving electric dipole-allowed Rydberg transitions. In this context, we propose an MW-mediated five-level pump-probe (P-Pr) lasers driven Ξ-type atomic system involving Rydberg states [figure 1 (left)]. The spontaneous decay channels originate due to the decay of atoms to the ground state from the closely lying middle excited states |2> and |3>(simultaneously coupled by P to the excited state |4>). MW drives the transitions between the atomic states (|4> and |5>) of the Rydberg atoms with exaggerated properties. In the presence of SGC, we have found that the system response to the Pr (connecting states |1> and |2>), substantially modifies [figure 1 (right)] at different Pr frequency regions and different MW strengths. Therefore, the SGC, enhancing the nonlinear coherent properties of the system, may play a salient role in realizing optical switches and the generation of optical solitons.

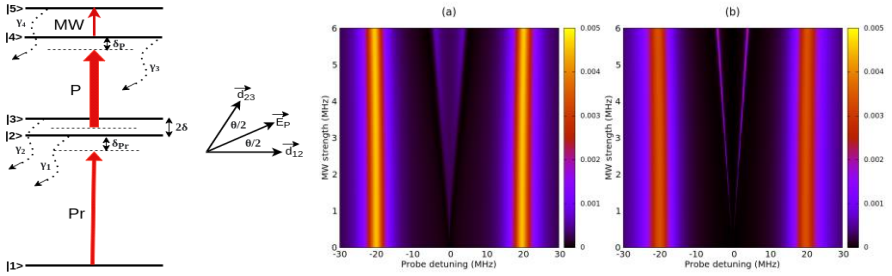

***Figure**: (Left) Schematic diagram of microwave-mediated five-level Ξ-type atomic system. γ_is (i = 1, 2, 3, 4) are the spontaneous decay rates. $|d_{jk}|$ (jk = 12, 23) are the related dipole moments. (Right) the variation of Doppler-free probe absorption as a function of both probe detuning and microwave strength in (a) the absence and (b) the presence of SGC.Pump strength (Ω_P = 10 MHz) and probe strength (Ω_{Pr}= 0.01 MHz) are fixed. The pump and microwave fields are in resonance.*

Keywords: Electromagnetically induced transparency (EIT), spontaneously generated coherence (SGC), microwave field, nonlinear optical response.

References:

[1] Boller, K. J., Imamoğlu, A., & Harris, S. E. (1991). Observation of electromagnetically induced transparency. *Physical Review Letters*, *66*(20), 2593.
[2] Wan, R. G., Kou, J., Li Jiang, Jiang, Y., and Gao, J. Y. (2011). Electromagnetically induced grating via enhanced nonlinear modulation by spontaneously generated coherence. *Physical Review A*, 83, 033824.

Confinement induced enhancement in entanglement measures of He-like isoelectronic ions

Koustav Das Chakladar*
Department of Physics, Aliah University, Action Area IIA/27, Newtown, Kolkata-160, India
*Corresponding author email id: koustavdaschakladar@gmail.com

The study of Quantum Entanglement in few-body atomic systems is one of the extremely promising fields of research in recent times [1]. The entanglement entropies like Von-Neumann entropy (S_{vn}) and linear entropy (S_{ln}) allow us to quantify the amount of entanglement between the constituent particles in a proposed system [2]. In this article, we studied ground state spatial entanglement between a two-electron He-like system under impenetrable spherical confinement.[3] We considered a simplistic explicitly correlated Hylleraas-type wavefunction and optimized its parameters by employing a variational framework for a certain strength of confinement. We then calculated the (S_{vn}) and (S_{ln}) of various He-like isoelectronic systems (Z=2-7) by varying the radius of confining potential. This wave function allows us to determine the entanglement entropies with reasonable accuracy for varying confinement strength. It was found that at a certain strength of confinement, the entanglement between two spatially correlated electrons becomes maximum, resulting in a confinement-induced enhancement in entanglement entropies. The radial position of the maximum entangled state is greater than the critical radius of the confined system which indicates that the highest entangled state appears inside the bound state domain. It is also found that the radial position of the maxima decreases as the atomic number increases (*see Figure 1*). The result suggests the possibility of tunability of degrees of spatial entanglement in electronic systems by various confining structures.

Result:

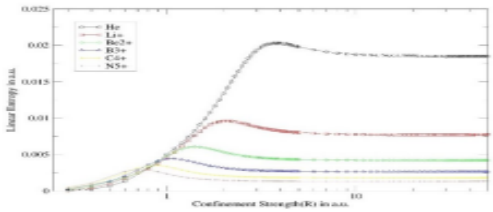

Figure-1

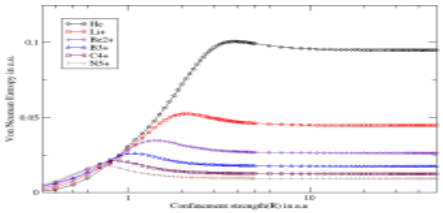

Figure-2

Figure: *Enhancement in (Figure 3) von Neumann entropy due to confinement strength for He-Like isoelectronic ions and (Figure 2) Linear Entropy due to confinement strength for He-Like isoelectronic ions*

Keywords: Quantum Entanglement, Von Neuman Entropy, Linear Entropy, Spherical Confinement

References:

[1] Mondal, S., Sen, K., & Saha, J. K. (2022). He atom in a quantum dot: Structural, entanglement, and information theoretical measures. *Physical Review A*, *105*(3), 032821.

[2] Kościk, P. (2023). On the Radial and Angular Correlations in a Confined System of Two Atoms in Two Dimensional Geometry. *arXiv preprint arXiv:2309.14116*.

[3] Kościk, P., & Saha, J. K. (2015). Entanglement in helium atom confined in an impenetrable cavity. *The European Physical Journal D*, *69*, 1-4.

Investigation of step edge based YBCO Josephson junction and Superconducting quantum interference devices

Mamta Dahiya*and Neeraj Khare
Department of Physics, Indian Institute of Technology Delhi, New Delhi-110016, India
*Corresponding author email id: jindmamta@gmail.com

Josephson junction (JJ) devices are an integral part of the development of electronic circuits, which can be used in various applications such as SQUID, Terahertz, microwave detection, etc (Shaikhaidarov et al., 2016). JJs are the basic elements of these circuits, which generally can be defined as sandwiching a barrier layer in between two superconductors. One of the simplest circuits is dc SQUID, which is made up of two JJs connected in parallel and coupled in a loop structure. Also, SQUID is a very sensitive magnetic field sensor for measuring subtle magnetic fields (Tafuri et al., 2013). In this study, we have fabricated $Y_1Ba_2Cu_3O_{7-x}$ (YBCO) based Josephson junction (JJ), and Superconducting quantum interference devices (SQUID) using lithography, pulsed laser deposition, and dry etching techniques on $SrTiO_3$ (STO) substrate using the optimized recipe. The growth of YBCO thin film along the c-axis on the STO substrate is confirmed using the X-ray diffraction technique. By analyzing the step-edge on the STO substrate using atomic force microscopy, the estimated value of step height is ~440 nm. Further, the transport measurement of fabricated devices is carried out using the four- probe technique, and liquid helium cryostat. The estimated values of critical temperatures for YBCO thin film, JJ, and SQUID device ~90, 89, and 88 K respectively. The value of critical current is obtained by conducting current-voltage measurements of the fabricated devices. Also, by biasing the SQUID device above critical current at 70 K, the measured field sensitivity by it corresponds to ~10^{-10} T.

Keywords: SQUID; magnetic sensor; critical current

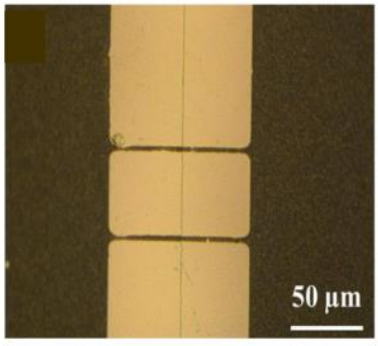

Figure: *SQUID device on STO substrate*

References:

[1] Shaikhaidarov, et al. (2016). *Physical Review Applied, 5*(2), 024010. doi: 10.1103/PhysRevApplied.5.024010.
[2] Tafuri, F., et. al. (2013).. *Journal of Superconductivity and Novel Magnetism*, *26*(1), 21–41. doi: 10.1007/s10948-012-17730.

Photometric and kinematic study of open clusters: King 6

Vaibhav Pandey[1,*], Apara Tripathi[1], Brijesh Kumar[2], Shantanu Rastogi[1]
[1] Deen Dayal Upadhyay Gorakhpur University, Gorakhpur-273009, India
[2] Aryabhatta Research Institute of Observational Sciences, Manora Peak, Nainital-263129
**Corresponding author email id: vaibhav.ankit10@gmail.com*

Open clusters are not trivial stellar systems. Their dynamical evolution is not yet fully understood. They are excellent targets for understanding issues related to galactic structure, stellar population, dynamical evolution, and star formation process in the Galaxy([2], [3], [4]). We present new UBVRI photometry open star clusters King 6. The data is collected from 104-cm Sampurnanand Optical Telescope, ARIES Nainital, using 2k x 2k CCD which covers about 13 x 13 arcmin^2 field on sky. Data reduction is done in a homogeneous manner. We could reach down to ~ 21 mag in the V band. GAIA DR3 archival astrometric data is used to determine membership probability, mean proper motion, and parallaxes for the member stars of the target field([1]). These may be used to determine the fundamental parameters (Reddening, age, distance), structural parameters, mass function, and mass segregation for the objects. The CCD photometry for King 6 is being reported for the first time.

Keywords: Star Cluster, Photometry, King 6, Parameters, Evolution.

References:

[1] Cantat-Gaudin, T., Jordi, C., Vallenari, A., Bragaglia, A., Balaguer-Núñez, L., Soubiran, C., Bossini, D., Moitinho, A., Castro-Ginard, A., Krone-Martins, A., Casamiquela, L., Sordo, R., and Carrera, R. A gaia dr2 view of the open cluster population in the milky way. A&A, 618:A93, 2018.
[2] WS Dias, H Monteiro, A Moitinho, JRD Lepine, G Carraro, E Paunzen, B Alessi, and L Villela. Vizier online data catalog: Updated parameters of 1743 open clusters (dias+, 2021). VizieR Online Data Catalog, pages J–MNRAS, 2021.
[3] Charles J. Lada and Elizabeth A. Lada. Embedded clusters in molecular clouds. Annual Review of Astronomy and Astrophysics, 41(1):57–115, 2003.
[4] Simon F Portegies Zwart, Stephen LW McMillan, and Mark Gieles. Young massive star clusters. Annual review of astronomy and astrophysics, 48:431–493, 2010.

Hybrid Quantum Engineering with photon-magnon coupling at room temperature for next generation quantum information devices

Kuldeep Kumar Shrivastava, Biswanath Bhoi, Rajeev Singh*
Nano-Magnetism and Quantum Technology Laboratory, Department of Physics, Indian Institute of Technology (Banaras Hindu University), Varanasi, 221005, Uttar Pradesh, Bharat.
**Corresponding author email id: rajeevs.phy@iitbhu.ac.in*

Photon-magnon coupled (PMC) hybrid systems hold great promise for applications in quantum processing technologies. Specially, controlling the interactions, including various types of anti-crossings, between photon (P) and magnon (M) modes is crucial for the development of information processing devices with desired tunability and scalability. Multimode PM coupling with switching features from level repulsion (LR)to level attractions (LA) is theoretically proposed and demonstrated through numerical simulations for two different hybrid systems i.e., two photon-one magnon mode (2-1 PM) and three photon-one magnon modes (3-1 PM). Although individual photon modes display dissipative couplings with the magnon mode, when designed as a 2-1 PMC system, one photon undergoes a transition to coherent coupling, while the other maintains its dissipative coupling with magnon. On the other hand, in the case of a 3-1 PMC system, their combination results in a shift to coherent coupling for one photon, a transition from dissipative to coherent coupling for the second photon while the third photon retains its dissipative coupling with magnon mode. The numerically calculated LR and LA due to coherent and dissipative coupling in these two PMC systems are presented in Fig. (c-e). Characteristic features of these multi-mode interactions (Fig. g-h)are analyzed with the help of our own developed quantum mechanical model just by controlling some parameters at room temperature.

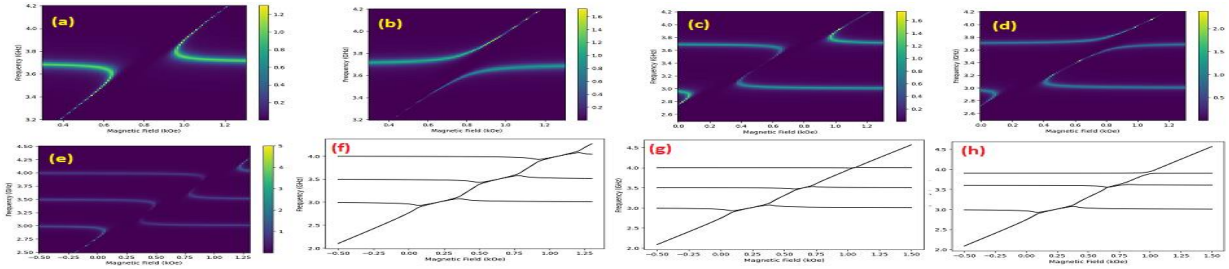

Figure: (a/ b)LA/ LRfor 1 magnon and 1photon mode, (c) 1 magnon and 2 photon modes showing LA for individual systems, (d) hybrid of (c) after parameter tuning shows LA+LR (e) 1 magnon 3 photon modes LA for individual systems, (f-h) eigen value curve for (e) after parameter tuning showing transition from LA to LR.

Keywords: photon, magnon, coupling, level attraction, level repulsion.

References:

[1] TiwariT, RoyD& Singh R (2020). Interplay of coherence and interaction in light propagation through waveguide QED lattice- arXiv preprint arXiv:2010.14935.
[2] Bhoi B**,** Kim B, Jeon H-C & Kim S-K(2022). Coupling induced transparency and absorption in a magnon-multiphoton hybrid system *J. Appl. Phys.* 132, 243901.
[3] ScullyM O and Zubairy M S, Quantum Optics (Cambridge University Press, 1997).
[4] Harder M, YaoB M, GuiY S& Hu C-M (2021). Coherent and dissipative cavity magnonics*J. Appl.Phys.* 129, 201101.

Imprints of spin on the solution and emission spectrum of accretion flows around black holes

Shilpa Sarkar[1]; Indranil Chattopadhyay[2]; Pu, Hung-Yi[3]; Mukherjee, Dipanjan[4]
[1]Harish-Chandra Research Institute (HRI), Prayagraj, India
[2]Aryabhatta Research Institute of Observational Sciences (ARIES), Nainital, India
[3]Department of Physics, National Taiwan Normal University, Taipei, Taiwan
[4]Inter-University Center for Astronomy and Astrophysics (IUCAA), Pune, India
**Corresponding author email id: shilpa.sarkar30@gmail.com*

We investigate accretion flows around rotating black holes (BHs) and obtain self-consistent transonic solutions in full general relativistic prescription. The flow is assumed to be viscous and radiative. Viscosity helps in the removal of angular momentum outwards, allowing matter to get accreted in wards. In addition, viscous heat dissipated makes the matter hotter. On the other hand, radiation mechanisms like bremsstrahlung, synchrotron, and their inverse-Comptonisations cools down the matter. Thus, the solution depends highly on the interplay between heating and cooling processes. In our work we investigate the entire energy–angular momentum parameter space and obtain both shocked and shock-free accretion solutions. Because of the spin in Kerr black holes, the event horizon is dragged to a region <2GM/c^2, increasing the efficiency of accretion process. Ample of works showed a rotating BH to yield high temperature solutions compared to a Schwarzschild BH. This suggests higher emission. Interestingly we have found a distinct annihilation line present only in extremely rotating BHs arising from regions very close to the central object. We have investigated further the other effects of spin on the spectrum obtained from accretion flows around BHs. We find efficiencies reaching >30% for maximally rotating BHs.

Keywords: Accretion, shocks, black holes, pairs, radiation.

Sunspot Number during Solar Cycle 23 and 24: Inferences on Asymmetry and Periodicities

Prithvi Raj Singh[1], Upendra Kr. Singh Kushwaha[1], Tarun Kumar Pant[2]
[1]Department of Physics, University of Allahabad, Allahabad-211003
[2]Space Physics Laboratory, VSSC, Thiruvananthapuram-695022, India
**Corresponding author email id: prithvisingh77@gmail.com*

To examine the asymmetry nature of the sunspot number (RGO data) during solar cycles 23 and 24 i.e., period 1996-2020. The present study indicates that solar activity (i.e., the sunspot number)is dominating in the northern (N) hemisphere during the rising phase of solarcycles 23 and 24, whereas the southern (S) hemisphere is dominating in the declining phase of the solar cycle23 and 24. The statistical significance of the asymmetry value (A) indicates real feature of the northern and southern hemisphere distribution of sunspot numbers.The absolute asymmetry analysis of sunspot numbers shows a periodical domination of the northern and southern hemispheres of the Sun for the period 1996-2020. The periodicities that are prominent in the asymmetry of the sunspot number have been investigated using R- RobPer, and Continuous Wavelet Transformation (WT) methods during a combined data set 1996-2020. These asymmetries reflect some essential properties of the prevailing solar processes which need tobe consistent with solar dynamo.

Keywords: Solar Activity, SSN, Northern and Southern hemisphere of the Sun

Evolution of QGP Fireball in the Early Universe

Naman[1,*], Yogesh Kumar[1], Poonam Jain[2], Vinod Kumar[3], Pargin Bangotra[4]
[1]Department of Physics, Hansraj College, University of Delhi, Malka Ganj, Delhi, India
[2]Department of Physics, Sri Aurobindo College, University of Delhi, Malviya Nagar, Delhi, India
[3]Department of Physics, University of Lucknow, Lucknow, U.P., India
[4]Department of Physics, Netaji Subhas University of Technology, Dwarka, Delhi, India
**Corresponding author email id: nbsverma@gmail.com*

The evolution of quark-gluon plasma (QGP) in the early universe is a key aspect of the Big Bang theory. The evolution of QGP fireball in the early universe is studied at the non-zero value of quark chemical potential. A theoretical-based model is used to determine thermodynamic variables with well-known Friedmann equations. The temperature and equation of state with respect to time is computed for the non-zero value of chemical potential. It plays a crucial role in shaping the universe's structure and is helpful in high energy particle collisions in laboratories like RHIC and LHC. Understanding the evolution of QGP via quasiparticle model helps unravel the universe's earliest moments.

References

[1] S. M. Sanches Jr, F. S. Navarra and D. A. Fogaca, Nucl. Phys. A **937**, 1 (2015)
[2] S. Borsanyi, Z. Fodor, C. Hoelbling, S. D. Katz, S. Krieg, C. Ratti, and K. K. Szabo, JHEP **9**, 1 (2010)
[3] M. I. Gorenstein and S. N. Yang, Phys. Rev. D **52**, 5206 (1995)
[4] A. Ray, S. Sanyal, Phys. Lett. B **726(1-3)**, 83 (2013)
[5] Y. Kumar, JPS Conf. Proc. **26**, 024028 (2019)
[6] J. Engels, J. Fingberg, F. Karsch, D. Miller and M. Weber, Phys. Lett. B **252**, 625 (1990)

Conversion of Axion Photon in Neutron star magnetospheres

Shubham Yadav*, M. Mishra, and Tapomoy Guha Sarkar
Department of Physics, Birla Institute of Technology & Science, Pilani, Pilani Campus
**Corresponding author email id: shubhamphy28@gmail.com*

The detection of axion dark matter could be possible through a narrow radio spectrum given out by neutron stars. In this work, we present how modified Tolman Oppenheimer Volkoff (TOV) system of equations (in the presence of magnetic field) affects the cooling rate and luminosities (photons, neutrinos and axions) within the possible axion mass range. We employ two different equation of states APR, FPS to generate the profiles. We obtain the axions and neutrino emission rate by including the Cooper-pair-breaking formation process (PBF) in the core and Bremsstrahlung process in the crust. We also examine the possibility of axion to photon conversion in the magnetospheres of neutron stars. We further investigate the impact of the magnetic field on the actual observables such as energy spectrum and conversion probability and its implication for X-ray flux.

Keywords: Neutron stars, Axions .

References:

[1] Yadav S, Mishra M, Sarkar TG, and Singh CR. Thermal Evolution and Emission Properties of Strongly Magnetized Neutron Star. 2022. arXiv: 2212.11652.

Formation of iso- and n- propanol in Interstellar medium: A theoretical study

Rachana Singh[1, 2], Manisha Yadav[1, 2], Shivani[2], Parmanand Pandey[1, 2], Aftab Ahamad[2], Pravi Mishra[1, 2]Alka Misra*[1], Poonam Tandon[2]

[1]Department of Mathematics and Astronomy, University of Lucknow, Lucknow, India

[2]Department of Physics, University of Lucknow, Lucknow, India

**Corresponding author email id: alkamisra99@gmail.com*

The emergence of life on Earth is hypothesized to have been initiated by the interstellar delivery of crucial ingredients necessary for life to develop. Alcohols are seen as fundamental building blocks for more intricate organic compounds, and their presence in the interstellar medium is of great interest in the study of the origins of life and the chemical processes occurring in space. The presence of i-Propanol has been observed in interstellar space near Sgr B2(N2), while n-Propanol has been identified in hot cores, with an abundance ratio of 0.6[1].In this study, we propose potential reaction pathways for the formation of both i-Propanol and n-Propanol in the interstellar medium by leveraging molecules primarily detected in interstellar environments. we employed Density Functional Theory (DFT) via Gaussian 16[2] software, allowing us to investigate plausible reaction mechanisms. Thermochemical changes, along with Frontier Molecular Orbital (FMO) analysis, are conducted to elucidate the reaction mechanisms.

References:

[1] A. Belloche, R.T. Garrod, O. Zingsheim, H.S.P. Müller, K.M. Menten, Interstellar detection and chemical modeling of iso-propanol and its normal isomer, Astron. Astrophys. 662 (2022) A110. https://doi.org/10.1051/0004-6361/202243575.

[2] M.J. Frisch et al., Gaussian 16 Rev. C.01, (2016).

Rotational Characteristics of the Sunusing SDO/AIA images at wavelength 1600 Å

Ved Prakash Gupta[1] *, Dr. Vivek Kumar Singh[1], Dr. Satish Chandra[2]
[1]SamHigginbottom University of Agriculture, Technology and Sciences, Prayagraj, [2]Pandit Prithinath (PG) College, Kanpur.
**Corresponding author email id: dr.ved_prakashgupta@rediffmail.com*

Temporal and spatial variations in solar rotation with accurate determination and its correlation with solar activities are interesting topic in solar physics since earlier. Solar rotation can be measured by tracking the tracers across the solar disk, or via spectroscopy, or via flux modulation method using radio waves, X-rays, and UV rays that emitted out in the space. Solar Dynamics Observatory, a space mission of NASA to study the magnetic behavior in the Sun. Onboard instrument SDO/AIA continuously observing the Sun and data can be used to estimate the rotation of solar atmosphere, which in turn provides information about change in solar magnetic field as variation in solar cycle. In present work possible variation in latitudinal solar rotation is estimated using flux modulation method. The SFD images at 1600Å and at a cadence of one image per day, obtained from SDO/AIA have been used for each year of the whole mission period (2011-2023) till now. In flux modulation method, the variation in flux emitted over the latitudinal bin(formed on equally separated latitude region of SFD images that extended from 80^{o}N to 80^{o}S) on solar disc generates annual time series at each latitude. Statistical tool LSP has been used to estimate periodic oscillations present in the time series.Solar Full Disk imageat 1600 Å shows ahighly complex and magnetically structured region lies between chromosphere and upper most layer of solar atmosphere called corona, in this regionphenomenon of rapid rising of temperature from relatively cool photosphere to much hotter corona takes place and this region is also responsible for generating solar wind in which charged particle is streamed outward from Sun to the solar system. Outcome of present work could help to build up the capability of forecasting solar variations that can affect space weather and life on the Earth.

Keywords: Solar rotation, Solar atmosphere, Transition region.

References:

[1] Bose S & Nagaraju K (2018). On the Variability of the Solar Mean Magnetic Field: Contributions from Various Magnetic Features on the Surface of the Sun. The Astrophysical Journal, 862:35 (8pp).
[2] Chandra S, Singh V K & Thomas S (2018). Study of Coronal Rotation using X-ray images observed by Hinode. International Astronomical Union, IAUS, 13(S340), 179-180.
[3] Mariska J T(1992). The Solar Transition Region. Cambridge University Press, Cambridge, 290
[4] Sharma J, Kumar B, Malik A K & Vats H O (2020). On the variation of solar coronal rotation using SDO/AIA observations. MNRAS 492, 5391–5398.
[5] SimõesP,Reid H A S,Milligan R O, & Fletcher L (2019). The Spectral Content of SDO/AIA 1600 and 1700 Å Filters from Flare and Plage Observations. The Astrophysical Journal, 870(2), 114–114

Fourier Ptychographic Microscopy as a metrological tool

Mukul Jaiswal*, Basab Chattopadhyay, Dag W. Breiby
Department of Physics, Norwegian University of Science Technology, Trondheim, 7491 Norway.
**Corresponding author email id: mukul.jaiswal@ntnu.no*

Microscopy is a cornerstone in medical and materials science research and is a field in rapid development. Computational imaging, in conjunction with microscopy, has significantly advanced image quality and information retrieval, circumventing the diffraction limit and offering new functionalities like quantitative phase contrast and post-exposure re-focusing. Recently, Fourier ptychographic microscopy (FPM) has emerged as a new technique, mitigating the trade-off between a wide field of view (FoV) and a high resolution.[1-3] By capturing multiple images from different illumination angles using partially coherent LED illumination, FPM computationally synthesizes high-resolution reconstructions, effectively enhancing the system resolution, while additionally providing quantitative phase information.

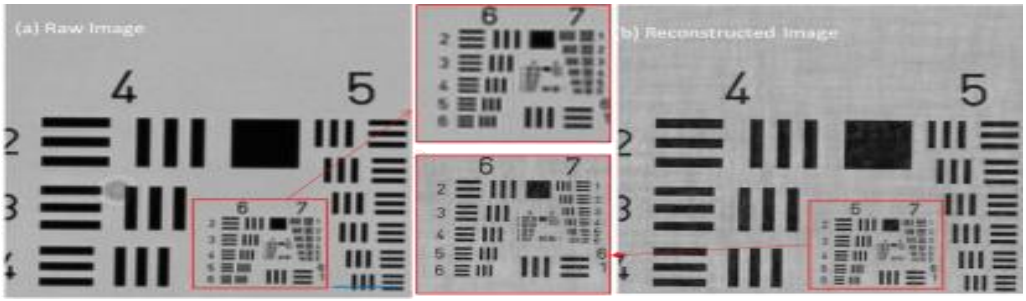

Fig. 1: USAF 1951 target imaging and reconstruction. a) Raw low-resolution image, b) Reconstructed high-resolution amplitude image. A region is zoomed in for clarity.

Here, we present some of our recent efforts towards high-precision metrology of the phase, contrast, and in-plane dimensions of 2D objects like histology.[3] A simple demonstration of the potential of FPM is given in Fig. 1, based on a resolution target. 9x9 low-resolution images were acquired using a 2x/NA 0.055 objective lens. The image quality after reconstruction is readily apparent by visual comparison. In the raw images, element 6 in group 6 can barely be discerned, whereas in the reconstructed image, element 6 in group 7 is clearly resolved. After an introduction to digitalization of microscopy along with machine learning and artificial intelligence, our ongoing efforts towards high-precision microscale measurements will be presented.

Keywords: Fourier Ptychography, Computational imaging, Phase contrast imaging.

References:

[1] Zheng, G., Horstmeyer, R., and Yang, C., (2013), "Wide-field, high-resolution Fourier ptychographic microscopy", *Nat. Photonics* 7(9), 739–745.
[2] Zheng, G., Shen, C., Jiang, S. et al., (2021) "Concept, implementations and applications of Fourier ptychography", *Nat Rev Phys* 3, 207–223.
[3] Tekseth, K.R., et al, (2023), "Mapping surface flaws on float glass through Fourier ptychographic quantitative phase imaging", *Appl. Phys. Lett.* 123, 021108.

Non-classical effects in superposition of three coherent states shifted in phase by an angle $\frac{2\pi}{3}$ to each other

Pankaj Kumar[1,*] and Rakesh Kumar[2]
[1]Department of Physics, Bhavan's Mehta Mahavidyalaya (V. S. Mehta College of Science), Bharwari, Kaushambi (U.P.) -212201, India.
[2]Department of Physics, C. M. P. Degree College, Prayagraj (U.P.)-211002, India.
Corresponding author email id: pankaj_k25@rediffmail.com

Abstract

A coherent state does not exhibit any non-classical effects like squeezing, higher-order squeezing, sub-Poissonian statistics and higher-order sub-Poissonian statistics etc. but superposition of two or more coherent states can exhibit one or more non-classical effects. In this paper we study squeezing of the most general Hermitian operator $X_\theta = X_1\cos\theta + X_2\sin\theta$, in the superposition state $|\psi\rangle = K[|xe^{i\phi}\rangle + |xe^{i(\phi+2\pi/3)}\rangle + |xe^{i(\phi-2\pi/3)}\rangle]$, of three coherent states $|xe^{i\phi}\rangle$, $|xe^{i(\phi+2\pi/3)}\rangle$ and $|xe^{i(\phi-2\pi/3)}\rangle$ shifted in phase by angle $2\pi/3$ to each other. Here Hermitian operators $X_{1,2}$ are defined by $X_1 + iX_2 = a$, the annihilation operator, x is a real number and ϕ is an arbitrary and only restriction on these is normalization condition of the superposed coherent state $|\psi\rangle$. We conclude that the superposed coherent state $|\psi\rangle$ exhibits squeezing of X_θ with some conditions on the parameters x, ϕ and θ, but its maximum squeezing is less than that of even coherent state. We have also studied sub-Poissonian photon statistics in the superposed state $|\psi\rangle$. Variations of variance of X_θ and Mandel's Q parameter with different parameters x, ϕ and θ have also been discussed.

Keywords: Quantum features of light; Coherent state; Squeezing; Displacement operator; Phase shifting operator.

References:

[1] Kumar R, Kumar P and Prakash H (2021), Squeezing of Longitudinal Spin Component in Spin Coherent State, National Academy Science Letters, Vol. 44, 443–445.
[2] Kumar P , Kumar R and Prakash H (2017), Enhancement of the Hong–Mandel Higher-Order Squeezing and Amplitude Odd-Power Squeezing in Even Coherent State by its Superposition with Vacuum State, Acta Physica Polonica A, Vol. 131, 1485-1490.
[3] Kumar P, Kumar R and Prakash H (2016), Simultaneous higher-order Hong–Mandel's squeezing and higher-order sub-Poissonian photon statistics in superposed coherent states, Optik, Vol. 127, 4826-4830.
[4] Kumar P and Kumar R (2013), Simultaneous higher-order Hong and Mandel's squeezing of both quadrature components in orthogonal even coherent state, Optik, Vol. 124, 2229-2233
[5] Prakash H, Kumar R and Kumar P (2011), Higher-order Hong–Mandel's squeezing in superposed coherent states, Optics Communications, Vol. 284, 289-293.

Spectroscopic Study of 3 Planetary Nebulae using *TANSPEC* from 3.6m Devasthal Optical Telescope

Atul Kumar Singh[1*], Arpan Ghosh[2], Rahul Anand[1], Saurabh Sharma[2], Shantanu Rastogi[1]
[1] Department of Physics, Deen Dayal Upadhyaya Gorakhpur University, Civil Lines, Gorakhpur, India 273009
[2]Aryabhatta Research Institute of Observational Sciences (ARIES) Manora Peak, Nainital, India 263001
**Corresponding author email id: atul10j@gmail.com*

This communication presents high-resolution optical and near-infrared spectra obtained during a single epoch for three Planetary Nebulae (PNe) utilizing the TANSPEC instrument mounted on the 3.6m Devasthal Optical Telescope (DOT). TANSPEC's spectral coverage ranges from 0.55 to 2.5 microns, providing a comprehensive view of the nebular features. Employing a narrow-slit technique, discrete regions within the PNe were targeted, revealing dominant H I, H_2, and various metallic lines in the spectra. Additional spectral elements, such as continuum emissions from the central star, C_2, CN, CO emissions, and warm dust continuum emissions, were observed. Comparative analyses of line profiles with existing theoretical predictions and previously published spectra were done,whichallowed us to interpret the physical processes driving the evolution of these PNe and enhance our understanding of their complex nature. This study contributes valuable insights into the composition, structure, and evolutionary dynamics of these celestial objects.

Keywords: Planetary Nebula, TANSPEC, IR- Spectroscopy

Effect of fullerene (C_{60}) on structural, morphological, and optical properties of methyl ammonium lead halide perovskite thin films

Virendra Kumar[1], Hitesh Kumar Sharma[2], Lokendra Kumar[3], Ashwani Kumar[4], Beer Pal Singh[1]
[1]Nanomaterial Laboratory, Department of Physics, C.C.S. University Meerut-250004, India [2]Meerut Institute of Technology, C.C.S. University, Meerut-250103, India
[3] Molecular Electronics Research Lab, Physics Department, Faculty of Science, University of Allahabad, Prayagraj 211002, India
[4]Nanosciencel Laboratory, Institute Instrumentation Centre, IIT Roorkee, Roorkee, 247667, India
**Corresponding author email id: drbeerpal@gmail.com*

In this study, we employed a two-step deposition technique to synthesize pure and Fullerene (C60)-based methyl ammonium lead iodide perovskite ($CH_3NH_3PbI_3$) thin films. The influence of Fullerene (C60) was investigated through X-ray diffraction (XRD), field emission scanning electron microscopy (FE-SEM), and energy-dispersive X-ray analysis (EDAX) on the perovskite thin films. Additionally, we examined the optical band gap of as-deposited Fullerene (C_{60})-based perovskite thin films using absorption and transmittance spectroscopy. The results revealed that the films exhibited a tetragonal crystal structure with compact morphology. By utilizing Williamson-Hall (W-H) analysis and the size-strain plot, we studied the effects of crystallite sizes and lattice strain on the peak broadening in the perovskite thin films. The W H models exhibited a linear fitted positive slope, indicating the presence of tensile strain in the crystal lattice of $CH_3NH_3PbI_3$ and $CH_3NH_3PbI_3$:C_{60}. The compact and extended nature of the Fullerene (C_{60})-based thin films was confirmed through surface morphology analysis and elemental analysis. Furthermore, the absorption spectra of the $CH_3NH_3PbI_3$:C_{60} perovskite thin films displayed maximum absorbance at a concentration of 1mg of C_{60}. These findings provide valuable insights into the structural and optical properties of Fullerene (C_{60})-incorporated perovskite thin films, contributing to the understanding and potential applications of these materials in various fields.

Keywords: Fullerene (C_{60}), Williamson-Hall (W-H) analysis, Size-strain Plot, X-ray diffraction, Elemental composition.

Charge and Mass Movement in alkali Metaborate

K.M. Mishra*, P.K. Pandey, F.Z. Haque[1]
Department of Physics, D.D.U. Gorakhpur University Gorakhpur
[1]Department of Physics, MANIT, Bhopal
**Corresponding author email id: kmmishra02@yahoo.com*

Using a high temperature solid state reaction approach with the oxides of the corresponding alkali metals and B_2O_3 as starting materials, the alkali metaborates $LiBO_2$, $NaBO_2$, and KBO_2 have been produced. Pressed pellets of these compounds' thermoelectric powers (S) and electrical conductivity (σ) is tested in the temperature ranging from the 440K to their respective melting points. Findings have been presented as plots of log σT Vs T^{-1} and log S Vs T^{-1}. It is noted that at a certain temperature for each solid, jumps by a factor of 10^2 and reaches a value on the order of 5 around 1000K. Each solid's S value exhibits an anomaly at a similar temp; this temp. is known as the phase transition temperature (T_P) of that solid. Utilizing a time dependency analysis of dc electrical conductivity, the ionic (σ_i) and electronic (σ_e) components of total conductivity have been assessed. It can be seen that the contribution of σ_i to σ is greater as compared to the 99 percent for every solid over T_P, and that below T_P, although it declines, it still remains near to 96 percent up to 500K.It has been determined, based on these findings, that each of such materials can be found in two distinct phases. Above the transition point, the phase is superionic, and below the transition point, it is mixed conductor. The temp. at which the phase transition occurs, denoted by the symbol T_P, can also be determined from the temp. dependence of magnetic and dielectric susceptibility investigations. In studies of σ, S, magnetic, and dielectric susceptibility, the T_P values have been seen to be consistent across all of these variables.

Keywords: Ionic conductivity, Electrical conductivity, Phase transition temperature, Thermo-electric Power, Electronic conductivity, Dielectric constants, Magnetic Susceptibility

Comparative analysis of the accuracy of two models in the calculation of the thickness of shock waves in condensed materials

M.K. Singh, R. K. Anand
Department of Physics (UGC Centre of Advanced Studies), University of Allahabad, Prayagraj, 211002, India
**Corresponding author email id: mithileshsingh@allduniv.ac.in*

In this work, the Navier-stokes equations of unidirectional magneto-hydrodynamic (MHD) shock waves in condensed-phase materials are solved to determine the thickness of the shock front considering the McQueen and Royce EoS models. For the comparative study of the accuracy of two models, the analytical expressions for the particle velocity, temperature, pressure, change-in-entropy, and bulk modulus within the shock transition region are obtained in view of McQueen and Royce EoS models. In the present study, the thickness of the MHD shock front is computed for titanium Ti6A14V, tantalum, stainless steel 304, aluminum 6061-T6, and oxygen-free high-conductive OFHC copper. Finally, the accuracy and validity of the two models for condensed materials are discussed.

Keywords: MHD, Shock-front thickness, Navier-stokes equation, condensed material

Theoretical investigations of the structural, spectroscopic, electrical, and nonlinear optical properties of the 4-dimethylamino pyridinium p-bromophenolate (4DMAPBP) crystal

Navneeta Kohli, Anuj Kumar
Department of Physics, Chaudhary Charan Singh University Meerut, Uttar Pradesh, India, 250004

The nonlinear optical materials (NLO) have gained great interest in research for applications in photoelectronics and photodevices [1]. In our present work, we have taken 4-dimethylamino pyridinium p-bromophenolate (4DMAPBP) [2] for the structural, spectroscopic, electronic and nonlinear optical behavior studies. All calculations are done using density functional theory (DFT) approach with the help of Gaussian 09W program package [3]. The title compound's dipole moment (μ), polarizability and hyper polarizability computed at 4.171869 Debye, 18.935583 x 10^{-24} esu, and 6.627 x 10^{-30} esu, respectively. Computed value of hyper polarizability is 17 times more than urea (total = 0.1947x10^{-30} esu) which confirms high nonlinear optical behavior of 4DMAPBP. Molecular electrostatic potential (MEP) surface was plotted for predicting active sites and relative reactivity towards electrophilic and nucleophilic attack. NBO analysis is used to explain formation of charge separated regions in the molecule due to the successful migration of electrons from donor to acceptor groups. The lower energy gap in the HOMO and LUMO explains the easier charge transfer interactions that take place within the title molecule. The Global reactivity parameters were also estimated using HOMO-LUMO. The intramolecular charge transfer and high hyperpolarizability show an important correlation between molecular structure and nonlinear optical properties of molecules. A comparison of calculated non-linear optical parameters such asmean polarizability (α_{total}) and first order hyper polarizability (β) of 4DMAPBP with several similar types of molecules has, further, helped in analyzing structure-property relation.

Keywords: Potential Energy Distribution (PED), Molecular Electrostatic Potential (MEP), NBO, HOMO-LUMO, Hyper polarizability.

References:

[1].Bass M, Enoch J M, VanStrylandEW, Wolfe W L (2001). Handbooks of optics IV, fiberoptics and nonlinear optics.2nded...NewYork:McGraw-Hill.

[2].Shalini S, Kirupavathy S S, Jerusha E, & Vinitha G (2018). 4-Dimethylamino pyridinium p-chlorophenolate a novel third order nonlinear optical single crystal: growth and characterization. Journal of Materials Science: Materials in Electronics.29(24), 21145-21156. https://doi.org/10.1007/s10854-018-0263-y

[3].Frisch, M et al. 2009 Gaussian 09, revision D. 01, Gaussian, Inc., Wallingford CT.

Zn(II) complex of diacetate(3,5 dimethyl 1H pyrazol N,N′): Structural, FTIR, NBO, HOMO-LUMO analysis using DFT and its activity against Trypanosoma Cruzi Bacteria

Varsha Rani, Anuj Kumar
Department of Physics, Chaudhary Charan Singh University Meerut, Uttar Pradesh, India, 250004
**Corresponding author email id: versharani91@gmail.com*

Trypanosoma cruzi is the protozoan parasite responsible for the cause of Chagas disease, a potentially devastating condition characterised by cardiac and gastrointestinal manifestations.Azole antimicrobial agents have been discovered to have antitrypanosomal activity by inhibition of ergosterol synthesis.In this present study we have reported theoretical study on molecular structure and FT-IR spectra of bioactive bis(3,5-dimethyl-4-nitro-1H-pyrazol-1-yl) methane (L) and diacetate(3,5-dimethyl-1H-pyrazol-N,N′)zinc(II) complex.Geometry optimization, electronic and biological properties have been calculated by Density Functional Theory (DFT) using(B3LYP)/6-311++g(d,p) basis set with the help of Gaussian 09 program package [1]. Hirshfeld surfaces and (NBO) analysis provides information about inter- and intra-molecular interactions respectively. We have calculated the molecular electrostatic potential (MEP) of titled complex which shows that molecule have several possible sites for electrophillic/nucleophillic attack in order of preference. HOMO-LUMO analysis has been utilized for the calculation of global reactivity parameters which are responsible for the physical, chemical and biological activities. Molecular docking studies verified the inhibitory nature of the title compounds against dihydrofolate reductase-thymidylate synthase (DHFR-TS) (PDB ID: 3HBB) and Trypanothione reductase (TR) (PDB code: 1BZL) proteins[2]. From docking studies we have calculated that the titled Zn complex exhibits binding energy -8.7 kcal/mol and -7.8 kcal/mol, while ligand having the binding energy -7.2 kcal/mol and -7.6kcal/mol with respect to target proteins.Assessment of anti Trypanosoma cruzi properties along with the drug-likeness parameter has revealed good drug-like behaviour of the Zn complex.

Keywords: Density Functional Theory (DFT), FT-IR spectra, Molecular Docking, HOMO-LUMO, Natural bond analysis (NBO)

References:

[1] Frisch, M et al. Gaussian 09, revision D. 01, Gaussian, Inc., Wallingford CT, 2009.
[2] Beaula T.J, Joe I.H, Rastogi V.K., Jothy V. B, (2015), Spectral investigations, DFT computations and molecular docking studies of the antimicrobial 5-nitroisatin dimer, Chem. Phy. Lett. vol. 624, 93-101.

Crystallization of Ge via ALILE process under ion irradiation

G Maity[1,2], T Meher[1], S Dhar[2], S. Ojha[3], R.Singhal[4], T. Som[5,6], D. Kanjilal[3], Shiv P Patel[1*]
[1]Department of Pure and Applied Physics, Guru Ghasidas Vishwavidyalaya (A Central University), Bilaspur-495009, India
[2]Department of Physics, Shiv Nadar University, Gautam Buddha Nagar-201314, India
[3]Inter University Accelerator Centre, Aruna Asaf Ali Marg, New Delhi-110067, India
[4]Department of Physics, Malaviya National Institute of Technology, Jaipur-302017, India
[5]Institute of Physics, Sachivalaya Marg, Bhubaneswar-751005, India
[6]Homi Bhabha National Institute, Training School Complex, Anushakti Nagar, Mumbai-400008, India
**Corresponding author email id: shivpoojanbhola@gmail.com*

To achieve crystallization of amorphous semiconductors at low temperatures, metal contact is made with which the semiconductor forms a eutectic phase known as metal induced crystallization (MIC). Al is used as a catalytic metal for layer exchange mechanism to crystallize semiconductor known as Aluminium Induced Layer Exchange (ALILE) process. In recent, ion beam irradiation have been used as tool to reduce the crystallization temeperature of Si and Ge [1-5]. The ion beam irradiation,athermal process, hasseveral advantages over thermal annealing such as spatial selectivity of samples, high precision, and lower processing time. In the present paper, the c-Al (50 nm)/a-Ge (50 nm) were deposited on thermally oxidized Si substrate utilizing thermal evaporation and e-beam evaporation, respectively. The samples were irradiated under 500 keV Xe^+ and Kr^+ ions at different fluences. A set of ion irradiated samples were post-annealed at 200°C for 6 hrs. The GIXRD confirms that the crystallization of a-Ge is achieved at 200°C at the lowest fluence of 7×10^{14} ions/cm^{-2} and crystallization increases with increasing ion fluence. The temperature dependent-Raman sectra on another set of samples irradiated at a fluence of 1×10^{16} ions/cm^{-2}which confirms the crystallization of a-Ge at 125°C. The crystallization of the sample irradiated with Xe^+ is better than that of Kr^+.

References:

[1] G. Maity, S. Ojha, S. Dubey, P. K. Kulriya, I. Sulania, S. Dhar, T. Som, D. Kanjilal, and Shiv P. Patel, CrystEngComm. **22,** (2020)666.
[2] G. Maity, R. Singhal, S. Ojha, A. Mishra, U. B. Singh,T.Som,S. Dhar, D. Kanjilal, and Shiv. P. Patel, J. Appl. Phys.**132**, (2022)095303.
[3] G. Maity, R. P. Yadav, R. Singhal, P. K. Kulriya,A. Mishra,T. Som, S. Dhar, D. Kanjilal,S. P. Patel.J. Appl. Phys. **129,** (2021) 045301.
[4] G. Maity, S. Dubey, Anter El-Azab, R. Singhal, S. Ojha, P. K. Kulriya, S. Dhar, T. Som, D. Kanjilal, and Shiv P. Patel, RSC Adv. **10**, (2020) 4414.
[5] G. Maity, R. Singhal, S. Dubey, S. Ojha, P. K. Kulriya, S. Dhar, T. Som, D. Kanjilal, and S. P. Patel, J. Non-Cryst. Solids **523,** (2019) 119628.

Effect of heavy metals (Zn and Cu) on growth parameters of Lycopersicum esculentum

Gautam Kumar*, Akrity Bharadwaj* and Justin Masih**
*Research Scholar, Department of Chemistry, Ewing Christian College, Prayagraj
**Associate Professor, Department of Chemistry, Ewing Christian College, Prayagraj
**Corresponding author email id: gkbhuvana111@gmail.com*

Environmental pollution is one of the most debated issues of contemporary times. One of the major effects of industrialization and urbanization is the over production of wastes in all forms and some of these wastes are totally infested and impregnated with toxic metals and heavy metals. One of the current problems of mankind is the accumulation of heavy metals in agricultural soil which can lead to several very detrimental effect on soil, plants and human beings.The aim of this study was to examine the accumulation and distribution of heavy metals(Zn and Cu) and to study their effect on various growth and physiological parameters of tomato plant *Lycopersicum esculentum*. Tomato plants were grown in clay pots containing soil and treated with different concentration (mg/kg soil) of Zinc (Zn; 50, 70 and 90) and Copper (Cu; 40, 60 and 75). The impact of heavy metal toxicity on shoot length, root length, number of leaf and other essential growth and physiological parameters was studied on 0, 18, 36 and 54 days after sowing (DAS). Atomic absorption spectroscopy technique was used to determine the concentration of heavy metalsin different parts of the plants i.e. root, shoot, leaf and fruit. It was observed that an increase in concentration of heavy metals adversely effectedthe growth parameters, chlorophyll content and other physiological parameters of the plants in plants.

Keywords: bioaccumulation, biomass, leaf area index, relative growth rate, heavy metal toxicity.

References:

[1] Murtić, S., Zahirović, Ć., Čivić, H., Karić, L., &Jurković, J. (2018). Uptake of heavy metals by tomato plants (Lycopersicum esculentum Mill.) and their distribution inside the plant. *Agriculture & Forestry/PoljoprivredaiSumarstvo*, *64*(4).

[2] Sbartai, H., Sbartai, I., Djebar, M. R., &Berrebbah, H. (2017). Phytoremediation of contaminated soils by heavy metals-" case tomato". *Acta Horticulturae*, (1159), 95-100.

[3] Rajalakshmi, K., & Banu, N. (2015). Extraction and estimation of chlorophyll from medicinal plants. *International Journal of Science and Research*, *4*(11), 209-212.

[4] Niţu, M., Pruteanu, A., Bordean, D. M., Popescu, C., Deak, G., Boboc, M., & Mustăţea, G. (2019). Researches on the accumulation and transfer of heavy metals in the soil in tomatoes-Solanum lycopersicum. In *E3S Web of Conferences* (Vol. 112, p. 03020). EDP Sciences.

[5] Mukhopadhyay, G. (2018). Atomic spectroscopy analysis of heavy metals in plants. *International Journal of Pharmaceutical & Biological Archives*, *9*(3), 175-179.

TB-mBJLDA approach to analyse structure, electronic and magnetic properties of cation substitution chalcopyrite $ZnMn_xGe_{(1-x)}As_2$

Anuj Kumar[*a,b], Aman Kumar[c], Sandeep Kumar Pundir[d], Nem pal Singh[a]
[a] School of Applied Sciences, Shri Venkateshwara University Gajraula - 244236, Uttar Pradesh, India
[b] Department of Physics, Mahamaya Government Degree College Sherkot, Bijnor - 246747, Uttar Pradesh, India
[c] Department of Physics, Keral Verma Subharti College of Science, Swami Vivekanand Subharti University Meerut, Uttar Pradesh, India
[d] Department of Physics, Lucknow University, Lucknow - 226007, Uttar Pradesh, India
**Corresponding author email id: jayamanlucky@gmail.com*

We have reported a thorough first-principal spin-polarized density functional calculation using linearized augmented plane wave (LAPW) approach for the structure, electronic profile, and magnetic properties of Mn-doped $ZnGeAs_2$. Tran-Blaha's modified Becke-Johnson (TB-mbJ) functional with local density approximation (LDA) utilized for the potential consideration. The structure, electronic and magnetic properties of $ZnMn_xGe_{(1-x)}As_2$ are analysed for the concentration range between $0 \leq X \leq 0.5$. Mn used for selective doping mechanism and replace Ge to develop high magnetism in the compound. The structural properties of doped material are almost similar for $0 \leq X \leq 0.5$. All the five compounds prepared by different Mn concentration show a half-metallic character with a p-type semiconducting nature. It is observed with increases Mn concentration in ZnGeAs2, bandgap increases in down state and up state showing degenerate semiconducting nature with effective zero band gap. The observed bandgap linearly increases with rate 1.85 eV in the range $0 \leq x < 0.25$ and after it decreases with rate of 0.27 eV for further after coming range $0.25 \leq x \leq 0.5$. The local charge density of Mn remains the same and magnetic momentum of all compounds remains unchanged. Mn-doped ZnGeAs2 compounds show a large spin moment and it may have possible applications for spintronics.

Keywords: Supercell, degenerate semiconductor, ferromagnetism

Investigation of structural, morphological, and dielectric properties of Nb-doped $BaTiO_3$ perovskite oxide

Ram Sundar Maurya[1], P. A. Alvi[1], Upendra Kumar[2]
[1]Department of Physical Sciences, Banasthali Vidyapith, Banasthali, Rajasthan, India
[2]Advanced Functional Materials Laboratory, Department of Applied Sciences, IIIT Allahabad, Prayagraj, India
*Corresponding author email id: drpaalvi@gmail.com, upendra.bhu512@gmail.com

The samples with A-site cation ordering $Ba_{1-x/2}Ti_{1-x}Nb_xO_3$ (BTN) with $0 \leq x \leq 0.010$ were synthesized via the conventional ceramic route by calcining at 1200^0C and sintered at 1350^0C. The preliminary study of the phase of prepared samples was determined through X-ray diffraction (XRD) analysis. The Rietveld refinement analysis indicates the tetragonal phase in BTN0 sample, whereas the doped samples exhibit a combination of tetragonal and cubic phases. Presence of Raman band at 308 cm^{-1} suggests the presence of tetragonal in all samples. The dielectric constant was observed to be 1500 (BTN0), 3000 (BTN5) and 1680 (BTN10) while tangent loss found 0.6 (BTN0), 0.04 (BTN5) and 0.07 (BTN10). All the sample shows same Curie temperature (120^0C) due to Ba-site cation ordering in the sample. Ferroelectric nature in all samples was also confirmed by modified Curie-Weis law. Based on the current studies, the present materials can be explored as a potential candidate for ferroelectric-memory devices, dielectric capacitor and energy harvesting applications.

Keywords: $Ba_{1-x/2}Ti_{1-x}Nb_xO_3$, dielectrics, Raman.

References:

[1] Maiti T, Guo R, Bhalla AS. Evaluation of experimental resumeof BaZrxTi1_xO_3 with perspective to ferroelectric relaxor family:an overview. Ferroelectrics. 2011;425:4-26. doi:10.1080/00150193.2011.644168.
[2] Kahn M. Influence of grain growth on dielectric properties ofNb-doped $BaTiO_3$. J Am Ceram Soc. 1971;54:455-457. doi:10.1111/j.1151-2916.1971.tb12384.x.
[3] Jeong CK, Lee JH, Hyeon DY, et al. Piezoelectric energy conversionby lead-free perovskite $BaTiO_3$ nanotube arrays fabricatedusing electrochemical anodization. Appl Surf Sci. 2020; 512:144784 .doi:10.1016/j.apsusc.2019.144784.
[4] Das Mahapatra S, Mohapatra PC, Aria AI, et al. Piezoelectricmaterials for energy harvesting and sensing applications: roadmapfor future smart materials. Adv Sci. 2021;8:2100864. doi:10.1002/advs.202100864.
[5] Mas_o N, Beltr_an H, Cordoncillo E, et al. Synthesis and electricalproperties of Nb-doped BaTiO3. J Mater Chem. 2006;16:3114-3119. doi:10.1039/b601251e.
[6] Ansaree MJ, Kumar U, Upadhyay S. Solid-state synthesis ofnano-sized Ba(Ti_{1_x}Snx)O_3 powders and dielectric propertiesof corresponding ceramics. Appl Phys A. 2017;123:432. doi:10.1007/s00339-017-1047.

Phonon Hydrodynamics in Graphene

Subhalaxmi Nayak, Cho Win Aung, Thandar Jaw Win, Sesha Vempati,Sabyasachi Ghosh
Indian Institute of Technology Bhilai, Kutelabhata, Khapri, Dist. Durg, Chhattisgarh 491001
subhalaxmin@iitbhilai.ac.in ,chowinaung@iitbhilai.ac.in, zawwin@iitbhilai.ac.in,
sesha@iitbhilai.ac.in, sabya@iitbhilai.ac.in

Phonons are the quantum of lattice vibration energy which act like quasi-particles. The interacting phonons depict hydrodynamic behavior at low frequency and long wavelength limits. Nowadays phonon hydrodynamics has become very popular because it has a strong contribution to the electrical and heat transport phenomena in crystalline material. It is an unusual phonon transport phenomenon that challenges the phonon scattering process in crystalline materials. Here, we analytically calculated various thermodynamic quantities like energy density, pressure, number density etc. for phonon hydrodynamics for crystalline graphene and compared them with the corresponding electron hydrodynamics case in graphene. Finally, all the terms corresponding to electrons, holes, and phonon will be added to obtain a general expression for the specific heat capacity. We have analyzed the specific heat capacity versus temperature for various cases and compared it with the traditional Dulong petit law.

Keywords: Phonon Hydrodynamics, Electron Hydrodynamics, Specific heat capacity of solids.

References:

[1] Cepellotti, A., Fugallo, G., Paulatto, L., Lazzeri, M., Mauri, F., & Marzari, N. (2015). Phonon hydrodynamics in two-dimensional materials. *Nature communications*, *6*(1), 6400.
[2] Lucas, A., & Fong, K. C. (2018). Hydrodynamics of electrons in graphene. *Journal of Physics: Condensed Matter*, *30*(5), 053001.

Synthesis and Catalytic Activity of a High Entropy Alloy Al-Cu-Fe-Ni-Ti for the De/Rehydrogenation of MgH_2

Yogesh Kumar Yadav[1], Thakur Prasad Yadav[1, 2], Mohammad Abu Shaz[1]
[1]Department of Physics, Institute of Science, Banaras Hindu University Varanasi, Uttar Pradesh-221005
[2]Department of Physics, University of Allahabad, Prayagraj, Uttar Pradesh-211002
Email: yogesh.yadav@bhu.ac.in (YKY);yadavtp@gmail.com (TPY); mashaaz@gmail.com (MAS)

In the present investigations, Al-Cu-Fe-Ni-Ti high entropy alloy nanoparticles have been used as a catalyst for hydrogen sorption in MgH_2. When MgH_2 is catalyzed by leached Al-Cu-Fe-Ni-Ti high entropy alloy catalyst, the onset desorption temperature drops from 421°C to 200°C. Furthermore, the leached Al-Cu-Fe-Ni-Ti high entropy alloy catalyst also improved the kinetics and absorbing 6 wt. % in 1.6 minutes at 300°C at 15 atm of hydrogen pressure. These are among the lowest MgH_2 desorption temperatures achieved with any other catalyst currently available. The research aims to investigate the hydrogen storage properties of high entropy alloys and to improve MgH_2 hydrogen storage properties using high entropy alloy Al-Cu-Fe-Ni-Ti catalysts. A workable catalytic mechanism of the Al-Cu-Fe-Ni-Ti high entropy alloy on MgH_2 has been proposed based on X-ray diffraction (XRD), transmission electron microscopy (TEM), scanning electron microscopy (SEM), and X-ray photoelectron spectroscopy (XPS) characterization.

Keywords: High Entropy Alloy, Hydrogen Sorption, Catalyst.

References:

[1] Pandey Sunita Kumari, P. Sunita Kumari, Bhatnagar Ashish, B. Ashish, Mishra S. S, M. S. S, Yadav T. P, Y. T. P, Shaz M. A, S. M. A, & Srivastava O. N, S. O. N. (0000). Curious Catalytic Characteristics of Al–Cu–Fe Quasicrystal for De/Rehydrogenation of MgH2. The Journal of Physical Chemistry C, 121, 24936-24944. doi: 10.1021/acs.jpcc.7b07336

[2] Srivastava, O. N., Yadav, T. P., Shahi, R. R., Pandey, S. K., Shaz, M. A., & Bhatnagar, A. S. H. I. S. H. (2015, September). Hydrogen energy in India: storage to application. In Proc Indian Natl SciAcad (Vol. 81, No. 4, pp. 915-937).

[3] Yadav, T. P., Kumar, A., Verma, S. K., & Mukhopadhyay, N. K. (2022). High-entropy alloys for solid hydrogen storage: Potentials and prospects. Transactions of the Indian National Academy of Engineering, 1-10.

Quantum transport and Shubnikov-de Haas (SdH) oscillations in $ZrTe_5$: An Experimental Study

Sanskar Mishra[1], Rajan Waliya[2], Dilip Bhoi[3], Prashant Shahi[1*], J-G Cheng[4], Yoshiya Uwatoko[3]
[1] Department of Physics, DDU Gorakhpur University, Gorakhpur, India
[2]University of Allahabad, Prayagraj, India
[3] Institute of Solid-State Physics, University of Tokyo, Tokyo, Japan
[4]Institute of Physics, Chinese Academy of Sciences, Beijing, China
**Corresponding author email id: prashantitbhu.shahi@gmail.com*

The electrical properties of any material system are quite sensitive to the states in immediate vicinity of the Fermi surface and therefore the knowledge of shape of Fermi surface, its energy dispersion and nearby statesare always important for any material system [1]. At very low temperature and in presence of strong magnetic field for pure materials, the electronic orbit is quantized called "Landau Quantization". Under the favorable conditions this quantization can be observed experimentally by measuring resistivity called Shubnikov-de Haas (SdH) oscillation or by susceptibility called de Haas-van Alphan (dHvA) oscillation. These observed oscillations rely on the interplay between Fermi surface and orbital quantization in presence of Magnetic field [2]. $ZrTe_5$ is topological material which hosts a large number of strange properties like peak in resistivity, sudden sign reversal in thermopower, non-saturating high magnetoresistance, topological phase transition etc [3]. It is the first candidate for the experimental realization of 3D Quantum Hall effect (QHE) [4]. All of the observed properties of this material are somewhere related to its complex nature of Fermi surface. In the present study we aim to figure out some properties of its Fermi surface by direct observation of Shubnikov de Haas (SdH) Oscillations at different temperature. The single crystals used for this study have been grown by Chemical Vapor Transport (CVT) method [3]. With the careful fitting of longitudinal and Hall resistivity of this sample we try to estimate the mobility and density of carriers. The above study offers valuable insights into the transport mechanism within the ZrTe5 system, potentially shedding light on the long-standing anomalous behavior observed in this material.

Keywords: Fermi Surface, Landau Quantization, Shubnikov de-Haas(SdH) oscillation.

References:

[1] G. N. Kamm, D. J. Gillespie, A. C. Ehrlich, T. J. Wieting, and F. Levy, "Fermi surface, effective masses, and Dingle temperatures of ZrTe5 as derived from the Shubnikovde Haas effect," *Phys. Rev. B*, vol. 31, no. 12, pp. 7617–7623, 1985, doi: 10.1103/PhysRevB.31.7617.
[2] Z. Ren, A. A. Taskin, S. Sasaki, K. Segawa, and Y. Ando, "Large bulk resistivity and surface quantum oscillations in the topological insulator Bi2 Te2 Se," *Phys. Rev. B - Condens. Matter Mater. Phys.*, vol. 82, no. 24, pp. 1–4, 2010, doi: 10.1103/PhysRevB.82.241306.
[3] P. Shahi *et al.*, "Bipolar Conduction as the Possible Origin of the Electronic Transition in Pentatellurides: Metallic vs Semiconducting Behavior," *Phys. Rev. X*, vol. 8, no. 2, pp. 1–13, 2018, doi: 10.1103/PhysRevX.8.021055.
[4] F. Tang *et al.*, "Three-dimensional quantum Hall effect and metal–insulator transition in ZrTe5," *Nature*, vol. 569, no. 7757, pp. 537–541, 2019, doi: 10.1038/s41586-019-1180-9.

Studies on Structural and Dielectric properties in Zr doped (1-x) $BaTiO_3$ – (x)$BiFeO_3$ Ceramics

Siddharth Pratap Singh*, Sindhu Singh, Anil Kumar
Material Synthesis Laboratory, Department of Physics and Electronics, Dr. Rammanohar Lohia Avadh University, Ayodhya 224001
*Corresponding author email id: physicistsiddharthsingh@gmail.com

In the current work, the bulk $\{Ba_{0.7}\ Bi_{0.3}\}\ \{(Ti_{0.7-y}\ Zr_y)\ Fe_{0.3}\}\ O_3$ with y = 0.0, 0.2, 0.3, 0.4 has been synthesized using the solid-state reaction method. The structural analysis reveals the formation of single-phase solid solution in the above composition. The crystal structure was found to be cubic for $x \leq 0.3$, while it becomes tetragonal for composition x = 0.4. Dielectric study shows the shift in T_C and decreases in the peak value with increased doping.

Keywords: Complex Perovskites, Solid state reaction, XRD, Dielectric properties

Comparison of Supercapacitive Performance of V_2O_5, CeO_2 and ZnO Thin Films

Jyoti Jangra, Sweety, Neelam, Amit Sanger*
Department of Physics, Netaji Subhas University of Technology, Azad Hind Faug Marg, Dwarka Sector 3, Delhi-110078
**Corresponding author email id: amit.sanger@nsut.ac.in*

Supercapacitors are attracting as it has fast charging discharging speed, long cycle life, high specific power and the ability to bridge the gap between batteries and capacitors. Supercapacitors can be of many types but we have compared three pseudo capacitors in which metal oxides are used as electrodes (Vanadium Oxide, Cerium Oxide and Zinc Oxide) which stores charges via fast redox reactions. We have prepared V_2O_5, CeO_2 and ZnO thin films by sputtering process in which plasma is created by ionization of pure gas i.e., Argon by means of potential difference. The characterizations are studied using X-Ray Diffraction, Field emission Scanning electron Microscopy, X-Ray Photoelectron Spectroscopy and the super capacitive property of the films were studied by cyclic voltammetry in electrolyte (0.5M Li_2SO_4in CeO_2, 1M Na_2SO_4 in V_2O_5, and 1M KOH in ZnO).

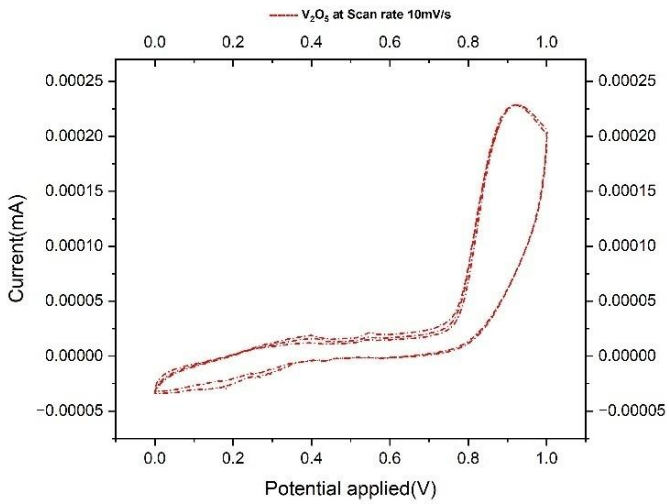

Figure: *Cyclic Voltammetry of 1M Na_2SO_4 in V_2O_5at Scan Rate 10mV/s*

Keywords: supercapacitor, thin film, sputtering

References:

[1] Sachin Kumar, Ghuzanfar Saeed, Ling Zhu, Kwun Nam Hui, Nam Hoon Kim, Joong Hee Lee (2021). 0D to 3D carbon-based networks combined with pseudocapacitive electrode material for high energy density supercapacitor: A review. Chemical Engineering Journal 403 (2021) 126352.

[2] Poonam, Kriti Sharma, Anmol Arora, S.K. Tripathi (2019). Review of supercapacitors: Materials and devices. Journal of Energy Storage 21 (2019) 801–825.

Drug descriptors with respect to CNTs diameters: An *ab initio* analysis

Neha Mishra and M. K. Dwivedi
Department of Physics, D.D.U. Gorakhpur University, Gorakhpur-273009, (U.P.)
**Corresponding author email id: mneha7109@gmail.com*

Carbon nanotubes (CNTs) are now adequate to cover almost all the fields of science and technology, including medical sciences. CNTs are cytotoxic, and hence their isolated drug behaviors are crucial. We have utilized Gaussian 09 with 6-31G* basis set using the Hartee-Fock method to calculate the drug descriptors like HOMO-LUMO gap, chemical potential, electron affinity, electrophilicity index, etc. for some CNTs. We have also calculated molar refractivity and logP through freely available code at http://www.scfbio-iitd.res.in/. The calculated values provide an understanding of the thermodynamical parameters and the nature of the interactions of the CNTs with living tissues and other biomaterials. Currently, we have found that the HOMO-LUMO gap and chemical potential decrease with respect to the radius of CNTs. In addition, we have also found that parameters like electron affinity, electrophilicity index, molar refractivity, and logP increase with CNT radii. Therefore, as the radius of CNT increases, it becomes more electrophilic, polarizable, and lipophilic. However, reactivity and binding interaction energy decreases as the radius increases.

Keywords: CNT, Hartee-Fock method, basis set, drug descriptors, Gaussian09.

References:

[1] Cook, G., & Dickerson, R. H. (1995). Understanding the chemical potential. *American Journal of Physics*, *63*(8), 737–742. https://doi.org/10.1119/1.17844
[2] Luo, J., Peng, L. M., Xue, Z. Q., & Wu, J. L. (2004). Positive electron affinity of fullerenes: Its effect and origin. *Journal of Chemical Physics*, *120*(17), 7998–8001. https://doi.org/10.1063/1.1691397
[3] Parthasarathi, R., Subramanian, V., Roy, D. R., & Chattaraj, P. K. (2004). Electrophilicity index as a possible descriptor of biological activity. *Bioorganic and Medicinal Chemistry*, *12*(21), 5533–5543. https://doi.org/10.1016/j.bmc.2004.08.013
[4] Sawant, P. D., Luu, D., Ye, R., & Buchta, R. (2010). Drug release from hydroethanolic gels. Effect of drug's lipophilicity (logP), polymer-drug interactions and solvent lipophilicity. *International Journal of Pharmaceutics*, *396*(1–2), 45–52. https://doi.org/10.1016/j.ijpharm.2010.06.008
[5] Slater, J. C. (1951). A simplification of the Hartree-Fock method. *Physical Review*, *81*(3), 385–390. https://doi.org/10.1103/PhysRev.81.385.

Structural and Optical Studies on $FAPbI_3$ and $FASnI_3$ Perovskite Thin Films

Ashok Vishwakarma and Lokendra Kumar*
Physics Department, University of Allahabad, Prayagraj-211002, U.P. India
**Corresponding author email id: lokendrakr@allduniv.ac.in*

Hybrid metal halide perovskites are suitable candidate for cost effective perovskite solar cells owing to its outstanding optoelectronic properties like high absorption coefficient, charge carrier mobility and suitable bandgap. We have fabricated lead based $FAPbI_3$ and lead free $FASnI_3$ perovskite thin films and its structural and optical properties has been studied by X-ray diffraction (XRD) and UV visible spectroscopy respectively. XRD pattern of $FAPbI_3$ film shows cubic α-phase $FAPbI_3$ perovskite and $FASnI_3$ film shows orthorhombic crystal structure. UV-visible spectra show complete absorption of visible spectrum for both $FAPbI_3$ and $FASnI_3$ perovskite films with suitable optical bandgap of 1.50eV and 1.37eV respectively. A high quality perovskite films are crucial to enhance photovoltaic performance of perovskite solar cells.

Keywords: Perovskite solar cells, lead free perovskite

References:

[1] Kim G., Min H., Lee K. S., Lee D. Y., Yoon S. M., Seok S. I. (2020), Impact of strain relaxation on performance of α-formamidinium lead iodide perovskite solar cells, Science 370, 108–112.
[2] Meng X, Lin J, Liu X, He X, Wang Y, Noda T, Wu T, Yang X, and Han L. (2019), Highly Stable and Efficient FASnI3-Based Perovskite Solar Cells by Introducing Hydrogen Bonding, Adv. Mater., 31, 1903721.
[3] Zhu Z., Jiang X., Yu D., Yu N., Ning Z. and Mi Q. (2022), Smooth and Compact FASnI3 Films for Lead Free Perovskite Solar Cells with over 14% Efficiency, *ACS Energy Lett.*, 7, 6, 2079–2083.
[4] Fan Y., Meng H., Wang L. and Pang S. (2019), Review of Stability Enhancement for Formamidinium Based Perovskite, Sol. RRL, 3, 1900215.

Internal Structure of MHD Shock Waves in a Two-Phase Gas-Particle Mixture: Awave front Approach

Anmol Singh*, R. K. Anand
Department of Physics (UGC Centre of Advanced Studied) University of Allahabad, Prayagraj-211002, India
**Corresponding author email id: anmolsingh@allduniv.ac.in*

We have solved the Navier-Stokes equations in a two-phase gas-particle mixture [1-2] to investigate the internal structure of magnetohydrodynamic MHD shock waves using wave-front approach [3]. The analytical expressions of gas dynamical variables, *i.e.*, particle velocity, temperature, pressure, and change-in-entropy distributions, have been derived within the shock transition region. Furthermore, we explored the effects on the structure of the shock-front due to the various parameters, such as the dynamical pressure (or viscosity), dust particles, ratio of specific heats of the mixture, Mach number, magnetic field, etc., on the shock formation distance within the shock transition region. The wave profiles are plotted and used to estimate the thickness of the MHD shock-front. The distributions of flow variables in theshock transition region have been discussed through figures and tables. The obtained analysis indicates that all the flow variables show considerable effects due to parameters throughout the shock formation zone. The present findings show that the mentioned flow fluid medium provides more reliable predictions about the internal structure of the shock-front in actual environments, as well as providing complete information for understanding this complex physical phenomenon in geophysical and astrophysical media.

Keywords: MHD Shock Waves; Shock-front Analysis; Dusty gas; Magnetic Field.

References:

[1] PaiS I, MenonS, & Fan ZQ(1980). Similarity solution of a strong shock wave propagation in a mixture of a gas and dust particles. Int. J. Eng. Sci.,18,1365-1373.
[2] Hamad H(1998). Behavior of entropy across shock waves in dusty gases.Z Angew Math Phys., 49 827-837.
[3] Anand R K, &Yadav, H C(2014). On the structure of MHD shock waves in a viscous non- ideal gas. Theor. Comput. Fluid Dyn. 28, 369-376.

Hydrogen Evolution Activity of Impurity-doped Triangulene GQD: A First Principles Study

Ashvin Kanzariya*[1], Shardul Vadalkar[2], L. K. Saini[1]and Prafulla K. Jha[2]
[1]Department of Physics, Sardar Vallabhbhai National Institute of Technology, Surat, Gujarat, India – 395007
[2]Department of Physics, Faculty of Science, The Maharaja Sayajirao University of Baroda, Vadodara, Gujarat, India – 390002
**Corresponding author email id: kanzariyaashvinbhai@gmail.com*

The hydrogen evolution reaction (HER) is a crucial electrochemical process for sustainable energy applications, such as hydrogen fuel production. Single atom catalysts[1] such as Platinum is highly efficient in catalyzing the HER, but encumbered by high cost, limited availability, susceptibility to poisoning, durability issues, and the persistent quest for alternative catalyst materials. Triangulene[2] is known for its unique electronic and structural properties, making it an intriguing candidate for catalytic applications.This study investigates the HER activity of pristine triangulene and triangulene molecules doped with boron (B), nitrogen (N), silicon (Si), phosphorus (P), and sulfur (S) atoms using density functional theory (DFT) calculations.IR spectroscopy offers complementary insights into the stability of pristine and doped triangulenegraphene quantum dots (GQDs). The interaction between an adsorbed hydrogen (H) atom and the GQDs is discerned through the analysis of binding energy,structural changes, Mullikan charge transfer, Induced dipole moment, shift in HOMO-LUMO electron density, and changes in the density of states (DOS) as well as employing techniques such as Quantum Theory of Atoms in Molecules (QTAIM), Non-Covalent Interaction (NCI) analysis, and Natural Bond Orbital (NBO) analysis.For effective Hydrogen Evolution Reaction (HER) activity, a small adsorption distance and minimal change in Gibbs free energy (ΔG_H) are essential. Unfortunately, pristine triangulene doesn't meet these criteria, as it has a high ΔG_H of 1.17 eV, making it unsuitable for HER.However, when we dope Si, P, and S onto the triangulene, we achieve significantly lower ΔG_H values of 0.05 eV, 0.02 eV, and 0.03 eV, respectively. This indicates their strong potential as catalysts for HER, as more active sites are created.These findings should inspire researchers to design and fabricate efficient, cost-effective GQDsfor HER applications.

Keywords: HER; Triangulene GQD; Density Functional Theory; Gibbs free energy;doping

References:

[1] A. Eftekhari, Electrocatalysts for hydrogen evolution reaction, Int. J. Hydrogen Energy. 42 (2017) 11053–11077. https://doi.org/10.1016/j.ijhydene.2017.02.125.
[2] V. Sharma, H.L. Kagdada, J. Wang, P.K. Jha, Hydrogen adsorption on pristine and platinum decorated graphene quantum dot: A first principle study, Int. J. Hydrogen Energy. 45 (2020) 23977–23987. https://doi.org/10.1016/j.ijhydene.2019.09.021.

On the Superhalogen Nature of $CH_{4-n}(BO_2)_n$ (n = 1-4) Molecules: A DFT Investigation

Jitendra Kumar Tripathi* and Ambrish Kumar Srivastava
Department of Physics, Deen Dayal Upadhyaya Gorakhpur University, Gorakhpur, 273009, Uttar Pradesh, India
**Corresponding author email id: jeettri432@gmail.com*

In this paper, we present a comprehensive investigation on the superhalogenbehavior of $CH_{4-n}(BO_2)_n$ molecules, where n varies from 1 to 4. Superhalogens are molecules or complexeswhose electron affinities (EAs) or vertical detachment energies (VDEs) is greater than that of chlorine (3.6 eV)[1]. They have received significant attention due to their potential applications in various fields, including catalysis and materials science etc. Our study employs the density functional theory (DFT) approach with the B3LYP [2,3] exchange-correlation functional and the 6-311++G(d,p) basis setusing the Gaussian 09 program [4].To analyze the superhalogenbehavior of these $CH_{4-n}(BO_2)_n$ molecules, we computed VDEs. Our findings highlightintrensting trends in the VDEs, providing valuable insights into the electron-capturing capabilities of these species. Specifically, the calculated VDE values for $CH_3(BO_2)^-$, $CH_2(BO_2)_2^-$, $CH(BO_2)_3^-$, and $C(BO_2)_4^-$ complexes are determined to be 4.90 eV, 5.67 eV, 5.64 eV, and 6.26 eV, respectively. These VDE valuesare higher than that of the electron affinity (EA) of chlorine,emphasizing the superhalogen nature of these organic compounds.These findings significantly advance our understanding of organic superhalogens and their potential applications in various fields.

Keywords: Organic Superhalogens, Density Functional Theory, Vertical Detachment Energies.

References:

[1] Gutsev, G. L., Boldyrev, A. I.. (1981) DVM-X_α calculations on the ionization potentials of MX_{k+1}^- complex anions and the electron affinities of MX_{k+1} "superhalogens". Chemical Physics, 56(3), 277-283.
[2] Becke, A. D. (1988). Density-functional exchange-energy approximation with correct asymptotic behavior. Physical review A, 38(6), 3098.
[3] C. Lee, W. Yang and R.G. Parr,(1988) Phys. Rev. B. 37, 785–789.
[4] Frisch, M. J., Trucks, G. W., Schlegel, H. B., Scuseria, G. E., Robb, M. A., Cheeseman, J. R., and Fox, D. J. (2009). 09, Revision D. 01, Gaussian. Inc., Wallingford, CT.

Temperature Dependent Electrical Characterization of Sb doped $Cs_3Bi_2I_9$ Single Crystals

Bharti[a], Anil K. Sharma[b], Jitendra Yadav[b], Ambreesh Kumar[b], Topeswar Meher[a], Dhirendra K. Chaudhary[b]*, Shiv P. Patel[a]*

[a] Department of Pure and Applied Physics, Guru Ghasidas Vishwavidyalaya, Bilaspur, 495009, India

[b]Centre of Renewable Energy, Prof. Rajendra Singh (Rajju Bhaiya) Institute of Physical Science for Study and Research, V. B. S. Purvanchal University, Jaunpur, 222003, India

**Corresponding author email id: phydhiren@gmail.com,shivpoojanbhola@gmail.com*

Lead-free perovskite single crystals have emerged as promising materials in various technological applications due to their eco-friendly nature and unique electronic properties. herein, single crystals of $Cs_3Bi_2I_9$ and $Cs_3Bi_2I_9$ doped with antimony (Sb) has been grown using inverse temperature crystallization with crystal size 4 to 5 mm. The physicochemical characterization of as synthesized crystals has been performed by various techniques such as Raman spectroscopy, X-ray diffraction (XRD), and UV-Vis. spectroscopy. Furthermore, the research delved into the intricate relationship between temperature and the electrical properties of these crystals. By subjecting the samples to a range of temperatures from 25°C to 135°C, the study systematically explored the variations in electronic behavior, both in doped and undoped conditions. This comprehensive analysis provided profound insights into the influence of temperature on the material's electronic characteristics. The outcomes of this study significantly enhance our understanding of the potential applications of these lead-free perovskite single crystals, particularly in electronic devices designed to function effectively across fluctuating temperature conditions.

References:

[1] Chaudhary, D. K., Dhawan, P. K., Patel, S. P., & Bhasker, H. P. (2021). Large area semitransparent inverted organic solar cells with enhanced operational stability using TiO2 electron transport layer for building integrated photovoltaic devices. *Materials Letters*, *283*, 128725.

[2] Ghosh, D., Chaudhary, D. K., Ali, Y., Chauhan, K. K., Prodhan, S., Bhattacharya, S., Barun Ghosh, D., Ray, P. K. , S. C., Bhattacharyya, S.; All-inorganic quantum dot assisted enhanced charge extraction across the interfaces of bulk organo-halide perovskites for efficient and stable pin-hole free perovskite solar cells; Chem. Sci., 2019, 10, 9530-954.

[3] Tailor, N. K., & Satapathi, S. (2020). Structural disorder and spin dynamics study in millimeter-sized all inorganic lead-free cesium bismuth halide perovskite single crystals. *ACS Applied Energy Materials*, *3*(12), 11732-11740.

[4] Wei, S., Tie, S., Shen, K., Zeng, T., Zou, J., Huang, Y., ... & Wu, J. (2021). High-Performance X-Ray Detector Based on Liquid Diffused Separation Induced Cs3Bi2I9 Single Crystal. *Advanced Optical Materials*, *9*(22), 2101351.

[5] Chonamada, T. D., Dey, A. B., & Santra, P. K. (2019). Degradation studies of Cs3Sb2I9: a lead-free perovskite. *ACS Applied Energy Materials*, *3*(1), 47-55.

Junction depth and profile studies for fabrication of Fine pixel pitch diodes in HgCdTe

Shring Jaiswal[1,2,*], Vanya Srivastav[2], Meenakshi Asthania[2], Gyanendra Sheoran[1]
[1]National Institute of Technology Delhi
[2]Solid State Physics Laboratory, DRDO
Corresponding author email id: shringjaiswal@nitdelhi.ac.in

$Hg_{1-x}Cd_xTe$ is an important II-VI semiconductor material used for the fabrication of Infrared Focal plane arrays (IRFPAs) with fine pitch and high pixel density. Two major device configurations p-on-n heterojunctions and n-on p homojunctions are being used for commercial production of these FPAs. We are using the n-on-p homojunction approach at SSPL because of standardization of the indigenous growth and fabrication technology. Generally, Boron (B^+) or Beryllium (Be^{2+}) ions are implanted to create homojunction n-on-p photodiodes in HgCdTe. The implantation process creates a shallow 0.5-1.0µm n-type region on HgCdTe surface. The junction is annealed to drive in the donor atoms. Present paper is for feasibility studies on the fabrication of 10/12 µm pixel pitch diodes in n-on-p configuration on HgCdTe for futuristic applications. A double dose of Boron ions was implanted in HgCdTe wafer with energy 130keV and 50keV @ 5×10^{13} ions/cm^2. Annealing studies were subsequently done to study the junction depth, profile and lateral extent. The Hall effect and resistivity have been measured in liquid-phase-epitaxial (LPE) HgCdTe layers at both room (300K) and liquid nitrogen (77K) temperatures [1]. The composition of the material covers the wavelength range from 3 to 5µm [2]. The process involves chemical etching of the thin (~0.1µm) layers of HgCdTe in dilute Bromine-Methanol (0.1%) solution followed by measurement of sheet resistance, depth profiles of active dopants, carrier concentration, mobility and type of carriers using differential Hall technique. Fig.1 shows the extracted junction depth and carrier profiles in one such case of annealing at 120°C for 90 minutes in nitrogen ambient. Selective-area ion implantation using a positive photoresist as the masking layer is used for the formation of n-on-p junction. Controlled experiments have been carried out to study the effect of masking on lateral extent of the junction which will determine the ultimate pixel pitch attainable using this technology.

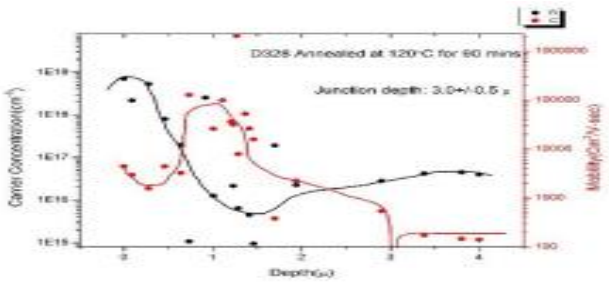

Fig.1: Variation of the carrier concentration and mobility with respect to the etch depth of the sample

Keywords: Differential Hall Effect, Mercury Cadmium Telluride, Resistivity, Hall Coefficient

References:

[1] Lou & Frye (1984). Hall effect and resistivity in liquid-phase-epitaxial layers of HgCdTe. J. Appl. Phys. 56, 2253–2267.
[2] Rogalski, Antoszewski, & Faraone (2009). Third-generation infrared photodetector arrays. J. Appl. Phys. 105(9).

Photophysical study on the fluorescence characteristics of 2,6-dihydroxy 4-methyl quinoline in polymeric micro-environment and neat solvents: Steady state, Time-resolved, and Computational (DFT/T-DFT, Molecular Docking) study

Rakesh Joshi[1],Shahid Husain[1], Nisha Fatma[1], Nupur pandey[1], Sanjay Pant[1*], and Hirdyesh Mishra [2*]
[1]Photophysics Laboratory, Department of Physics, Centre of Advanced Study, DSB Campus, Kumaun University, Nainital- 263002, India.
[2]Physics Section MMV, Department of Physics, Banaras Hindu University, Varanasi-221005, India.
**Corresponding author email id: hmishra@bhu.ac.in, sanjayphotophys@gmail.com*

In the present paper work we report the spectral, decay and photophysical properties of 2,6-dihydroxy 4-methyl quinoline in a few polymer (PVA, PVC, PMMA and CA) matrices. The effect of polymers: polarity, proticity and free volume has been studied by steady state and time resolved measurements. Absorption spectra are nearly identical for all the polymers but the emission spectra shows some shift in these polymers. Observed multi-exponential decays are explained on the basis of free as well as hydrogen-bonded species and also trapping in various excited state geometries of the matrix. Besides,the molecule 2,6-dihydroxy4-methylquinoline is characterized by theoretically also using fluorescence spectroscopy in several polar and non-polar solvents. Both the absorption and fluorescence spectra displayed solvatochromism. Experimental calculations are compared to the computed FT-IR, FT-Raman, and UV–vis spectra. Theoretical and observed spectra are found to be very comparable. Various polar protic and polar aprotic solvents are used to investigate the electronic solvation properties of the title compound using the TD-DFT/IEFPCM model (B3LYP for UV–Vis, NBO, NLO, HOMO-LUMO and MEP). The occurrence of charge transfer in a molecule is explained by Natural Bond Orbital (NBO) analysis [1].The title compound's kinetic stability and reactivity are demonstrated using thermodynamic, Fukui function, MEP, and Frontier Molecular Orbital (FMO) functions. The substance under research has excellent NLOproperties.Molecular docking studies are used to investigate ligand–protein interactions, and to show the insulin inhibitor activity of the chemical under research [2].

Keywords: DFT/TD-DFT, Electronic spectra, HOMO-LUMO, NBO, NLO.

References:

[1] S. Xavier, S. Periandy& S. Ramalingam (2015).*NBO, conformational, NLO, HOMO-LUMO, NMR and electronic spectral study on 1-phenyl-1-propanol by quantum computational methods*. Spectrochimica Acta Part A: Molecular and Biomolecular Spectroscopy, 137, 306-320.

[2] A. Saral, P. Sudha, S. Muthu, S. Sevvanthi & A. Irfan (2022). *Molecular structure spectroscopic Elucidation, IEFPCM solvation (UV-Vis, MEP, FMO, NBO, NLO), molecular docking and biological assessment studies of lepidine (4-Methylquinoline)*. Journal of Molecular Liquids, 345, 118249.

Targeting Multiple G-quadruplex DNA: A Molecular Dynamics Study of Perylene Di-imide in Explicit Solvent

Vandana Mishra[1], Rakesh Kumar Tiwari[2*]
Deen Dayal Upadhyaya Gorakhpur University Gorakhpur, U.P., India
Department of Physics, Deen Dayal Upadhyaya Gorakhpur University Gorakhpur, U.P. India
**Corresponding author email id: drrkt@yahoo.com*

It is well known that the guanine quadruplex molecule (G-DNA) are arguably the most important non canonical DNA structure. It have a potential anti cancer significance and several compound have been discovered and evaluated as favorable G-quadruplex binder with anti cancer activity. Here starting from a promising hit with a perylene di-imide, which is binding of terminal telomeric G-quadruplex inhibiting terminal. In this study we performed a total of 100ns molecular dynamics binding simulation of perylene di-imide to the DNA duplex and two G quadruplex in explicit solvent. finally molecular dynamics simulation help to explain the stabilization effect of selected compound.

References:

[1] Routh ED, Creacy SD, Beerbower PE, Akman SA, Vaughn JP, Smaldino PJ (March 2017). "A G-quadruplex DNA-affinity Approach for Purification of Enzymaticacvly Active G4 Resolvase1". Journal of Visualized Experiments. **121** (121). *doi*:*10.3791/55496*. *PMC5409278*. *PMID 28362374*

[2] Largy E, Mergny J, Gabelica V (2016). "Chapter 7. Role of Alkali Metal Ions in G-Quadruplex Nucleic Acid Structure and Stability". In Astrid S, Helmut S, Roland KO S (eds.). *The Alkali Metal Ions: Their Role in Life (PDF)*. Metal Ions in Life Sciences. Vol. 16. Springer. pp. 203–258. *doi*:*10.1007/978-3-319-21756-7_7*. *PMID 26860303*

[3] Sundquist WI, Klug A (December 1989). "Telomeric DNA dimerizes by formation of guanine tetrads between hairpin loops". Nature. **342** (6251): 825–9. *Bibcode*:*1989Natur.342..825S*. *doi*:*10.1038/342825a0*. *PMID 2601741*. *S2CID 4357161*

[4] Sen D, Gilbert W (July 1988). "Formation of parallel four-stranded complexes by guanine-rich motifs in DNA and its implications for meiosis". Nature. **334** (6180): 364–6. *Bibcode*:*1988Natur.334..364S*. *doi*:*10.1038/334364a0*. *PMID 3393228*. *S2CID 4351855*

Large hyperpolarizability and nonlinear optical activity of the adsorbed complex of *para*-aminobenzoic acid and 7-diethylamino 4-methyl coumarin

Shradha Lakhera, Kamal Devlal, Meenakshi Rana*
Department of Physics, School of Sciences, Uttarakhand Open University, Haldwani, 263139, Uttarakhand, India
Corresponding author email id: mrana@uou.ac.in

Previously, we have experimentally investigated the optical limiting activity and large nonlinearity of *para*-aminobenzoic acid and 7-diethylamino 4-methyl coumarin [1,2]. The large values of hyperpolarizability of $29.99\times10^{-30}$and 18.46×10^{-30} esu were obtained for *para*-aminobenzoic acid and 7-diethylamino 4-methyl coumarin. Additionally, the optical limiting threshold was found to be 1.64×10^{13} W/m^2 and 2.04×10^{13} W/m^{2}for *para*-aminobenzoic acid and 7-diethylamino 4-methyl coumarin. Motivated by the results, herein we have reported the nonlinear optical characteristics of a combination of *para*-aminobenzoic acid and 7-diethylamino 4-methyl coumarin.

The combined complex of both molecules was designed. The amino and carboxyl groups were observed to behave as strong donor and acceptor sites in the complex. The band gap of the adsorbed complex (3.6 eV) was found more suitable.The value of first-order hyperpolarizabilityof the complex (94.75×10^{-30} esu)suggests the improved nonlinear optical responses of the introduced complex. Additionally, the negative value of second-order hyperpolarizability suggests the possibility of the occurrence of reverse saturable absorption in the complex [3]. The reported work gives theoretical insights into the nonlinear optical properties of the combination of *para*-aminobenzoic acid and 7-diethylamino 4-methyl coumarin. Thus, the reported work makes a strong foundation for pursuing the experimental work with the combination of two compounds *para*-aminobenzoic acid and 7-diethylamino 4-methyl coumarin.

Keywords: adsorption; benzoic acid; hyperpolarizability; Nonlinear optics; coumarin

References:

[1] Lakhera, S, Rana M, Devlal K, Sharma S, Chowdhury P, Dhuliya V, Panwar S, Purohit LP, Dhanusha A, Girisun TC (2023) Exploring the Nonlinear Optical Limiting Activity of Para-Aminobenzoic Acid by Experimental and DFT Approach. Journal of Photochemistry and Photobiology A: Chemistry, 114987. https://doi.org/10.1016/j.jphotochem.2023.114987.

[2] Lakhera, S, Rana M, Devlal K, Sharma S, Chowdhury P, Dhanusha A, Girisun TC (2023) Nonlinear Optical and Optical Limiting Activity of 7-Diethylamino-4-methylcoumarin/dimethyl formamide solution, Journal of Photochemistry & Photobiology, A: Chemistry.

[3] Lakhera, S, Rana M, Devlal K, Influence of Adsorption of Gold and Silver Nanoclusters on Structural, Electronic, and Nonlinear optical properties of Pentacene-5, 12-dione: A DFT study, *Opt Quant Electron* (2023). **55**, 178. https://doi.org/10.1007/s11082-022-04422-z

Tight Binding Hamiltonian and Quasi Particle Spectrum of Single Layer Graphene

Mamta Yadav, Piyush Masih and Sarita Khandka.
Department of physics, Faculty of Science, SHUATS, Prayagraj, 211007.
my.mamtayadav19@gmail.com; piyush.masih@shuats.edu.in; sarita.khandka@shiats.edu.in

Using Tight Binding Hamiltonian for monolayer graphene, expression for dispersion relation is obtained usingGreen Function Technique. During the calculations nearest neighbour and next nearest neighbour hopping along with onsite coulomb interaction are considered. The result shows no gap at Dirac point and Dirac cone is obtained for different values ofnext nearest neighbour hopping (t').

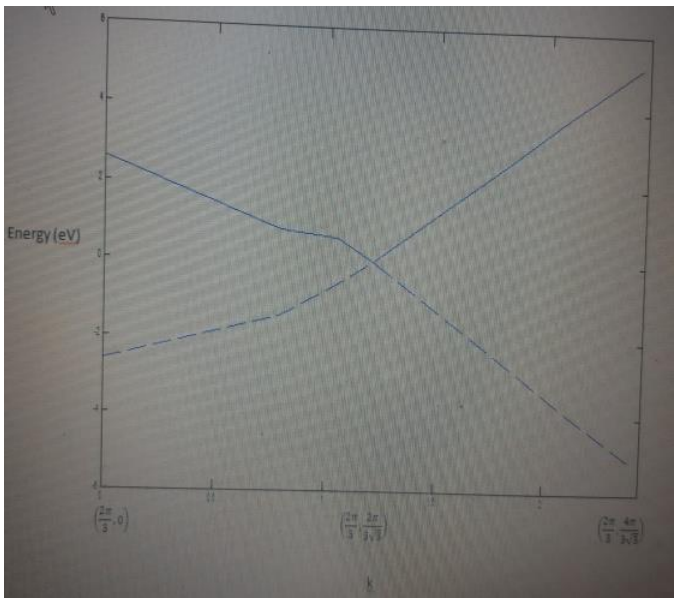

Fig.1:Quasi-particle energy versus k (t=2.6eV, t'=0eV, U=0.1eV) for single layer graphene.

Keywords: Monolayer Graphene, Tight binding Hamiltonian, Dispersion Relation.

References:

[1] Kumar S. and Ajay (2013). Quasi-particle spectrum and density of electronic states in AA- and AB- stacked bilayer graphene, The European Physical Journal B, 86,111.
[2] Geim A. K. and MacDonald (2007). Graphene: Exploring carbon flatband, Physics Today, 60,8,35.

Structural, Dielectric, and Transport Properties of La_2FeMnO_6 Double Perovskite

Baniya Meena[1], Sandeep Chatterjee,[2] Anup Ghosh[1, *]
[1]Material Research Laboratory, Department of Physics, Banaras Hindu University (BHU), Varanasi, India-221005
[2]Department of physics, Indian Institute of Technology BHU, Varanasi, India-221005
[*]*Corresponding author email id: akghosh@bhu.ac.in; anupkg66@gmail.com*

Polycrystalline sample La_2FeMnO_6 has been synthesized by the high temperature solid-state reaction method. Rietveld refinement of powder X-ray diffraction data confirms the cubic phase with space group *pm-3m* (221). Temperature dependent dc resistivity,measured in temperature range 160-300 K, clearly indicates the semiconducting nature of La_2FeMnO_6. Resistivity data was analyzed withthermally activated conduction mechanismsby the Arrhenius and Variable range hopping of small polarons. The activation energy of the charge carriers is found to be 0.0640, 0.079 eV below the charge localization temperature (T_{CL}~228 K) and 0.131, 0.147 eV above that charge localization temperature (T_{CL}) corresponds to the Arrhenius and Variable range hopping of small polaronsrespectively.The dielectric behavior is explored over a wide frequency (1KHz –1 MHz) and temperature (125–300 K) ranges which showsthat the La_2FeMnO_6exhibits a high dielectric constantand low loss at room temperature.Temperature dependent dielectric constant and dielectric loss reveal the relaxation behavior of La_2FeMnO_6. A single relaxation peak has been detected in imaginary part of the impedance(Z'')whichreveals the contribution of grain boundaries at lower frequency regime become evident from the complex impedance spectroscopic and modulus studies. The corresponding activation energy of charge carriersis estimated from the Arrhenius fittings.The nature of the temperature-dependent unitless exponent function describethe 'Non-overlapping Small Polaron Tunnelling' (NOST) mechanism in La_2FeMnO_6double perovskite.Magnetization measurement reveals the complex environment of ferrimagnetic and antiferromagnetic interactions. This material appears to be a very interesting candidate for various applications that need room temperature high dielectric constant.

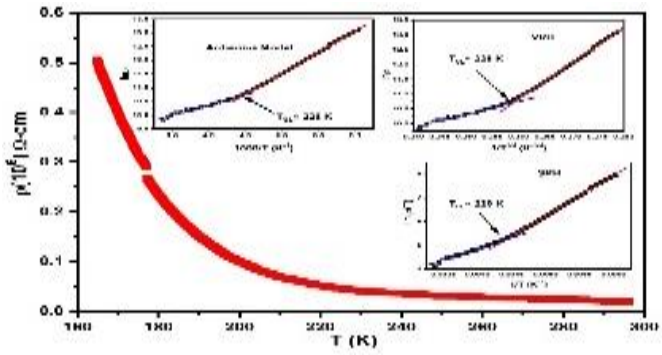

Fig -1. *Temperature dependent resistivity, and the inset of the figure represent the fitting of resistivity data with Arrhenius, Variable range Hopping and Small Polaron Hopping conduction mechanism for La_2FeMnO_6.*

Keywords: Double perovskites, high dielectric constant, Impedance spectroscopy, magnetic complexity.

The correlation between band gap & urbach energy with dielectric parameters of thickness dependent SnS thin film

Vinita[1], Chandra Kumar[2], B.K. Singh[1,3*]
[1]Department of Physics, Banaras Hindu University (BHU), Varanasi-221005, India
[2]University Centre for Research & Development, Chandigarh University, Mohali-140413, Punjab
[3*]Discipline of Natural Sciences, PDPM Indian Institute of Information Technology, Design, and Manufacturing, Jabalpur 482005, India
**Corresponding author email id: bksingh@bhu.ac.in*

Abstract: Here we report the room-temperature deposition of SnS thin film through thermal the evaporation technique.The effect of thickness on SnS thin film and its influence on band gap (E_g), Urbach energy (E_u), dielectric constant (ε), and dielectric loss (tanδ) have been investigated using UV-Visspectroscopy. TheSEM and AFM images showed that the SnSfilms are nearly uniform, homogeneous, and crack-free. The average particle sizes of SnS films are in the range of 90 nm-116 nm. It is observed that as thicknessincreases, the values of E_g and E_u systematically decrease whereas the values of dielectric constant and dielectric loss systematically increase. The correlation between Eg and Eu with dielectric constants is explainedby the Bohr model, i.e.,$E_u \propto 1/\varepsilon_r^2$ and $E_g \propto 1/\varepsilon_r^2$. In the present investigation, it has been proposed that an increase in the values of E_g and E_u, leads to a decrease in the tunneling probability of electrons from the valence band to the conduction band, which may result in a decrease in the value of the dielectric loss. Present investigations clearly suggest that the value of dielectric loss is effectively controlled by E_g.Thus, this investigation contributes to understanding the interconnection between the optical and dielectric properties of SnS thin film and successfully demonstrates the decrease in dielectric constant with increasing disorder(Urbach energy).

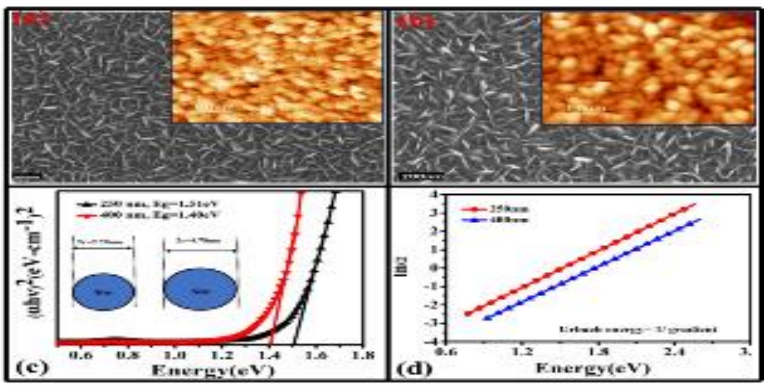

Figure: *1(a-b) SEM image(inset AFM), (c-d) energy-gap and Urbach energy of SnSfilm*

Keyword: Thin film,AFM, Bandgap, Urbach energy, Dielectric parameters.

Simulation study of n-CdS/p-Si heterojunction solar cell using SCAPS-1D

Shalini Srivastava*, Vineet Kumar Singh
Department of Physics, DDU Gorakhpur University, Gorakhpur, 273009, India
**Corresponding author email id: shalinisrivastava775@gmail.com*

Abstract

In this simulation study, we proposed a new silicon heterojunction (n-CdS/p-Si) solar cell as a potential candidate for photovoltaic application. The performance of n-CdS/p-Si heterojunction solar cell suffers from interface imperfection. Based on simulation, this paper has established a model to correlate the defect density and cell performance. Deep trap density, shallow trap density, interface defect density, and electron selective layer thickness are simulation parameters. The cell's performance is worsened by interface traps rather than deep or shallow traps. In this simulation study, the heterojunction solar cell's champion power conversion efficiency is ~ 18.72%.

Keywords: Solar energy material, defects, semiconductor, thin films, interface defect

DNA-quadruplex Single molecular structure determination using computational methods and investigating its dynamic behavior through molecular dynamic simulation

Jwala Ji Prajapati [1, 2], Ramesh Kumar Yadav[1], Umesh Yadava[2]
[1]Department of Physics, B.R.D. Post Graduate College, Deoria, Uttar pradesh 274001, India,
[2]Department of Physics, Deen Dayal Upadhyaya Gorakhpur University, Gorakhpur, 273009 India.
jwalajisjlt@gmail.com(JJP), rkybrd@yahoo.in(RKY), u_yadav@yahoo.com(UY)

We provide results from a simulation of molecular dynamics and a conformational analysis of the DNA quadruplex, whose crystal structure has been described in the literature. The DNA quadruplex's coordinates, which are the sequence d(GGGGTTTTGGGG)4, were obtained from the protein data bank (PDB ID:1d59). The DNA quadruplex model was created, and then the molecule underwent a 100ns simulation of molecular dynamics. At regular intervals of 10 ns, the dynamical pathway's trajectories are examined. X3DNA software is used to assess the shape and conformation of the time evolution trajectory utilizing plots for root mean square deviation (RMSD) and root mean square fluctuation (RMSF). The collected results were compared to the information on the DNA quadruplex crystal structure that was at hand. The collected information reveals several fascinating details.The MD simulation was carried out in the Desmond Suite's OPLS (Optimized Potential for Liquid Simulation)-implemented NPT ensemble coupled using OPLS.Using the particle mesh ewald sum approach, long-range coulombic forces are evaluated. Backbone helicoidal and torsion angle parameters were examined, and the results are shown in the results and discussions.We have come to the conclusion that the DNA G-quadruplex may be incredibly important in the development of some deadly diseases.This finding may make it easier to do further research on DNA quadruplex structures in telomeric regions of living cell’s chromosomes.

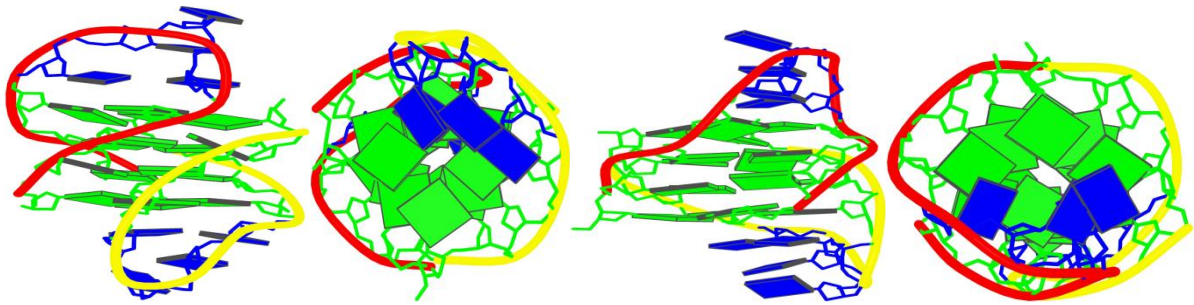

Fig.Single molecular structure of DNA G-quadruplex and its conformation

References:

[1] Spiegel J., Adhikari S., Balasubramanian S. The Structure and Function of DNA G-Quadruplexes. *Trends Chem.* 2020;2:123–136. doi: 10.1016/j.trechm.2019.07.002.
[2] Burge S., Parkinson G.N., Hazel P., Todd A.K., Neidle S. Quadruplex DNA: Sequence, topology and structure. *Nucleic Acids Res.* 2006;34:5402–5415. doi: 10.1093/nar/gkl655.
[3] Ma Y., Iida K., Nagasawa K. Topologies of G-quadruplex: Biological functions and regulation by ligands. *Biochem. Biophys. Res. Commun.* 2020;531:3–17. doi: 10.1016/j.bbrc.2019.12.103.
[4] Huppert J.L., Balasubramanian S. G-quadruplexes in promoters throughout the human genome. *Nucleic Acids Res.* 2007;35:406–413. doi: 10.1093/nar/gkl1057.

Li ion conductivity properties of Garnet structured Niobate and Tantalate oxides

Saiqua Siddiqui, Brajendra Singh*
Materials Chemistry Laboratory, Centre of Material Sciences, University of Allahabad, Prayagraj, India
**Corresponding author email id: brajendr@allduniv.ac.in; brajendr@gmail.com*

In order to overcome the safety concerns, the garnet type oxide materials have been employed as the solid state electrolyte in lithium-ion batteries.In this study, Pb-containing Nb and Ta-doped garnet type compositions weresynthesized to investigate the effect of doping on the structure and ionic conductivity of $Li_7La_{2.8}Pb_{0.2}Zr_{1.8}Nb_{0.2}O_{12}$ (LLPZNbO) and $Li_7La_{2.8}Pb_{0.2}Zr_{1.8}Ta_{0.2}O_{12}$ (LLPZTO) oxides. The XRD patterns revealed a single phase for these garnet structured oxides. The influence of the presence of Pb, Nb, and Taatoms on the structure and Li-ion conductivity of parent composition $Li_7La_3Zr_2O_{12}$wasinvestigated. The dopant Pb was found in La sublattice, whereas Nb and Ta were doped at Zr site, resulted in variations in the ionic conductivity of the compositions. All the doped materialsexhibited cubic garnet structuresimilar to undoped $Li_7La_3Zr_2O_{12}$.Novocontrol impedance analyzer (Alpha-A high performance frequency analyzer) was used to record the impedance measurements from room temperature (25°C) to 450°C in the frequency range of 1Hz to 40 MHz. At 300°C, the Ta doped garnet composition $Li_7La_{2.8}Pb_{0.2}Zr_{1.8}Ta_{0.2}O_{12}$ showed higher conductivity of 6.0×10^{-2} S/cm as compared to Nb doped composition LLPZNbO (1.0×10^{-2} S/cm) and undoped parent composition (3.4×10^{-2} S/cm).The Almond-West formula was used to calculate the ac conductivity (ac), hopping frequency (p), and frequency exponent (n) of the compositions. Furthermore, the modulus spectra explained the conductivity nature of the compositions. The shifting in the modulus peaks towards higher frequency in the doped composition at higher temperature suggested the presence of thermally generated dielectric relaxation phenomenon and the hopping of charge carriers.

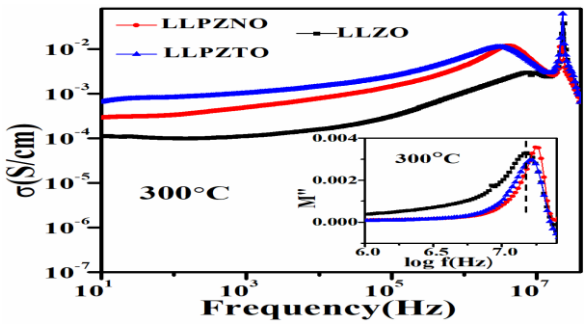

Fig.1 Conductivity plot of garnet compositions $Li_7La_3Zr_2O_{12}$, $Li_7La_{2.8}Pb_{0.2}Zr_{1.8}Nb_{0.2}O_{12}$ and $Li_7La_{2.8}Pb_{0.2}Zr_{1.8}Ta_{0.2}O_{12}$ at 300°C. Inset figure shows the modulus spectra of the prepared garnet compositions to demonstrate the shifting of modulus peak.

Keywords: Solid electrolytes, ceramics, ionic conductivity, modulus.

References:

[1] Thangadurai V, Weppner W (2005).$Li_6ALa_2Nb_2O_{12}$ (A=Ca, Sr, Ba): A New Class of Fast Lithium Ion Conductors with Garnet-Like Structure. J. Am. Ceram. Soc. 88, 411-418.
[2] Siddiqui S, Singh D, Singh P, Singh B (2023) Structural, optical, microstructure, and giant dielectric behavior of parent, Cu and Sr doped $La_{0.55}Li_{0.35}TiO_{3-\delta}$. J. Am. Ceram. Soc. 106, 6732-3742.

Enhanced upconversionand optical thermometric performance in $GdVO_4:Er^{3+}/Yb^{3+}$ phosphor via incorporation of Li^+ ion

Madan M. Upadhyay* and Kaushal Kumar
Optical Materials & Bio-imaging Research Laboratory, Department of Physics, Indian Institute of Technology (Indian School of Mines), Dhanbad-826004, India
**Corresponding author email id: madan.iitism@gmail.com*

$GdVO_4$phosphor doped with Er^{3+}/Yb^{3+} and $Er^{3+}/Yb^{3+}/Li^+$ ions was successfully produced by the high temperature solid state reaction approach.The crystal structure of $GdVO_4$ was found to have a tetragonal phase using X-ray diffraction study. The morphological analysis reveals the presence of particles at a micro scale. The upconversionluminescence upon 980 nm laser diode excitationshows the emission bands in green and red regions owing to characteristic emission of Er^{3+}ion.Pump power analysis and energy level diagram were used to explain the observed emissions. Temperature-dependent upconversion spectra were recorded in order to determine the suitability of the produced phosphors as a non-contact temperature sensor.The temperature sensitivity of the phosphors was determined by utilizing the emission bands arising from thermally coupled and non-coupled levels of the Er^{3+}ion. Furthermore, thermal stability, colour coordinate study and anti-counterfeiting application were also explored.

Keyword: Solid-state reaction, Upconversion, Optical thermometry, anti-counterfeiting

References:

[1]Huang X., HuangK., Chen L., Chen N., Lei R., Zhao S., &Xu S. (2020). Effect of Li^+/Mg^{2+} co-doping and optical temperature sensing behavior in $Y_2Ti_2O_7$: Er^{3+}/Yb^{3+}upconverting phosphors. Optical Materials,107, 110114.

[2] Jin Y., Li K., Chen H., Fang F., Li Y., Lin H., ... & Ma L. (2023). Non-contact thermometer behaviour of $(Y_{0.5}In_{0.5})_2O_3$: Yb^{3+}, Er^{3+}solid solution. Dalton Transactions, 52(29), 10005-10012.

[3] Vega M., Martin I. R., Cortés-Adasme E., & Llanos J. (2022). Enhanced red up-conversion emission in Er^{3+}/Yb^{3+}co-doped $SrSnO_3$ for optical temperature sensing based on thermally and non-thermally coupled levels. Journal of Luminescence, 244, 118687.

Structure, Relative energy, Dissociation pathways, Transition states and Thermochemical analysis of some Interstellar molecules: A theoretical study

Siddhartha Bhattacharjya[1], Narayan C. Bera[2] and Indranil Bhattacharyya*[3]
[1]Department of Physics, Derozio Memorial College, Rajarhat Road, Gopalpur, Kolkata-700136
[2]Department of Physics, Narasinha Dutt College, 129 Belilious Road, Howrah-711101
[3]Department of Physics, AcharyaPrafulla Chandra College, New Barrackpore, Kolkata- 700131
**Corresponding author email id: indranil@apccollege.ac.in*

The field of astrochemistry and astrobiology has gained immense attention to the scientists due to the recent development in high precession telescope used in space mission to study the composition of different interstellar media and planetary atmosphere.Small nitriles are abundant in the interstellar region and the presence of *CN*-group acts as precursors of prebiotic substance. It is observed that the radiation environment such as *UV* radiation and ionization radiation process leads to different isomerization of molecules.Out of the recent detections, Voyager-II found the existence of CH_3CN, CH_2CHCN and CH_3CH_2CN in the surface of Titan (Saturn's largest moon). The existence of acetonitrile (CH_3CN), acrylonitrile (CH_2CHCN) and propionitrile (CH_3CH_2CN) and their iso-nitrile, isomers are detected in recent observation.The presence of -CN fragment in the molecule makes these molecules possible precursor amino acids and finally biological molecules, hence these are often considered as a prebiotic substance towards the origin of life. The detailed mechanism of the dissociation and reaction pathways is still a challenging to the researchers. The presence of -SiNfragment in place of –CN plays an important role in characterizing the properties of some respective interstellar molecules.

In this study we have used density functional *B3LYP* method followed by high level ab-initio methods to study the relative stability and dissociation pathways of iso-nitriles substances. The nitriles are more stable compared to its isomeric form. The reported structural parameters, structure of transition states, vibrational frequencies, thermochemical calculations along with the heat of formation and dipole moments yield good with available reported experimental results. We reported six dissociation channels of CH_3NC, CH_2CHNC and CH_3CH_2NC. Out of all these dissociation channels the most favourable channel consists of HCN product having dissociation energy of~78 kcal/mole,~16 kcal/mol and 6-7 kcal/mol forCH_3NC, CH_2CHNC and CH_3CH_2NC molecules respectively.The detailed study of CH_2CHSiN and CH_3CH_2SiN has also been done and the relative energy as well as the dissociation pathways along with the transition states between corresponding isomers and thermochemical studies has been done and interesting properties are shown.

References:

[1] Mariia A.Lukianova et al. Radiation Physics and Chemistry **180** (2021) 109232.
[2] Kameneva V. Svetlana et al. Radiation Physics and Chemistry **141** (2017) 363.

Magnetic field enable efficient separation process for Fe doped perovskite manganites from water and its photocatalytic degradation properties

Brajendra Singh[a*], Priyanka Singh[a], Saiqua Siddiqui[a] and Mukul Gupta[b]
[a]Materials Chemistry Laboratory, Centre of Material Sciences, University of Allahabad, Prayagraj -211002, India
[b]UGC-DAE Consortium for Scientific Research, University Campus, Khandwa Road, Indore 452 001, India
**Corresponding author email id:* brajendr@gmail.com; brajendr@allduniv.ac.in

The treatment of chemical dyes containing waste water is very necessary to protect the environment and life of living beings. Nowadays, photocatalytic process is becoming favored for wastewater purification. It is very essential to remove photo catalyst from water and degradation of chemical dyes in quick time. Magnetic field dependent separation process can be very productive to show effective result in industrial applications. In this work, We have documented (i) efficient separation of Fe doped perovskite manganites photocatalysts from water using magnetic field (ii) the photocatalytic degradation of chemical dyes present in wastewater. These Fe doped perovskite manganites ceramic photocatalysts are first calcined and then sintered at 1050^{o}C for 12 hours. Ceramics are characterized by X-ray diffraction (XRD), Soft X-ray absorption spectroscopy (SXAS), Fourier transform infrared spectroscopy (FTIR) and UV–visible diffuse reflectance spectroscopy (DRS). SXAS studies show the presence of Mn (Mn^{+3}/Mn^{+4}) and Fe (Fe^{+3}/Fe^{+4}) mixed valences in Fe doped perovskite manganites. Optical band gap is found in visible light range for Fe doped perovskite manganites. Parent manganite degrades 83% indigo carmine in 5 minutes, 92 % chemical dye methyl orange in 20 minutes and 84% crystal violet in 10 minutes. Fe doped perovskite manganite take lesser time to degrade these dyes. Parent and Fe doped manganites can be separated in 60 seconds from wastewater. These properties of Fe doped samples are also compared with Ti and Ru doped manganite samples.

Keywords: Synchrotron X-ray absorption, dye degradation, magnetic separation, mixed valences, wastewater treatment.

References:

[1] KatheresanV., KansedoJ., LauS. Y.,(2018) Efficiency of various recent wastewater dye removal methods: A review, J. Environ. Chem. Eng. 6, 4676-4697.
[2] Singh B, Singh P, Siddiqui S, Singh D and Gupta M (2023) "Wastewater treatment using Fe doped perovskite manganites by photocatalytic degradation of methyl orange, crystal violet and indigo carmine dyes in tungsten bulb / sun light" Journal of Rare Earths 41, 1311-1322
[3] Singh B., Singh P. (2020) Ru doping effect on the structural, electronic, transport, optical and dye degradation properties of layered Li_2MnO_3, SN Appl. Sci. 2, 506-519.
[4] Deshmukh A.V., Patil S.I., Bhagat S.M., Sagdeo P.R., Choudhary R.J., Phase D.M., (2009) Effect of iron doping on electrical, electronic and magnetic properties of $La_{0.7}Sr_{0.3}MnO_3$, J. Phys. D: Appl. Phys. 42, 185410-185414.

The catalytic activity of CSF admixed with SWCNT on Hydrogenation Properties

Rashmi Kesarwani[a], M A Shaz[a]
[a]Hydrogen Energy Centre, Department of Physics, Banaras Hindu University, Varanasi, 221005, India

Here, we outline and explore the impact of the addition of CsF made from alkaline earth fluoride on the enhancement of absorption, desorption, and cyclability of the cutting-edge hydrogen storage material MgH_2. Cesium fluoride (CsF), which was utilized as an additive in this study, had the highest fundamental electronegativity difference of all the fluorides at 3.19, compared to NbF_5, one of the best-known catalysts for MgH_2 to date, at 2.38. Because MgH_2 is ionic and has a polar covalent nature, it will quickly react with CsF, which is highly ionic. The catalysts, Magnesium Fluride and Cesium Hydride , are produced when CsF interacts with MgH_2. Additionally, the onset desorption temperature for MgH_2 + CSF and the catalysts (MgH_2+SWNT+CSF) is 261°C and 231°C, respectively, which is 95°C and 125°C lower than MgH_2 that has been ball milled. The H_2 absorption for MgH_2 catalyzed by CSF is discovered to be 6.0 % in 5 minutes at 290 ^oC. The hydrogen absorption for SWNT+ CsF catalyzed MgH_2 is 6.16 wt% in 2 minutes at 290^oC. Even after 15 cycles, MgH_2+SWNT+ CsF storage capacity is still 6.00 wt. %, consistent with the great cyclability. A suitable catalytic mechanism based on X-ray diffractionand Scanning Electron Microscopic studies has been presented for catalysts on hydrogen sorption in MgH_2.

Keywords: Hydrogen Storage, Metal Hydride, MgH_2, SWNT and CSF

High compression thermal properties of semiconductors from Equation of States

Prachi Singh[1], Shivam Srivastava[1], Chandra K. Dixit[1], and Anjani K. Pandey[2]
[1]Department of Physics, Dr. Shakuntala Misra National Rehabilitation University, Lucknow, Uttar Pradesh
[2]Institute of Engineering and Technology, Dr. Shakuntala Misra National Rehabilitation University, Lucknow, Uttar Pradesh

In present the work, we have theoretically predicated some important thermoelastic properties of nanomaterials such as Gruneisen parameter and lattice constant of nanomaterials by using three different Equation of States (EOS): (I)modified Lenard Jones EOS, (II) Shankar EOS and (III) Universal Tait EOS for CdSe and CdS nanomaterials. The result shows that the Gruneisen parameter decreases as compression increases and the lattice constant also decreases with increasing compression.

Keywords- High compression, Semiconductor, Equation of states, Lattice constant, Gruneisen parameter.

Magnetocapacitance properties of heterostructured $MnO_2/La_{0.7}Pb_{0.3}MnO_3/MnO_2$ manganite systems

Brajendra Singh[a*], Priyanka Singh[a], Saiqua Siddiqui[a] and Mukul Gupta[b]
[a]Materials Chemistry Laboratory, Centre of Material Sciences, University of Allahabad, Prayagraj-211002, India
[b]UGC-DAE Consortium for Scientific Research, University Campus, Khandwa Road, Indore 452001, India
**Corresponding author email id: brajendr@allduniv.ac.in; brajendr@gmail.com*

The Magnetoelectric (ME) coupling in material has attracted researcher's attention due to its potential applications in sensing, as spinelectronic devices and in energy harvesting. Conventional materials show this coupling due to the controlled ferroelectric polarization with the change in magnetic field.Magnetocapacitance (MC) effect has been used to explore the magneto electric coupling due to the spin and charge degree of freedom in materials. In this work, we have explored the magnetocapacitance properties of heterostructures with MnO_2 and room temperature magnetic $La_{0.7}Pb_{0.3}MnO_3$ bulk powder samples keeping LPMO sample sandwiched between MnO_2 layers ($MnO_2/La_{0.7}Pb_{0.3}MnO_3/MnO_2$ systems). We have found huge positive and negative magneto capacitance in these hetrostructures at low magnetic field and low frequencies. X-ray diffraction pattern confirms the single phase of used $La_{0.7}Pb_{0.3}MnO_3$ and MnO_2 samples. UV–visible Diffuse Reflectance Spectroscopy (DRS) shows Optical band gap 4.47 eV for MnO_2 while LPMO has multiple optical band gaps at 3.85 and 1.3 eV. X-ray absorption spectroscopy(XAS) shows the mixed valence states of Mn (Mn^{+3} and Mn^{+4}) in LPMO while MnO_2 shows only Mn^{+4} valence state of Mn. Maximum magnetocapacitance is found ~40% at 1kHz frequency in 1.8T magnetic field in double layered heterostructure. Single Layered hetrostructure ($MnO_2/La_{0.7}Pb_{0.3}MnO_3/MnO_2$) shows ~30% magnetocapacitance while dotted manganites system shows ~15% magetocapac itance at 1kHz frequency in 1.8T magnetic field. Single layered hetrostructure ($MnO_2/La_{0.7}Pb_{0.3}MnO_3/MnO_2$) system also shows the negative magnetocapacitance ~20% in MHz frequencies.

Keywords: Magnetocapacitance, band gap, hetrostructure, perovskite manganite, magnetic

References:

[1] Catalan G. (2006), Magnetocapacitance without magnetoelectric coupling. Appl. Phys. Lett. 88,102902-102904.
[2] Singh B (2016)Ru^{4+} induced colossal magnetoimpedance in Ru doped perovskite manganite at room temperature, Phys. Chem. Chem. Phys. 18, 12947-12951
[3] Singh B (2015)Room temperature large positive and negative magnetocapacitance in CaMn 0.95 Fe 0.05 O 3− δ, Materials Letters 156, 76-78
[4] Singh M.P., Prellier W., Simon C., Raveau B. (2005) Magnetocapacitance effect in perovskite-superlattice based multiferroics. Appl. Phys. Lett. 87, 022505-022507.

Study on formation and structural stability of an AB_5 type multicomponent $TiVCoNiMn_2$ high-entropy alloy

Abhishek Kumar[1*], M. A. Shaz[1], N.K. Mukhopadhyay[2], and Thakur Prasad Yadav[1,3]
[1]Hydrogen Energy Centre, Department of Physics, Institute of Science
Banaras Hindu University, Varanasi-221005, India
[2]Department of Metallurgical Engineering, Indian Institute of Technology (Banaras Hindu University), Varanasi-221005, India
[3]Department of Physics, Faculty of Science, University of Allahabad, Prayagraj-211002, India
**Corresponding author email id: abhishek.physics.bhu@gmail.com*

Recent theoretical and practical investigations have concentrated on the intriguing research subject of multicomponent high entropy alloys (HEAs), opening up a new field since they offer enhanced mechanical and functional qualities compared to ordinary alloys based on a single primary element. Multicomponent HEAs contain five or more than five primary elements, with concentrations ranging from 5 to 35 atomic percent [1, 2]. We examined the microstructure and mechanical characteristics of AB_5 type as-cast and annealed $TiVCoNiMn_2$ HEA. Thermo-Calc was used for phase prediction, and Meidma's model calculated the mixing enthalpy and other thermodynamic parameters. This AB_5 type as-cast $TiVCoNiMn_2$ HEA has a mixing enthalpy of ~-15.6 kJ/mol and an atomic radius mismatch of ~10.03%. This AB_5 type HEA was synthesised using a 35 kW radio frequency induction furnace, and validation of the BCC phase with lattice parameter 2.95 Å was done with XRD profile analysis. For thermal stability of phase, we annealed the as-cast AB_5 type HEA for 24 hours at 1000°C, identifying intermetallic phases. The elemental composition and surface morphology of these as-cast and annealed HEAs were evaluated using SEM and EDX. We perform the hardness test at a 200 g load for 15 seconds. There was no significant difference in hardness between the annealed (795 HV) and as-cast samples (806 HV). This HEA is synthesised by combining hydride and non-hydride-forming elements. Which could be ideal for use as a hydrogen storage material. It is worth promising the hydrogen properties of these classes of HEAs, such as hydrogen ab/de-sorption [3, 4].

Keywords: Multicomponent, High Entropy Alloys, BCC phase, Vickers hardness.

References:

[1] Yadav TP, Kumar A, Verma SK, Mukhopadhyay NK (2022) High-Entropy Alloys for Solid Hydrogen Storage: Potentials and Prospects. Transactions of the Indian National Academy of Engineering 7: 147-156.
[2] Kumar A, Yadav TP, Mukhopadhyay NK (2024) Hydrogen storage in high entropy alloys. Towards Hydrogen Infrastructure 1: 133-164.
[3] Kumar A, Yadav TP, Mukhopadhyay NK (2022) Notable hydrogen storage in Ti–Zr–V–Cr–Ni high entropy alloy. International Journal of Hydrogen Energy 47: 22893-22900.
[4] Kumar A, Yadav TP, Shaz MA, Mukhopadhyay NK (2024) Hydrogen storage properties in rapidly solidified TiZrVCrNi high entropy alloys. Energy Storage

Topological Hall Effect in $(Mn_{1-x}Fe_x)_{3.25}Ge$ (x = 0.4) Hexagonal Magnet

Vishal Kumar, Gaurav K. Shukla, Nisha Shahi, and Sanjay Singh
School of Materials Science and Technology, Indian Institute of Technology (Banaras Hindu University)
Varanasi 221005, India
**Corresponding author email id: ssingh.mst@iitbhu.ac.in*

Topologically protected nontrivial spin structures attract significant interest in condensed matter physics for their utilization in low-power-consumption spintronics devices, memory devices, etc. The topological Hall effect (THE) is an additional Hall resistivity in the system arising from real-space Berry curvature picked up by conduction electrons passing through the nontrivial spin texture. Compared to expensive neutron diffraction measurements, THE is often used as a cost-effective tool to investigate nontrivial spin texture in the materials. In the present manuscript, THE in the $(Mn_{1-x}Fe_x)_{3.25}Ge$ (x = 0.4) alloy is studied using magneto-transport measurements. Maximum THE is found in the system at about 0.65 μΩ cm at 150 K, in contrast to the pristine Mn_3Ge with zero THE. The strong temperature variation of THE suggests that the noncoplanar spin structure due to competition among the magneto-crystalline anisotropy, antiferromagnetic coupling, and ferromagnetic exchange interaction is the main source of THE in the present system. Herein, it is shown that chemical doping can be an effective way to induce THE in the material with vanishing THE in its parent phase.

Keywords: frustration, magnetic anisotropy, magnetic texture, topological hall effect

References:

[1] Nagaosa, Naoto, et al. (2010) "Anomalous Hall effect." Reviews of modern physics 82.2: 1539.
[2] Wang, Wenhong, et al. (2016) "A centrosymmetric hexagonal magnet with super stable bi-skyrmion magnetic nanodomains in a wide temperature range of 100–340 K." Advanced Materials 28.32: 6887-6893.
[3] Bruno, P., V. K. Dugaev, and M. Taillefumier. (2004) "Topological Hall effect and Berry phase in magnetic nanostructures." Physical review letters 93.9: 096806.
[4] Liu, Jun, et al. (2020) "Magnetic transition behavior and large topological Hall effect in hexagonal $Mn_{2-x}Fe_{1+x}Sn$ (x= 0.1) magnet." Applied Physics Letters 117.5.

Optical and Structural Study of Large Band Gap-MoO_3 Semiconductor Thin Films

Sumit Kumar [a]*, Amit Kumar Singh Chauhan [a], Govind [b]
[a] Department of Physics, D.D.U. Gorakhpur University, Gorakhpur-273009, India
[b] National Physical Laboratory (CSIR-NPL), New Delhi-110011
**Corresponding author email id: sumittripathi01121991@gmail.com*

This paper presents an in-depth diffraction study of thin films composed of molybdenum trioxide (MoO_3); a semiconductor characterised by its wide band gap. MoO_3 thin film have garnered significant interest due to their potential application in various optoelectronics device. Understanding the structural properties and crystallographic characteristics of MoO_3 thin films is crucial for optimizing their performance in this application. The diffraction analysis, primarily conducted using (X-ray) diffraction (XRD) techniques, offers a comprehensive investigation into the crystallographic attributes of MoO_3 thin films. The encompasses an exploration of thin film's crystal structure, lattice parameter, preferred orientation, and crystallographic defects. Furthermore, it examines the influence of deposition at various temperatures ranging from 800℃- 950℃, growth condition and the structure features of MoO_3 thin films. The photoluminescence study suggests strong optical response of the grown films.

Keywords: MoO_3, XRD, thin film, PL, crystal structure, CVD

Study of transition from collective to non-collective behavior in ^{114}Te through CNS Model

Aalakh Kumar[1, *], Mamta Prajapati[1], Nidhi Goel[1], and Somnath Nag[1] [1]Dept. of Physics, Indian Institute of Technology (BHU), Varanasi – 221005 (U.P.), India
**Corresponding author email id:* aalakhkumar.rs.phy22@itbhu.ac.in

The tellurium nuclei with two protons outside the ^{100}Sn core are known to exhibit vibrational character at low spin which evolves into rotational characteristics with the increase in spin. In the previous work by I. Thorslund [1], the rotational bands were reported to attend smooth band termination and the bands were explained to be based on coupling of the two proton particles with deformed (2p-2h) states of the Sn-core. The deformed 2p-2h configuration coupled with neutrons outside the closed shell was the reason for the terminating bands in the even Sn isotopes. For Sb isotopes, terminating bands involve configuration namely a 3p-2h structure. In ^{114}Te, terminating bands involve 4p-2h configuration.

To identify the onset of non-collective behaviour across the yrast decay path in ^{114}Te cranked Nilsson-Strutinski model (CNS) calculations [2, 3] were applied. This model involves parameters derived for A = 110 region [2] and the configurations are labeled by the number of particles in different high-*j* orbitals outside a closed core. The calculation minimizes the energy with respect to the deformation parameters (ε_2, ε_4, γ). Model addresses nice result in absence of pairing correlations. Non collectivity is observed to evolve around I ~ 13^- (see Fig. 1). Details will be discussed during the conference.

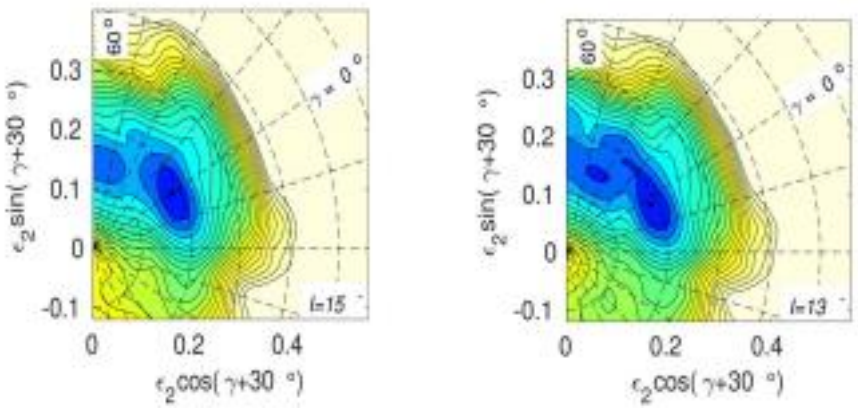

Fig1: Total energy surfaces at spins 13ħ and 15ħ for a general scan run. The contour line separation is 0.25 MeV.

References:

[1] I. Thorslund, et al. , Phys. Rev. C, **52**, R2839(1995)
[2] A. V. Afansjev, D. B. Fossan, G. J. Lane, and I. Ragnars, Phys. Rep. **322**, 1 (1999),and references therein.
[3] T. Bengtsson and I. Ragnarsson, Nucl. Phys. **A436**, 14 (1985).

Shelf life prediction of liner material

Anupama Devi [#1], Khayanath Mitra [#1], Shivam Tiwari [1], Tanu Srivastava [2], S. Krishna Mohan[2], Pralay Maiti[*1]
[1]School of Materials Science and Technology, Indian Institute of Technology BHU,
Varanasi, 221005, India [2]Defense Research & Development Laboratory, DRDO, Hyderabad
500058, India
[#]First two authors equally contributed for this work.
Corresponding author email id: pmaiti.mst@itbhu.ac.in

In contemporary society, it is widely acknowledged that the absence of polymers would render daily life exceedingly challenging. Elastomers, a class of polymers, have widespread application in both industrial and everyday contexts [1].Polymeric materials are widely utilized in various applications in everyday life [1]. These materials exhibit superiority over conventional materials primarily due to their remarkable versatility and great capacity for adjustment. Polymers have extensive application in a diverse range of items, encompassing dielectrics, corrosion and erosion inhibition, electromagnetic interference (EMI) shielding, fuel cells employed for energy storage [2], as well as sensors. One of the specific uses of such materials are in thermal barrier, coating rockets, missile and other systems used in space and defense. Each liner material exhibits different properties according to their chemical structure and composition and shelf life [3]. In this study, accelerated thermal aging of the liner material, silicone- hollow glass microsphere composite (LDAM) has been studied along with the determination of its life span. The effect of such aging on the thermal properties of LDAM has been studied using thermogravimetry. Activation energy of the process has been determined to be in the range of 45-55 KJmol $^{-1}$.The results have been compared with already reported silicon polymers. Shelf life of LDAM composite has also been determined using Arrhenius model. Stochastic model has been applied to determine the lower and upper limits of shelf life. Shelf life of LDAM is found to be 24 years with 28 and 18 years of upper and lower error limits.

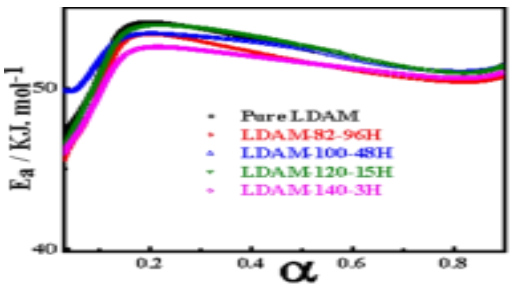

Fig 1. Activation energy vs. conversion curve of samples annealed at highest time for indicated temperatures

Keywords: Silicone polymer; degradation behavior; mechanical properties; shelf-life estimation.

References:

[1].Shit, S. C. & Shah, P. M. Edible Polymers: Challenges and Opportunities. *J. Polym.* **2014**, 1–13 (2014).
[2].Tiwari, S., Devi, A., Dubey, D. K. & Maiti, P. Induced Piezoelectricity in Cotton-Based Composites for Energy-Harvesting Applications. *ACS Appl. Bio Mater.* **6**, 1536–1545 (2023)
[3].Das, S. N. & Chaudhuri, A. R. Estimation of life of an elastomeric component: A stochastic model. *Def. Sci. J.* **61**, 257–263 (2011).

Thermochemical Energy Storage Materials and Their Potential Applications

Deepali Shukla[1], Amritanshu Shukla[1,*], Alka Misra[2], Manisha Yadav[1,2], Rachana Singh[1,2], Parmanand Pandey[1,2], Pravi Mishra[1,2]

[1]Department of Physics, University of Lucknow

[2]Department of Mathematics and Astronomy, University of Lucknow

**Corresponding author email id: shukla_as@lkouniv.ac.in*

Significant climate change has placed a pressing requirement for the utilisation of cleaner energy resources and thermal energy storage based systems, ranging from domestic to industrial applications, can heavily contribute for the same. Thermal Energy Storage System stores energy when available in abundance to be used at a later time. It is further divided in three types: Sensible Heat Storage (SHS), Latent Heat Storage (LHS), and Thermochemical Energy Storage (TCES).Sensible Heat Storage stores the energy by increasing the temperature of the materials and releases it by decreasing it. Latent Heat Storage uses the latent heat of the Phase Change Materials to store or emit energy. Thermochemical Energy Storage (TCES) uses reversible chemical reactions to store or release energy [1].

The TCES materials have advantage over other two types of thermal energy storage materials as these have Volumetric Energy Density about five to ten times higher than that of LHS and SHS materials [2]. The capacity of TCES (120-250 kWh/t) is also higher than LHS (50-150 kWh/t) and SHS (10-50 kWh/t) [3]. Therefore, TCES material is more efficient than LHS and SHS materials. Salt hydrates such as Na_2S, and LiCl are common materials used in TCES systems. $CaCl_2$ with an energy density of 1.47GJ/m^3, a heating rate of 10 K/min, and complete dehydration at 110 ˚C is an acceptable TCES material. In order to improve the efficiency, various studies have been already done. Examples include composite materials such as Silica Gel-$CaCl_2$, which has been studied to increase the thermal conductivity of pure $CaCl_2$ [4].Similarly, $SrBr_2$ with an energy density of 2.26 GJ/m^3 is a good TCES material.[4].

It is important to note that the utilization of even the most promising TCES materials gets limitedand much research and development work is called for due to large volume change, decreasing stability of materials under repetitive cyclesand required study of the heat transfer rate[5]. Currently, work is underway in this direction and a brief review of the topic along with the current status will be presented.

Keywords: Clean Energy Resources, Thermal Energy Storage, Thermochemical Energy Storage

References:

[1] Diaz PM (2016). Analysis and Comparison of different types of Thermal Energy Storage Systems: AReview. Journal of Advances in Mechanical Engineering and Science, Vol. 2(1), 33-46.

[2] Dizajia H B, Hosseinib H (2018). A review of material screening in pure and mixed-metal oxide thermochemical energy storage (TCES) systems for concentrated solar power (CSP) applications. Renewable and Sustainable Energy Reviews, 98, 9-26.

[3] Sarbu I, Sebarchievici C (2018). A Comprehensive Review of Thermal Energy Storage. Sustainability, 10(1), 191.

[4] Lin J, Zhao Q, Huang H, Mao H, Liu Y, Xiao Y (2021). Applications of low-temperature thermochemical energy storage systems for salt hydrates based on material classification: A review. Solar Energy, 214, 149-178.

[5] Clark R J, Mehrabadi A, Farid M (2020). State of the art on salt hydrate thermochemical energy storage systems for use in building applications. Journal of Energy Storage, 27, 101145.

Polymer translocation: Effects of periodically driven confinement

Manish Dwivedi[1], Swarn Lata Singh[2]and Sanjay Kumar[1*]
[1]Department of Physics, Banaras Hindu University, Varanasi 221005, India
[2]Physics Section, MMV, Banaras Hindu University Varanasi, 221 005, India
**Corresponding author email id: ksanjay@bhu.ac.in*

We study the influence of driven confinement on the translocation dynamics of a linear polymer chain in a good solvent through a cone-shaped pore. Using the Langevin Dynamics simulations, we calculate both the first attempt time and translocation time as a function of the position of the back wall and apex angle α. As the in vivo, confining environment is inherently dynamic, we extended present study to explore the consequences of periodically driven back wall and apex angles on the translocation dynamics. Our findings reveal that the translocation time initially decreases as the driving frequency increases, but increases after a certain frequency. The frequency at which the translocation time is found to be minimum is referred to as the resonance activation. Analyzing the distribution of translocation times around this frequency renders interesting information about the translocation process. We further explore the translocation dynamics by calculating the residence time of individual monomers, shedding light on the microscopic aspects of the process.

Keywords: Polymer translocation, Resonance activation.

References:

[1] Fiasconaro A., Mazo J. J. and Falo F. 2018. Translocation time of periodically forced polymer chains. Physical Review E, 82, 031803.
[2]J. Cohen A., Chaudhuri A. and Golestanian R. 2011. Active Polymer Translocation through Flickering Pores. Physical Review Letters, 107, 238102.

One-pot synthesis of binary nickel ferrite -reduced graphene oxide nanocomposite as stable and high-performance supercapacitor electrode material

G K Gupta, and Amit Srivastava
Department of Physics, TDPG College, VBS Purvanchal University, Jaunpur-222001, India

In the present study, we have successfully used an integrative approach to fabricate a three dimensional hierarchical electrode material constructed by $NiFe_2O_4$/rGO nanostructure via a facile hydrothermal method and subsequently studied its electrocapacitive performances. The structural and morphological characteristics of as-synthesized $NiFe_2O_4$/rGO nanostructure have been characterized by X-ray diffraction (XRD), Raman spectroscopy, Transmission electron microscopy (TEM), Scanning electron microscopy (SEM) and X-ray photo spectrometer (XPS). The electrocapacitive performances of the as-synthesized sample have been evaluated by galvanostatic charge-discharge (GCD), cyclic voltammetry (CV) and electrochemical impedance spectroscopy (EIS) using a three electrode system with 3 M KOH electrolyte solution. As-prepared hierarchical electrode material exhibits specific capacity ~ 362.46 Fg^{-1} at a current density of 0.65 Ag^{-1}, suggesting good rate capability. $NiFe_2O_4$/rGO nanostructure electrode material exhibits a significant high energy…. and power density as…, respectively. Furthermore, the as-synthesized nanocomposite harvest a superior cycling stability over 2000 cycles without obvious capacitance attenuation. The $NiFe_2O_4$/rGO provides rapid pathways for electron transfer and diminish the ion diffusion routes due to $NiFe_2O_4$ over rGO sheets, which ultimately results in exceptional electrochemical properties. Henceforth, the unique morphological features, outstanding conductivity & favorable cyclic stability render $NiFe_2O_4$/rGO nanocomposite as a promising and prospective advanced electrode material for supercapacitor in the field of energy storage-conversion application.

Analysis of High Pressure EOS on the Structural Properties of Gallium Compounds

Shipra Tripathi[1], Shivam Srivastava[1], Prachi Singh[1] Anjani K. Pandey[2] and Chandra K. Dixit[1]
[1]Department of Physics, Dr. Shakuntala Misra National Rehabilitation University, Lucknow, Uttar Pradesh
[2]Institute of Engineering and Technology, Dr. Shakuntala Misra National Rehabilitation University, Lucknow, Uttar Pradesh
**Corresponding author email id: shipraofau@gmail.com*

In this particular research, theoretical projections of the bulk modulushave undertaken, first pressure derivative of isothermal bulk modulus and the Grüneisen parameter (γ) for materials like GaN, GaAs, GaP and GaSb across varying compression values (V/V_0) by using three well known Equation of State (EOS) viz. Brennan-Stacey EOS, Vinet EOS and Tait EOS. These EOSs are also been tested for the basic requirements revealed from the fundamental thermodynamics for the limit of extreme compressions, as given by Stacey. It is found that at low compressions, the three EOSs viz Tait EOS, Vinet EOS and Brennan-Stacey EOS gives exactly the similar results for theoretical prediction of pressure, Bulk modulus and first pressure derivative of isothermal Bulk Modulus.

Keywords: EOS, Bulk modulus, high pressure, lattice parameter, volume compression ratio

MoS_2 assisted self-assembly of P3HT and PCPDTBT polymers thin film-based Schottky diode

Pankaj Kumar*, Sarita Yadav, Anchal Kishore Singh+, Naresh Kumar+, Lokendra Kumar
Physics Department, University of Allahabad, Prayagraj-211 002 (U.P.), India
+Physics Department, MNNIT-Allahabad, Prayagraj-211 002, (U.P.) India
Corresponding author email id: pankajkumar.gangwar@yahoo.co.in

Polymer thin films enhanced charge carrier mobility is very important for better electronic device applications. The study of polymer chain orientation within the microstructure of polymer is crucial. Here, we have examined the MoS_2-assisted crystallinity and electrical charge transport properties of Poly[2,6-(4,4-bis-(2-ethylhexyl)-4H-cyclopenta[2,1-b;3,4-b′]dithiophene)-alt-4,7(2,1,3-benzothiadiazole)] (PCPDTBT) and Poly (3-hexylthiophene) (P3HT) via a self-assembly process. We observed a significant change in the structure and optical properties of PCPDTBT and P3HT using MoS_2 nanosheets at various concentrations in chlorobenzene. We obtained highly crystalline and oriented film morphology PCPDTBT and P3HT with MoS_2 nanosheets. Optical and Structural studies of films have been studied using UV-visible absorbance and grazing incidence X–ray diffraction (GIXD). MoS_2 nanosheets confirmed with TEM and UV-visible absorbance. The electrical charge transport properties of these films have been investigated with Schottky diode configuration ITO/PCPDTBT/Al and ITO/P3HT/Al. The current density – voltage (J–V) characteristics are used for extracting the device parameters. MoS_2-assisted trap density is also calculated by J–V characteristics at room temperature. We observed that highly crystalline P3HT films with MoS_2 nanosheets showed less traps than PCPDTBT- MoS_2 films.

Keywords: Poly (3-hexylthiophene) (P3HT), PCPDTBT, Schottky diodes, Molybdenum disulphide (MoS_2)

Extraordinary electrical and thermal transport in Co-based Heusler alloys

Gaurav K.Shukla and Sanjay Singh
School of Materials Science and Technology IIT(BHU)-VARANASI-221005
**Corresponding author email id:* gauravshukla571996@gmail.com

The performance limitations of conventional electronic materials impose a major problem in the era of digital transformation. Consequently, extensive research is being conducted on the development of quantum materials that may overcome such limitations, by utilizing quantum effects to achieve remarkable performances. The well-known Hall effect is the appearance of transverse voltage due to Lorentz force in the current-carrying conductor placed in the perpendicular magnetic field [1]. The anomalous Hall effect(AHE)-an additional Hall resistivity in ferro magnetic material even in the absence of a magnetic field gained immense interest for its possible application in spintronics, memory devices, etc. [1,2]. The anomalous Nernst effect (ANE), which is AHE's thermoelectric counterpart, can be utilized as energy harvesting material, where a longitudinal thermal gradient can achieve the pronounced transverse electrical signal [3]. The origin of large AHE and ANE is related to the quantum mechanical Berry phase in momentum space, which purely depends upon the band structure of the material [4]. Therefore, the topological materials are prominent for the realization of large AHE and ANE, due to the large Berry curvature originating from their topological band structure such as the Weyl points/nodalline [5].Considering the potential of Heusler-based topological material, the oral presentation will cover some of our recent work [*Phys. Rev. B 104, 195108 (2021), Appl. Phys. Lett.*123, 052402 *(2023)]* focusing on AHE and ANE in the Co-based Heusler alloys specifically topological semimetal.

Keywords: Hall Effect; Weyl point/nodal line; Berry curvature; First principles calculation; Magneto- transport;

References:

[1] N.Nagaosa, J.Sinova,S.Onodaet.al.,AnomalousHalleffect,Rev.Mod.Phys.82,1539(2010).
[2] G. K. Shukla, J. Sau, N. Shahi, A. K. Singh, M. Kumar,and S. Singh, Anomalous Hall effect from gapped nodal line in the Co_2FeGe Heusler compound, Phys. Rev. B 104, 195108 (2021).
[3] S.N.Guin, K.Mannaetal., Anomalous Nernst effect beyond the magnetization scaling relation in the ferromagnetic Heusler compound Co_2 MnGa, NPG Asia Mater. 11, 16 (2019).
[4] D.Xiao,M.-C.Changet.al.,Berryphaseeffectsonelectronicproperties,Rev.Mod.Phys.82,1959(2010).
[5] A.Burkov,Topological semi-metals,Nat.Mater.15,1145(2016).

Weyl Fermion semimetal and topological Fermi arcs in NbAs

Md Tanwir Alam, Devendra Prasad Singh
University Department of Physics, Bhupendra Narayan Mandal University, Madhepura, Bihar, India

Weyl semimetal is a crystal whose low energy electronic excitation behave as Weyl fermions. It has received world wide attention in the era of condensed matter physics. Experimental research shows that Weyl semimetals are rarely found in nature. Expermimetal researchs finds Weyl semimetal state in NbAs .Method used in the experiment is the combination of both soft X-ray and ultraviolet photoemission spectroscopy.Experiment observed Weyl cone,Weyl nodes in the bulk, and the Fermi arcs.Weyl semimetal received attention in few last years due to their classification of symmetry protected topological phases beyond insulators and unusual transport phenomena and provide emergent condensed matter realization of Weyl fermion. Weyl fermion does not exist as a fundamental particle in the standard model.

Keywords: Weyl semimetal, Weyl fermion, NbAs, X-ray, Photoemission spectroscopy, Fermi arcs

Elevating Selective Ethanol detection based on unlocking the Potential of Accordion Structured MXene

Satyam Tripathi[1,2*] , Pratima Chauhan[2]
[1]Centre of Material Sciences, IIDS, University of Allahabad, Prayagraj, U.P.
[2]Advanced Nanomaterials Research Laboratory, U.G.C. Centre of Advanced Studies, Department of Physics, University of Allahabad, Prayagraj, U.P.
**Corresponding author email id: satyam.phd2022@allduniv.ac.in*

Two-dimensional (2D) transition-metal carbides (Ti3C2Tx) MXene have received much attention due to their exciting prospects for application in gas sensing. Large surface area, metallic conductivity, and the functionalization potential all are key characteristics of MXene. These materials have optimum gas selectivity and responsiveness among 2D materials. By using HF etching, we developed exfoliated MXene from MAX phase of Ti3AlC2. The William-Hall (W-H) plot estimated the size of the crystallite to be 9.90 nm. The calculated optical band gap was found 3.8 eV. The complete disappearance of aluminum (Al) layers was confirmed by the XRD peak shift and the accordion-like morphology confirmed by FESEM images. The experimental findings demonstrate the fact that Ti3C2Tx incorporation improves the sensitivity, the repeatability, and the selectivity of chemo-resistive sensors that are sensitive to oxygencontaining VOCs (volatile organic compounds) such as acetone, ethanol, methanol, propanol, and hexane. The fabricated MXene based sensor was tasted under exposure of aforementioned VOCs at 600 ppm. The initial finding illustrates that ethanol is the most sensitive VOC. The fabricated Ti3C2Tx sensor yielded response (%) at the concentrations of 50, 100, 200, 300, 400 and 500 ppm as 1.78, 2.63, 3.42, 4.28, 5.05, and 5.47%, respectively under purging ethanol. The maximum response at room temperature (RT) operable ethanol sensor was calculated as 5.65% at 600 ppm under 54% of relative humidity (RH). The outcomes demonstrate rapid responses/recovery of 5s and 8s, respectively.

Key-words: MXene, VOCs, Sensor, W-H plot.

Conformational analysis of 3-aminosalicylic acid: Quantum chemical and spectroscopic approach

Shahid Husain[1*], Sanjay Pant[1] and Mohan Singh Mehata[2]
[1]Photophysics Laboratory, Department of Physics, Centre of Advanced Study, DSB Campus, Kumaun University, Nainital- 263002, India.
[2]Laser Spectroscopy Laboratory, Department of Applied Physics, Delhi Technological University, Bawana Road, Delhi - 110042, India.
**Corresponding author email id: shahidbinmalik@gmail.com*

Salicylic acid (SA) is frequently used in the synthesis of organic compounds as well as in food preservation and as a plant hormone. It is extensively utilized in many skin care products to control hard skin, acne, corns, psoriasis, warts, and keratosis pilaris [1,2]. Quantum chemical calculations on 3-aminosalicylic acid (3ASA) (monomer and dimer) have been performed using DFT and TD-DFT theories in the ground and excited states. The optimized geometric bond lengths and bond angles in the ground state were closer to the available theoretical and experimental values of the parent molecule i.e. salicylic acid. The absorption and emission spectra of 3ASA in solvents have been estimated by TD-DFT and correlated with the available experimental results. The computed absorption and emission spectra of monomer and dimer are in correlation with each other. The absorption and emission spectra of 3ASA were also observed experimentally in different solvents and compared with theoretically obtained results. Moreover, the natural bond orbital (NBO) analysis shows that intramolecular charge transfer (ICT) contributes significantly to stabilizing the molecular system. In the case of dimer, H-bonding plays a dominant role in stabilizing the molecular framework. Furthermore, the calculated nonlinear optical (NLO) properties suggest that 3ASA can be considered in NLO applications.

Keywords: 3ASA, DFT/TD-DFT, electronic spectra, NBO parameters, dimer.

References:

[1] Suresh, S., Gunasekaran, S., & Srinivasan, S. (2014). Spectroscopic (FT-IR, FT-Raman, NMR and UV–Visible) and quantum chemical studies of molecular geometry, Frontier molecular orbital, NLO, NBO and thermodynamic properties of salicylic acid. *SpectrochimicaActa Part A: Molecular and Biomolecular Spectroscopy*, *132*, 130-141.

[2] Seo, J., Warnke, S., Gewinner, S., Schöllkopf, W., Bowers, M. T., Pagel, K., & von Helden, G. (2016). The impact of environment and resonance effects on the site of protonation of aminobenzoic acid derivatives. *Physical Chemistry Chemical Physics*, *18*(36), 25474-25482.

Probing the Charge Transfer Mechanism and Dielectric Relaxation of $Cs_3Bi_2I_9$ Single Crystal via AC Impedance Spectroscopy

Jitendra Yadav[a], Anil K. Sharma[a], Ambreesh Kumar[a], Bharti[b], Parasmani Rajput[c], Manvendra Kumar[d], R. J. Choudhary[e], Shiv P. Patel[b], Dhirendra K. Chaudhary[a,f]*, Sanjay Mathur[f]*

[a]Centre of Renewable Energy, Prof. Rajendra Singh (Rajju Bhaiya) Institute of Physical Science for Study and Research, V. B. S. Purvanchal University, Jaunpur, 222003, India

[b]Department of Pure and Applied Physics, Guru Ghasidas Vishwavidyalaya, Bilaspur, 495009, India

[c]Beamline Development and Application Section, Bhaba Atomic Research Centre, Trombay, Mumbai-85

[d]Shri Vaishnav Vidyapeeth Vishwavidyalaya Campus: Indore – Ujjain Road, Indore – 453111

[e]UGC-DAE Consortium for Scientific Research, Indore-452017

[f]Institute for Inorganic Chemistry, University of Cologne, Greinstrasse 6, 50939 Cologne, Germany

**Corresponding author email id- phydhiren@gmail.com,*

In recent years, Lead-free metal halide Pervoskite materials have paved significant attention from the scientific community owing to their exceptional optoelectronic characteristics and environmental friendly nature. Herein, we have successfully grown a single crystal of $Cs_3Bi_2I_9$ of ~5 mm size and investigated the dielectric relaxation and conduction mechanisms using temperature-dependent impedance spectroscopy correlated with modulus spectroscopy. We observed negative temperature resistance coefficient (NTRC)-type characteristics in impedance study and both complex impedance and electrical modulus studies have suggested the temperature dependent transition from Debye to non-Debye type relaxation in the material. Moreover, the estimated activation energy in $Cs_3Bi_2I_9$ single crystal is found to be $299 \pm 10\ meV$. Our systemic study demonstrates the basic understanding on $Cs_3Bi_2I_9$ single crystal, which is a promising candidate for high-performance Pervoskite-based optoelectronic devices.

References:

[1].Bechir, M.B. and M.H. Dhaou, *Study of Charge Transfer Mechanism and Dielectric Relaxation of CsCuCl3 Perovskite Nanoparticles.* Materials Research Bulletin, 2021. **144**: p. 111473

[2].Pradhan, D.K., et al., *Studies on structural, dielectric, and transport properties of Ni0.65Zn0.35Fe2O4.* Journal of Applied Physics, 2014. **115**(24)

[3].Paul, R., et al., *Temperature-activated dielectric relaxation in lead-free halide perovskite single crystals.* Journal of Physics D: Applied Physics, 2022. **55**(41): p. 415301.

Effect of Shock Strength on the Shock-front Structure in Van der Waal's gases

Sewa Singh and Raj Kumar Anand
Department of Physics, University of Allahabad, Allahabad-211002, India
Corresponding author email id: sewasingh705@gmail.com

The structure of viscous Shock-front has been investigated in a van der Waal's gases between the uniform boundary conditions $x = -\infty$ and $x = +\infty$ considering the flow to be viscous and one dimensional. The exact solutions for the flow parameters, particle velocity, pressure, temperature, and change-in-entropy in the shock transition region have been obtained under the quantitative analysis of the equation of state for van der Waal's gases. The effects due to the shock strength are analyzed on the structure and the flow variable of the gases. The results confirm that the shock-front thickness decreases with increasing the shock strength.

Keywords: Shock-front; Rankine-Hugoniot (RH) relations; van der Waal's gas; viscosity; non idealness parameter.

Hierarchical Nanorod-Induced Thermal Conductivity Modulation in ZnO/PEDOT: PSS Composite Films

Shivam K. Singh[1], Anil K. Sharma[2], Jitendra Yadav[2], Bharti[3], Savita[1,2], Giridhar Mishra[1*], H. P. Bhasker[4], Punit K. Dhawan[1], Shiv P. Patel[3], Dhirendra K. Chaudhary[1*]

[1]Department of Physics, Prof. Rajendra Singh (Rajju Bhaiya) Institute of Physical Sciences for Study and Research, V. B. S. Purvanchal University, Jaunpur-222003, India.

[2]Centre for Renewable Energy, Prof. Rajendra Singh (Rajju Bhaiya) Institute of Physical Sciences for Study and Research, V. B. S. Purvanchal University, Jaunpur-222003, India.

[3]Department of Pure and Applied Physics, Guru Ghasidas Vishwavidyalaya, Bilaspur, 495009, India

[4]Department of Physics, C.M.P. Degree College, University of Allahabad, Allahabad-211002, India.

**Corresponding author email id: phydhiren@gmail.com; giridharmishra@rediffmail.com*

In this study, composite films comprising ZnO nanorods and poly(3,4-ethylenedioxidthiophene):poly(4-styrenesulfonate) (PEDOT:PSS) has been synthesized using a sol-gel method, and their thermo-physical properties has been systematically investigated. Various characterization techniques were employed to analyze the structural, thermal, and optical properties of the composite. The film thickness, determined through cross-sectional Field emission scanning electron microscopy (FESEM), was measured at 900 nm, with an average nanorod diameter of approximately 250 nm. Thermal properties of the composite films were studied in the temperature range of 273 K to 353 K. For ZnO nanorods/PEDOT:PSS, the thermal conductivity, diffusivity, and specific heat were found to be 1.609 W/mK, 0.6465 mm^2/s, and 2.489 MJ/m^3K, respectively, at 353 K. Meanwhile, for ZnO/PEDOT:PSS films, these values were determined to be 1.495 W/mK, 0.4930 mm^2/s, and 3.033 MJ/m^3K at 353 K. These findings provide valuable insights into the thermal behavior of the composite films, offering potential applications in various scientific and technological fields.

Reference:

[1].Du, Yong, Kefeng Cai, Shirley Z. Shen, Weidong Yang, Jiayue Xu, and Tong Lin. "ZnO flower/PEDOT: PSS thermoelectric composite films." *Journal of Materials Science: Materials in Electronics* 27 (2016): 10289-10293.

[2].Hata, S., Taguchi, K., Oshima, K., Du, Y., Shiraishi, Y., & Toshima, N. (2019). Preparation of Ga-ZnO Nanoparticles Using Microwave and Ultrasonic Irradiation, and the Application of Poly (3, 4-ethylenedioxythiophene)-poly (styrenesulfonate) Hybrid Thermoelectric Films. *ChemistrySelect*, *4*(22), 6800-6804.

Effect of lattice boundary on Anderson Localization of nonclassical light in optical waveguide arrays

Shubradeep Majumder,* Amit Rai
Jawaharlal Nehru University, New Delhi
Corresponding author email id: shubradeepmajumder3@gmail.com

We study the effect that the boundary of a one-dimensional lattice has on Anderson localization of quantum states of light in a finite optical waveguide array in which neighbouring waveguides are evanescently coupled and controlled disorder is introduced. By investigating the quantum properties of the output when different quantum states of lights are injected to the waveguide we show enhancements of localization and quantum features because of the boundary.

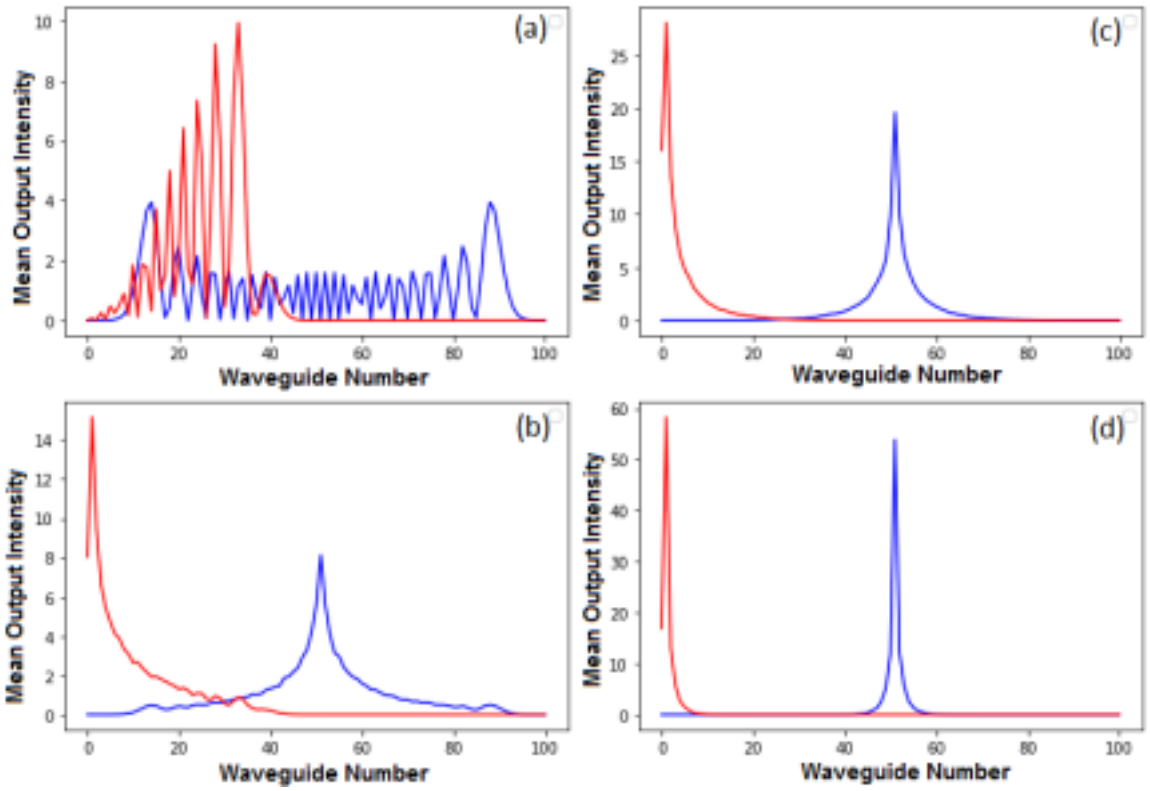

Figure caption: Mean output intensity of waveguide array for two input condition 1st (solid red line) and 50th(solid blue line). The disorder parameter of system were fixed as (a) $\Delta = 0$, (b) $\Delta/C = 0.5$, (c)$\Delta/C = 1$, (d) $\Delta/C = 3$

Keywords: Anderson localization, quantum states.

References:

[1] P. W. Anderson, Phys. Rev. 109, 1492 (1958).
[2] C. Thompson, G. Vemuri, and G. S. Agarwal, Phys. Rev. A 82, 053805 (2010).
[3] S. Majumder, A. Rai, and G. Vemuri, Journal of Optics 25, 105201 (2023).

Bidirectional Quantum Teleportation via penta-modal Entangled Coherent Cluster- State as the quantum channel by employing prevalent Linear Optical Elements

Ankita Pathak*, Ravi S. Singh#
Photonic Quantum-Information and Quantum Optics Laboratory, Department of Physics, Deen Dayal Upadhyaya Gorakhpur University, Gorakhpur (U.P.), 273009, India.
Corresponding author email id: pathak18.phy@gmail.com; #yesora27@gmail.com

Because of remarkable entangling characteristics Entangled Coherent-Cluster-states (ECCS) have attained paramount importance in recent years due to their robustness against prevalent noise as well as in novel quantum information processing tasks [1].

We worked out a proposal for bidirectional quantum teleportation (BQT) utilizing prevalent linear optical elements such as beam splitters, phase shifters and ideal photon number resolving detectors in which a penta-modal ECCS is exploited as the quantum channel. Our proposal paves the way for simultaneous exchange of quantum-information, encoded in bi-dimensional Hilbert space spanned by two coherent bases vectors differing in phases by π [2], between two different parties (Alice and Bob). Unlike standard quantum teleportation [3], where information transmission is typically unidirectional, our approach gives both parties (Alice and Bob) the right to transmit the quantum information independently usingnon-local C-NOT operation. A heralded detection of photons in labs of Alice and Bob followed by classical communications of even and odd photon-numbers and local unitary operations in both labs, impeccably, demonstrates the completion of our protocol.

Keywords: Bidirectional Quantum Teleportation, Entangled Coherent States, Bell-pair state, Linear Optical Elements

References:

[1] Bhatti, D. and Barz, S. (2023), Generating Greenberger-Horne-Zeilinger States using Multiport Splitters, Phys. Rev. A 107, 033714
[2] RalphT. C.,Munro W. J., Milburn G. J. (2001).Quantum Computation with Coherent States, Linear Interactions and Superposed Resources.Phys. Rev.,65,042313.
[3] Bennett C. H., Brassard G., Crépeau C., Jozsa R., Peres A., and Wootters W. K.(1993). Teleporting an unknown quantum state via dual classical and Einstein-Podolsky-Rosen channels.Phys. Rev. Lett.70, 1895.

Raman Spectroscopy of Fe ion implanted InGaAs epilayer grown using MBE

Anita Rani,Rakesh Kumar Pandey*, Suresh Kumar Jangir, Soni Kumari, Anubha Jain, Dushyant Kumar, Yateesh Kumar Mishra, Monika Kumari, MVG Padmavati, Puspashree Mishra
Solid State Physics Laboratory, DRDO, Lucknow Road, Timarpur, Delhi, India
Corresponding author email id: rakeshpandey.sspl@gov.in, anitamirdha05@gmail.com

Terahertz radiation lies between the microwave and infrared regions of the electromagnetic spectrum and offers many potential applications in areas such as imaging, spectroscopy, communication, and sensing. The possibility of 1.5 μm fiber laser coupling and several favorable properties e.g., ultra-short carrier life time with high resistivity, and mobility enables InGaAs-based material best suited for terahertz PCA-based applications. Molecular beam epitaxy (MBE) is preferred method to grow high-quality InGaAs epilayers for terahertz devices. Ion implantation is usually carried out to modify the electrical and optical properties of semiconductors. Fe ion implantation in InGaAs is known to create deep midgap acceptors, provide additional defect centres to those related to implantation damage and offer both the high resistivity and the ultrashort carrier lifetimes required for terahertz (THz) applications [1].Here, we report Fe ion implantation in $In_{0.53}Ga_{0.47}As$ films at different energies with constant dose. The $In_{0.53}Ga_{0.47}As$ films used in this experiment have been grown on semi-insulating GaAs (001) using molecular beam epitaxy (MBE) at substrate temperature ~510C. Films have been implanted with Fe at 150 keV, 175 keV and 200 keV energies in negative ion beam implanter. Raman Spectroscopy is performed on implanted samples as well as pristine samples for structural analysis. Scattering by LO modes is allowed by the Raman selection rules in backscattering geometry from an (001) orientated substrate. In an InGaAs alloy, the optical phonons exhibit a two-mode behaviour, this means InAs- and GaAs- like modes exist over the whole composition range. In $In_{0.53}Ga_{0.47}As$, the two LO modes are observed at 239 cm^{-1} and 269.5 cm^{-1} for pristine sample. The GaAs- like peak is dominated over InAs- like peak because of higher polarizability of GaAs bond compared to InAs bond. For higher implantation dose of Fe at energies 150 keV, 175 keV, 200 keV respectively, the peaks broadens and the InAs- like peak merges with GaAs peaks due to structural disorder created in sample and this results a plateau between 220 cm^{-1} and 270 cm^{-1} [2].

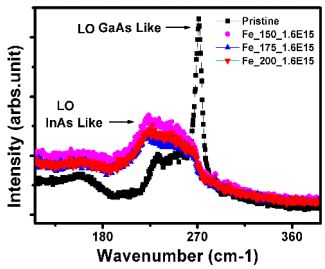

Figure 1: Raman spectra of pristine and ion implanted InGaAsgrown using MBE system

References:

[1] C. Carmody, H. H. Tan, C. Jagdish, A. Gaarder, S. Marcinkevicius, Appl. Phys. Lett. 22, 82, (2003).
[2] S. HernaHndez, B. Marcos, R. CuscoH, N. Blanco, G. GonzaHlez-DmHaz, L. ArtuHs, 87, 721, (2000).

Detection of melamine in milk using molecular imprinting polymerization (MIP) based fiber optic probe

Jyoti[1], R. K. Verma[1]*
[1]Department of Physics, University of Allahabad
*Corresponding author email id: rkverma@allduniv.ac.in

Excessive adulteration of melamine in milk leads to kidney and urinary tract diseases. In the year 2007, urinary tract adverse in 294000 children, and the death of 6 children were reported due to excessive adulteration of melamine in milk [1,2]. In this present work, the fabrication of fiber optic probes has been done for highly sensitive and selective detection of melamine in milk. Probes were initially synthesized with TiO_2 nanoparticles using the sol-gel method and further coated with an additional layer of molecular imprinting polymerization technique as shown in Figure 1. It has been obtained that the MIP-coated probe is highly selective to melamine and a sensitivity of 0.363 nm/mM was obtained. A quick time response of 4-8 seconds and the limit of detection and limit of quantification values of 1.128 mM and 2.790 mM were obtained. Other performance parameters like full width half maximum and figure of merit were also measured in this experimental work.

Keywords: Molecular Imprinting, Melamine, Adulteration, TiO_2 nanoparticles, Fiber optic sensors

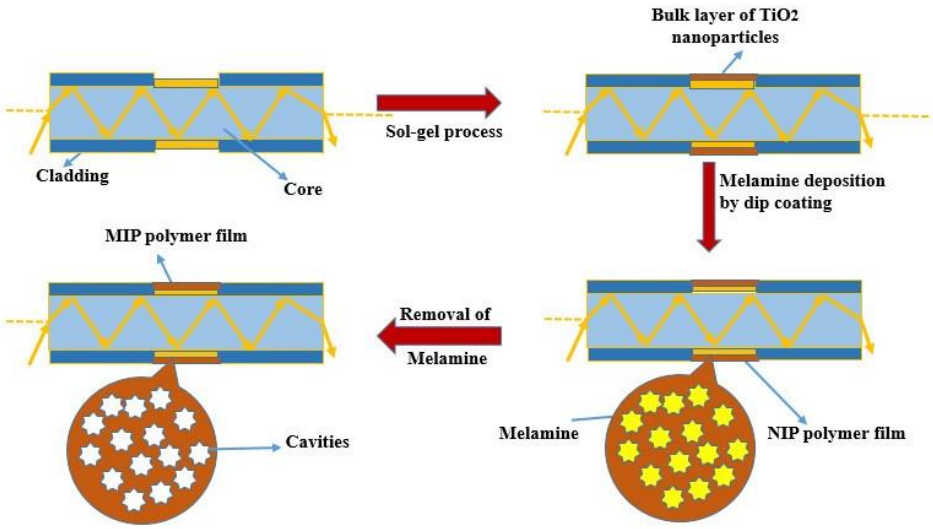

Figure 1. Fabrication of fiber optic probe by Molecular Imprinting Polymerization technique

References:

[1] Lei, H., Su, R., Haughey, S. A., Wang, Q., Xu, Z., Yang, J.,& Sun, Y. (2011). Development of a specifically enhanced enzyme-linked immunosorbent assay for the detection of melamine in milk. Molecules, 16(7), 5591-5603.

[2] Brown, C. A., Jeong, K. S., Poppenga, R. H., Puschner, B., Miller, D. M., Ellis, A. E., & Brown, S. A. (2007). Outbreaks of renal failure associated with melamine and cyanuric acid in dogs and cats in 2004 and 2007. Journal of Veterinary Diagnostic Investigation, 19(5), 525-531.

First Principles Studies of Opto-electronic, Spectroscopic and Molecular Docking of Olivacine Drug

Abhinav Mishra*, Dipendra Sharmaand Sugriva Nath Tiwari
Department of Physics, D.D.U. Gorakhpur University, Gorakhpur-273009, India
(abhinav.phy94@gmail.com, d_11sharma@rediffmail.com, sntiwari123@rediffmail.com)*
**Corresponding author email id: abhinav.phy94@gmail.com*

A semisynthetic isomer of ellipticine,olivacine drug belongs to the family of natural alkaloids; which possesses analgesic, antibacterial and antipyretic properties. It is a model anti-cancer drug acting as topoisomerase II inhibitor. The mechanism of action and antineoplastic properties of olivacine are ascribed to its intercalative binding into DNA helices. Thepresent paper reports DFT investigation of the structure, electro-optical properties, infrared, Raman, UV-Vis and NMR analysis of the olivacine. Frontier orbitals (HOMO and LUMO), MEP surface and density of states (DoS) along with NLO analysis of the drug have been examined. Furthermore, inhibitory activity and binding sites of olivacine with three isomerase transcriptases (PDB Id: 1did, 2ypi and 1xig) have been elucidated by molecular docking technique.

Keywords: Olivacine, DFT, HOMO-LUMO, Topoisomerase II Inhibitor, Molecular Docking

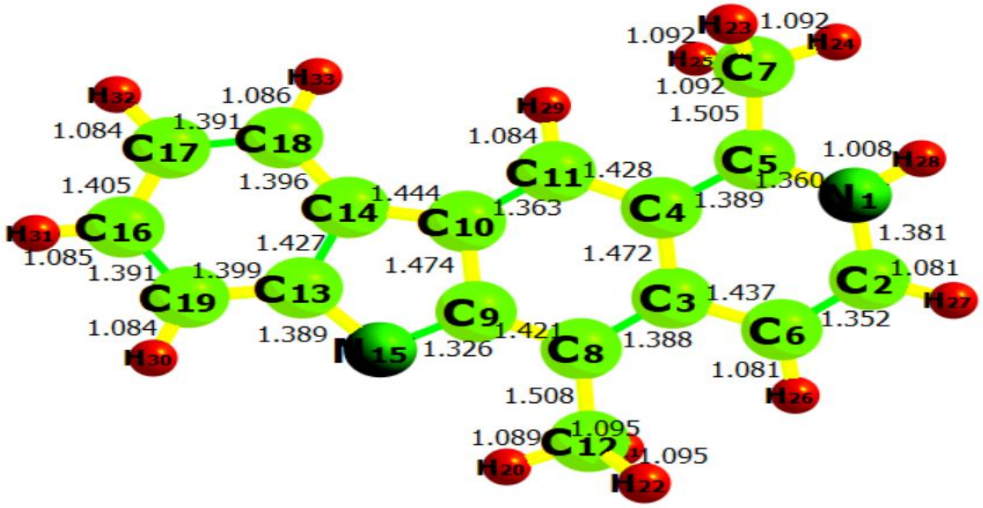

Fig.1:Optimized structure of olivacine drug.

References:

[1] Wenkert Ernest & Dave K G (1962). Synthesis of olivacine. Journal of American Chemical Society, 84 (1), 94–97.
[2] Mishra A, Sharma D&Tiwari SN (2023). Theoretical Investigation by Density Functional Theory and Molecular Docking of a Naturally Occurring Anticancer Drug: 9-Hydroxyellipticine. Recent Advances in Nanotechnology ICNOC 2022. Springer Proceedings in Materials,28, 117-123.
[3] Mishra A, Sharma D & Tiwari S N (2023). DFT and Molecular Docking Studies of an Antiviral Drug: Molnupiravir. Indian Journal of Pure & Applied Physics, 61, 810-812.

Utilizing Fe_3O_4@PEI@Ag Metallic Magnetic Microspheres Substrate for Surface-Enhanced Raman Spectroscopy (SERS) in the Detection of Organic Pollutant Dyes

Dev Kumar, Akanksha Yadav, Anil Kumar Yadav*
Crystal growth& Raman lab Department of Physics, Chaudhary Charan Singh University, Meerut UP- (250004)
Email:devphysics369@gmail.com,akansha.9793@gmaail.com
**Corresponding author email id: anilsaciitb@gmail.com*

In our current research, our primary objective is to detect extremely low concentrations of organic pollutants, specifically harmful dyes such as Malachite Green (MG) and Crystal Violet. These substances pose significant risks to both human health and the environment. To detect these t organic pollutants, we have synthesized Fe_3O_4@Ag magnetic nanoparticles (microspheres) and employed a Surface-Enhanced Raman Spectroscopy (SERS) method.The process of creating these microspheres can be summarized in three steps:Initially, we synthesized Fe_3O_4 particles using a hydrothermal method.Subsequently, we coated Polyethyleneimine (PEI) on these microspheres, resulting in Fe_3O_4@PEI microspheres.Next, we deposited silver nanoparticles onto the Fe_3O_4@PEI microspheres, resulting in the formation of Fe_3O_4@PEI@Ag composite magnetic microspheres.The deposition of silver (Ag) onto the Fe_3O_4@PEI microspheres has been thoroughly characterized using various techniques, including X-ray diffraction (XRD), field emission scanning electron microscopy (FE-SEM), and elemental analysis through Energy Dispersive X-ray Analysis (EDAX). In the XRD pattern, distinct diffraction peaks were observed at 2θ values of 38.15° (111) and 44.35° (200), confirming the presence of crystalline metallic silver nanoparticles with a cubic structure. Additionally, the magnetic properties of these microspheres have been assessed using a Superconducting Quantum Interference Device (SQUID) and absorbance by UVspectrometer. Furthermore, we have successfully determined the lowest detection limit for all two dyes using the SERS method with a Raman spectrometer. The surface morphology of the deposited Ag (Silver) on Fe_3O_4 microspheres was identified using Field Emission Scanning Electron Microscopy (FE-SEM). The magnetic saturation (MS) values for Fe_3O_4@Ag microspheres were measured at 32.1 emu/g.The maximum absorbance peak of Fe_3O_4@Ag microspheres was observed at 456 nm by UV spectroscopy.Finally, we detect the lowest detection limit of these two dyes 10^{-8} and 10^{-10} via the SERS method.

Keywords: Surface-Enhanced Raman Spectroscopy (SERS), Malachite Green (MG), magnetic nanoparticles, Polyethyleneimine (PEI)

The behavior of Raman active phonon mode for β-$(Al_xGa_{1-x})_2O_3$ alloys

Jayanta Bhattacharjee,[1,2*] and S. D. Singh[1,2]
[1]Accelerator Physics and Synchrotrons Utilization Division, Raja Ramanna Centre for Advanced Technology, Indore 452013, India
[2]Homi Bhabha National Institute, Training School Complex, Anushakti Nagar, Mumbai 400094, India
Corresponding author email id: jayanta@rrcat.gov.in, jayanta.jagat1991@gmail.com

Aluminium (Al) substituted β-Ga_2O_3 alloy has attracted paramount attention because of bandgap engineering, where the bandgap can be tuned from 4.5 eV to 6.9 eV[1]. Phonon modes of an alloy have an important role in their electronic transport and thermal conducting properties. Hence, the phonon mode behaviour of β-$(Al_xGa_{1-x})_2O_3$alloy has been investigated from Raman spectroscopy for Al compositions up to x= 0.444. The alloy shows mixed-mode behaviour, where low frequency (100-200 cm^{-1}) and high frequency (500-800 cm^{-1}) modes correspond to translation and libration of (Ga_IO_{IV}) tetrahedral chain and stretching and bending of (Ga_IO_{IV}) tetrahedral chain, respectively remain intact throughout the composition range ($x \leq 0.444$) and display one-mode behaviour. On the other hand, medium frequency (300-500 cm^{-1}) phonon modes related to the deformation of ($Ga_{II}O_{VI}$) octahedra and (Ga_IO_{IV}) tetrahedra chains show sudden change such as appearance (disappearance) of new (existing) phonon modes as shown in Fig. 1. The appearance (disappearance) of new (existing) modes with the Al substitution correspond to the Al-O (Ga-O) sublattices and they display two-mode behaviour[1]. The existence of two sublattices is further supported by the preferential occupation of the Al atom at the octahedral site in comparison to the tetrahedral site in nearly the whole composition range. The observation of phonon modes related to translation and libration of (Ga_IO_{IV}) tetrahedral chain up to an Al composition of 0.444 indicates that the monoclinic lattice's long-range periodicity is maintained throughout the investigated Al composition range.

Keywords: Mixed-mode; Raman spectroscopy; Ultra-wide bandgap semiconductors

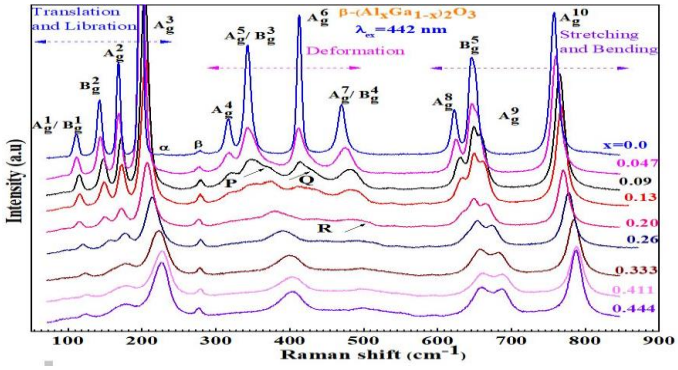

Figure 1. Raman spectra of β-$(Al_xGa_{1-x})_2O_3$ alloys for different Al compositions. The appearance of new phonon modes has been denoted by P, Q, and R. Peaks indicated by symbol 'β' is related to the plasma line of the laser.

References:

[1] Bhattacharjee J, Singh S D (2023), Observation of mixed-mode behaviour of Ramanactive phonon modes for β-$(Al_xGa_{1-x})_2O_3$ alloys. Appl. Phys. Lett. 122, 112101.

Role of Er_2O_3/WS_2 Nanocompositeto Enhance Optical and Morphological Properties

Naresh mandhan, Vidyotma yadav, and Akanksha pandey, Tanuja mohanty *
[1]Jawaharlal Nehru University, New Delhi, India;
*Corresponding author email id: tanujajnu@gmail.com

Tungsten disulfide (WS_2) is a transition metal di-chalcogenide (TMD) arranged in a layered form where each layer is connected by a Van der Waals force. The TMDs atoms are covalently bound to each other within the layer, forming an X-M-X arrangement, where M represents the metal and X represents the chalcogenide. WS_2 among other TMDs possess unique optical and morphological properties. The Nanocomposite of Er_2O_3/WS_2 can be synthesized providing required conditions. In this work, quantum dots of $WS_2$and Er has been synthesized using liquid phase exfoliation method. Initially a paste by mortar and paste to 1 hr with DMSO(10mg/ml) then magnetic stirrer for 0.5 hr with 1.2k rpm at room temperature. After that a bath sonication of WS_2 powder was performed for 71 hrs for effective exfoliation of WS_2 quantum dots (QDs).The same is repeated for Er_2O_3 but for 22 hrs of bath sonication. The ultrasonic waves help weakening of Van der Waals bonding between the layers as well as decrease the lateral size with time. Determining the size from XRD analysis and Morphological studies by TEM(Transmission Electron Microscopy) has confirmed the successful synthesis of Er2O3/WS_2.The UV-Visible absorption(Bandgap increases with increases in concentration of Er) and fluorescence spectroscopy have been conducted on the samples to study the effect on optical properties.Fig 1(a) depicts the UV-Visible absorption spectra and Tauc's plot is also presented in inset of this figure.The estimated values of bandgaps of WS_2 and Er_2O_3/WS_2 with 5%,7.5% and 10% concentrations are 4.170eV, 4.190eV, 4.193 and 4.197eV respectively. The enhancement in band gap is indicating the decrease in size of nanocomposite which can be a milestone to enhance the optical performance in device fabrication. The alteration in the Er_2O_3/WS_2 bandgap may be attributed to changes in the electronic energy band brought on by Charge Transfer Process(Er to WS_2). The emission fluorescence spectra are recorded for excitation wavelength at 350nm are presented in Fig. 1(b). A broad emission is observed with a red shift(Near IR Region) from WS_2 QDs to Er_2O_3/WS_2 Nanocompositewith different concentration variations.

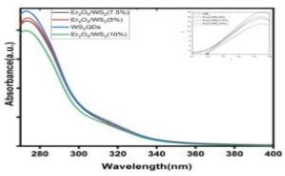

Fig. 1(a)

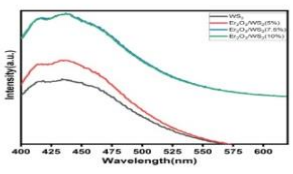

Fig. 1(b)

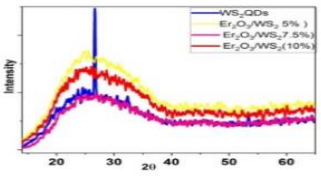

Fig. 1(c)

Fig. 1: (a) UV-Visible absorption spectra (Inset: Tauc's plot) (b) Fluorescence spectra at 350nm excitation (c) XRD Spectra of WS2 QDs and Er_2O_3/WS_2 nanocomposite.

Keywords: WS_2QDs, Er_2O_3(Erbium Oxide), UV-Visible Spectroscopy, Fluorescence spectroscopy, TEM

References:

[1] Bora Larionette & Mawlong P.L.et.al (2020). Journal of Colloid and Interface Science. **561**, 519-532.
[2] Sakthivel J & Chandrasekaran A.et.al(2022), New J. Chem.**46**,17066.

Nonlinear Absorption of High Powercosh-Gaussian Laser Beam in Carbon Nanotubes

Kaisar Ali[1], Sujeet Kumar[1], Arvind Kumar[1], Asheel Kumar[1]*, S P Mishra[2] and Ashish Varma[2]
[1]Plasma Physics Research Group, Department of Physics, University of Allahabad, Prayagraj-211002, India
[2]Laser Plasma and Material Research Group, Department of Physics, K. N. Govt. P. G. College, Gyanpur, Bhadohi-221304, India
**Corresponding author email id: asheel2002@gmail.com*

In this present study, we investigate the nonlinear absorption of high powercosh-Gaussian laser beam in array of carbon nanotubes. The laser beam propagates normally to the parallel aligned carbon nanotubes. The electric field profile of laser beam produces the electrostatic restoration force due to displaced electron and ion cylinder. This net restoration force with respect to ion cylinder and electron cylinder causes the nonlinearity. An analytic expression of high-power laser beam absorption coefficient is derived. The resonant absorption is achieved as the laser beam frequency approaches near the effective surface plasmons frequency $\omega \sim \omega_{pe}/\sqrt{2}$. The laser beam absorption process is tuned by varying the laser beam decentered parameter, carbon nanotube length, radius, density, and collisional frequency. This enhanced and tunable absorption of laser beam in carbon nanotubes might have application in the heating process.

Keywords: Absorption Coefficient, Carbon Nanotube, Surface Plasmon Frequency, Decentered Parameter, Collisional Frequency.

References:

[1] Yadav, M., Mandal, S., & Kumar, A. (2019). Nonlinear absorption and harmonic generation of laser in an assembly of CNT's. Physics of Plasmas, 26(7).
[2] Tiwari, P. K., & Tripathi, V. K. (2004). Stimulated Raman scattering of a laser in a plasma with clusters. Physics of Plasmas, 11(4), 1674-1679.
[3] Kumar, A., Mishra, S. P., Kumar, A. & Varma, A., (2023) Electron Bernstein wave aided cosh-Gaussian laser beam absorption in plasma, Optik 273, 170436.

Squeezing enhanced coherent anti-Stokes Raman spectroscopy (CARS)

Taj Kumar[1], Gaurav Shukla[1], Priyanka Sharma[1], Anand Kumar[1], Krishna Mohan Mishra[1], Aviral Kumar Pandey[1], Devendra Kumar Mishra[1]*
[1]Department of Physics, Institute of Science, Banaras Hindu University, Varanasi 221005, India
Corresponding author email id: kndmishra@gmail.com

The sensitivity of coherent anti-stokes Raman spectroscopy (CARS) [1] is limited by the shot-noise from the probe fields. We present the theoretical analysis of a squeezing-enhanced version of CARS that overcomes the shot-noise limit with enhancement of the Raman signal and inherent background suppression, while remaining fully consistent with conventional Raman spectroscopy methods. We introduce the Raman sample between two phase-sensitive optical parametric amplifiers [2] that squeeze the light along orthogonal quadrature axes, and then perform estimation of phase using the quantum detection technique, where the quantum enhancement is gained over the classical scenario. Our work may find potential applications in chemical sensing [3], and non-invasive imaging and sensing of biological samples.

Keywords: Coherent anti-stokes Raman spectroscopy (CARS), Optical parametric amplifiers.

References:

[1] Pezacki, J. P., Blake, J. A., Danielson, D. C., Kennedy, D. C., Lyn, R. K., & Singaravelu, R. (2011). Chemical contrast for imaging living systems: molecular vibrations drive CARS microscopy. *Nature chemical biology*, *7*(3), 137-145.
[2] Hanlon, E. B., Manoharan, R., Koo, T., Shafer, K. E., Motz, J. T., Fitzmaurice, M., ... & Feld, M. S. (2000). Prospects for in vivo Raman spectroscopy. *Physics in Medicine & Biology*, *45*(2), R1
[3] Baumgartner, R., & Byer, R. (1979). Optical parametric amplification. *IEEE Journal of Quantum Electronics*, *15*(6), 432-444.

Surface-enhanced Raman Scattering(SERS): An effective tool for trace-level detection of melamine in milk using gold-based substrate

Akanksha Yadav, Dev Kumar, Dr. Anil K. Yadav*
Department of Physics, Chaudhary Charan Singh University, Meerut 250004 India
Email: akanksha.9793@gmail.com,
**Corresponding author email id: anilsaciitb@gmail.com*

There is a considerable demand for techniques for on-site food contamination analysis. Even though on-site food testing with portable Raman spectroscopy is widespread, achieving this objective with quick detection and a budget-friendly substrate can be difficult. In the present research, we used the Surface-enhanced Raman Scattering (SERS) technique to find traces of melamine, a food contaminant, in samples of milk powder. We designed a quick and effective method for creating paper that functions as a SERS-active substrate and contains gold nanoparticles (AuNPs) that have been reduced by polyethylene glycol. To confirm the formation of AuNPs, synthesized AuNPs were characterized using a UV-Vis spectroscope and absorption maxima was observed about 520 nm. Further, to know their size and morphology particles were analyzed by transmission electron microscopy(TEM) indicating 20-30 nm spherical AuNPs. The developed substrate was successfully characterized for SERS analysis using a probe dye Rhodamine 6 G (R6G), for which limit of detection (LOD) 10^{-8} M was achieved. Further, different concentrations of spiked powder milk samples were evaluated using SERS detection technique. We successfully detected traces of melamine in spiked milk samples which is as low as 0.10 ppm. As a result, our technique offers enormous potential for field-based detection of melamine in milk as well as other contaminants in dairy products.

To study the third harmonic generation and growth rate of stimulated Raman scattering using Hermite cosh Gaussian laser beam

Taruna[1], Niti Kant[2] and Oriza Kamboj[1]
[1]Lovely Professional University, Punjab, India
[2]University of Allahabad, Prayagraj, India
Corresponding author email id: tarunaazad875@gmail.com

This study delves into Stimulated Raman scattering occurring within a plasma medium subjected to an applied magnetic field. As the laser beam travels through the plasma, it undergoes a transformation into both an upper hybrid wave and a down-shifted sideband wave. The interaction between the incident laser and the sideband wave gives rise to the generation of a nonlinear ponderomotive force, which acts on plasma electrons, leading to the excitation of the upper hybrid wave. Simultaneously, this interaction parametrically couples the incident wave with the upper hybrid wave, thereby inducing the stimulation of the sideband. Utilizing a fluid model and nonlinear current density analysis, we precisely ascertain the characteristics of the nonlinear ponderomotive force, including the dispersion relation and growth rate, particularly within the weakly relativistic regime. Furthermore, the paper formulates equations describing the third harmonic Raman instability, underscoring the pivotal roles played by plasma and laser parameters, in conjunction with the strength of the electric field. These findings carry substantial implications for the advancement of plasma-based technologies.

Keywords: Stimulated Raman Scattering, Upper Hybrid Wave, Nonlinear Ponderomotive Force, Non linear Current Density, Growth Rate.

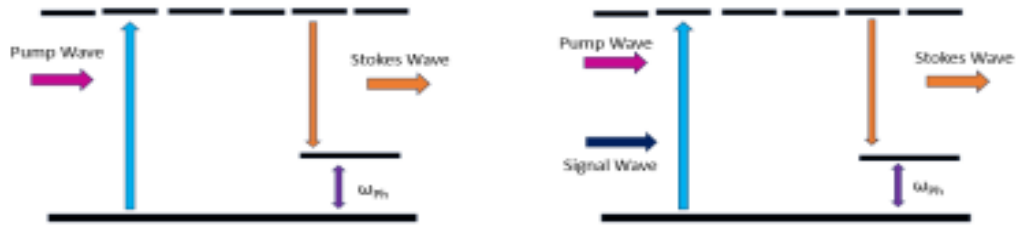

Figure 1: Schematic Diagram of Stimulated Raman Scattering.

References:

[1] A.Khaleefa, Z. S., Mahdi, S. S., & Yaseen, S. K. (2020, March). Numerical Analysis of CW Raman Amplifier in Silicon-on-Insulator Nano-Waveguides. In IOP Conference Series: Materials Science and Engineering (Vol. 757, No. 1, p. 012022). IOP Publishing.
[2] Ali, A. H., Kamboj, O., & Kant, N. (2022, May). Study of growth rate of backward Raman scattering in plasma with density ripple. In Journal of Physics: Conference Series (Vol. 2267, No. 1, p. 012015). IOP Publishing.
[3] Paknezhad, A., &Dorranian, D. (2013). Third harmonic stimulated Raman backscattering of laser in a magnetized plasma. Physics of Plasmas, 20(9).

Enhanced Vis-NIR Absorption using $Ti_xZr_{1-x}N$ $Ti_xSc_{1-x}N$ and $Ti_xMg_{1-x}N$ based Plasmonic Grating

Yajvendra Kumar[1], Manmohan Singh Shishodia[2*] , Beer Pal Singh[3]
[1.] Department of Physics, D.P.B.S.P.G.CollegeAnupshahr, Bulandshahr, India-203390
[2.] Department of Applied Physics, Gautam Buddha University, Greater Noida, India-201312
[3.] Department of Physics, Chaudhary Charan Singh University Meerut, India-250004
**Corresponding author email id:* manmohan@gbu.ac.in

Ternary Transition Metal Nitrides (TMNs) such as $Ti_xZr_{1-x}N$ $Ti_xSc_{1-x}N$ and $Ti_xMg_{1-x}N$ are emerging as effective and alternative plasmonic materials for Vis-IR spectra [1]. These transition metal nitrides have an edge on coinage metals (e.g., Au, Ag, and Al etc.) due to their CMOS compatibility, low optical losses, better corrosion and abrasion resistance, higher hardness, and thermal stability at high temperature. This is now well known that, traditional TMNs such as TiN, ZrN, and HfN shows plasmonic tunability in UV and Visible spectral region. Alloying these binary TMNs such as TiN with Zr, Sc, and Mg can extend their plasmonic response to the NIR range, especially in the telecommunication window. In the present work, we investigate the plasmonic properties of $Ti_xZr_{1-x}N$ $Ti_xSc_{1-x}N$ and $Ti_xMg_{1-x}N$-based plasmonic gratings. Specifically, the dispersion characteristics and the plasmonic length scales, namely surface plasmon polaritons wavelength (λ_{SPP}), penetration depth into metal (δ_m)/dielectric (δ_d), and surface plasmon polaritons propagation length (δ_{SPP}) are estimated and their comparison with, the most commonly used plasmonic materials e.g., Au and Ag is done. One-dimensional metallic lamellar grating can significantly enhance the light absorption by virtue of diffraction and excitation of surface plasmon polaritons at the metal-dielectric interface [2, 3]. This results in the subwavelength confinement and hence the greater absorption in the absorbing layer near grating. The enhanced absorption can be tuned in different spectral regions by controlling grating parameters such as the grating period, grating height, grating aspect ratio etc. and the composition of these ternary alloys. Here, ternary transition metal nitrides have been assessed for their suitability in Vis-NIR wavelength range.

References:

[1] Kassavetis S., Bellas D. V., G. Abadias, E. Lidorikis, and Patsalas P., (2017) "Infrared Plasmonics with Conductive Ternary Nitrides'', ACS Appl. Mater. Interfaces 9, 10825
[2] Shishodia M. S. and Perera A. G. U., (2011) "Heterojunction plasmonic midinfrared detectors", J. Appl. Phys. 109, 043108.
[3] Barnes W. L., (2006) "Surface plasmon-polariton length scales: a route to sub-wavelength optics", J. Opt. A: Pure Appl. Opt. 8, S-87.

Pressure Sensor Utilizing High Birefringence Photonic Crystal Fiber

Sudhir Kumar[1], Monika Goyal[2], Binay Prakash Akhouri[1] and Mohit Sharma[3]
[1]*Department of Physics, S. S. Memorial College, Ranchi University Ranchi, India*
[2]*Department of Physics, Dronacharya Degree College, Kurukshetra - 136119, India*
[3]*Department of Physics, SLAS, Mody University of Science and Technology, Lakshmangarh, Rajasthan, India*

This study presents a concept for a highly sensitive Photonic Crystal Fiber sensor with high birefringence and low confinement losses. The sensor is specifically designed for pressure detection applications. The Photonic Crystal Fiber structures under consideration incorporate additional air holes in the core region for achieving high birefringence. The proposed photonic crystal fiber structures were analyzed using the full vectorial Finite Element Method (FEM) numerical simulations. The study focused on investigating the sensitivity, confinement losses, effective refractive index, and modal birefringence characteristics of these structures. It is reported that the proposed PCF structures possess a notable degree of relative sensitivity, a significant level of birefringence, and minimal confinement losses across a range of analytes.

Keywords: Pressure sensor; photonic crystal fiber; fiber sensors; integrated optics.

Lead Silicate Giant Nonlinear Photonic Crystal Fiber for Optical Communication Applications

Abhishek Kumar, Manoj Mishra, Brajraj Singh and Mohit Sharma
Department of Physics, SLAS, Mody University of Science and Technology, Lakshmangarh, Rajasthan, India

This work introduces a novel Lead silicate (SF57) photonic crystal fiber (PCF) with eleven concentric rings of air holes. The PCF promises to yield very large nonlinearity $\sim 13169\ \mathrm{W^{-1}km^{-1}}$ at $0.75\ \mu m$, $\sim 8607\ \mathrm{W^{-1}km^{-1}}$ at $1.064\ \mu m$ and $\sim 4640\ \mathrm{W^{-1}km^{-1}}$ at $1.55\ \mu m$. The PCF has two zero dispersion at wavelength $0.3\ \mu m$ and $1.50\ \mu m$. The current recorded value of nonlinearities is the highest to date. The PCF possesses a significantly small optical mode field, resulting in a substantial nonlinearity that renders it highly appropriate for creating supercontinuum and optical communication.

Keywords: Nonlinearity; photonic crystal fiber; Super continuum generation; Single Mode.

Potential of laser induced breakdown spectroscopy (LIBS) technique coupled with chemometric methods for the detection of nutritional and toxic element in dry fruits

Tejmani Kimar[1], A. K. Rai[1]*
[1]Laser Spectroscopy Research Laboratory (LSRL)
Department of Physics
University of Allahabad, Prayagraj, 211002
**Corresponding author email id: awadheshkrai@gmail.com*

Laser-induced breakdown spectroscopy (LIBS) is gaining much attention due to its unique capability for monitoring the major and minor constituents present in any phase (solid, liquid, or gas) of samples. In the present work, we have conducted qualitative and quantitative investigations of essential and trace heavy elements present in health-beneficial dry fruits (almonds, dates, raisins, and cashew) using laser-induced breakdown spectroscopy. For an accurate elemental exposure using the LIBS technique, the local thermo-dynamic equilibrium of the laser-induced plasma was established and verified using the McWhirter criterion based on the electron density in the plasma. Earlier, our LIBS detector was optimized. For the quantification of elements, the standard calibration-free (CF)-LIBS method was applied. Using our LIBS system, nutritional elements such as aluminium (Al), magnesium (Mg), calcium (Ca), iron (Fe), potassium (K), zinc (Zn), and sodium (Na) and toxins like lead (Pb), chromium (Cr), and copper (Cu) were detected in dry fruits. The elemental quantification of dry fruit contents was validated using the standard atomic absorption spectroscopy (AAS) method. Principal component analysis (PCA) has been used to classify the different dry fruits on the basis of their major and minor continents present in the samples.

Keywords: LIBS, Elemental analysis, Dry fruits, AAS, Atomic Absorption Spectroscopy, Chemometric methods

Silver-BP-Graphene based Surface Plasmon ResonanceBiosensor for Sensing Biomolecules

Awadhesh Kumar and S. K. Srivastava*
Department of Physics, Institute of Science, Banaras Hindu University, Varanasi-221005.
**Corresponding author email id: sanjay_itbhu@yahoo.com*

The sensitivity of a surface plasmon resonance (SPR) biosensor, consisting of the BK-7 prism, silver, and 2D materials primarily black phosphorous (BP) and graphene, is aimed to be improved by this work. Angular interrogation techniques are employed in the proposed device, and a wavelength of 633 nm is utilized. The silver layer has been optimized to a thickness of 55 nm. In terms of sensitivity (S), a value of 175 deg/RIU, a detection accuracy (DA) of 12.2, and a quality factor (QF) of 154.9 RIU-1 are demonstrated by our results. The sensing medium refractive indices are taken to range from 1.33 to 1.41. This structure can be deemed suitable for the detection of biomolecules and other analytes.

Keywords: surface plasmon resonance (SPR), sensitivity, graphene, biomolecules, BK-7 prism

Tunable Nonlinear Current Density Generation by Beating of Two High Power Laser Beams in Plasma Embedded with Nanocluster

Sujeet Kumar[1], Kaisar Ali[1], Arvind Kumar[1], Asheel Kumar[1]*, S P Mishra[2] and Ashish Varma[2]
[1]Plasma Physics Research Group, Department of Physics, University of Allahabad, Prayagraj-211002, India
[2]Laser Plasma and Material Research Group, Department of Physics, K. N. Govt. P. G. College, Gyanpur, Bhadohi-221304, India
Corresponding author email id: asheel2002@gmail.com

In this paper, we study the generation of nonlinear current density by the interaction of two copropagating high power Hermite-cosh-Gaussian (HChG) laser beams in nanoclustered plasma medium. It is assured that nanocluster become ionize owing to the interaction of intense electromagnetic radiation of laser field with it and hereafter clusters are converted into the plasma plume balls. As the interaction process takes place, each electromagnetic radiation of laser beam conveys the oscillatory velocity to the both medium electrons. The two copropagating HChG laser beams might be undergoes to the beat process of wave with beat wave number $k = k_1 - k_2$and frequency $\omega = \omega_1 - \omega_2$ and surely a nonlinear force acts on electron associated with nanoclustered plasma which is generally termed as ponderomotive force. An expression of generation of nonlinear current density is analytically derived by using the nonlinear oscillatory velocity and nanoclustered plasma density. The effective surface plasmons oscillation is become resonant as the beat wave frequency becomes the $\sqrt{3}$ times the electron plasma frequency causes the much more generation of current density in clusteredplasma. The nonlinear current density is tuned and controlled by cluster radius, cluster density, beam decentred parameter, electron-neutral collisional frequency and laser mode index m. This enhanced and tunable nonlinear current density might have possible applications in terahertz radiation generation, anomalous resistivity, harmonic generation, and many more.

Keywords: Mode index, Collisional frequency, Decentered parameter, Ponderomotive force, Oscillatory velocity.

References:

[1] Kumar, A., Kumar, A., Mishra, S. P., Yadav, M. S., & Varma, A. (2022). Plasma wave aided heating of collisional nanocluster plasma by nonlinear interaction of two high power laser beams. Optical and Quantum Electronics, 54(11), 753.
[2] Siahmazgi, R. N., &Jafari, S. (2021). Soft X-ray emission from an anharmonic collisional nanoplasma by a laser–nanocluster interaction. Journal of Plasma Physics, 87(3), 905870312.
[3] Varma, A., & Kumar, A. (2021). Electron Bernstein wave aided beat wave of Hermite-cosh-Gaussian laser beam absorption in a collisional nanocluster plasma. Optik, 245, 167702.

Computation of Start Oscillation Current in a Gyroklystron Amplifier

Nazish Fatima Siddiqui*, Dipendra Sharma, Madan Singh Chauhan
Department of Physics, Deen Dayal Upadhyaya Gorakhpur University, Gorakhpur-273009
**Corresponding author email id: nazishfatima.nfs@gmail.com*

The gyroklystron is a high-power coherent radiation source that has been intensively developed for various applications, such as millimeter-wave radars, RF plasma heating systems, spectroscopy, and high-gradient linear accelerators. Due to its fast-wave nature and extended interaction structure, gyroklystron amplifiers are considered strong contenders for high-power generation in the millimeter and submillimeter wave bands. The gyroklystron functions as a high-power microwave tube amplifier, combining the characteristics of a multicavity klystron with the energy extraction method of a cyclotron resonance maser instability, similar to a gyrotron. Its operation is similar to conventional klystrons, with the exception that electron bunching occurs in the azimuthal direction instead of the axial direction, and larger overmoded cylindrical cavities are utilized, allowing them to operate at higher frequencies and with greater cavity sizes. The gyroklystrons currently under development have been built to exceed the average and peak output limitations of conventional amplifiers.

To optimize device performance, the primary design characteristics of the gyroklystron include the choice of RF structure, electron beam, magnetic field, drive signal parameters, and start oscillation current. Additionally, the gyroklystron exhibits a large number of competitive modes. To ensure effective operation, it is crucial to excite the operating mode in the interaction cavity while suppressing the competitive modes. As a result, the design of the gyroklystron's start oscillation current becomes a crucial parameter for the device's efficient operation. This parameter enables the investigation of conditions that can produce self-oscillations and excite other competing modes in the device. Preventing oscillations is a significant concern for gyroklystrons, as they not only contaminate the desired output spectrum but can also easily destroy the frequency of interest by draining its power. Therefore, modifying the beam current, magnetic field, cavity size, and cavity quality factor is essential to prevent oscillations.

In this paper, a numerical code has been developed to compute the start oscillation current of a 35 GHz gyroklystron amplifier operating at the fundamental electron cyclotron frequency in the TE_{01} mode. The calculated start oscillation current is found to be greater than the operating current, ensuring the stability of the device. Additionally, the effect of the electron beam velocity ratio (α) and quality factor on the start oscillation current has been studied in detail through parametric analysis.

Keywords: Microwave tubes, fast-wave device, millimeter-wave amplifier.

Study the Emission Feature of the Slowest Target Fragments Released in the Interaction of ^{84}Kr+Em 1 A GeV

D. Sharma[1], B. Kumari[1], M. K. Singh*[1], V. Singh[2]
[1]Department of Physics, IAH, GLA University, Mathura-281406, India
[2]Department of Physics, School of Physical and Chemical Sciences, Central University of South, Bihar, Gaya 824236, India
**Corresponding author email id: singhmanoj59@gmail.com*

A significant obstacle to explaining the mechanism of nucleus-nucleus interactions is the study of the processes that take place in the participant and spectator parts of interacting nuclei, and in particular, the interaction between these processes, which is significant given the central nature of the reactions [1, 2]. These issues can be resolved with the use of nuclear emulsion experiments, which offer a full 4π angular coverage and enable the estimation of projectile fragment charges as well as the nearly threshold-less identification of particles as shower, grey, or black particles [3]. The multiplicity distributions for the slowest target fragments (black particles) released in encounters of ^{84}Kr ions with emulsion nuclei at 1 A GeV were examined as a function of collision centrality. To identify the procedure leading to the creation of secondary particles, the collected data was also compared with the other available experimental data and found consistent results [4, 5].

Keywords: RHIC, Target Fragment

References:

[1] Singh M. K. et al., (2011). Two source emission behavior of projectile fragments alpha in ^{84}Kr interactions at around 1 GeV per nucleon. Indian J. Phys. 85, 1523-1533.
[2] Liu F. H., (2003). Multiplicity Distribution of Relativistic Charged Particles in Oxygen-Emulsion Collisions at 3.7A GeV. Chin. J. Phys. 41, 486-496.
[3] Singh M. K. et al., (2022). Emission characteristics of the target fragments at relativistic energy. Int. J. Mod. Phys. E 31, 2250036(1-10).
[4] Kamel S. et al., (2021). Emission characteristics of target black fragments in ^{16}O-Emulsion collisions at 3.7 A GeV. Int. J. Mod. Phys. E 30, 2150042(1-10).
[5] Abdallah N., (2023). Studies of the angular distribution of the grey particles in ^{16}O-emulsion collision at 3.7A GeV. Int. J. Mod. Phys. E 32, 2350006.

Application of the Nuclear Emulsion Techniques in Rare Event Search

P. Chaudhary[1], B. Kumari[1], M. K. Singh*[1] V. Singh[2]
[1]Department of Physics, IAH, GLA University, Mathura-281406, India
[2]Department of Physics, School of Physical and Chemical Sciences, Central University of South, Bihar, Gaya 824236, India
**Corresponding author email id: singhmanoj59@gmail.com*

The nuclear emulsion detector has played a significant role in several notable successes and discoveries in particle physics [1]. Nuclear emulsion detectors have the finest spatial resolution for monitoring ionizing particle tracks of all tracking tools utilized in particle physics [2, 3]. Due to improvements in digital read-out via high-speed automated scanning and the ongoing advancement of emulsion gel design, the emulsion method interest is currently at the forefront of physics research [4]. Particularly for specialized applications in neutrino physics and other leading-edge sciences, they are unmatched for the topological detection of short-lived particles [5]. In fact, this manuscript will highlight the enormous potential of emulsion detectors in applied research.

Keywords: Nuclear Emulsion, Neutrino Physics.

References:

[1] U. Rawat et al., (2023). Emission characteristics of the shower particles produced in the interaction of ^{84}Kr with emulsion 1 GeV per nucleon. J. Kor. Phys. Sci. 83, 411-415.
[2] Kajal et al, (2022). Emission feature of the singly-charged and doubly-charged projectile fragments emitted in the interaction of $^{84}Kr_{36}$ + Em at 1 GeV per nucleon. Int. J. Mod. Phys. E, 31, 2250073(1-8).
[3] Singh M. K. et al., (2020). Study of emission characteristics of the projectile fragments produced in the interaction of $^{84}Kr_{36}$ with nuclear emulsion detector at 1GeV. Chin. J. Phys. 67, 107-112.
[4] Singh M. K. et al., (2009). Photographic Nuclear Emulsion Detector: Past, Present and Future. J. PAS (Physics Science). 15, 166-175.
[5] Ariga A. et al., (2020). Nuclear Emulsions. Detectors for Particles and Radiation, Springer, 2, Chapter 9, 383-438.

Theoretical Modelling of Relativity for Faster-than-Light Particles

Vivek Kumar Srivastava*, Alok Kumar Verma
Department of Physics, Prof. Rajendra Singh (Rajju Bhaiya)
Institute of Physical Sciences for Study and Research,
Veer Bahadur Singh Purvanchal University, Jaunpur-222003, India.
Corresponding author email id: shubhoniam.1312@gmail.com

Beyond Einstein's special theory of relativity, a new dimension in physics has been revealed through the study of particles traveling faster than the speed of light. The non-existence of such superluminal particles was refuted by introducing the concept of causality principle(Bilaniuk & Sudarshan, 1969; Srivastava et al., 2023; Thouless, 1969). Different attempts to detect the superluminal particles in terrestrial laboratories were counterintuitive(Issifu et al., 2021; Lee et al., 2015; Musha, 2020; Wong, 2019). The abortive endeavor for detection was the result of the obscure nature of the transformation gamma factor in superluminal physics (Hill & Cox, 2012; Sutherland & Shepanski, 1986).To establish the transformation relations in superluminal physics, parametrized gamma factor has been introduced. Based on the two categories of gamma factors, real and imaginary, transformation relations have been introduced. These transformation relations do not include the simultaneous effect of the measurements based on the photon and tachyon. The simultaneous measurement with respect to photon and tachyon educe the concept of time lag and position lag in stationary frame. Moreover, transformation relations for position and time are deduced with an unveiled gamma factor. Hereto, velocity addition relation is also obtained for the superluminal particle. This study renders the possibilities for existences of faster than speed of light particles in the realm of physical world.

Keywords: Faster-than-light particles, Photon, Gamma factor.

References:

[1] Bilaniuk, O. M. P., & Sudarshan, E. C. G. (1969). Causality and space like signal. *Nature*, *223*(5204), 386–387. https://doi.org/10.1038/223386b0.
[2] Hill, J. M., & Cox, B. J. (2012). Einstein's special relativity beyond the speed of light. *Proc. R. Soc. A*, *468*(2148), 4174–4192. https://doi.org/10.1098/rspa.2012.0340.
[3] Issifu, A., Rocha, J. C. M., & Brito, F. A. (2021). Confinement of Fermions in Tachyon Matter at Finite Temperature. *Adv. High Energy Phys.*, *2021*, 1–22. https://doi.org/10.1155/2021/6645678.
[4] Lee, T. E., Alvarez-Rodriguez, U., Cheng, X.-H., Lamata, L., & Solano, E. (2015). Tachyon physics with trapped ions. *Phys. Rev. A*, *92*(3), 1–6. https://doi.org/10.1103/PhysRevA.92.032129.
[5] Musha, T. (2020). Hypercomputation and Negative Entropy. *Trans Eng Comput Sci*, *1*(2), 1–11. https://doi.org/10.13140/RG.2.2.29202.68809.
[6] Srivastava, V. K., Verma, A. K., & Vaish, G. (2023). Different Aspects of Faster Than Light Particles and Its Impact in Physical Reality. In R. K. Shukla (Ed.), *Challenges and Opportunities in Science : A Multidisciplinary Perspective* (First, pp. 141–155). Aryabhat Publication House.
[7] Sutherland, R. I., & Shepanski, J. R. (1986). Superluminal reference frames and generalized Lorentz transformations. *Phys. Rev. D*, *33*(8), 2896–2902. https://doi.org/10.1103/PhysRevD.33.2896.
[8] Thouless, D. J. (1969). Causality and Tachyons. *Nature*, *224*, 506. https://doi.org/10.1038/224506a0.
[9] Wong, B. (2019). Existence of Tachyons and their Detection. *RRJoPHY*, *8*(2), 23–26.

Application of Neutrino Physics in Different Fields

B. Kumari*[1], M. K. Singh[1], V. Singh[2]
[1]Department of Physics, IAH, GLA University, Mathura-281406, India
[2]Department of Physics, School of Physical and Chemical Sciences, Central University of South, Bihar, Gaya 824236, India
Corresponding author email id: babitak15mar@gmail.com

Today, cosmology, astrophysics and elementary particle physics are all centered around the neutrino [1]. A small elementary particle, the neutrino is separate from the atom. It is a real thing in nature with a very low mass, no charge, and half spin [2]. As a result of its incredibly weak interactions with other matter particles, millions of neutrinos fall on us every second and pass through our bodies undetected. It is possible for neutrinos to detect nuclear weapons, speed up international communication, and even demonstrate the existence of elusive dark matter. In this manuscript we will summarize the neutrino properties, detection techniques and its application in different fields [3-5].

Keywords: Neutrino physics, Application of neutrino.

References:

[1] Jose S. et al., (2016). Neutrino and its application . Research J. Pharm. & Tech. 9, 474-478.
[2] Pascoli S. (2018). Neutrino physics. Proceedings of the ESHEP, Maratea, Italy. 6 213-259.
[3] Fermi E. (1934). An attempt to a β rays theory. Nuovo Cim. 11, 1-20.
[4] Reines F. et al., (1956). The neutrino. Nature. 178, 446-449.
[5] Cowan C. L et al., (1956). Detection of the Free Neutrino: a Confirmation. Science 124, 103-104.

Application of Particle Accelerators

Kajal*[1], M. K. Singh[1], P. K. Khandai[2]
[1]Department of Physics, IAH, GLA University, Mathura-281406, India
[2]Department of Physics, Ewing Christian College, Allahabad 211003, India
Corresponding author email id: kajalattri255@gmail.com

The use of the particle accelerator, which was created by particle physicists to comprehend the origins of the cosmos and find new particles, is also playing an important role in applied science/medicine [1]. The majority of our lives will be directly impacted by particle accelerators most directly through different uses [2, 3]. The accelerator technology is not limited to the discovery of different physics but also playing important role in medical science to secure human lives. In this manuscript we will focus on the different applications (such as search of rare events and also in medical science) of the accelerator technology [4,5].

Keywords: Particle accelerator, its applications.

References:

[1] Gourlay S. (2022). Challenges of Future Accelerator for Particle Physics Research. Front. Phys. 10, 20520(1-10).
[2] Amaldi U. (1999). Cancer therapy with particle accelerators. Nuclear Physics A. 654, 375c-399c. [3] Amaldi U. (1998). Hadrontherapy in the world and the programmes of the TERA Foundatio. Tumori. 84, 188-199 .
[3] ShiltsevV.(2020). Superbeams and Neutrino Factories - Two Paths to Intense Accelerator-Based Neutrino Beams. Mod Phys Lett A. 35, 2030005.
[4] Orecchia R. et al., (1998). Particle beam therapy (hadrontherapy): basis for interest and clinical experience. Eur. J. Cancer. 34, 459-468.

Study of vector charmonium and axial vector electromagnetic Dalitz decays

Arti Mishra*and V. Prasad
Department of Physics, Nehru Gram Bharti (Deemed to be University), Kowa-Jamunipur-Dubawal, Prayagraj 221505, Uttar Pradesh, India,
*Corresponding author email id: artimisra2601@gmail.com

We perform the numerical study of electromagnetic Dalitz decays $V \to \ell^+\ell^- P$ [1]within a framework of Vector Meson Dominance model, where V is either vector charmonium J/ψ and $\psi(3686)$ mesons or axial vector $b_1(1235)$ meson, $\ell(= e, \mu)$ are leptons and P[1]$(=\pi^0, \pi^\pm, \eta, \eta'$ ...) are the spin-zero pseudoscalar mesons. The di-lepton invariant mass-dependent Transition Form Factor (TFF) in these decays describes the deviation from the standard point-like prediction of the quantum electrodynamics (QED). Thus, TFF is a sensitive probe of the inner structure of the involved hadrons. TFF also acts as input in the theoretical calculation of the light-by-light hadronic contribution to the anomalous muon magnetic moment, whose experimental value is deviated by 4.2σ from the Standard Model prediction. We calculate the numerical values of the branching fractions of the electromagnetic Dalitz decays $V \to \ell^+\ell^- P$ using both point-like QED theory and multipole approximation theory in which the possible intermediate resonances of ρ, ω and $\boldsymbol{\phi}$ are taken into account. As shown in Fig. 1, our numerical study reveals that the expected branching fraction of $J/\psi \to e^+e^-\pi^0$ is significantly enhanced after considering the intermediate resonances of ρ and ω and very close to its experimental measurement [1]. The number of signal events for $b^{(0,\pm)}(1235) \to \ell^+\ell^-\pi^{(0,\pm)}$ is expected to be more than 100 events in the 10 billion of BESIII J/ψ data. Thus, the BESIII J/ψ data may allow the first measurement of the electromagnetic Dalitz decays of $b^{(0,\pm)}(1235) \to \ell^+\ell^-\pi^{(0,\pm)}$.

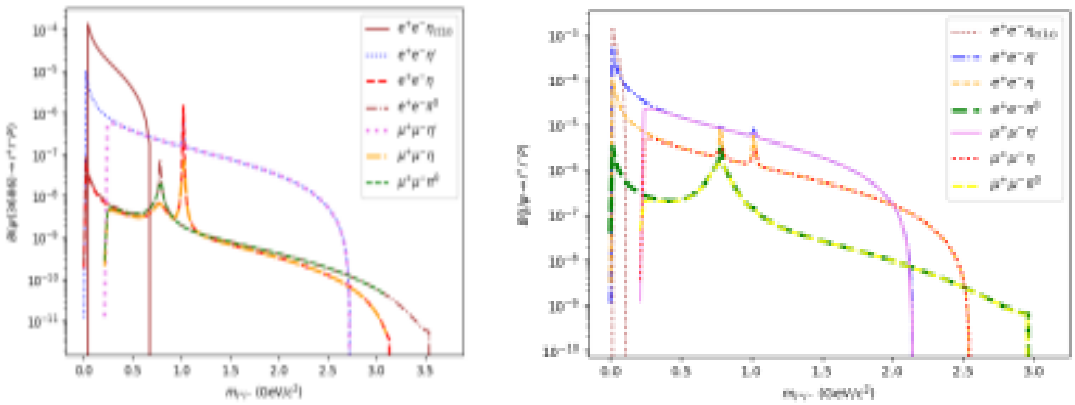

Fig. 1: Expected branching fractions of $J/\psi \to \ell^+\ell^- P$ (left) and $\psi(3686) \to \ell^+\ell^- P$ (right) including intermediate resonances of ρ, ω and $\boldsymbol{\phi}$ as a function of di-lepton invariant mass spectrum.

Keyword: Electromagnetic Dalitz decay, Quantum electrodynamics, Transition Form Factor, BESIII experiment.

References:

[1] Mishra A. and Prasad V. (2023). Prospects of Electromagnetic Dalitz Decays of Charmonium Mesons. Journ. of NGBU 12, 22-33

Probing the Transit Timing Variations in the TrES-2 system with TESS data

Shraddha Biswas[1], Parijat Thakur[1], Ing-Guey Jiang[2], John Southworth[3], Li-Hsin Su[2]
[1]Guru Ghasidas Vishwavidyalaya (A Central University), Bilaspur (C.G.)-495009, India;
[2]Department of Physics and Institute of Astronomy, National Tsing-Hua University, Hsinchu, Taiwan
[3]Astrophysics Group, Keele University, Staffordshire, ST5 5BG, UK
[*]*Corresponding author email id: parijat@associates.iucaa.in*

Transit timing variations (TTVs) are proving to be a very valuable tool in the field of exoplanetary detection (Agol et al. 2005). Up to now, WASP-4 (Wilson et al. 2008) and WASP-12 (Hebb et al. 2009) are the most promising candidates for presenting TTVs. Here, we have considered the hot Jupiter TrES-2b due to the close proximity to its host star. Being a space-based telescope and sowing to its longer uninterrupted time-series observations compared to the ground-based telescopes, the Transiting Exoplanet Survey Satellite (TESS) is used to search for timing anomalies in previously known exoplanets. For our work, we have considered total 214 transit light curves of TrES-2b, which include 47 recently observed transits of TESS, 59 from the Exoplanet Transit Database (ETD) and 108 from the literature to investigate the possibility of transit timing variation (TTV).

We found that the sequence of transits occurred 68.45 s later than had been predicted, which may be due to the gravitational influence of an additional planet and the estimated False Alarm Probability (FAP) is below the threshold level of FAP = 5%, that means short-term periodic TTV in the timing residuals of the hot Jupiter is not detected, indicating the absence of an additional body in the orbit close to the hot Jupiter in this system. The absence of short-term periodic TTV in the timing residuals motivates us to explore the possibility of long-term TTV, which may be induced due to either orbital decay or apsidal precession. To explore the other possible origins of TTV, the orbital decay and apsidal precession ephemeris models are fitted to the transit time data and we found that the constant- period is a worse fit than both the apsidal precession and orbital decay models. For instance, long-term transit-timing for TrES-2b have revealed a secular decrease in the orbital period at a rate of $\approx 8.86 \pm 2.1$ ms yr^{-1}, based on transit-timing measurements spanning 15 yr, which has been interpreted as the effect of tidal orbital decay (Maciejewski et al. 2016, 2018; Patra et al. 2017; Yee et al. 2020). Tidal orbital decay is suspected to occur especially for hot Jupiters, with the only observationally confirmed case of this being WASP-12. The period change rate of $(-6.94 \pm 1.65) \times 10^{-10}$ for TrES-2b appears to be the same order of the measured orbital decay of WASP-12b. In recent years, astronomers have invoked the Bayesian information criterion (BIC; Schwarz 1978) to identify the theoretically correct model, the best model minimizes the chosen information criterion. The ΔBIC metric favors the orbital decay model over a constant period by a value of 12.05, but it does not favor the apsidal precession model over a constant period. In order to confirm these findings, further high-precision transit, occultation and radial velocity observations of the system would be worthwhile.

Keywords: Transit timing variations, Hot Jupiters, Transiting Exoplanet Survey Satellite, Exoplanet Transit Database, False Alarm Probability.

References:

[1] Agol E., Steffen J., Sari R., Clarkson W., 2005, MNRAS, 94, 262
[2] Wilson, D. M., Gillon, M., Hellier, C., et al. 2008, ApJL, 675, L113
[3] Hebb, L., Collier-Cameron, A., Loeillet, B., et al. 2009, ApJ, 693, 1920
[4] Maciejewski, G., Dimitrov, D., Fernández, M., et al. 2016, A&A, 588, L6
[5] Patra, K. C., Winn, J. N., Holman, M. J., et al. 2017, AJ, 154, 4
[6] Yee, S. W., Winn, J. N., Knutson, H. A., et al. 2020, ApJL, 888, L5
[7] Maciejewski, G., Fernández, M., Aceituno, F., et al. 2018, AcA, 68, 371

Deriving the Equation of State of Quark-Gluon Plasma: A Modified Liquid Drop Model in Magnetic and Non-Magnetic Environments

K. Arjun*, A. M. Vinodkumar, and Vishnu MayyaBannur
Department of Physics, University of Calicut, Kerala, India
*Corresponding author email id: arjunk_dop@uoc.ac.in

Quark-gluon plasma (QGP), believed to have existed shortly after the Big Bang, plays a central role in high-energy nuclear physics and astrophysical research [1]. To understand its behavior under different conditions, we've introduced a modified liquid drop potential model. This model, using Mayer's Cluster expansion [2], treats quarks and gluons as quasiparticles influenced by the QGP environment. Remarkably, it aligns well with lattice data for pressure and energy density, even at temperatures below the critical point ($T < T_c$) [3]. Additionally, it shows strong agreement with magnetized QGP lattice data at temperatures exceeding 113MeV [3].

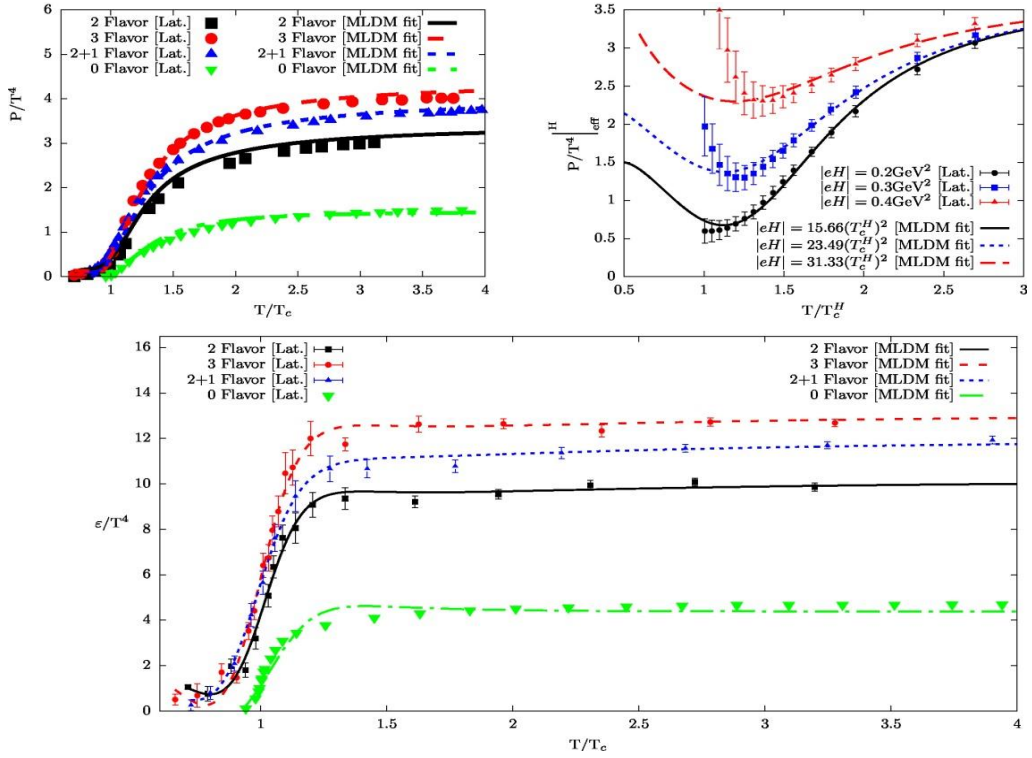

Fig1: Pressure and Energy density, scaled by $1/T^4$ are plotted against scaled temperature for various environments. The model is specified with [MLDM fit] *and the lattice data is specified with* [Lat.].

Keywords: Statistical Mechanics, QGP, quasiparticle, High Energy Physics

References:

[1] K. Yagi, T. Hatsuda, and Y. Miake, Quark-Gluon Plasma From Big Bang to Little Bang (Cambridge University Press, 2008)
[2] J. E. Mayer, J. Chem. Phys. 18, 1426 (1950).
[3] G. S. Bali et al., J. High Energy Phys. 2014 (8), F. Karsch et al., Phys. Lett. B 478, 447 (2000).

Quarkonium dissociation properties of hot QCD medium at momentum-anisotropy in the N-dimensional space using Quasi-particle Debye mass with finite baryonic chemical potential

Siddhartha Solanki and Vineet Kumar Agotiya
Department of Physics, Central University of Jharkhand, Ranchi, 835-222, India.
**Corresponding author email id: siddharthasolanki2020@gmail.com*

The analytical exact iteration method has been used to calculate the N-dimensional radial Schrodinger equation with the real part of complex valued potential and it is generalized to the finite value of anisotropy (ξ), temperature and baryonic chemical potential. In N-dimensional space the energy eigen values have been calculated for any states (n, l). The present results have been used to study the properties of quarkonium states (i.e., the binding energy and mass spectra in the N-dimensional space). The influences of anisotropy (ξ) on the dissociation temperature (T_D) have also been investigated for the ground state of quarkonia at N=0 and μ=300MeV. The anisotropy in oblate case, thus obtained, makes the dissociation temperature (T_D) higher as compared to the isotropic case. It has also been observed that the binding energy obtained by using Leading order Debye mass is greater than that of quasi-particle Debye mass depending upon the baryonic chemical potential [1].

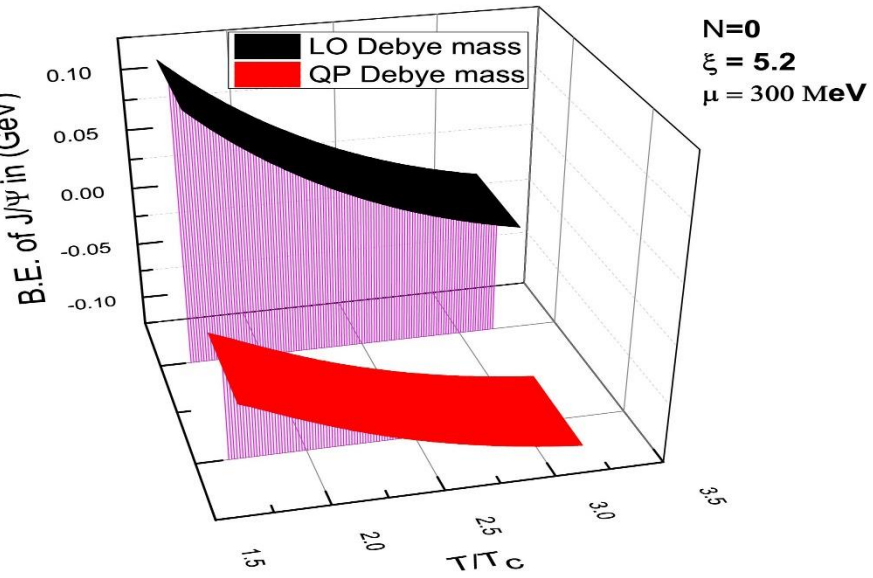

Fig: *Comparison of leading order and quasi-particle Debye mass for J/ψ binding energywith temperature at fixed value of μ = 300MeV, ξ = 5.2 and N = 0.*

Keywords: Real part of complex-valued potential, Debye mass, Momentum anisotropy, dimensionality number and baryonic chemical potential.

References:

[1] Solanki S, Lal M and Agotiya V K (2022). "Study of Differential Scattering Cross-section using Yukawa term of medium-modified Cornell potential" Advances in high energy physics journal, vol.2022, Article ID 1456538.

Quark condensate, Dynamic mass of hadrons and particle ratios based on three flavour Nambu - Jona Lasinio model

Nasir Ahmad Rather*, Saeed Uddin, Sameer Ahmad Mir, Iqbal MohiUd Din
Jamia Millia Islamia (Central University), Delhi-110025, India
**Corresponding author email id: nasirrather345@gmail.com*

The quantum chromodynamics (QCD) is a well-established theory of strong interactions. It deals with two extreme forms of strongly interacting matter, one heated to trillion degrees called QCD quenched and the other one being the cold to near absolute zero called QCD vacuum. While the perturbative aspects of QCD have been thoroughly studied its non-perturbative aspects (i.e., QCD vacuum regime) is studied by using effective field theories. One such effective field theory employed to study some of its non-perturbative aspects is the NJL model. Using NJL model, we showcase through a detailed study the intricate interplay between chiral symmetry breaking, quark condensate formation and generation of constituent quark mass. We then calculate the hadron dynamic mass (m^*) and the particle ratios of different hadronic species at various chemical potential (μ_B) and temperature (T) at varying centre of mass energies ($\sqrt{S_{NN}}$). We found a good match between theoretical and experimental results.

Hyperon Production and Hard-Core Hadronic Interactions in Relativistic Nuclear Collisions

Sameer Ahmad Mir*, Saeed Uddin, Nasir Ahmad Rather, Iqbal MohiUd Din
Department of Physics, Jamia Millia Islamia (Central University), New Delhi, 110025-India.
Corresponding author email id: sameerphst@gmail.com

In the present study we calculate the anti-baryon to baryon ratios in the in ultra-relativistic heavy-ion collisions at BRAHMS, RHIC energies as well as in the p-p collisions at LHC energies by using Hadron Resonance Gas (HRG) Model. We have incorporated a crucial aspect of baryonic interaction viz. the hard-core repulsive interaction. This essentially leads to a finite-size or an excluded volume type effect. As a result, the equation of state of the HRG is modified. The method adopted here is thermodynamically consistent as proposed by Rischke et al. This approach has been used in the present theoretical framework for studying the behaviour of the hot and dense hadronic matter at freeze-out. Using the above method, we have calculated several anti-baryons to baryons ratios and studied their dependence on the centre of mass energy of the colliding nuclei. We have found that the theoretical results are quite consistent with the experimental data after fixing certain parameters viz. the baryonic, strange, and electric chemical potentials, the temperature and the hard-core sizes of baryons and anti-baryons.

Keywords: Hardon Resonance Gas, Rischke Method, Particle Ratios, Heavy Ion Relativistic Collisions.

Molecular Vibrations of n-Annulene PAHs: A Bridge to Understanding Cosmic PAH Emissions

Vishnu Patel*, Anju Maurya, Shantanu Rastogi
Department of Physics, Deen Dayal Upadhyaya Gorakhpur University Gorakhpur, Civil lines, Gorakhpur - 273009
**Corresponding author email id: vishnu.phy17@gmail.com*

The IR spectra of objects associated with dust and gas- including evolved stars, reflection nebulae, the interstellar medium, star-forming regions and galaxies- are dominated by emission features at 3.3, 6.2, 7.7, 8.6, 11.2, and 12.7 micron, the so-called unidentified infrared (UIR) bands. These bands are generally attributed to the IR fluorescence of Polycyclic Aromatic Hydrocarbon molecules and related species. Annulenes are interesting derivatives of polycyclic aromatic hydrocarbon (PAH) molecules that can have aromatic, non-aromatic and anti-aromatic character. DFT computations are performed using B3LYP functional in conjugation with 6-31Gd basis set through the GAMESS suit of programs. [14]-Annulene, [18]-Annulene, [22]-Annulene and [26]-Annulene are studied. The computed IR spectra of each molecule in neutral and cation are reported. The variation in bond lengths, charge distribution and vibrational frequencies with increasing number of carbon atoms and corresponding PAHs: Pyrene ($C_{16}H_{10}$), Coronene ($C_{24}H_{12}$), Ovalene ($C_{32}H_{14}$) and circumanthracene ($C_{40}H_{16}$). All Annulenes have unique vibrational signature between 910 -980 cm^{-1}, which is due to C-H out of plane vibrations. The C-H stretch mode (3030-3040 cm^{-1}) in neutral molecules has highest intensity and the C-H out of plane vibrational mode (880 - 890 cm^{-1}) and C=C stretch vibrational modes are dominant in nature. The C-H stretch mode is vanishing in cation just as in PAH molecules. In cation the C-H out of plane vibrational mode is most intense.

Keywords: Interstellar molecules; DFT; Charge distribution; IR spectra; Aromatic infrared bands

Batalin-Fradkin-Vilkovisky Quantization of Christ-Lee Model

Ansha S. Nair, Saurabh Gupta
Department of Physics, National Institute of Technology Calicut,
Kozhikode - 673 601, Kerala, India
**Corresponding author email id: anshsuk8@gmail.com*

We analyse the constraint structure and subsequently quantize the Christ-Lee model within the framework of Batalin-Fradkin-Vilkovisky (BFV) formalism in both polar as well as Cartesian coordinates. We obtain Becchi-Rouet-Stora-Tyutin (BRST) invariant gauge fixed action and derive the nilpotent and absolutely anti-commuting (anti-)BRST charges and gauge fixing functions in both coordinate systems.

Keywords: BFV formalism, BRST symmetries, Christ-Lee model.

A new paradigm in the consistent extraction of surface and volume symmetry energy using the relativistic application of coherent density fluctuation model

Praveen K. Yadav[1*], Raj Kumar[1], and M. Bhuyan[2]
[1]School of Physics and Materials Science, Thapar Institute of Engineering and Technology, Patiala, Punjab - 147004
[2]Center for Theoretical and Computational Physics, Department of Physics, Faculty of Science, University Malaya, Kuala Lumpur - 50603, Malaysia
**Corresponding author email id: praveenkumarneer@gmail.com*

Over the years, traditional bulk properties such as binding energy, quadrupole moment, and shell correction have shown to be reliable means for predicting shell closure near and far away from the β-stability line. However, moving close to the dripline, the dominance of neutron-proton asymmetry, also referred to as isospin asymmetry, starts to take over. Nuclear symmetry energy is one of the observables that depends on the isospin asymmetry. However, one caveat of using symmetry energy is that the quantity of nuclear matter is defined in the momentum space, and finite nuclei are defined in the coordinate space [1]. The coherent density fluctuation model (CDFM) has served as a viable tool for translating symmetry energy from momentum space to coordinate space while verifying existing experimental shell closure and even predicting novel shell and/or sub-shell closure [1-4].Recently, the incorporation of newly fitted relativistic energy density functional (relativistic-EDF) within the CDFM formalism helped tackle the Coester-band problem, which helps to explore the nuclear lan dscape, including the super-heavy region reliably [3]. Moreover, a new approach has been proposed for the calculation of surface and volume terms of symmetry energy using the non-relativistic prescription within the CDFM formalism, which is meant to provide more realistic results of the surface and volume components [4]. In the present work, taking cues from the proposed non-relativistic prescription [4], we proposed novel application of relativistic-EDF for surface properties to explore the existence of shell closure in the medium mass region while verifying the experimental constraint range of the volume and surface components.

Keywords: Isospin Asymmetry, Symmetry Energy, Relativistic Mean-Field, Coherent Density Fluctuation Model.

References:

[1] Yadav, P. K., Kumar, R., & Bhuyan, M. (2022). Isospin dependent properties of the isotopic chains of Scandium and Titanium nuclei within the relativistic mean-field formalism. Chinese Physics C, 46(8), 084101.
[2] Yadav, P. K., Kumar, R., & Bhuyan, M. (2023). Persistence of the N= 5 0 shell closure over the isotopic chains of Sc, Ti, V and Cr nuclei using relativistic energy density functional. Modern Physics Letters A, 2350114.
[3] Yadav, P. K., Kumar, R., & Bhuyan, M, (Inprogress).
[4] Gaidarov, M. K., de Guerra, E. M., Antonov, A. N., Danchev, I. C., Sarriguren, P., & Kadrev, D. N. (2021). Nuclear symmetry energy components and their ratio: A new approach within the coherent density fluctuation model. Physical Review C, 104(4), 044312.

Effect of low-lying levels on the fusion cross-section using microscopic nuclear potential with the coupled channel approach

N. Jain[1*], Raj Kumar[1] andM. Bhuyan[2]
[1]School of Physics and Materials Science, Thapar Institute of Engineering and Technology, Patiala-147004, Punjab, India
[2]Center for Theoretical and Computational Physics, Department of Physics, Faculty of Science, University of Malaya, Kuala Lumpur 50603, Malaysia
**Corresponding author email id: njain_phd20@thapar.edu*

We have investigated the fusion dynamics for an illustrative case of $^{18}O+^{148}Nd$ and $^{18}O+^{150}Sm$ reactions at energies near and below the Coulomb barrier using the coupled channel (CC) CCFULL code [1] with the microscopic nuclear potential. The nuclear potential used in CC calculations is obtained from the Woods-Saxon potential. In the present work, we have incorporated the recently developed microscopic R3Y NN potential and densities obtained from the self-consistent relativistic mean-field approach [2,3] for the NL3* parameter set. Quadruole and hexadecapole transition to low-lying states in projectile and target as well as the coupling effect of positive Q value neutron transfer are included in the CC calculations. The calculated results from microscopic nuclear potential is further compared with the M3Y, WS potential and the experimental data [4, 5]. It is observed from the results that the R3Y NN potential with various intrinsic degrees of freedom shows closer agreement with the experimental data than those for the M3Y and Woods-Saxon potentials, mainly at sub-barrier energies.

Keywords: Higher order coupling, fusion cross-section, Relativistic mean-field, neutron transfer channel.

References:

[1] Hagino, K., Rowley, N., & Kruppa, A. T. (1999). A program for coupled-channel calculations with all order couplings for heavy-ion fusion reactions. *Computer Physics Communications*, ***123*****(1-3)**, 143-152.
[2] Satchler, G. R., & Love, W. G. (1979). Folding model potentials from realistic interactions for heavy-ion scattering. *Physics Reports*, ***55*****(3)**, 183-254.
[3] Bhuyan, M., & Kumar, R. (2018). Fusion cross section for Ni-based reactions within the relativistic mean-field formalism. *Physical Review C*, ***98*****(5)**, 054610.
[4] Broda, R., Ishihara, M., Herskind, B., Oeschler, H., Ogaza, S., & Ryde, H. (1975). Heavy-ion fusion cross sections. *Nuclear Physics A*, ***248*****(2)**, 356-376.
[5] Charity, R. J., Leigh, J. R., Bokhorst, J. J. M., Chatterjee, A., Foote, G. S., Hinde, D. J., Newton, J. O., Ogaza, S., Ward, D. & Ward, D. (1986). Heavy-ion induced fusion-fission systematics and the effect of the compound-nucleus spin distribution on fission-barrier determination. *Nuclear Physics A*, ***457*****(2)**, 441-460.

The experimental intensity analysis of the Pb L-subshells through keV electron impact

Kailash Verma, Namita Yadav, Kumar Ankit Upadhayay, Raj Singh, R Shanker, Rajneesh Kumar
Banaras Hindu University, Varanasi-221005
**Corresponding author email id: kailash233226@gmail.com*

The collision of atoms or molecules by the impact of electrons gives different phenomenon i.e. ionization, excitation, polarization of atoms, fragmentation of molecules, electron backscattering, X-ray emission etc.[1] The study of these phenomenon have a great importance in dealing different fields of physics .The experimental data of electron matter interaction describes different theoretical models which determine the internal structure as well as dynamics of atoms and molecules. Our objective is to analyze the X-ray intensity of L-subshells of Pb by impact of electron (energy range:-16-30 keV). An electron beam of specific energy has been interacted with Pb of thickness 0.5 mm [2]. With the help of Si-PIN X-ray detector, produced X-rays have been detected. The analysis and recording of the detected X-rays have been performed through the MCA software. The intensities of L X-rays from different subshells of Pb in impact of 16-30 keV electrons have been determined. The results will be compared with the Monte Carlo simulation using PENELOPE code [3].

Keywords: Monte Carlo, ionization, X-ray

References:

[1] Goel S K, Singh M J, Shanker R (1998). Efficiency measurement of a Si(Li) detector below 6.0 keV using the atomic-field bremsstrahlung, Indian J. Phys. 72A (1), 65-71.

[2] Yadav N, Bhatt P, Singh R, Llovet X, Shanker R (2012). Total M-shell X-ray yields from a thick Pt target irradiated by 10–25 keV electrons. Journal of Electron Spectroscopy and Related Phenomena,185, 23– 26.

[3] Singh B, Prajapati S, Kumar S, Singh B K, Llovet X, Shanker R (2018). Measurement of the angular distribution of thick target bremsstrahlung produced by 10–25 keV electrons incident on Ti and Cu targets. Radiation Physics and Chemistry, 150, 82–89.

Exploring the Nuclear Modification Factor and Anisotropic Flow in Heavy Ion Collisions at LHC Energies

Aditya Kumar Singh, Aviral Akhil, and Swatantra Kumar Tiwari*
Department of Physics, University of Allahabad, Prayagraj- 211002, U.P
**Corresponding author email id: Sktiwari4bhu@gmail.com*

In this work, we have analysed the Nuclear Modification Factor and Anisotropic Flow in the relativistic heavy-ion collisions at the Large Hadron Collider (LHC) energies. Our analysis relies on the Boltzmann Transport Equation (BTE) within the relaxation time approximation (RTA) to interpret experimental data. We have used the Tsallis statistics as the initial distribution and incorporate the Tsallis Blast wave (TBW) model to describe the equilibrium distribution function governing particle production evolution in the BTE. We have fitted the transverse momentum spectra in Pb-Pb, p-Pb, and Xe-Xe collisions at LHC energies ($\sqrt{s_{NN}}$ = 5.02 TeV and 5.44 TeV). We have conducted fits for the nuclear modification factor measured in Pb-Pb collisions (R_{PbPb}), which encompasses $\pi^{\pm}, K^{\pm}, p+\overline{p}, K^{*0}+\overline{K^{0*}}, \phi$. Similarly, we extend this analysis to p-Pb collisions (R_{pPb}), involving $\pi^{\pm}, K^{\pm}, p+\overline{p}$ at LHC energy of $\sqrt{s_{NN}}$ = 5.02 TeV, spanning the spectrum from central to peripheral collisions. Furthermore, our investigation extends to fitting anisotropic flows ($v_2, v_3, and v_4$) for identified hadrons, such as pions, kaons, and protons, in both Pb-Pb and Xe-Xe collisions at LHC energies across various centrality categories. Our comprehensive approach effectively fits the experimental data for p_T spectra and nuclear modification factors up to p_T= 8 GeV, providing insightful interpretations of anisotropic flow data up to p_T= 10 GeV. Our findings reveal notable trends, including the decline of both the average transverse flow velocity ($< \beta_r >$) and the kinetic freeze-out temperature (T) with increasing peripheral collisions. We have observed that azimuthal modulation amplitudes (ρa) for $v_2, v_3, and v_4$) increase as one progresses from central to peripheral collisions, consistently observed in both Pb-Pb and Xe-Xe nucleus interactions.

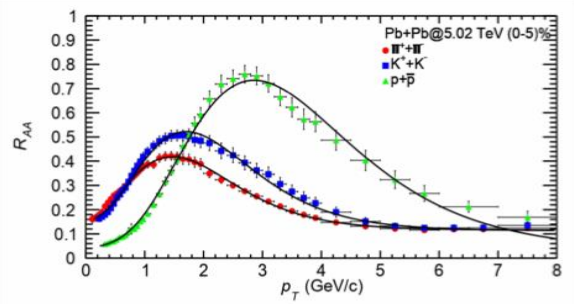

RAA spectra of pions, kaons and protons for 0-5%centrality in Pb-Pb collisions [1]

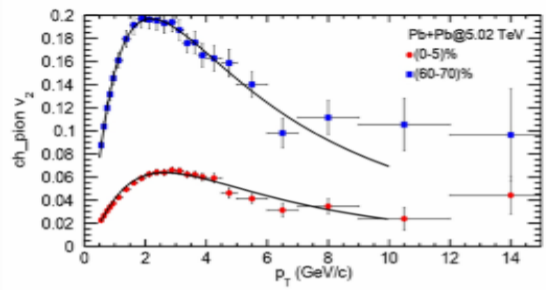

v2 for pions at Pb-Pb collisions for the 0-5% and 60-70% [2]

References:

[1] Shreyasi Achrya et al. Production of charged pions, kaons, and (anti-)protons in *Pb-Pb* and inelastic *pp* collisions at $\sqrt{s_{NN}}$ = 5.02 TeV. *PhysRevC.101.044907*

[2] S. Acharya et al. Anisotropic flow of identified particles in *Pb-Pb* collisions at $\sqrt{s_{NN}}$ = 5.02 TeV. JHEP09(2018)006

A study of multi-strange hadrons production in Pb+Pb collisions at $\sqrt{sNN}$= 2.76 TeV and $\sqrt{sNN}$ = 5.02 TeV using HYDJET++ model

Gauri Devi[1*], Arpit Singh[1]
[1] *Department of Physics, Institute of Science, Banaras Hindu University (BHU), Varanasi, 221005, India and Corresponding author: B. K. Singh*[1†,2]
[2] *Discipline of Natural Sciences, PDPM Indian Institute of Information Technology Design & Manufacturing, Jabalpur, 482005, India*

The (multi-) strange hadrons have freeze out temperature close to the phase transition temperature and have small hadronic interaction cross-sections and thus provide valuable information about the early (partonic) stage of relativistic heavy-ion collisions. φ-meson($s\bar{s}$) and Ω-baryon(sss) are pure combination of strange quarks, therefore they are not affected by the light shower partons at high p_T [1]. For the present work, we have used HYDJET++ [2] model to study the production of multi-strange hadrons in *Pb+Pb* collisions at $\sqrt{s_{NN}} = 2.76$ Tev and $\sqrt{s_{NN}} = 5.02$ TeV. We have simulated the data for four centrality intervals i.e., 0-5%, 0-10%, 30-40%, and 60-80% at both energies. We have calculated p_T-spectra and elliptic flow (v_2) of φ-meson and Ω-baryon. Further, we have compared the HYDJET++ results with the ALICE experimental data [3, 4] and with different phenomenological models such as HIJING, VISHNU [5], and AMPT model [1]. We find that the HYDJET++ model provides a good description of the experimental results in comparison to other simulation models. The elliptic flow (v_2) shows partonic collectivity and mass ordering effect at low p_T. v_2 as a function of p_T shows centrality dependence at both the energies. Further, we have calculated nuclear modification factors (R_{AA}, and R_{CP}) which provide information about the jet quenching phenomena. We observed that nuclear modification factors of multi-strange φ and Ω hadrons show less suppression towards peripheral collisions which is in accordance with the experimental results. The Ω to φ ratio show an enhancement as a function of p_T and exhibit a smooth trend at both the collision energies.

Keywords: Quark Gluon Plasma, Multi- strange Hadrons, Strangeness Enhancement.

References:

[1] Y. J. Ye, J. H. Chen, Y. G. Ma, S. Zhang and C. Zhong, Chin. Phys. C 41 (2017) no.8, 084101 doi:10.1088/1674-1137/41/8/084101.
[2] P. Lokhtin, L. V. Malinina, S. V. Petrushanko, A. M. Snigirev, I. Arsene and K. Tywoniuk, Comput. Phys. Commun. 180 (2009), 779-799 doi:10.1016/j.cpc.2008.11.015.
[3] S. Acharya *et al.* [ALICE], Phys. Lett. B 802 (2020), 135225 doi:10.1016/j.physletb.2020.135225.
[4] S. Acharya *et al.* [ALICE], Phys. Rev. C 106 (2022) no.3, 034907 doi:10.1103/PhysRevC.106.034907.
[5] B. B. Abelev *et al.* [ALICE], JHEP 06 (2015), 190 doi:10.1007/JHEP06(2015)190.

Quadrupole deformation of the hypernuclei in the few-body model

Murshid Alam* and Md. Abdul Khan
Department of Physics, Aliah University, Newtown, Kolkata-700160
Corresponding author email id: alammurshid2011@gmail.com

Hypernuclei are the subatomic systems containing at least one baryon ((viz., Λ, Σ, Ξ, etc.) having strangeness degree of freedom together with ordinary nucleons in conventional nuclei. Fermionic hyperon (Y), being dissimilar from nucleons, do not face Pauli blocking and can penetrate deep inside the host nucleus. And due to the attractive nature of YN and YY interactions, foreign hyperons lead to impurity effects both in single and double hyperon hypernuclei. When deep inside the core, hyperon(s) attract their surrounding nucleons playing a ``glue-like" role in nuclear medium which significantly modify nuclear properties, resulting in an increase in the population of dripline nuclei as well as introducing changes in their binding mechanism. Among several structural properties of the hypernuclei, quadrupole deformation is very significant and interesting because it gives a clear picture of the possible shape of impure nuclei. Hence, the deformation features of hypernuclei have recently piqued the curiosity of researchers working on exotic hypernuclei. Following the work of Hagino et al., initially a preliminary value of the deformation parameter $\beta = 0.3$ is chosen to reproduce the quadrupole moment of magnesium (Mg) isotopes. Thereafter, we derived an extra term with a second-order appearance of β, and this lead to a better result consistent with the experimental values of Mg isotopes. In the Woods-Saxon (WS) density distribution, the quadrupole deformation parameter is introduced as a function of the surface diffuseness parameter. We have also focused on the quadrupole moment, deformation parameter, binding energy, and root mean square radii of single- and double-hyperon hypernuclei. In our few-body model approach (core +Y+Y), for the two-body subsystem core+Y, we solved the Schrödinger equation directly using an effective Core-Y potential derived by single folding calculation. And for the three-body model calculation, we have employed hyperspherical harmonics expansion method (HHEM) involving two Jacobi variables using hyperon-hyperon (Y-Y) potential clubbed with the folding model potential derived for the Core-Y pair. For the Y-Y interaction, we have made choices among Nijmegen potential models. The results of our calculation will be presented during the conference.

Keywords: Hypernuclei, Glue-like role, hyperon-hyperon interaction, quadrupole moment.

References:

[1] Hagino K., Lwin N. W., &Yamagami M., (2006). Deformation parameter for diffuse density. Physical Review C, 74, 017310.
[2] Xue H. -T. et al., (2023). Deformation and spin-orbit splitting of Λ hypernuclei in the Skyrme-Hartree-Fock approach. Physical Review C, 107, 044317.
[3] Garcilazo H., & Valcarce A., (2016). D*ΞN bound state in strange three-body systems. Physical Review C, 93, 064003.

Use of isospectral potential in the search of resonances in exotic ^{24}O

Mahamadun Hasan*, Md Abdul Khan†
Department of Physics, Aliah University, Newtown, Kolkata-700160, India
*Corresponding author email id: *mahamadun.hasan@gmail.com; †drakhan.rsm.phys@gmail.com*

The advent of dedicated radioactive-ion beam (RIB) facilities and rapid advancements in technology together have revealed numerous exciting phenomena in modern subatomic physics. In recent years, nuclear physicists have paid significant attention to the physics of exotic weakly bound nuclear systems, particularly those formed near nuclear drip lines. One of the most exciting weakly bound systems identified near the neutron dripline is the ^{24}O because of its N/Z ratio (=2.0) which is greater than those of the ordinary stable nuclei. On the other hand, it is the heaviest bound isotope of the oxygen chain. Here we will apply a hyperspherical three-body (^{22}O + n + n) cluster model to compute the bound state energy and wave function for the chosen set of two-body phenomenological potentials. This in turn will be used to derive a new one-parameter family of potential which is strictly isospectral with the original three-body effective potential by the use of supersymmetric quantum mechanics (SSQM). The ground state energy and wave function of ^{24}O standard GPT n-n potential and SBB core-n (^{22}O - n) potential are utilized to solve the three-body Schrodinger equation in hyperspherical coordinates. As the three-body effective potential has a skinny-wide barrier followed by a shallow well even for the lowest partial waves, one may expect low-lying resonances at sub-barrier energies due to trapping of the particle in the well-barrier region. For effective trapping, we made use of the ground state energy and wave function to construct a one-parameter family of isospectral potentials. The parameter will be adjusted to develop a deep well followed by an enhanced repulsive barrier, having the capability of trapping particle(s) with positive energy E>0. The probability of particle trapping within the well barrier combination is calculated for various positive energies. A plot of which against energy will show a peak at resonance energy. WKB approximation is then used to calculate the width of resonance with identified resonance energy. Computed resonance energies and widths are compared with the available experimental data which are in excellent agreement. The results of the calculation will be presented during the conference.

Keywords: Exotic-nuclei, Nuclear dripline; Resonance; Isospectral potential; Hyperspherical harmonics.

References:

[1] Li J et al, (2021). Recent progress in Gamow shell model calculations of drip line nuclei. Physics 3, 977997.
[2] Gogny D et al, (1970). A smooth realistic local nucleon-nucleon force suitable for nuclear Hartree-Fock calculations. Phys. Lett. B, 32, 591-595.
[3] Sack S et al, (1954). The elastic scattering of protons by alpha particles. Phys. Rev., 93, 321.
[4] Jones M D et al, (2015). Two-neutron sequential decay of ^{24}O. Phys. Rev. C, 92, 051306(R).
[5] Tshoo K et al, (2012). N = 16 Spherical Shell Closure in ^{24}O. Phys. Rev. Lett, 109, 022501.
[6] Hoffman C R et al, (2011). Observation of a two-neutron cascade from a resonance in ^{24}O. Phys. Rev. C, 83, 031303 (R).
[7] Khan M, Hasan M et al, (2021). Hyperspherical three-body model calculation for the bound and resonant states of the neutron dripline nuclei $^{42,44}Mg$ using isospectral potential. Nucl. Phys. A, 1015, 122316.
[8] Hasan M et al, (2022). Study of resonances in exotic neutron-rich ^{14}Be by the use of isospectral potential. Jour. Phys.: Conf. Ser. 2349**,** 012024.

Effect of Octupole deformation in Pb-Pb collisions at 5.02 TeV using HYDJET++ model

Saraswati Pandey[1], Satya Ranjan Nayak[1], and B. K. Singh[1, 2]
[1]Department of Physics, Institute of Science,
Banaras Hindu University, Varanasi, 221005, INDIA. and
[2]Discipline of Natural Sciences, PDPM Indian Institute of Information
Technology Design Manufacturing, Jabalpur-482005, INDIA.
Corresponding author email id: saraswati.pandey13@bhu.ac.in

We present the study of the role of octupole deformation in non-spherical most-central Pb-Pb collisions at 5.02 TeV by employing Monte-Carlo HYDJET++ model. Motivated by the dis crepancies in the v_2-to-v_3 puzzle found in Pb-Pb collisions and the low-energy nuclear structure calculations of nuclear deformation, we first study the basic observables necessary for any study in heavy-ion collisions. HYDJET++ (hydrodynamics plus jets) is an event generator developed to study heavy-ion collisions at RHIC as well as LHC energies, performing simulation by superimposing soft state and the hard state simultaneously and independently. It meticulously treats soft hadroproduction as well as hard parton production, also examining the known medium effects. Incorporated physics and the corresponding simulation procedure can be found in the articles [1]. Using HYDJET++ model, we study the transverse momentum (p_T) spectra and anisotropic flow (v_2 and v_3) of primary charged hadrons with different parameters in two geometrical configurations: body-body and tip-tip type of Pb-Pb collisions. We observe that the transverse momentum spectra is dependent on the strength of octupole deformation parameter. $\langle v_2 \rangle$ and $\langle v_3 \rangle$ in body-body collisions show weak positive correlation with β_3 while average anisotropic flow in tip-tip collisions are weakly correlated to β_3 in most-central collision region.

Keywords: Heavy-Ion Collisions, Anisotropic flow, nuclear deformations,

References:

[1] I. Lokhtin, et al. Computer Physics Communications 180, 779 (2009)

Impact of Sidereal Effects on DUNE Sensitivity to Neutrino Standard Oscillation Parameters

Shashank Mishra, Saurabh Shukla, L. Singh, Venktesh Singh
Department of Physics, Central University of South Bihar, Gaya
**Corresponding author email id: skm.qft@gmail.com*

The sidereal effect refers to the variation in experimental observations due to the Earth's rotation and its position relative to distant celestial objects. This phenomenon is particularly significant in fields such as astrophysics and particle physics, where precise measurements are crucial for understanding the fundamental laws of the universe. Non-isotopic nature of Phenomenon of Lorentz invariance violation could lead to the sidereal effects in neutrino oscillation. For long-baseline neutrino experiments, these variations could leads to departure form there standard nature. We have investigated the impact of LIV induced sidereal effect on the sensitivity of DUNE to standard neutrino oscillation parameters.

Keywords: Lorentz Invariance Violation, Neutrino Oscillation, DUNE, Sidereal effect.

Resistive Plate Chambers (RPCs): Innovations, Unconventional Materials, and Multifaceted Applications in Particle Physics and Beyond

*Deepak Mishra, Shashank Mishra, Saurabh Shukla, Subhasis Parhi, L. Singh, Venktesh Singh
Department of Physics, School of Physical and Chemical Science, Central University of South Bihar, Gaya
*Corresponding author email id: *deepakmishra@cusb.ac.in*

Resistive Plate Chambers (RPCs) stand as quintessential innovations in the realm of particle physics, seamlessly blending precision and versatility. This mini-review delves into the intricacies of RPCs, shedding light on their fundamental principles, operational mechanisms, and diverse applications. RPCs, characterized by their excellent time resolution, efficiency, and cost-effectiveness, have emerged as indispensable tools in high-energy physics experiments. Their remarkable performance in particle tracking, triggering, and identification has paved the way for groundbreaking discoveries in the field of nuclear and high-energy physics. This abstract encapsulates our current work on non-fridgle materials and non-conventional shapes of RPCs. Additionally, this abstract explores the diverse range of applications for RPCs, including their role in particle physics experiments, medical imaging, and cosmic-ray detection. Overall, RPCs continue to play a crucial role in advancing our understanding of fundamental particles and have promising applications in various scientific and industrial fields.

Keywords: Resistive Plate Chamber, Instrumentation, Detector physics.

Perspective of Quantum Gravity from Symmetries in Einstein Gravity

Jitesh Kumar[@], Rohit K. Gupta[1], Supriya Kar[@], R. Nitish[2], and Sunita Singh[*]
[1]Dyal Singh College, University of Delhi, New Delhi, India.
[@]Department of Physics and Astrophysics, University of Delhi, New Delhi, India.
[2]Miranda House, University of Delhi, New Delhi, India.
[*]Kirori Mal College, University of Delhi, New Delhi, India.
**Corresponding author email id: jitesh.astrophysics@gmail.com*

We revisit an order two anti-symmetric U(1) gauge theory in a setup to modify the covariant derivative in presence of its gauge field strength[1]. It is shown that the new curvatures derived with the modified gauge theory in bulk on $R \times S_4$ corresponds to the boundary gravity [2]. In particular, the boundary gravity is shown to incorporate quantum topological correction $B_2 \wedge F_2$ to the Einstein-Hilbert action in (3+1). The boundary quantum gravity ensures microscopic multi black holes[3] . In addition the isometries in Einstein's Gravity were explored to derive an effective potential which in turn is shown to agree with the topological correction(s) derived otherwise in an emergent gravity scenario from gauge theory.

Keywords: Boundary gravity, Modified gauge theory, emergent curvatures.

References:

[1] A. K. Singh, K. P. Pandey, S. Singh, and S. Kar, "Discrete torsion, de Sitter tunneling vacua and AdS brane: U(1) gauge theory on D4-brane and an effective curvature," J. High Energy Phys., vol. 2013, no. 5, p. 33, May 2013, doi: 10.1007/JHEP05(2013)033.
[2] R. K. Gupta, S. Kar, R. Nitish, and M. Verma, "Exact Geometries from Boundary Gravity," Int. J. Theor. Phys., vol. 62, no. 3, pp. 1–10, Mar. 2023, doi: 10.1007/s10773- 023-05325-9.
[3] S. M. Carroll, Spacetime and Geometry. Cambridge University Press, 2019.

Band structure of Neutron Deficient Br Isotopes

S. Tiwari[1], T. Trivedi[1*], A. Mukherjee[2], S. Bhattacharya[3], R. Palit4[4], Biswajit Das[4], Vishal Malik[4], S. Nag[5], M. Prajapati[5], S. Kumar[6], S. V. Jadhav[4], B. S. Naidu[4], A. V. Thomas[4], S. Thorat[3], A.K. Jain[3]
[1]Department of Physics, University of Allahabad, Prayagraj- 211002, India
[2]Department of Pure and Applied Physics, Guru Ghasidas Vishwavidyalaya, Koni, Bilaspur-495009, India
[3]Amity Institute of Nuclear Science & Technology, Amity University, Noida-201313, India
[4]Department of Nuclear and Atomic Physics, Tata Institute of Fundamental Research, Mumbai-400005, India
[5]Department of Physics, IIT(BHU), Varanasi-221005, India
[6]Department of Physics and Astrophysics, University of Delhi, Delhi-110007, India
**Corresponding author email id:* ttrivedi1@gmail.com

The neutron-deficient Br isotopes have attracted considerable attention as they exhibit many interesting phenomena like shape coexistence, octupole correlation, chirality etc. For instance, the presence of interconnecting transitions between negative and positive parity bands along with measured B(E1)/B(E2) ratio and enhanced B(E1) transition strength establishes octupole correlation in the ^{73}Br nucleus [1]. A similar band structure with enhanced E1 transitions has been reported in the ^{76,78}Br nuclei [2,3]. The odd A ^{77}Br nucleus lies in between these two well-studied nuclei and represents an ideal case to look for such an interesting features. Recently, we performed an experiment to study high spin states of ^{77}Br using ^{65}Cu(^{19}F, αp2n) fusion evaporation reaction at a beam energy of 80 MeV. The Indian National Gamma Array (INGA) at TIFR, Mumbai consisting of 18 Compton-suppressed clover detectors [4] was used to identify the decaying gamma rays. The clover detectors were arranged as a combination of 3, 3, 3, 2, 3, and 4 clovers corresponding at angles 157°, 140°, 115°, 65°, 40° and 90° with respect to the beam direction. The collected data was sorted in the γ-γ matrices using the MARCOS program. These γ-γ matrices have been used to build the level structure. The yrast band has been confirmed up to spin 29/2+ and new inter-connecting γ- ray transitions were placed in the level scheme. These enhanced interlinking transitions may be an indication of octupole correlations in this nucleus.

References:

[1] S. Bhattacharya *et al*., Phys. Rev. C 100, 014315 (2019).
[2] W.Z. Xu *et al*., Phys. Lett. B 833, 137287 (2022).
[3] C. Liu *et al*., Phys. Rev. Lett. 116, 112501 (2016).
[4] R. Palit. *et. al*., Nucl. Instrum. Methods Phys. Res., Sect. A 680, 90 (2012).

Quarkonium Suppression in Heavy-ion Collision at 5.02 TeV, Large Hadron Collider Energy.

Mayank Kumar Mishra, Prashant Kumar Srivastava.
Physics and Material Science Department,
Madan Mohan Malaviya University of Technology, Gorakhpur- 273010, INDIA
**Corresponding author email id: mayankmishra0203@gmail.com*

Production and suppression of heavy quarkonium states is one of the most studied topics in heavy ion collision field. Recently the experimental data regarding quarkonia suppression has been obtained and analysed by CMS and ALICE collaboration at $\sqrt{S_{NN}}$ = 5.02 TeV. In this article, we would like to provide the physical interpretation to these data by using our recently proposed hybrid kinetic model for quarkonia suppression. we have improved our model by incorporating another physical process, which regenerates the singlet quarkonia states in addition to the regeneration by radiating a soft gluon. We proceeded forward with our improved model calculations to obtain the variation of nuclear modification factor for different quarkonia states with respect to centrality at $\sqrt{S_{NN}}$ = 5.02 TeV. Further, we have calculated the nuclear modification of charmonia states with respect to bottomonia states. We have compared these model results with the experimental data at $\sqrt{S_{NN}}$ = 5.02 TeV, LHC energy.

Keywords:QGP- Quark Gluon Plasma, CMS-Compact Muon Solenoid, ALICE- A Large Ion Collider Experiment, Pb + Pb- Lead Ion Collision, LHC- Large Hadron Collider

References:

[1] T. Matsui and H. Satz,J/ψ Suppression by Quark-Gluon Plasma Formation, Phys. Lett. B 178, 416 (1986).
[2] N. Brambilla et al.,non-Perturbative analysis of various mass generation by Gluonic dressing effect with the Schwinger-Dyson formalism in QCD, Eur. Phys. J. C 71, 1534 (2011).
[3] P. K. Srivastava, M. Mishra and C. P. Singh, Colour Screening scenario for quarkonia suppression in a quasiparticle model compared with data obtained from experiments at the CERN SPS, BNL RHIC and CERN LHC,Phys. Rev. C 87, 034903 (2013).
[4] P. K. Srivastava O. S. K. Chaturvedi, Lata Thakur, Heavy Quarkonia in a potential model: binding energy, decay width and survival probability, Eur. Phys. J. C 78, 440 (2018).

Comparative study of Quarkonium Suppression at various energy using a hybrid kinetic model.

Praduman Chauhan, B. K. Pandey, P. K. Srivastava.
Physics and Material Science Department,
Madan Mohan Malaviya University of Technology, Gorakhpur- 273010, INDIA
**Corresponding author email id: pradumanmau03@gmail.com*

Heavy-ion collision is an emerging area of research field. One of its aims is to search of QGP, an exotic phase of strongly interacting matter. One of the signals to detect and study this exotic phase is quarkonium suppression. Recently, by CMS and ALICE collaboration, the experimental data has been obtained and analysed for quarkonium suppression at 2.76, 5.02 and 8.16 TeV energy for various colliding species. In this article we would like to yield the corporeal explanation and analysis to these data by using our recently proposed hybrid kinetic model. The exercise will help us to stablished that our kinetic model consistently explains the production and suppression of various quarkonia states over a wide range of collision energies starting from BNL, RHIC to CERN, LHC.

Keywords: ALICE- A Large Ion Collider Experiment, **BNL-** Brookhaven National Laboratory, **RHIC-** Relativistic Heavy Ion Collider, **LHC-** Large Hadron Collider, **QGP-** Quark Gluon Plasma

References:

[1] P. K. Srivastava O. S. K. Chaturvedi, Lata Thakur, Heavy Quarkonia in a potential model: binding energy, decay width and survival probability, Eur. Phys. J. C 78, 440 (2018).
[2] Victor Feuillard (for the ALICE collaboration), Measurement of Quarkonium production in ALICE, arXiv:2101.03857 [nucl-ex] (2011).
[3] Victor Feuillard (for the ALICE collaboration), Overview of Quarkonium production in ALICE, arXiv:2212.11524 [nucl-ex] (2022).

Effect of Magnetic Field in Quasi Particle Model

Kumari Ambika, P. K. Srivastava.
**Corresponding author email id: sdev62415@gmail.com*

Divulging the explicit nature of QCD medium is a crucial issue in lattice QCD and phenomenological models. Various model prototype such as MIT Bag model, Quasiparticle model are devised to study QGP behavior at high temperature, pressure and other input quantities. In the recent past, practitioners in this field have proposed that the evolution of QGP medium, produced in collider experiments, is under the influence of a strong magnetic field. In this work, we have started to construct a hybrid model to study the thermo-dynamical properties of QGP and, under the effect of magnetic field. In this regard we have used quasiparticle model for our endeavor and implemented the landau quantization scheme to disseminate the effect of magnetic field in the equation of state (EOS) for QGP. We will study the various properties which are parametrized as the function of baryon density (chemical potential) and temperature. From our preliminary results, we have shown different thermo-dynamical, transport and magnetic properties QGP.

Keywords: QGP- Quark Gluon Plasma, **QCD-** Quantum Chromodynamics, **EOS -**Equation of State

References:

[1] P. K. Srivastava, S. K. Tiwari, C. P. Singh, Phys. Rev. D 82 014023, (2010); P. K. Srivastava, C. P. Singh, Phys. Rev. D 85 114016, (2012).
[2] A. Ayala, C. Dominguez, S. Hernandez-Ortiz, L. Hernández, M. Loewe, D. M. Paret, and R. Zamora, Physical Review D 98 (2018).
[3] V. M. Bannur, Phys. Lett. B362, 7 (1995).

Energy Difference in Valence Mirror Nuclei

Y. P. Singh[1*], V. Kumar[1], A. Choudhary[1], Gobind Ram[1], A. Shukla[1], Manoj Kumar Sharma[1], Y. Kumar[2], P. Jain[3]and D. Negi[4]
[1]Department of Physics, University of Lucknow, Lucknow, Uttar Pradesh – 226007, India
[2]Department of Physics, Hansraj College, University of Delhi, Delhi – 110019, India
[3]Department of Physics, Sri Aurobindo College, University of Delhi, Delhi - 110017, India
[4]Department of Physics, MIT, Manipal Academy of Higher Education, Manipal, Karnataka – 576104, India
**Corresponding author email id: yogendrapratap2015@gmail.com*

Mirror nuclei show strong similarities in their excited states, which has been thoroughly studied in the past and indicates the isospin symmetry [1]. Mirror nuclei are just a pair of nuclei (Z_1, N_1) and (Z_2, N_2) with the number of the protons and neutrons exchanged ($Z_1 = N_2$, $Z_2 = N_1$). The similarities of the spectra can also be found in pairs of valence mirror nuclei [2]. Valence mirror nuclei have different magic cores, but they still have the same numbers of valence protons Z_v and valence neutrons N_v, in the major shell, respectively (e.g., N_1=82, Z_1=50+k and N_2=50+k, Z_2 =50). Such pairs of valence mirror nuclei have also been referred to as quasi mirror nuclei [3, 4].

In the present work we are looking macroscopic effect in valence mirror nuclei. Casten's [5-8] basic postulate is that nuclei with same values of NpNn will have the same structures. Therefore, mirror energy difference in valence mirror nuclei (VMED) with respect to NpNn had been calculated to see the effect of NpNn on VMED. We applied the yrast filter concept corresponding to our limitation of an unbroken magic core. If we consider only the low spin states of the yrast band the condition of unbroken magic core will normally hold up to a certain excitation energy.

Keywords: Mirror Nuclei, Pseudo Mirror Nuclei, Valence Mirror Nuclei, NpNn

References:

[1] Wilkinson, D. H. (1969). Isospin in Nuclear Physics. Amsterdam: North-Holland Publishing Company.
[2] Wirowski, R., Yan, J., Brentano, P. von, Dewald, A., & Gelberg, A. (1988), Valence mirror nuclei. Journal of Physics G, 14, L195 - L199.
[3] Prade, H., Enghardt, W., Fromm, W. D., Jager, H. U., Kaubler, L., Keller, H. J., Kostov, L. K., Stary, Winkler, F., G., & Westerberg, L. (1984). New Positive-Parity States and the Shell-Model Description of ^{111}Sn. Nuclear Physics A 425, 317 - 344.
[4] Enghardt, W., Prade, H., Jager, H. U., H. J. Kaubler, F. Stary, & Kostov, L. K. (1986). Microscopic Structure of Semimagic Nuclei with 82 Neutrons or 50 Protons. Annalender Physik(Leipzig) 43, 424 - 442.
[5] Casten, R. F. (1985). NpNn systematics in heavy nuclei. Nuclear Physics A, 443, 1 - 28. [6] Casten, R. F., Brentano, P. Von, Gelberg, A., & Harter, H. (1986). Collectivity: a comparison of collective model, NpNn and F-spin approaches with empirical systematic. Journal of Physics G: Nuclear Physics 12, 711 - 716.
[6] Theuerkauf, J., Harter, H., Brentano, P. Von, & Casten, R. F. (1987). Z. Physics A 326 65.
[7] Casten, R. F. (1986). Nuclei far off stability in the NpNn scheme. Physical. Review C 33, 1819 - 1822.

Magnetic field effect on the meson masses in the two flavor quark meson model

Suraj Kumar Rai
Department of Physics, Acharya Narendra Dev Kisan P. G. College Babhnan, Gonda, India 271313
**Corresponding author email id: surajrai050@gmail.com*

The two flavor Polyakov loop augmented quark meson model (PQM) with proper accounting of fermionic vaccume fluctuations is used to investigate the effect of magnetic field. In the two flavour PQM model psudoscalar (π; η) and scalar (σ; a_0) mesons are the chiral partners. We have studied the thermal evolution of masses of chiral partners in external magnetic field (eB). The mass degeneration of chiral partners signalling $SU_A(2)$ symmetry restoration. At higher magnetic field $SU_A(2)$ symmetry restores at higher temperature.

Keywords: Strong Interaction, Sigma model, Magnetic Field, Chiral Symmetry

Role of Time-Dependent Magnetic Field on Strange Quark Matter

Vansh Batra[1,†], Yogesh Kumar[1], Poonam Jain[2], Vinod Kumar[3], Pargin Bangotra[4]
[1]Department of Physics, Hansraj College, University of Delhi, Malka Ganj, Delhi, India
[2]Department of Physics, Sri Aurobindo College, University of Delhi, Malviya Nagar, New Delhi, India
[3]Department of Physics, University of Lucknow, Lucknow, U.P., India
[4]Department of Physics, Netaji Subhas University of Technology, Dwarka, Delhi, India
**Corresponding author email id: vanshbatra0412@gmail.com*

In this study, the behavior of strange quark matter under the influence of time-dependent magnetic fields (TDMF) is investigated. The interaction between magnetic fields and quark matter is a complex and relatively unexplored area of research, with potential implications for our understanding on both fields such as fundamental particle physics and astrophysics. Our research employs theoretical models to explore the effects of TDMF on strange quark matter. We examine how these fields influence the properties of strange quark matter, including its equation of state, and other relevant parameters. Our findings shed light on the intricate interplay between magnetic fields and strange quark matter, offering valuable insights into the behavior of matter under extreme conditions. Finally, our results are useful with TDMF. It paves the way for future investigation that may uncover new phenomena and applications related to the unusual properties of strange quark matter in the presence of dynamic magnetic fields.

References

[1] G. H. Bordbar and A. Peyvand, Res. Astron. Astrophys. 11, 851 (2011)
[2] S. Borsanyi, Z. Fodor, C. Hoelbling, S. D. Katz, S. Krieg, C. Ratti and K. K. Szabo, JHEP 9, 1 (2010)
[3] S. Chakrabarty, Phys. Rev., D 54, 1306 (1996)
[4] J. C. Collins and M. G. Perry, Phys. Rev. Lett. 34, 1353 (1975)
[5] Y. Kumar, JPS Conf. Proc. 26, 024028 (2019)
[6] E. Broderick, M. Prakash and J. M. Lattimer, Phys. Lett. B 531, 167174 (2002)
[7] J. D. Anand, N. Chandrika Devi, V. K. Gupta, and S. Singh, Astrophys. J. 538, 870 (2000)

Exploring the polarization of high-energy photons in fundamental studies with J-PET detector

Deepak Kumar[1,2,3*], Sushil Sharma[1,2,3]and Pawel Moskal[1,2,3]
on behalf of J-PET collaboration
[1]Faculty of Physics, Astronomy, and Applied Computer Science, Jagiellonian University, Poland.
[2]Total-Body Jagiellonian-PET Laboratory, Jagiellonian University, Kraków, Poland
[3]Center for Theranostics, Jagiellonian University, Cracow, Poland
Corresponding author email id: d.kumar@doctoral.uj.edu.pl

Abstract

The Jagiellonian Positron Emission Tomograph (J- PET) is a multiphoton detector used in both medical research and fundamental physics [1,2,3]. This state-of-the-art detection system relies on plastic scintillators as the active detection material, coupled with a triggerless data acquisition system [4,5]. At J- PET, research focuses on measuring the angular correlation in the photons produced when the electron (e^-) annihilates with its antiparticle positron (e^+). By analysing these correlations, one can gain insight into phenomena such as quantum entanglement [6,7] and potential violations of discrete symmetries in the charged leptonic sector [3,8]. J- PET has shown to be able to estimate the polarization of photons based on the Compton process [9]. This allows not only the exploration of applications in medical imaging(by measuring the polarization correlation of annihilation photons), but also the construction of a set of unique operators to study symmetry violations [8].

This contribution gives a comprehensive overview of the experimental techniques used and highlight the groundbreaking capabilities of J- PET with emphasis on fundamental studies.

Acknowledgement

We acknowledge support from the Foundation for Polish Science through the TEAMPOIR.04.04.00-00-4204/17 program, the National Science Centre of Poland through Grants No. 2021/42/ A/ST2/00423, 2021/43/B/ST2/02150, 2019/35/B/ST2/03562, Jagiellonian University via Project No. CRP/0641.221.2020, and the SciMat and qLife Priority Research Area budget under the auspices of the program Excellence Initiative—Research University at Jagiellonian University

References:

[1] Moskal P.&Stępień E.Ł (2021). Positronium as a biomarker of hypoxia. Bio-Algorithms and Med-Systems, 17 (4), 199-202.
[2] Moskal P., et. al. (2021). Positronium imaging with the novel multiphoton PET scanner. Science Advances, 7, eabh4394.
[3] Moskal P., et. al. (2021). Testing CPT symmetry in ortho-positronium decays with positronium annihilation tomography. Nature Communications, 12, 5658.
[4] Korcyl G., et al. (2018). Evaluation of Single-Chip, Real-Time Tomographic Data Processing on FPGA -SoC Devices. IEEE Trans. Med. Imaging 37, 2526.
[5] Sharma S., et.al. (2023). Efficiency determination of J-PET: first plastic scintillators-based PET scanner. EJNMMI Phys. 10, 28.
[6] Hiesmayr B. C. and Moskal P. (2019). Witnessing Entanglement In Compton Scattering Processes Via Mutually Unbiased Bases. Sci. Rep. 9, 8166.
[7] Sharma S., Kumar D.& Moskal P. (2022). Decoherence Puzzle in Measurements of Photons Originating from Electron-Positron Annihilation. Acta Phys. Polonium. A 142(3), 428-435.
[8] Moskal P., et al. (2016). Potential of the J-PET Detector for Studies of Discrete Symmetries in Decays of Positronium Atom - a Purely Leptonic System. Acta Phys. Polonium. B 47, 509.
[9] Moskal P., et.al. (2018). Feasibility studies of the polarization of photons beyond the optical wavelength regime with the J-PET detector. Eur. Phys. J. C 78, 970.

Unravelling the recent heightened γ -ray activity from 4C 31.03 Observed by Fermi-LAT telescope

Aminabi T[1], Dr S Sahayanathan[2], Dr C D Ravikumar[1].
[1]Department of Physics, University of Calicut.
[2]Astrophysical Sciences Division, BARC.
Corresponding author email id: thekkothaminabi@gmail.com

Fermi-LAT has recently reported heightened gamma-ray activity from the multi-messenger source 4C 31.03 in January. This marks the first instance of such heightened activity since its initial discovery. Following this, the IceCube Collaboration conducted a search for muon neutrino events stemming from the same source. The timing analysis of the gamma-ray light curve with 1day as well as 12-hour binning clearly revealed three epochs of enhanced gamma ray activity.

We could observe a noteworthy curvature in the gamma-ray spectrum during the periods of high activity, with a decrease in flux at higher energies. Additionally, the shortest timescale for a doubling of the flux, coinciding with the onset of the heightened activity, was found to be 7.17 hours. Furthermore, an estimate places the lower limit for the location of the gamma-ray emission region at approximately 10^{17} centimeters. This suggests that the emission may originate from the inner regions of the molecular torus or the outer edges of the broad-line region. Interestingly, the modeling of a simultaneous broadband spectral energy distribution (SED) using templates of synchrotron, synchrotron self-Compton, and external Compton processes indicates that the observed gamma-ray flux during these episodes can be well accounted for by the external Compton process involving infrared photons from the torus.

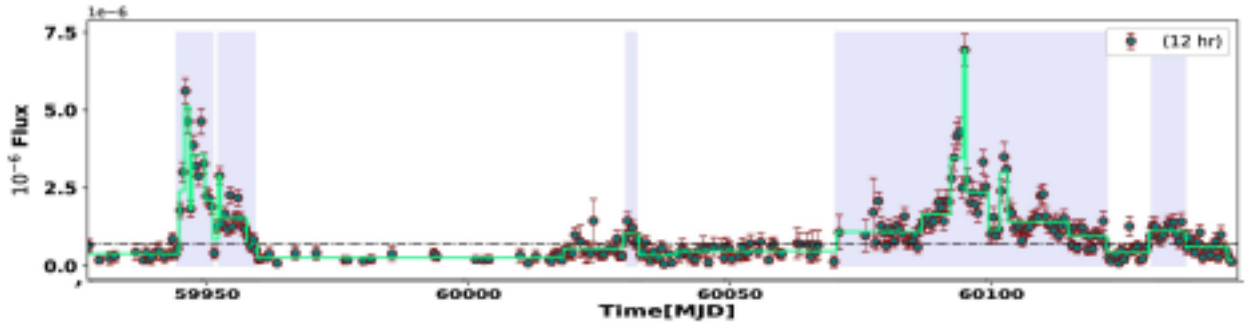

***Figure**: 12-hour binned gamma-ray light curve showing the phases of flux enhancement in shaded areas. The highest flux reported is more than 60 times the average value.*

Keywords: Active galaxies, jets, quasars, non-thermal emission.

Reference:

[1] M. Meyer, J. D. Scargle and R. D. Blandford, Characterizing the Gamma-Ray Variability of the Brightest Flat Spectrum Radio Quasars Observed with the Fermi LAT, ApJ 877 (2019) 39 [1902.02291].

Study of thermodynamic properties and eigen functions for heavy Quarkonia in the presenceof magnetic field

Rishabh Sharma, Siddhartha Solanki, Manohar Lal and Vineet Kumar Agotiya
Department of Physics, Central University of Jharkhand, Ranchi 835-222

We study the behavior of eigen functions for higher excited states of Charmonium & Bottomonium. Here we employed the medium modified form of Cornell potential which is modeled properly for short as well as long distances. In this paper we are using the quasi-particle Debye mass in the presenceof magnetic field which intuitively helps us to understand the effect of magnetic field on thermodynamical properties of heavy Quarkonia. We also study the free energy of quark-antiquark pair in presence quasi-particle Debye mass with magnetic field.

Fabrication of reactive sputtered deposited MoS_2 thin films based NO_2 gas sensor

ShresthaTyagi*, Beer Pal Singh
Department of Physics, Chaudhary Charan Singh University, Meerut 250004, India.
**Corresponding author email id: shresthatyagi67@gmail.com*

One of the most prevalent air pollutants, NO_2, is mostly produced by vehicle emissions, the burning of fossil fuels, and the commercial production of nitric acids, and poses a serious threat to the ecosystem. Therefore, the development of a highly sensitive and selective sensor for environmental safety is needed. In the present work, we report the controlled synthesis of Cu-functionalized MoS_2 thin films using a reactive co-sputtering technique for NO_2 sensors. Structural and surface morphological properties were studied using XRD and FESEM analysis, respectively. The study of surface chemistry and defects of as-prepared samples was carried out using X-ray photoelectron spectroscopy and photoluminescence spectroscopy, respectively. The sensing performance of pure MoS_2 and Cu-MoS_2 thin films was studied towards different nitrogen dioxide (NO_2) gas concentrations at the optimum working temperature of 100°C. The Cu-MoS_2 thin-film sensor has excellent NO_2 sensitivity, stability, and selectivity over NH_3, CO, and H_2 gases. Due to its exceptional performance, the proposed MoS_2 thin-film-based sensor may be employed for low (2 ppm) NO_2 detection in a low operating temperature regime.

Keywords: MoS_2; Reactive co-sputtering; Nitrogen dioxide; Gas sensor.

References:

[1] S. Tyagi, A. Kumar, A. Kumar, Y.K. Gautam, V. Kumar, Y. Kumar, B.P. Singh, Enhancement in the sensitivity and selectivity of Cu functionalized MoS_2nanoworm thin films for nitrogen dioxide gas sensor, Mater. Res. Bull. 150 (2022) 111784

Facile synthesis of doped (rGO) CuO and undoped CuO Nanostructures for Energy Storage Devices

Deepanshi Tyagi[a], Rahul Singhal[b], Beer Pal Singha[*]
[a]Department of Physics, Chaudhary Charan Singh University Campus, Meerut- 250004, INDIA
[b]Department of Physics and Engineering Physics, Central Connecticut State University, New Britain, CT 06050,USA
**Corresponding author email id: drbeerpal@gmail.com*

In the present work, we report doped (rGO) CuO and undoped CuO nanostructures synthesized by hydrothermal method. The pure CuO and doped-CuO nanostructures were synthesized through redox reactions between CuCl2•2H2O and reduced graphene oxide (rGO) without using any reducing agent. The structural analysis was determined by XRD while the surface morphology and elemental analysis was examined by FE-SEM coupled with EDAX. The optical band gap is determined by UV-Vis spectrophotometry. XRD revealed the presence of monoclinic phase of all synthesized samples. The average crystallite size of the synthesized doped-CuO nanostructures was found to be 10.65 nm and pure CuO nanostructures was found to be 20.29 nm. Surface morphology obtained from FE-SEM revealed agglomeration in synthesized samples. Tauc's plots were used to determine the optical band gap of the nanostructures using spectroscopic measurements. Further characterizations and utilization for energy storage devices are under processing.

Keywords: CuO nanstructures, Reduced Graphene Oxide (rGO), X-ray diffraction, Field Emission Scanning electron microscope.

Studies on MoS_2 nanoflowers obtained by hydrothermal method

Vanshika Bhardwaj[1,*], Beer Pal Singh[1], Rahul Singhal[2]
[1]Department of Physics, C.C.S University Campus, Meerut-250004, India
[2]Department of Physics and Engineering Physics, Central Connecticut State University
New Britain, CT, U.S.A
**Corresponding author email id: vanshikabhardwaj8@gmail.com*

In this present work, flower-like MoS_2 nanostructures were synthesized at different temperature by a facile hydrothermal route. The structure and surface morphology of the as-prepared MoS_2 specimens were examined by X-ray diffraction (XRD) and field-emission scanning electron microscopy (FESEM). The chemical composition and the purity of the samples was verified by X-ray photoelectron spectroscopy (XPS). The XRD results indicated the formation of randomly stacked layers of MoS_2. The crystallite size for the corresponding peak of the as-prepared MoS_2 nanostructures was calculated by XRD pattern using Scherrer's formula. The FESEM images revealed the formation of flower-like porous MoS2 nanostructures. The growth of two-dimensional nanosheets on the surface during the reaction finally made the MoS_2 to have a three-dimensional flower-like structure.

Keywords: MoS_2 nanoflowers, Hydrothermal method, X-ray Diffraction, FESEM.

Development of Ultra-broad light emitting garnet phosphor based on energy transfer mechanism for white light emitting device and optical thermometry applications

Neeraj Kumar Mishra*and Kaushal Kumar
Optical Materials and Bio-imaging Research Laboratory, Department of Physics, Indian Institute of Technology (Indian School of Mines), Dhanbad-826004, India.
**Corresponding author email id: neeraj.17dr000663@ap.ism.ac.in*

Blue light pumped, Ce^{3+} doped garnet structure-based phosphors have been used widely for phosphor-coated white light emitting device (pc-WLED) purposes. But WLED prepared with this type of phosphors suffer from low color rendering index (CRI) and higher correlated color temperature (CCT) values owing to the deficiency of red components in its emission spectrum. To overcome this challenge, authors have prepared Ce^{3+}/Cr^{3+} co-doped $Gd_3Al_4GaO_{12}$ garnet phosphor which is capable of emitting ultra-broad (470 nm – 850 nm) light emission via utilizing an energy transfer mechanism from Ce^{3+} to Cr^{3+} under blue light (450 nm) excitation.

The crystal structure and phase purity of the prepared sample have been examined using the X-ray diffraction pattern of the sample. The optical studies of the sample have been inspected using diffused reflectance and photoluminescence spectra systematically. Further, the temperature-dependent PL spectra were measured to check the thermal stability and thermal response characteristics of the dopants. For the commercial application of the sample, the selected sample was used for fabricating the WLED device by combining it with a blue LED chip (InGaN). The voltage stability of the prepared WLED has been tested by measuring voltage-dependent electroluminescence spectra. Moreover, the CRI and CCT values of the fabricated pc-WLED were measured and it was found that these values are better than some of the already commercially available pc-WLED. In addition to this application, the sample also has been checked for contactless optical thermometry application using the luminescence intensity ratio (LIR) technique. Thus, the prepared phosphor could be used for pc-WLED and contactless optical thermometry purposes.

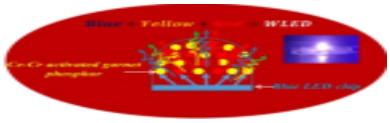

Figure 1. Schematic representation of the fabricated pc-WLED.

Keywords: Garnet, energy transfer, electroluminescence, and optical thermometry, etc.

Reference

[1] Fang, M. H., Bao, Z., Huang, W. T., & Liu, R. S. (2022). Evolutionary generation of phosphor materials and their progress in future applications for light-emitting diodes. *Chemical Reviews*, *122*(13), 11474-11513.
[2] Mishra, N. K., Kumar, A., & Kumar, K. (2023). Development of ultra-broad band light emitting single phase garnet phosphor based on energy transfer mechanism and its applications in optical temperature sensing and WLED. *Journal of Alloys and Compounds*, *947*, 169440.

Agro-Based Wastes as Precursor for Synthesis of CNTs Using Pyrolysis Method

Akrity Bharadwaj, Gautam Kumar, Justin Masih
Department of Chemistry, Ewing Christian College, Prayagraj
**Corresponding author email id: singhakritybharadwaj@gmail.com*

There is a compelling challenge to produce cost-effective carbon nanotubes (CNTs) from sustainable biomass resources as competitive carbon precursors. The mass production of nano-porous carbons is an established process, the first patents of which date back to the beginning of the 20th century. This present work proposes a "green" method for obtaining carbon nanoparticles. The process is simple, eco-friendly, and effective.

This study discusses various green processes of synthesis of CNTs via pyrolysis. This work focuses on the synthesis of activated carbon and carbon nanotube (AC@CNT) composites through an environmentally friendly method obtained from coconut shells through various routes. The aim of this study is to find and summarize various economical and environmentally friendly ways to produce carbon nanotubes from readily available coconut shells, which may be used in the future to remove natural heavy metals through adsorption. The precursor was carbonized at high temperature and pressure followed by chemical activation with KOH, H_3PO_4, $CaCl_2$, Ferrocene, etc. Physical characterization of the prepared nanoparticles was carried out using FTIR, SEM and X-ray diffraction.

Keywords: green synthesis, carbon nanotube (CNT), sustainable, activated carbon, biomass**.**

References:

[1] Wedad A. Al-Onazi, M.H.H. Ali and Tahani Al-Garni (2021). Using Pomegranate Peel and Date Pit Activated Carbon for the Removal of Cadmium and Lead Ions from Aqueous Solution, Hindawi Journal of Chemistry, Volume 2021,13 pages.
[2] J. B. Njewa, E. Vunain and T. Biswick (2022). Synthesis and Characterization of Activated Carbons Prepared from Agro-Wastes by Chemical Activation, Hindawi Journal of Chemistry, Volume 2022, 13 pages.
[3] Asih Melati, G. Padmasari, R. Oktavian, F. A. Rakhmadi (2022). A comparative study of carbon nanofiber (CNF) and activated carbon based on coconut shell for ammonia (NH3) adsorption performance, Applied Physics A Material Science & Processing (2022), 128:211.
[4] M. C. Tonucci, Leandro V. A. Gurgel, S. F. de Aquino (2015). Activated carbons from agricultural byproducts (pine tree and coconut shell), coal, and carbon nanotubes as adsorbents for removal of sulfamethoxazole from spiked aqueous solutions: Kinetic and thermodynamic studies, Elsevier, Industrial Crops and Products,74 (2015),111–121.
[5] A Melati and E Hidayati (2016). Synthesis and characterization of carbon nanotube from coconut shells activated carbon, Journal of Physics: Conference Series, 694 (2016), 012073.

Tunable electro-optical and dielectric features of CdS quantum dots doped isothiocynate-based nematic liquid crystal composites

Prabhat Singh Raghav[1], Sandeep Kumar[2,3] and Gautam Singh[1*]
[1]Department of Applied Sciences, Amity University, Uttar Pradesh, Noida,201313, India.
[2]Raman Research Institute, C.V. Raman Avenue, Sadashivanagar, Bengaluru 560080, India
[3]Department of Chemistry, Nitte Meenakshi Institute of Technology, Yelahanka, Bengaluru 560064, India
* *Corresponding author email id: gsingh6@amity.edu*

In the recent past, semiconducting quantum dots (QDs) have gained popularity as dopant to nematic liquid crystal (NLC) materials in order to tune their optical, electro-optical and dielectric properties, useful for the next-generation high-performance display and non-display devices [1-3]. To the best of our knowledge, among the semiconducting QDs, CdS QDs are not being much explored as dopant to tune the physical properties of NLC materials and hence required the detailed investigations. Herein, we report the effect of CdS QDs (diameter ~3.5 nm) on the electro-optical and dielectric properties of isothiocynate-based NLC material, 1-(trans-4-Hexylcyclohexyl)-4-isothiocyanatobenzene (6CHBT) using cross-polarised optical microscope and dielectric spectroscopic techniques. Threshold voltage (electro-optical parameter) of CdS QDs-6CHBT composites is found to be higher than the pure 6CHBT. Similarly, the dielectric properties (real dielectric permittivity (ε′) and dielectric anisotropy (Δε)) of the composites are also enhanced as compared to the pure 6CHBT. However, the decrease in activation energy related to the short-axis molecular relaxation of 6CHBT with increase in the dopant (i.e., CdS QDs) concentration is observed. The observed changes in the physical properties of composites as compared to pure sample could be attributed to the plausible interaction among QDs and NLC molecules. Our results clearly indicate that CdS QDs could significantly tune the electro-optical and dielectric properties of 6CHBT, NLC. We certainly believe that such composites would be useful for the fabrication of tunable photonic devices and test beds to understand the interaction among the QDs and NLC molecules.

Keywords: CdS QDs, nematic liquid crystal, electro-optical, dielectric spectroscopy

References:

[1] Bisoyi, H.K. & Kumar, S. (2011). Liquid-crystal nanoscience: An emerging avenue of soft self-assembly. *Chem. Soc. Rev.*, 40, 306–319.
[2] Mirzaei, J., Rezinov, M. & Hegmann, T. (2012). Quantum dots as liquid crystal dopants. *J. Mater. Chem. C*, 22, 22350-22356.
[3] Singh, G., Fisch, M. R. & Kumar, S. (2016). Emissivity and electro-optical properties of semiconducting quantum dots/rods and liquid crystal composites: A Review. Reports on Progress in Physics, 79, 056502.

Simultaneous Extraction of Charge Carrier Mobility and Total Contact Resistance in an Organic Field Effect Transistors

Samayun Saikh*, Nikhitha Rajan, Ayash Kanto Mukherjee
Department of Physics, Indian Institute of Technology Patna
*Corresponding author email id: *samayun_2021ph35@iitp.ac.in*

The charge carrier mobility is extracted from transfer characteristics of an Organic-Field-Effect-Transistor (OFET) by fitting classical Metal-Oxide-Semiconductor-Field-Effect-Transistor (MOSFET) equations into OFET experimental data [1]. This mobility value does not reflect gate field dependency. Although, MOSFET equation is fitted to OFET data, MOSFET equations is not included the effect of high contact resistance (R_C) [2]. The former device possesses high contact resistance at source and drain contact region [3]. Few methods such as Four-Probe-Method [4], Transfer-Line-Method [5], Kelvin-Probe-Microscopy [2] and Transition -Voltage- Method (TVM) [6]exist to extract R_C. All these Method come with their own difficulties to practice at laboratory. In this report, a simple and generic expression has been derived to extract the total contact resistance and gate filed dependent charge carrier mobility simultaneously from the characteristics of an OFET while biased at linear region. This derived expression is applied to the characteristics of OFET based on 6,13-Bis (triisopropylsiylethynyl) Pentacene, commonly known as TIPS Pentacene. TVM is also applied to the same OFET characteristics to extract R_C for comparison with the extracted values of R_C by derived expression.

Keywords: Contact Resistance, Mobility, Organic Field Effect Transistor, Transition Voltage Method.

References

[1] Bittle, E. G., Basham J. I., Jackson, T. N., Jurchescu, O. D., & Gundlach, D. J. (2016). Mobility overestimation due to gated contacts in organic field-effect transistors. *Nature communications*, *7*(1), 10908.

[2] Waldrip, M., Jurchescu, O. D., Gundlach, D. J., &Bittle, E. G. (2020). Contact resistance in organic field-effect transistors: conquering the barrier. *Advanced Functional Materials*, *30*(20), 1904576.

[3] Hong, K., Yang, S. Y., Yang, C., Kim, S. H., Choi, D., & Park, C. E. (2008). Reducing the contact resistance in organic thin-film transistors by introducing a PEDOT: PSS hole-injection layer. *Organic electronics*, *9*(5), 864-868.

[4] Chesterfield, R. J., McKeen, J. C., Newman, C. R., Frisbie, C. D., Ewbank, P. C., Mann, K. R., & Miller, L. L. (2004). Variable temperature film and contact resistance measurements on operating n-channel organic thin film transistors. *Journal of applied physics*, *95*(11), 6396-6405.

[5] Xu, Y., Minari, T., Tsukagoshi, K., Chroboczek, J. A., &Ghibaudo, G. (2010). Direct evaluation of low-field mobility and access resistance in pentacene field-effect transistors. *Journal of Applied Physics*, *107*(11).

[6] Wang, S. D., Yan, Y., &Tsukagoshi, K. (2010). Transition-voltage method for estimating contact resistance in organic thin-film transistors. *IEEE Electron Device Letters*, *31*(5), 509-511.

Novel $Ag_2Cu_2O_3$ Nanoparticles for High-Capacity Supercapacitor

Arvind Kumar*, Mukesh P, Lakshmisagar G, Akshay Hegde
Department of Physics NITK Surathkal, India, 575025
**Corresponding author email id: arvindkumar12695@gmail.com*

In today's world, the surging demand for high-energy-density devices, driven by the proliferation of electronic appliances and hybrid vehicles, necessitates the development of energy storage solutions capable of delivering rapid bursts of power. Supercapacitors have emerged as a prominent choice to meet this energy supply requirement owing to their exceptional energy storage capabilities. Achieving these high-energy attributes relies on the intricate design of electrode materials in tandem with appropriate electrolytes. In this investigation, we introduce a pioneering nanomaterial, $Ag_2Cu_2O_3$, synthesized via a straightforward one-pot method. Our primary aim is to delve into the electrochemical characteristics of $Ag_2Cu_2O_3$ nanoparticles, specifically in the context of their potential as electrode materials for supercapacitors. Through meticulous galvanostatic charge-discharge experiments, we have unveiled the remarkable specific capacity of $Ag_2Cu_2O_3$, which stands at 731 F/g when exposed to a 2M KOH electrolyte at a current density of 1 A/g. Notably, it is noteworthy that no existing literature or reports currently exist on the utilization of $Ag_2Cu_2O_3$ nanomaterial as an electrode material for supercapacitors. This research makes a substantial contribution to the ongoing developments in high-energy-density supercapacitor technology, thereby paving the way for innovative energy storage solutions in the realm of electronic devices and hybrid vehicles.

Microwave assisted synthesis of multi-metallic nanofluids and performance for biomedical applications

Ajit Kumar Maddheshiya*, Phool Singh Yadav
Condensed Matter Physics Research Laboratory, Department of Physics, University of Allahabad, Prayagraj 211002, U.P., India
**Corresponding author email id: ajitmdd@gmail.com*

The noble trimetallic nanoparticles are made up of three different metals. These noble trimetallic nanoparticles have wonderful, promising properties and can be used in a wide range of innovative applications. Due to rampant misuse of antibiotics, certain bacterial organisms have developed resistance against them as a result of genetic modifications, rendering a lot of the traditionally used antibiotics ineffective. The functioning of these nanofluids is controlled by their composition, shape, and size. Controlled synthesis of these nanomaterials is a popular research area because of the biomedical applications associated with their shape, optimum content, biocompatibility, and flexible chemistry. This article reports exploring the antimicrobial performances of multimetallic nanofluids (NFs) as potential anti-bacterial agents for the future. We have used a one-pot microwave-assisted reduction approach to synthesize the trimetallic NFs. The UV–Vis spectroscopy results indicate that a clear single plasmon resonance peak within the 518–541 nm range. Furthermore, NFs were subjected to characterization by HRTEM, XRD, SEM, etc. The NFs have an average size of 5–15 nm and are spherical in shape. Superior synergism between mono-metal features is provided. This had a profound effect on the antibacterial activity as the trimetallic Au-Pt-Pd was found to be the most effective against both the gram-negative and gram-positive bacterial strains. In comparison to the considerable research on bimetallic nanoparticles, trimetallic nanostructures have only just begun to be thoroughly investigated in terms of their properties and applications.

Keywords: Trimetallic nanofluids; antimicrobial, metals nanoparticles,

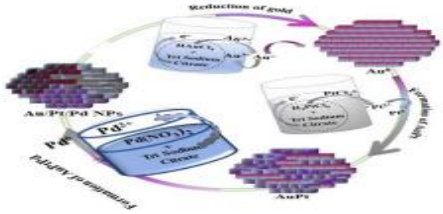

Fig.1. *Schematic depiction of the mechanistic interpretation for the formation of the trimetallic Au-Pt-Pd NFs*

References:

[1] Yadav, N., Yadav, R. R., & Dey, K. K. (2022). Microwave assisted formation of trimetallic AuPtCu nanoparticles from bimetallic nano-islands: why it is a superior new age biocidal agent compared to monometallic & bimetallic nanoparticles. *Journal of Alloys and Compounds*, *896*, 163073.

[2] Maddheshiya, A. K., Yadav, N., Yadav, S., Yadav, P. S., & Yadav, T. P. (2023). Facial Synthesis of the trimetallic Au-Pt-Pd nanofluids and performance for Methylene blue degradation. *Materials Letters*, 134735.

Carbon dots induced vertical alignment of planar anchored isothiocynate-based thermotropic nematic liquid crystal material

Srashti Tomar[1,2], PriscillaP[1], Prabhat Singh Raghav[1], Sandeep Kumar[3,4] and Gautam Singh[1,a)]
[1]Department of Applied Physics, Amity Institute of Applied Sciences, Amity University Uttar Pradesh, Noida 201313, India.
[2]Physics Department, Deshbandhu College (University of Delhi), Kalkaji 110019, New Delhi, India.
[3]Raman Research Institute, C.V. Raman Avenue, Sadashivanagar, Bengaluru 560080, India.
[4]Department of Chemistry, Nitte Meenakshi Institute of Technology, Bengaluru 560064, India.
**Corresponding author email id: gsingh6@amity.edu*

The vertical alignment of nematic liquid crystal (NLC) materials is the key for their ubiquitous versatile display and other photonic devices. The doping of quantum dots (QDs) into NLCs has been proven to be one of new techniques to verticallyalign NLC molecules without using any alignment layer [1]. However, the effect of QDs (ex. Carbon dots, CDs) on alignment of NLCs in planar anchored ITO sample cells has not been greatly investigated. Consequently, we have studiedthe effect of CDs (diameter ~7-8 nm)as a dopanton alignment of isothiocynate-based NLC,namely,1-(trans-4-Hexylcyclohexyl)-4-isothiocyanatobenzene (6CHBT) filled into planar anchored sample cells using polarising optical microscope and dielectric spectroscopy. Interestingly, induced vertical alignment of 6CHBT is observed in the planar anchored sample cells by the CDs (concentration ≥0.2 wt%) at room temperature. The presence of short axis molecular relaxation in the CDs-6CHBT composites at 0V also confirms the induced vertical alignment. Temperature dependent optical texture and dielectric studies further confirm thermal stability of induced vertical alignment. It appears that the interaction between CDs and NLC molecules is stronger than the interaction among the NLC molecules and planar anchored ITO substrates and which results in the induced vertical alignment. We believe that our findings would shed more light on the current understanding of the dynamics of interaction of CDs and NLCs useful for development of advanced soft composite materials for fabrication of high-performance flexible displays and other non-display devices [2-4].

Keywords: Carbon dots, nematic liquid crystal, electro-optical, dielectric spectroscopy

References:

[1] Priscilla P et al. (2023). Recent advances and future perspectives on nanoparticles-controlled alignment of liquid crystal displays and other photonic devices. Crit. Rev. Solid State Mater. Sci., 48(1), 57–92.
[2] Eskalen H. (2020). Influence of carbon quantum dots on electro–optical performance of nematic liquid crystal.Appl Phys A.,126(9),708.
[3] Pandey FP, Rastogi A, Singh S.(2020).Optical properties and zeta potential of carbon quantum dots (CQDs) dispersed nematic liquid crystal 4′- heptyl-4-biphenylcarbonitrile (7CB). Optical Materials.,105,109849.
[4] Neha, Singh G, Kumar S, Malik P, Supreet.(2023). Recent trends and insights into carbon dots dispersed liquid crystal composites. Journal of Molecular Liquids.,384,122225.

Enhancing Electrochemical Performance through Sn Substitution in WO_3 Nanoflower

Harishchandra S. Nishad and Pravin S. Walke*
National Center for Nanosciences and Nanotechnology, University of Mumbai
**Corresponding author email id: harish_pw@nano.mu.ac.in*

Materials scientists are desperately chasing nanoscale materials and their engineering in order to develop superior energy storage devices. In this context, metal cation substitution in the pseudocapacitive metal oxide nanomaterials are extremelyfavoured. This work designates the investigation of enhancing electrochemical performance through the incorporation of Sn cations in the WO_3 matrix. We have systematically investigatedeffect of Sn substitution into WO_3 nanoflowers via a facile one-step hydrothermal method. The prepared Sn-doped WO_3 has employed as electrode materials for Quasi-Solid State Asymmetric Supercapacitors (QSSAS). Electrochemical analysis highlighted significant enhancement in the specific capacitance of 138 F g^{-1} (Sn-doped WO_3) from 72 F g^{-1} (WO_3) at 1 A g^{-1}. Furthermore, a temperature-dependent study revealedsix times improvement in the specific capacitance as temperature rises. The measured specific capacitance values are 109 F g^{-1}, 139 F g^{-1}, 194 F g^{-1}, 301 F g^{-1}, and 603 F g^{-1} at temperatures 10 °C, 20 °C, 30 °C, 40 °C, and 50 °C, respectively. Furthermore, the performance of the QSSAS constructed using the Sn-doped WO_3 nanoflowers as an anode. The device showcases remarkable stability, retaining 97.51% of its initial performance after 2500 cycles. This longevity is coupled with an energy density of 8 W h kg^{-1} and a power density of 6400 W kg^{-1}. These advantageous characteristics are attributed to increased conductivity, enhanced diffusion capacity, and robustness resulting from multiple redox active sites. The findings underscore the promising electrochemical attributes of tin-substituted WO_3, highlighting its potential as a viable pathway for advancing electrode material development in energy storage applications.

Keywords: Sn-doped WO_3, Nanoflower, Quasi-Solid State Asymmetric Supercapacitors, Pseudocapacitor.

NH_4Cl modified TiO_2 layer for efficient planar perovskite solar cells

M. S. Patel[1,3], R. P. Yadav[2], Preeti Shukla[1] and Lokendra Kumar[1*]
[1]Molecular Electronics Research Laboratory, Physics Department, University of Allahabad, Prayagraj-211 002
[2]Department of Physics, Deen Dayal Upadhyay Govt. P.G. College, Saidabad, Prayagraj- 221508, India
[3]Present Address: Department of Physics, Nehru Gram Bharati University, Prayagraj- 221505, India
**Corresponding author email id: lkumarau@gmail.com*

The interface between perovskite and transport layers plays a vital role in improving the performance of perovskite solar cells. Herein, we report a unique way to improve the interface between TiO_2 acting as an electron transport layer (ETL) and perovskite layer via defect passivation by NH_4Cl. NH_4Cl modified TiO_2 layer resulted as an ameliorator in the growth of perovskite film in terms of interface, crystallinity, absorbance and photovoltaic performance. Fractal analysis is performed on Scanning Electron Microscopy (SEM) images of perovskite thin films fabricated onto unmodified and modified TiO_2 substrates to calculate the fractal dimension and Hurst exponent. The estimated value of fractal dimension/ Hurst exponent is found to be larger/smaller for the perovskite thin film grown on 60s NH_4Cl modified TiO_2 substrate as compared to other.The larger the value of fractal dimension higher will be surface jaggedness which provide a better interface between the perovskite and hole transport layer. The perovskite solar cell fabricated on NH_4Cl modified TiO_2 layers improves the charge transport, minimised the trap state density and enhance the power conversion efficiency from 6.65% to 9.13%.

Keywords: Electron transport layer, Surface morphology, Fractal dimension, Perovskite solar cell.

Temperature-Induced Degradation Modelling of Perovskite Solar Cells

Anand Pandey [1*], Ankush Bag[1,2]
[1] Centre for Nanotechnology, Indian Institute of Technology Guwahati, Guwahati 781039, India
[2] Department of Electronics and Electrical Engineering, Indian Institute of Technology Guwahati, Guwahati 781039
**Corresponding author email id: anandpandeyau@gmail.com*

Perovskite photovoltaics (PSCs) attracted much attention in the scientific community due to their superior charge transport properties, large diffusion length, and ambipolar charge transport. Due to these excellent properties, PSCs achieved a power conversion efficiency of 25.7 % last year[1]. However, PSCs are degraded under moisture, humidity, temperature, and light[2]. However, the operational thermal stability of perovskite materials and their devices is a matter of concern for their commercialization[3].The operational thermal stability is one of the key issues that hurdle their commercialization. Therefore, besides achieving high power conversion efficiency (PCE), understanding the device degradation kinetics of PPVs is necessary for their reliability and failure under thermal stress. In this work, Arrhenius type and linear degradation schemes have been adopted to understand the degradation kinetics of $FAPbI_3$ and multifunctional FTPA-modified $FAPbI_3$ PSCs. Further, various figures of merit such as acceleration factor, degradation factor, mean lifetime, and activation energy have been deduced by fitting the PCE degradation data onto the above-said kinetic models. These figures of merit have been correlated with other defect-determining factors such as micro-strain and Urbach's energy. This study suggests that FTPA modification in PSCs may improve their thermal stability, lifetime, and decelerate their aging time. Our findings suggest that intrinsic stability, thermal stability, and mean lifetime of studied devices are strongly correlated with micro-structural defects.

Keywords: Perovskite solar cells, Reliability, Defects, Modeling, Stability.

References:

[1] Y. Tong, A. Najar, L. Wang, L. Liu, M. Du, J. Yang, J. Li, and K. Wang, Adv. Sci. **9**, 2105085 (2022).
[2] S. T. Thornton, G. Abdelmageed, R. F. Kahwagi, and G. I. Koleilat, J. Chem. Technol. Biotechnol. **97**, 810 (2022).
[3] A. Pandey and L. Kumar, Phys. B Condens. Matter **628**, 413566 (2022).
[4] M. Li, R. Sun, J. Chang, J. Dong, Q. Tian, H. Wang, Z. Li, P. Yang, H. Shi, C. Yang, Z. Wu, R. Li, Y. Yang, A. Wang, S. Zhang, F. Wang, W. Huang, and T. Qin, Nat. Commun. **14**, 573 (2023).
[5] D. B. Khadka, Y. Shirai, M. Yanagida, K. Uto, and K. Miyano, Sol. Energy Mater. Sol. Cells **246**, 111899 (2022).

Dielectric and Thermal Investigation of Carbon Nanotubes Doped Nematic Liquid Crystal

Rama Shanker Gupta[a], Nidhi Pandey[a], Sudhanshu Pandey[a], Anoop Kumar Srivastava[b*]
[a]Department of Physics, United University,Rawatpur, Jhalwa, Prayagraj-211012,India
[b]Department of Applied Science and Humanities, Institute of Engineering and Technology,
Dr. Rammanohar Lohia Avadh University, Ayodhya-224001, India
**Corresponding author email id: srivastava_anoop@rediffmail.com*

Dielectric and thermal properties of pristine liquid crystal (LC) and carbon nanotubes (CNTs) doped liquid crystals were investigated. The improved dielectric responses were observed in CNTs doped liquid crystal. The electrical conductivity of CNTs doped LC was higher than pristine LC. Dielectric anisotropy and hence the improved threshold volage was observed in CNTs doped LC. The heat capacity in CNTs doped LCs was five time higher than that of pristine LC. The thermal conductivity was increased by more than two time in CNTs doped LC as compared to pure LC.

Keywords: Liquid Crystals, Carbon Nanotubes, Threshold voltage, Dielectric anisotropy, Conductivity.

Persistence of invaded multiplex ecosystems

Dweepabiswa Bagchi*, D. V. Senthilkumar
Indian Institute of Science Education and Research Thiruvananthapuram

Numerous studies have typically highlighted the detrimental consequences of invasions on an isolated ecosystem patch or a simple network of connected but very similar ecosystem patches. However, numerous species co-exist and interact in a real ecosystem. A complex network, consisting of motifs of two or more interacting species is thus a much more suitable framework for studying ecosystems. The apropos complex network that characterizes such an ecosystem is a multiplex or a multi-layered network. The multiplex has layers that are motif specific.

We investigate 3 distinct ecological multiplexes under invasion from external species. We quantify the criteria for the increase in extinction risk of these multiplex ecosystems under invasion. We identify the system states that can be considered 'danger states' (high extinction risk) and the states that can be termed 'resistive states' (low extinction risk). Moreover, we quantify the persistence of the entire network, corresponding to the collected interplay of invasion strength and higher-order trophic and non-trophic interactions ([1],[2]). Our results also demonstrate the advantage of multiplex network structure of ecosystems.

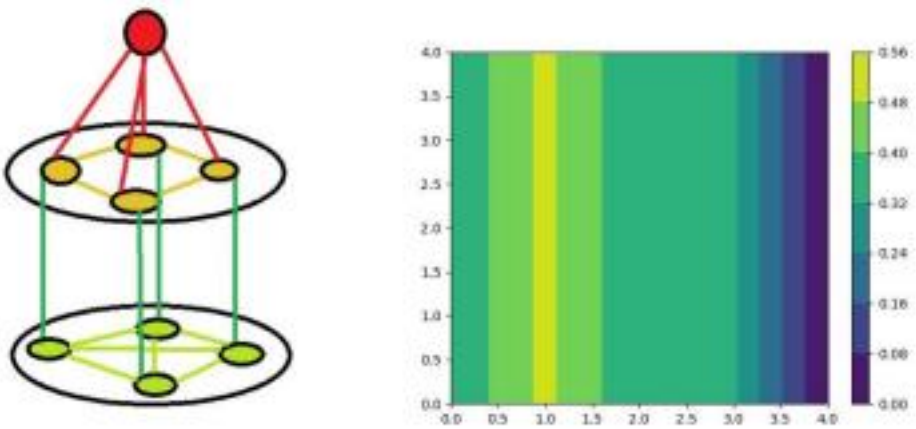

..

Left: Representative scheme of multiplex network under invasion. Right: corresponding 'danger zones' where network synchronizes w.r.t invasion and intra-patch dispersal values

References:

[1] Grilli J, Barabás G, Michalska-Smith M. J., Allesina S (2017). Higher-order interactions stabilize dynamics in competitive network models. Nature, volume 548, pages 210–213

[2] Sauve A. M. C, Fontaine C, Thébault E (2014). Structure–stability relationships in networks combining mutualistic and antagonistic interactions. Oikos, 123, 378–384

Porous transition metal dichalcogenide (TMD) nanomaterial for sensing application

Pratibha Patel, Dr. Kajal Kumar Dey*
Centre for Nanoscience & Technology, Prof. Rajendra Singh (Rajju Bhaiya) Institute of Physical Science for Study and Research, VBSPU Jaunpur-222003, U.P. India.
**Corresponding author email id: itstiyash@gmail.com*

A sensor is an electronic device that senses the changes in its surrounding physical phenomenon as input (Heat, Temp, Gas, Moisture, Motion etc.) and produces an output in the form of a signal. Our day-to-day lives are frequented by sensor devices such as biometric sensors, water alarms, moisture sensors, thermometersetc. Fresh innovations are a constant pursuit in sensor-based research aiming to improve their efficiency in terms of sensitivity, stability and environmental friendliness. Different materials and their various avatars are being investigated for the same. Transition metal dichalcogenides (TMD), such as molybdenum disulphide (MoS_2), have demonstrated considerable potential for sensing applications due to their high surface-to-volume ratio, an abundance of surface-active sites for chemical adsorption and the presence of anion (such as Sulphur) vacancies.[1]MoS_2 has shown strong potential in this regard due to its layered structure with covalent and Van der Waals bonds, ease of transition from bulk to 2D structure, tunable band gap, low contact resistance and lack of surface dangling bond which enhance the sensing. Our aim in this work is to investigate the performance of porous MoS_2 based sensors for soil moisture sensing. Porous nanomaterials can show enhanced specific surface area, tunable pore volume, and accessible active surface sites for trapping the molecules. A simple hydrothermal method was utilized to fabricate the hollow MoS_2 particles. The as-synthesized samples were characterized by FESEM, EDS and FT-IR.We are hopeful that the outcomes of this research will provide new insights and further advance the field of sensing.

Keywords: Transition Metal Dichalgonides, MoS_2, Sensor, Porous nanomaterials

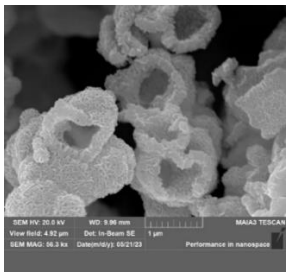

Fig.1.FESEM image of Porous MoS_2

References:

[1].Kumar, N. et al. (2022). Highly sensitive hierarchical MoS 2 nanoflowers for in-situ soil moisture sensing. Sens and Actuators B: Chemical 2.

Novel Hybrid Evolutionary Algorithm for Precise Nano-Optimization of Graphene Allotropes

Pawan Mishra[1*], Shashi Prakash Tripathi[2], Pooja[3]
[1,3]Department of Electronics and Communication Engineering, University of Allahabad, India
[2] Department of Applied Mathematics and Computer Science, Liverpool John Moores University, England
**Corresponding author email id- pawanmishra@allduniv.ac.in*

This research introduces an Evolutionary based Differential Evolution Algorithm with Parallel Optimization (EDEPO) strategy for the systematic exploration of optimal atomic configurations in two-dimensional graphene-like carbon lattices. Departing from conventional approaches, EDEPO fuses the prowess of Evolutionary Algorithms with the efficiency of Differential Evolution and the scalability of parallel processing. This integrated methodology aims to expedite the search for stable carbon atom arrangements. The optimization process involves a hybridization of the evolutionary algorithm and the Differential Evolution technique, synergistically leveraging their complementary strengths. The primary objective is to identify stable carbon atom arrangements under specified conditions, such as density, shape, and unit cell size. The fitness function, crucial for guiding the optimization, is framed as the total potential energy of the atomic system, ensuring a comprehensive evaluation of structural stability. Within this framework, the discrete atomic model is refined, and atom interactions are modelled using a tailored potential function, specifically designed for carbon and hydrocarbon materials. This contributes to a more accurate representation of atomic behaviours within intricate structures. Crucially, the parallel processing approach significantly accelerates computation time without compromising accuracy. The obtained results are rigorously validated, showcasing the efficiency of EDEPO in discovering stable atomic arrangements. Furthermore, the research presents diverse examples of new 2D materials generated through the algorithm, each characterized by distinct mechanical properties. EDEPO emerges as a robust and efficient tool for atomic arrangement exploration, contributing to advancements in material science and computational optimization.

Keywords: Nano-level optimization, Graphene Derivatives, Evolutionary Algorithm, Parallel Processing

Reference :

[1] Yu, X., & Gen, M. (2010). Introduction to evolutionary algorithms. Springer Science & Business Media.
[2] Cranford, S. W., & Buehler, M. J. (2011). Mechanical properties of graphyne. *Carbon*, *49*(13), 4111-4121.
[3] Wang, Y., Lv, J., Zhu, L., & Ma, Y. (2010). Crystal structure prediction via particle-swarm optimization. Physical Review B, 82(9), 094116.
[4] Babicheva, R. I., Dahanayaka, M., Liu, B., Korznikova, E. A., Dmitriev, S. V., Wu, M. S., & Zhou, K. (2020). Characterization of two carbon allotropes, cyclicgraphene and graphenylene, as semi-permeable materials for membranes. Materials Science and Engineering: B, 259, 114569.
[5] Bahmann, S., & Kortus, J. (2013). EVO—Evolutionary algorithm for crystal structure prediction. *Computer Physics Communications*, *184*(6), 1618-1625.
[6] John, C., Owais, C., James, A., & Swathi, R. S. (2020). Swarm Intelligence Steers a Global Minima Search of Clusters Bound on Carbon Nanostructures. The Journal of Physical Chemistry C, 125(5), 2811-2823

Green synthesis and dielectric study of Fe_2O_3

Sandeep Kumar, Deepash Shekhar Saini*
Department of Physics, Deen Dayal Upadhyaya Gorakhpur University, Gorakhpur 273009, India
**Corresponding author email id: dssainiddugu@gmail.com*

The ecological biosynthesis of iron oxide nanoparticles garnered great attention due to its low cost, eco-friendly, and non-toxicity. Iron oxide (Fe_2O_3) nanoparticles were synthesized using aloe vera leaf extract. Complex impedance, complex dielectric permittivity, electrical conductivity, and, electrical modulus measurements are carried out as a function of temperature (40-500 ℃), and frequency (100-10^6 Hz). The well-fitted Nyquist plot reveals the sintered sample's grain, grain boundary, and electrode polarization effect in the temperature range of 100-500 ℃. The real part of dielectric permittivity shows two behaviors from 40 ℃ to 180 ℃ (10^6-10) it decreases and between 180 to ℃-500 ℃ (10-10^4) increases and decreases with frequency. The tangent (tanδ) loss also showed two natures, a decreasing trend from 40 ℃ to 180 ℃ and increases from 180 to ℃-500 ℃. The ac conductivity spectra are explained using Jonscher's power law. The complex modulus plot ($M''vs\ M'$) shows alike behavior to Nyquist plots at different temperatures. The imaginary part of modulus (M'') is interpreted on the basis of the Kohlraush-William-Watts (KWW) function. The AC conductivity shows metal-to-semiconductor (weak insulator) transition.

Keywords: Green Synthesis, AC conductivity, Impedance, Metal-semiconductor.

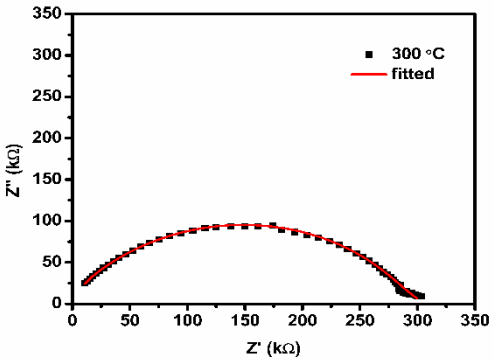

Figure.1. Complex impedance plane plot (Z'' vs Z') at 300℃

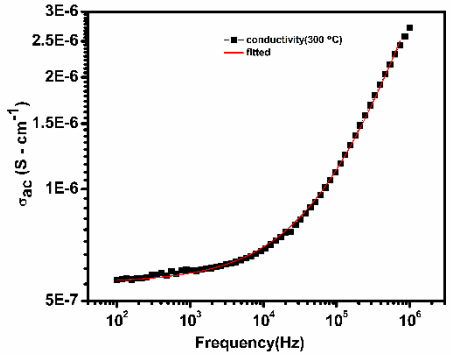

Figure. 2. log-log plot of frequency-dependent ac conductivity at 300 ℃

References:

[1] Abdullah, J. A. A., Salah Eddine, L., Abderrhmane, B., Alonso-González, M., Guerrero, A., & Romero, A. (2020). Green synthesis and characterization of iron oxide nanoparticles by pheonix dactylifera leaf extract and evaluation of their antioxidant activity. *Sustainable Chemistry and Pharmacy*, *17*.

[2] Kouhbanani, M. A. J., Beheshtkhoo, N., Taghizadeh, S., Amani, A. M., &Alimardani, V. (2019). One-step green synthesis and characterization of iron oxide nanoparticles using aqueous leaf extract of Teucrium polium and their catalytic application in dye degradation. *Advances in Natural Sciences: Nanoscience and Nanotechnology*, *10*(1).

[3] Qayoom, M., Shah, K. A., Pandit, A. H., Firdous, A., & Dar, G. N. (2020). Dielectric and electrical studies on iron oxide (α-Fe2O3) nanoparticles synthesized by modified solution combustion reaction for microwave applications. *Journal of Electroceramics*, *45*(1), 7–14.

Thermal and Acoustical Properties of Zinc Doped $MgFe_2O_4$–Ethylene Glycol Nanofluids

Avinash Chandra Rai*, Vivek Kumar Srivastava, Alok Kumar Verma
Department of Physics, Prof. Rajendra Singh (Rajju Bhaiya)
Institute of Physical Sciences for Study and Research,
Veer Bahadur Singh Purvanchal University, Jaunpur-222003, India.
*Corresponding author email id: avinash.pgc9@gmail.com

Spinel ferrite nanoparticles are recognized as an advanced material due to their physical, structural, optical, electronics, magnetic, chemical, and thermal properties (Ostafijchuk et al., 2015; Sharma et al., 2017).Ultrasonic attenuation is required for the non-destructive evolution of materials, which can improve the scrutinizing ability of materials for industrial applications (Mishra et al., 2013; Verma et al., 2010).Here, we have synthesized $MgFe_2O_4$ and Zn doped $MgFe_2O_4$ nanoparticles via sol-gel method. Structural analysis of the both nanoparticles have been done using X-ray diffraction (XRD) patterns. Particle size and morphological analysis of the synthesized nanoparticles have been done using Transmission Electron Microscope (TEM). Synthesized nanoparticles have been suspended in ethylene glycol to prepare the ferrite based nanofluids. Ultrasonic attenuation and particle size distribution (PSD) of the suspended particles in the base matrix have been studied with the help of Acoustical Particle sizer. Temperature and concentration dependent thermal conductivities of the nanofluids have been determined using transient plane source method. Effects of doping and temperature on the thermal and acoustical properties of the prepared ferrite based nanofluids have been discussed.

Keywords: Acoustical particle sizer, Ultrasonic Attenuation, Thermal conductivity, Nanofluids

References:

[1] Ostafijchuk, B. K., Bushkova, V. S., Moklyak, V. V., Ilnitsky, R. V. (2015). Synthesis andmagnetic microstructure of nanoparticles of zinc-substituted magnesium ferrites. *Ukr. J. Phys.*,60, 1234–1242.
[2] Sharma, R., Thakur, P., Kumar, M., Barman, P. B., Sharma, P., Sharma, V. (2017).Enhancementin A-B super-exchange interaction with Mn2+ substitution in Mg-Zn ferrites as aheating source in hyperthermia applications*Ceram. Int.,* 43, 13661–13669.
[3] Mishra G., Singh D., Yadawa P. K.,Verma S.K., Yadav R.R. (2013). Study of copper/palladium nanocluster using acoustical particle sizer. *Platinum Metals Rev.* 57, 186-191.
[4] Verma S.K., Yadav R.R., Yadav A.K. and Joshi B. (2010). Nondestructive evaluations of gallium nitride nanowires, *Mat. Lett*. 64, 1677-1680.

Atomic structure calculations of encapsulated lithium atom inside fullerene cage

Mobassir Ahmad*, Biplab Goswami, Jobin Jose and Raghavan K Easwaran
Department of Physics, Indian Institute of Technology Patna, Bihar, 801103, India
**Corresponding author email id: mobassir_2121ph06@iitp.ac.in*

Since its discovery, the fullerene [1] has attracted both theoretical and experimental groups in the disciplines of both basic and applied physics. This special species has a unique soccer ball like shape made by the carbon atoms leaving a hollow cage inside. It can encapsulate small atoms or molecules which make a considerable modification of physical properties in both fullerene and confined atom. As fullerene is quite stable and inactive in nature, the encapsulated atoms are practically isolated from the surroundings, which makes them suitable for several applications such as quantum computing, spintronics, etc.

Theoretically the effect of the fullerene cage on the encapsulated atom can be realized by different model potentials bypassing the structural and geometrical complications of fullerene. Here, we use a simpler model potential called as Annular Square Well (ASW) which is added to the Hamiltonian of the lithium atom [2]. ASW is a short range attractive annular well which takes the form of a spherical shell. The effective nuclear potential of the atom with ASW potential is shown in figure 1. We use the Multi-configuration Dirac Hartree-Fock (MCDHF) method to compute the atomic energy levels. Later the transition parameters including the lifetime of different levels are also computed. Changing the depth of the ASW model, we can alter the energy levels, lifetimes and transition strengths [3]. So, by controlling the model potential depth as tuning parameter, the atomic energy levels can be set suitably for quantum memory applications. As atomic decoherence is one of the challenging factors to perform efficient quantum memory protocols like Electromagnetically Induced Transparency (EIT) in bare atomic media, the encapsulated atom can be a good candidate for performing EIT where the decoherence effect can be controlled by the confining potential depth as tuning parameter.

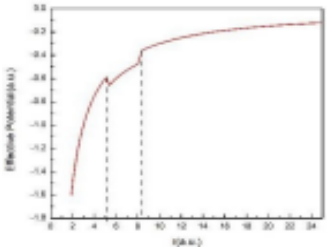

Figure 1: *Effective nuclear potential of the confined lithium atom inside fullerene cage*.

Keywords: Endohedral fullerene, Atomic structure calculation, MCDHF method, EIT.

References:

[1] Kroto H. W., Heath J. R., O'Brien S. C., Curl R. F., and Smalley R. E. (1985). C60: Buckminster fullerene. Nature, 318,162–163.
[2] Dolmatov V. K., Baltenkov A.S., Coonerede J.P. and Manson S.T. (2004), Structure and photoionization of confined atoms, Radiation Physics and Chemistry, 70(1), 417-433.
[3] Saha S. and Jose J. (2020), Shanon Entropy a Predictor of Avoided Crossing in Confined atoms, Int. J. Quant. Chem., 120, E26374.
[4] Ma L., Slattery O. and Tang X. (2017). Optical quantum memory based on electromagnetically induced transparency. Journal of Optics, 19(4), 043001.

Study of dielectric properties of silver nanoparticles (Ag-NPs) dispersed nematic liquid crystal 4'-n-Heptyl-4-cyanobiphenyl (7CB)

Ankur Srivastava[a*], Sindhu Singh[a], Anoop K. Srivastava[b] Anil Kumar[a]
[a]Department of Physics and Electronics, Dr. R. M. L. Avadh University Ayodhya
[b]Department of Applied Science & Humanities, I.E.T., Dr. R. M. L. Avadh University, Ayodhya
Corresponding author email id: ankursrivastava6001@gmail.com

In the present work, silver nanoparticles (Ag-NPs) were dispersed at a room temperature nematic liquid crystal 4'-n-Heptyl-4-cyanobiphenyl (7CB) at the concentration of 0.2, 0.4, 0.6 and 0.8 wt%. The dielectric properties of pristine and NPs dispersed in different concentrations into host nematic LC have been studied. Dielectric studies show that the presence of the Ag-NPs modulates the effective longitudinal component ($\varepsilon_{\parallel}'$) of the dielectric permittivity while has no effect on the transverse component ($\varepsilon_{\perp}'$). The birefringence, parallel and perpendicular components of permittivity and conductivity was found to be dependent on temperature and concentration of Ag-NPs into host nematic LC.

Keywords: Nematic liquid crystal; Ag-NPs; anisotropy; conductivity; permittivity

Antibacterial activity of $ZnO/CoFe_2O_4$ magnetic nanocomposite for gram-positive and gram-negative bacterial strains

Anand Kumar Vishwakarma[a], Sneha Tripathi[b], Bhim Sen Yadav[a], Sarvesh Kumar[a], Shivesh Sharma[b], Naresh Kumar[a,*]

[a]Department of Physics, Motilal Nehru National Institute of Technology Allahabad, Prayagraj

[b]Department of Biotechnology, Motilal Nehru National Institute of Technology Allahabad, Prayagraj

**Corresponding author email id: nsisodia@mnnit.ac.in*

We report on the synthesis of $ZnO/CoFe_2O_4$[ZnO/CFO] magnetic nanocomposite and explore their antibacterial properties for gram-positive and gram-negative species. ZnO/CFO nanocomposite was synthesized via hydrothermal and sol-gel method. Structural analysis of the synthesized samples revealed that the nanocomposite exhibited the inverse spinel structure of $CoFe_2O_4$, alongside the wurtzite hexagonal phase of ZnO (Figure 1). The shifting of bands in FTIR spectra from 416 cm^{-1} to 439 cm^{-1} and 581 cm^{-1} to 597 cm^{-1} at octahedral and tetrahedral positions has suggested the attachment of ZnO on the surface of $CoFe_2O_4$ nanoparticles. The direct bandgap values were estimated to be 2.75 eV for $CoFe_2O_4$ and 3.00 eV for $ZnO/CoFe_2O_4$ by UV-Vis-DRS spectra. Morphological analysis revealed an agglomerated and irregular structure for both $CoFe_2O_4$ and ZnO nanoparticles. The TEM images provided insight into the average particle sizes, which were determined to be 15 nm for $CoFe_2O_4$ and 33 nm for ZnO.Interestingly, the saturation magnetization (M_S) of the ZnO/CFO nanocomposite decreased by 40%, from 65.4 emu/g to 39.3 emu/g, demonstrating its suitability for magnetic separation from biological systems.The nanocomposite's antibacterial efficacy was assessed against both gram-positive and gram-negative species at different concentrations (specifically, 1600, 1200, 800, and 400 µg) using the agar well diffusion assay. The results demonstrated a significant increase in antibacterial activity, with approximately 35.4% inhibition observed for *B. subtilis*, around 32.3% inhibition for *S. aureus*, approximately 9% inhibition for *E. coli*, and roughly 14.5% inhibition for *P. aeruginosa* among the tested bacterial strains (Figure 2).Additionally, bacterial growth patterns were investigated at various concentrations (5, 2.5, 1.25, 0.625, 0.15625, and 0.078125 mg/mL) of the ZnO/CFO nanocomposites using the micro-broth dilution method. Notably, all examined bacterial strains exhibited the highest degree of growth inhibition when exposed to a concentration of 5 mg/mL of the nanocomposites.

Keywords: Cobalt ferrite, Zinc oxide, Hydrothermal, Nanocomposite, Antibacterial activity

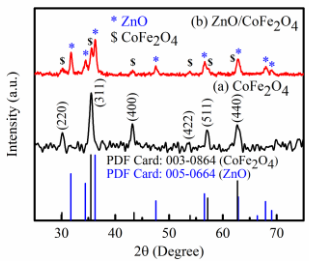

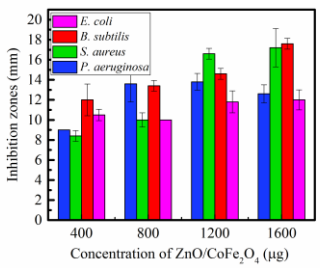

Figure 1: *XRD patterns of (a) $CoFe_2O_4$ NPs and (b) $ZnO/CoFe_2O_4$ NCs* & **Figure 2:** *Bar diagram representing the diameter of inhibition zones vs sample concentration for all studied bacteria.*

Electrical Characterization of ZnPc-based Organic Schottky Diodes

Nargis Khatun*, AKM Maidul Islam
Department of Physics, Aliah University, Newtown, Kolkata-700160, India
**Corresponding author email id: nargis2796@gmail.com*

Organic semiconductors (OS) have recently emerged as promising prospects due to their wide variety of potential applications in low-cost, flexible electronic devices, such as OFETs, solar cells, and sensors [1]. All of these devices require forming an active semiconducting layer on a suitable substrate, depending upon the application, and the charge transfer process at the junction determines the device's functionality [2]. Therefore, understanding the charge transport process at the interfaces is vital to designing high performance OE devices. Amidst many devices, the metal/semiconductor junction-based device, such as the Schottky diode, is of particular significance because Schottky diodes serve as the foundation for many devices, including field-effect transistors and solar cells. ZnPc is a suitable OS whose temperature response considerably impacts the crystal structure of films and is expected to affect the interfacial properties, essentially allowing the tenability of the metal/semiconductor junction functionalities. Therefore, the temperature response of the Schottky behaviour of such devices has paramount significance in enhancing the device performance, like hole mobility, the turn-on voltage, junction barrier height, series resistance, ideality factor, etc. So, in order to address the above parameters, in this study, ZnPc-based Schottky diodes are fabricated in Al/ZnPc/ITO device configuration. The comprehensive electrical performance was investigated using current-voltage (I-V) characteristics before and after annealing the device. Different regions of charge conduction mechanisms were visible. At higher voltages, conduction is dominated by the space charge-limited conduction mechanism (SCLC). Upon heating, hole mobility was increased by almost an order of magnitude, and the series resistance of this device decreased after applying heat. After annealing, the barrier height reduction was observed from 0.87 eV to 0.75 eV, which reduced the turn-on voltage.

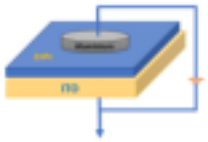

(a) (b)

Fig.1(a) Schematic diagram of Schottky diode, (b) I-V characteristics of the device

Keywords: Zinc phthalocyanine, Schottky diodes Interface, Mobility, Conductivity, Series resistance

References:

[1] Spanggaard, H., & Krebs, F. C. (2004). A brief history of the development of organic and polymeric photovoltaics. *Solar Energy Materials and Solar Cells*, *83*(2-3), 125-146. [2] Petraki, F., & Kennou, S. (2009). Investigation of the interfaces formed between ITO and metal phthalocyanines (NiPc and CoPc) by photoelectron spectroscopy. *Organic Electronics*, *10*(7), 1382-1387.

Highly efficient room temperature hydrogen gas sensor using Pd-capped PdMg alloy thin films

Durvesh Gautam, Yogendra K. Gautam*
Smart Materials and Sensor Laboratory, Department of Physics, CCS University Campus
Meerut, Uttar Pradesh, 250004, India
Corresponding author Email id: ykg.iitr@gmail.com

The pursuit of efficient and reliable hydrogen gas sensors has gained paramount importance due to the increasing demand for clean energy applications and the potential hazards associated with hydrogen leakage. In this present work, Pd-capped PdMg alloy thin film has been studied for its hydrogen gas sensing application. DC/RF magnetron sputtering was used to deposit the Pd-capped PdMg alloy thin films at room temperature on glass substrates. By varying the deposition power of the sputtering target Pd, three samples have been prepared. The structure and surface morphology of the as-prepared Pd-capped PdMg alloy specimens were examined by X-ray diffraction (XRD) and field-emission scanning electron microscopy (FESEM). The chemical composition and purity of the samples were verified by X-ray photoelectron spectroscopy (XPS)and elemental analysis through Energy Dispersive X-ray Analysis (EDAX). Furthermore, using a two-probe approach, in situ hydrogen gas sensing measurements are performed to a known hydrogen gas concentration by using a hydrogen sensing setup. In measurements for hydrogen gas sensing, the sensor's performance is evaluated in terms of sensitivity, selectivity, response time, and stability. this is found that the change in electrical resistance for the sensor during the hydrogenation/dehydrogenation process is reversible at room temperatures. The $Mg_{40}Pd_{60}$ sensor's response time was observed to be 5s, while the minimum recovery time after dehydrogenation at room temperature is 3 min. We observed that the sensor was mechanically stable as the composition of Pd was increased for numerous hydrogenation/dehydrogenation cycles. These results indicate that our hydrogen gas sensor is designed with exceptional selectivity, sensitivity, and stability, ensuring precise detection even in high-humidity atmospheres.

Keywords: PdMg alloy, Hydrogen gas, DC/RF magnetron Sputtering, XRD, FESEM.

Photocatalytic production of aniline by nitro-compound over highly recyclable Pd nanoparticles supported on ZnO nanostructures

Sagar Vikal*[1], Yogendra K. Gautam[1]
[1]Smart Materials and Sensor Laboratory, Department of Physics, Ch. Charan Singh University, Meerut, Uttar Pradesh 250004, India.
**Corresponding author email id: Sagarvikal97@gmail.com*

Photocatalytic reduction of organic pollutants has gained significant attention due to its potential as an effective and sustainable remediation technique. Nitrobenzene, a toxic and persistent aromatic pollutant, poses a serious threat to environmental and human health. Palladium-doped ZnO nanoparticles (Pd-doped ZnO NPs) were synthesized through the hydrothermal method. The XPS analysis confirmed the doping of Pd with ZnO NPs, and the XRD spectra show a decreasing trend in crystallite size (CS) of synthesized NPs with increased Pd concentration. FESEM study reveals the nanorods like surface morphology of pure ZnO nanoparticles, irregular nanorod & sphere particle like shape of Pd-doped ZnO nanoparticles. UV-vis spectroscopy was used to estimate the optical properties and chemical bonding of the prepared Pd-doped ZnO NPs, respectively. Further the study of catalytic activity of Pd-doped ZnO photocatalyst showed that doping increases the product yields up to 86 % and reduces the reaction time. The most appealing outcome was obtained with 0.08 wt% Pd-doped ZnO nanoparticles that shows maximum reduction of nitrobenzene to aniline at a catalyst load of 20 mg. Up to six successive treatment cycles is confirmed for their reusability. This will limit the risk of nanotoxicity and aid the cost-effectiveness of the overall reduction process.

Keywords: ZnO Nanoparticles, Palladium, Photocatalyst, XPS, Nitrobenzene.

Structural and transport properties of pulsed laser deposition grown $La_{0.7}Sr_{0.3}MnO_3$ thin film on $LaAlO_3$ substrate

Bharat K. Gupta[1], Nikhil Kumar[1,*]
[1]Department of Physics, Deen Dayal Upadhyay Gorakhpur University, Gorakhpur, Uttar Pradesh 273009, India
[*]*Corresponding author email id: nik.jnu@gmail.com*

Half metallic ferromagnetic material shows good magnetic and conducting properties at room temperature. $La_{0.7}Sr_{0.3}MnO_3$ (LSMO) is a leading member of half metallic ferromagnetic material family which has great interest for application in development of facile and flexible electronics and spintronic devices. We have deposited epitaxial thin film of LSMO of 100nm thickness on single crystal $LaAlO_3$ (LAO) substrate with compressive strain of 3.19% by pulsed laser deposition (PLD) technique. In thin film growth by PLD, substrate temperature, oxygen partial pressure, laser pulse energy density, substrate to target distance, strain induced due to lattice mismatch between substrate and thin film, cooling environment and pressure significantly influence the transport and magnetic properties of grown LSMO thin film. The structural characterization shows that grown film is in single phase having orthorhombic structure. Magnetization versus applied field (M-H) measurement of LSMO/LAO film at 5K reveal the saturation magnetization M_s= 117.5emu/cm^3, residual magnetism M_r = 36emu/cm^{3}and coercive field value H_c=0.3kOe while the film exhibit M_s= 27.6 emu/cm^3, M_r = 12.8emu/cm^{3}and H_c = 30Oe at 300K. The ferromagnetic transition temperature T_c (Curie temperature) and metal to insulator transition temperature T_{MI} of film are investigated by magnetization versus temperature measurement and transport measurement and we found around 316K and 312K respectively. We also observed surface roughness of 4.35 nm using atomic force microscopy (AFM).

Keywords: PLD, Thin film, half metallic ferromagnetic, Spintronics.

Acknowledgements:

BKG acknowledges the funding support from IUAC, New Delhi, for the junior research fellow position and for AFM measurements under Dr. Indra Sulania. NK acknowledges DST Inspire Faculty Project grant IFA-216. We also acknowledge the support of PLD facility, XRD and magnetization measurements using SQUID-VSM magnetometers from UGC-DAE CSR, Indore Centre under Dr. Ram Janay Choudhary.

References:

[1] Wang K., Tang M. H., Xiong Y., Li G., Xiao Y. G., Zhang W. L., Wang Z. P., Li Z. & He J. (2017). Epitaxial growth and magnetic/transport properties of La0.7Sr0.3MnO3 thin films grown on SrTiO3 with optimized growth conditions. *RSC Adv.*, vol. 7, no. 50, pp. 31327–31332.
[2] Panchal G., Choudhary R. J. & Phase D.M. (2018). Magnetic properties of La0.7Sr0.3MnO3 film on ferroelectric BaTiO3 substrate. *J. Magn. Magn. Mater.*, vol. 448, pp. 262–265.
[3] Cesaria M., Caricato A. P., Maruccio G. & Martino M. (2011). LSMO - Growing opportunities by PLD and applications in spintronics. *J. Phys. Conf. Ser.*, vol. 292 012003.

Copper-doped TiO_2 thin films as a potential charge transport layer in Perovskite solar cell

Vivek Dhuliya[1], L. P. Purohit[1*]
[1]Department of Physics, Gurukula Kangri (Deemed to be University), Haridwar, 249404, Uttarakhand, India
**Corresponding author email id: lppurohit@gkv.ac.in*

Titanium dioxide (TiO_2) thin films have emerged as one of the most promising metal oxides due to their unique properties and low cost(Zhang et al., 2018). TiO_2 thin films are widely used in photovoltaic solar cells as transparent conductive oxide layers as well as electron transport layers (ETL) due to their low-cost fabrication, high light transmissivity, stability, etc(Hu et al., 2020). In the present work, Copper doped TiO_2 (Cu-TiO_2) thin films, were deposited over the glass substrates using the spin coating method. Five samples S_1 S_2, S_3, S_4, and S_5 were prepared with Copper doped in doping percentages 0,0.5, 1.0, 1.5, and 2.0% respectively were prepared with different film thicknesses.

The UV-Vis spectra suggest that all the samples have transmittance >80% in the 300-700 nm wavelength range. The values of the band gap for samples S_1, S_2, S_3, S_4, and S_5 were in the range of 3 to 4 eV. The electrical conductivity for samples was observed using current-voltage (I-V) measurements.XRD analysis gave peaks corresponding to the indices of the anatase phase of the crystallinity of the film. The FESEM images were obtained to analyze the morphological properties of the films. The doping of Cu does change the morphology of the TiO_2 films however, the increment in the concentration of Cu increases the size of the flakes, and a uniform texture of the film was obtained as compared to TiO_2 films. The EDS images confirmed the concentration of the Cu in the prepared films.

The overall characterizations suggest that among the five samples, S_3 exhibits the desired properties very well.Thus, the designed thin film was found promising electron transport layer in perovskite solar cells.

Keywords: Titanium dioxide; Copper; Spin coating; hydrothermal; UV-Visible Spectroscopy

References:

[1] Hu, W., Yang, S., & Yang, S. (2020). Surface Modification of TiO2 for Perovskite Solar Cells. *Trends in Chemistry*, *2*(2), 148–162. https://doi.org/10.1016/j.trechm.2019.11.002

[2] Zhang, H., Zhang, Q., Lv, Y., Yang, C., Chen, H., & Zhou, X. (2018). Upconversion Er-doped TiO2 nanorod arrays for perovskite solar cells and the performance improvement. *Materials Research Bulletin*, *106*, 346–352. https://doi.org/10.1016/j.materresbull.2018.06.014

Facile Synthesis of $MoSe_2$ Nanosheets as Promising Electrode Material for Supercapacitor Device Application

Divya Singh, Ashwani Maurya, Saurav K. Ojha, Animesh K. Ojha*
Department of Physics, Motilal Nehru National Institute of Technology Allahabad, Prayagraj-211004, India
**Corresponding author email id: animesh@mnnit.ac.in*

In the changing era of modern electronics and renewable energy, the energy storage materials find many applications in hybrid electric vehicles, portable electronic and wearable device. Transition metal dichalcogenides (TMDs) (e.g., $MoSe_2$, MoS_2, WSe_2, WS_2, and WTe_2) having 1D and 2D layered structures is being studied as promising material for Supercapacitor application [1]. $MoSe_2$ has layered structure and has a higher electrical conductivity than MoS_2, WSe_2, and WS_2 [2].The layered structure $MoSe_2$ is synthesized by one-step Hydrothermal method. The structural and morphological characterizations of prepared $MoSe_2$is done by using X-ray diffraction and SEM. Comparing the XRD data (Fig.1) with reference data (JCPDF card No– 290914) confirms the formation of highly crystalline hexagonal phase of $MoSe_2$ which is semiconducting in nature. Fig.2Show the results of CV measurements done at various scan rates (10 to 200 mV/s) in fix potential window of -0.05 to 0.55 V. The specific capacitance of $MoSe_2$ electrode as calculated form CV curves at different scan rate is turn out to be 529 F/g, at scan rate of 10mV/s, in 3M KOH electrolyte with optimal cycling stability.

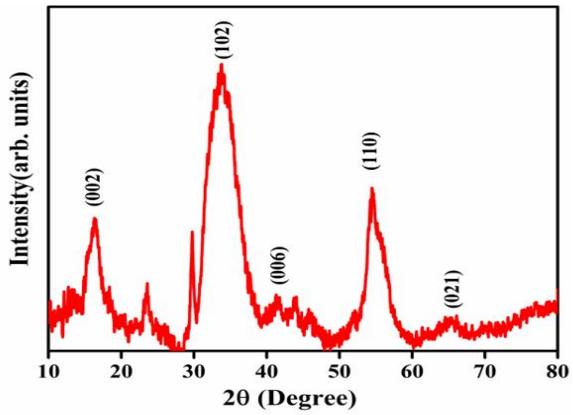

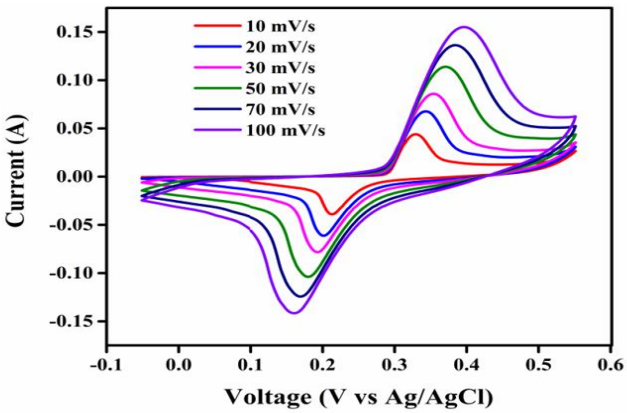

Fig.1. *XRD pattern of $MoSe_2$* ***Fig.2.*** *CV curve of $MoSe_2$ electrode at various scan rates.*

Keywords: $MoSe_2$, Hydrothermal Method, supercapacitor.

References:

[1] Nath, M., & Rao, C. N. R. (2001). MoSe2 and WSe2 nanotubes and related structures. Chemical Communications, (21), 2236-2237.

[2] Singh, D., Ojha, S. K., Maurya, A., Preitschopf, T., Fischer, I., & Ojha, A. K. (2023). Controlled synthesis of 2H-WSe2@ rGO nanocomposites: An efficient electrode material for high performance asymmetric supercapacitor device application. Journal of Alloys and Compounds, 968, 171828.

Actinidia Deliciosa Assisted Reduced Graphene Oxide: An Eco-friendly and Efficient Electrode Material for Energy Storage Application

Ashwani Maurya*, Divya Singh, Saurav K. Ojha, Animesh K. Ojha
Department of Physics, Motilal Nehru National Institute of Technology Allahabad, Prayagraj-211004, India
**Corresponding author email id: ashwanim765@gmail.com*

Carbon-related materials are promising electrode materials for energy storage devices, as they offer a very high specific area[1]. Reduction of graphene oxide (GO) is an efficient way to obtain graphene in large quantities[2]. Graphene oxide (GO) is reduced with a reducing agent to obtain rGO. But, most of the reduction methods for reducing GO into rGO involved the use of chemicals, which are very toxic in nature and they are also not environment friendly. Therefore, the green approach for reduction of GO into rGO is the subject of great research interest for the researchers[2]. Herein, we have reduced GO with an eco-friendly and cost-effective approach using actinidia deliciosa (AD) juiceas a green reducing agent.The X-ray diffraction (XRD) patterns of the synthesized materials, as shown in Fig. 1 (red colour),show peak at 2θ = 10.5°, confirming the formation of GO[2].However,the peak is shifted towards higher 2θ values (24°–26°) after reduction, indicating the successful reduction of GO into rGO[2]. The value of specific capacitance (SC) calculated from cyclic voltammetry (CV)curves (see Fig. 2), turns out to be 104 F/g at 5 mV/s scan rate. The present report shows that the AD assisted rGO is a promising electrode material for supercapacitor applications.

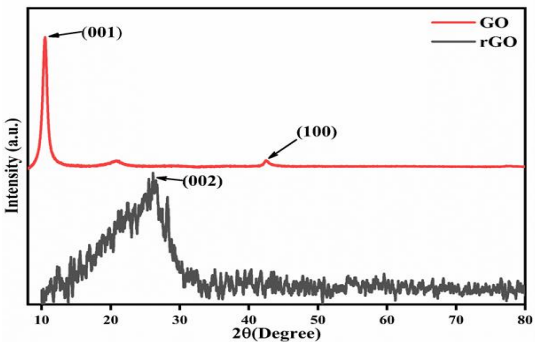

Fig. 1. XRD spectra of GO and rGO.

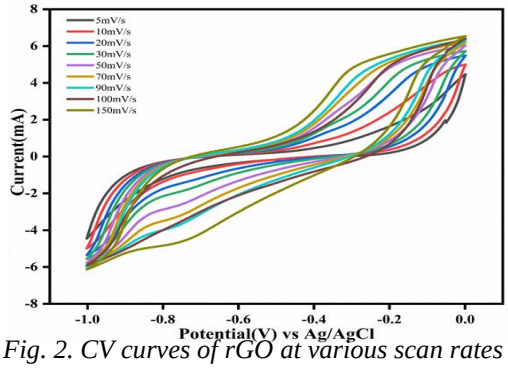

Fig. 2. CV curves of rGO at various scan rates

Keywords: Supercapacitor, Graphene, Actinidia deliciosa, Green reducing agent

References :

[1] Singh, A., & Ojha, A. K. (2020). Coal derived graphene as an efficient supercapacitor electrode material. Chemical Physics, 530, 110607.

[2] Singh, A., Ahmed, B., Singh, A., & Ojha, A. K. (2018). Photodegradation of phenanthrene catalyzed by rGO sheets and disk like structures synthesized using sugar cane juice as a reducing agent. Spectrochimica Acta Part A: Molecular and Biomolecular Spectroscopy, 204, 603-610.

Electrical properties of highly aligned P3HT solution processed thin films

Imran[1], Preeti Shukla[2], C. K. Singh[2], Shikha Jaiswal[1*], Lokendra Kumar[2]
[1]Department of Physics, Feroze Gandhi College,Raebareli (U.P.)
[2]Department of Physics, University of Allahabad, Prayagraj-211 002 (India)
**Corresponding author email id: shikhajk@gmail.com*

It is a key challenge to achieve long-range ordering in the morphology of conjugated polymers for efficient charge transport in organic electronic devices. The efficiency and working mechanism of organic electronic devices strongly depend on the structure and crystallinity of active semiconducting polymers. Conducting polymers has received much attention due to the demand for light and flexible electronic equipment. Poly(3-hexylthiophene) (P3HT) has much more excellent stability than most conducting polymers because of the sulphur hetero-aromatic ring structure and its solubility in common organic solvents such as chloroform, chlorobenzene, Di-chloromethane, and toluene. In this study, we examine the combined effect of solvents chloroform (CF) and toluene (TLN) over the crystallization and orientation of P3HT when cast on-center and off-center. The thin film was deposited on Fluorine doped tin oxide (FTO) substrate via off-center and on-center spin coating. The surface morphology is studied by AFM. The structural analysis is observed using grazing angle X-ray diffraction. Further, the Schottky diodes in Al/P3HT/FTO configuration are fabricated, and their current density-voltage characteristics are subsequently compared for extracting the electronic parameters of the device.

Keywords: P3HT, conjugated polymers, Schottky diodes.

References

[1] K. Singh and R. Prakash, Organic Schottky diode based on conducting polymer–nanoclaycompositeRSC Adv. 2, 5277 (2012).
[2] V. Singh, A. K. Thakur, S. S. Pandey, W. Takashima, and K. Kaneto, Role of Morphology on Photoluminescence Quenching and Depletion Width Formed at the Interface of Aluminum and Poly(3-alkylthiophene)Japanese Journal of Applied PhysicsPart 1 48, 061503 (2009)
[3] V. Singh, A. K. Thakur, S. S. Pandey, W. Takashima, and K. Kaneto, Evidence of photoluminescence quenching in poly(3=hexylthiophene-2,5-diyl) due to injected charge carriersSynth. Met. 158, 283 (2008).
[4] Vivek Chowdhary, Rajiv Kumar Pandey, Rajiv Prakash, Arun Kumar SinghSelf-assembled H-aggregation induced high performance poly (3-hexylthiophene) Schottky diode December 2017 Journal of AppliedPhysics 122(22):225501
[5] Vivek Chowdhary, Naresh, Arun Kumar Singh Solubility dependent trap density in poly (3-hexylthiophene) organic Schottky diodes at room temperatureMarch 201Synthetic Metals 250:88-93
[6] N.E. Persson, J. Rafshoon, K. Naghshpour, T. Fast, P.-H. Chu, M. McBride, B. Risteen, M. Grover, E. Reichmanis, Nucleation, growth, and alignment of poly (3-hexylthiophene) nanofibers for high-performance OFETsACS Appl. Mater. Interfaces 9 (2017) 36090–36102.
[7] P.R. Berger, M. Kim, J. Polymer solar cells: P3HT:PCBM and beyond, Renew. Sustain. Energy 10 (2018) 013508
[8] J. Song, K.-H. Kim, E. Kim, C.-K. Moon, Y.-H. Kim, J.-J. Kim, S. Yoo,Lens free OLED with 50% external quantum efficiencyvia external scattering and horizontally oriented emitters, Nat. Comm. 9 (2018) 3207.
[9] Y. J. Lin and Y. M. Chin, Defect-dependent carrier transport behavior of polymer:ZnOomposites/electrodeposited CdS/indium tin oxide devices J. Appl. Phys. 116, 173709 (2014).
[10] Y. M. Chin, Y. J. Lin, and D. S. Liu, Enhancement of carrier mobility in poly (3-hexylthiophene)by incorporating ZnOnanoparticlesThin Solid Films 548, 453 (2013)

Electrically polarized lanthanum substituted hydroxyapatite-barium strontium titanate composite shows enhanced osteoblast activities and inhibits *S. aureus* bacteria

Doctor Rojaleen Lenka, Debansh Samanta Singhar, Subhasmita Swain*, Tapash R. Rautray
Biomaterials and Tissue Regeneration Lab, Centre of excellence, Institute of Technical Education and Research, Siksha 'O' Anusandhan (Deemed to be University), Bhubaneswar – 751030, Odisha, India
**Corresponding author email id: subhasmitaswain@soa.ac.in*

Piezoelectric barium titanate (BT), hydroxyapatite (HA), and composites based on these have been used for various biomedical applications for several years. Advantages offered by these composites, such as bio-inertness, osteoconductivity, high compressive strength, biocompatibility and biodegradability, make them a potential candidate for dental and orthopaedic use. This investigation was carried out to prepare a revised implantable bone filler composite, i.e., barium strontium titanate (BST) / lanthanum substituted HA (La-HA), and to investigate the proliferation rate of human osteoblast-like cells (MG63), osteogenic expression and bacterial viability of *Staphylococcus aureus* on the composite specimen. Two composite specimens, namely 10%LaHA-10%BST and 10%LaHA-20%BST, were synthesized. It was found from thermally stimulated depolarization current (TSDC) measurement that, at 492 °C, the N-poled BST-La-HA composite exhibits a peak current density at 550 °C, and maximum charge was found to be stored. La ion release from the composite enhanced the antimicrobial behaviour of the sample. MG63 cell proliferation rate, osteogenic gene expressions as well as antibacterial nature was maximized in 10%-LaHA-20%-BST, contrary to 10%-LaHA-10%-BST.

Keywords: BST, hydroxyapatite, osteogenicity, polarization.

References:

[1] Swain, S., Kumari, S., Swain, P., &Rautray, T. (2022). Polarised strontium hydroxyapatite–xanthan gum composite exhibits osteogenicity in vitro. *Materials Today: Proceedings*, *62*, 6143-6147.

[2] Fukada, E., & Yasuda, I. (1957). On the piezoelectric effect of bone. *Journal of the physical society of Japan*, *12*(10), 1158-1162.

[3] Chen, Q. Z., Wong, C. T., Lu, W. W., Cheung, K. M. C., Leong, J. C. Y., & Luk, K. D. K. (2004). Strengthening mechanisms of bone bonding to crystalline hydroxyapatite in vivo. Biomaterials, 25(18), 4243-4254.

Silver doped HA-Xanthan gum microspheres exhibiting promising result in combating bacteria *in vitro* for bone tissue engineering

Monalisa Pradhan[†], Sunita Das[†], Subhasmita Swain, Tapash Ranjan Rautray[*]
Biomaterials and Tissue Regeneration Lab, Centre of Excellence, Siksha 'O' Anusandhan (Deemed to be University), Bhubaneswar, Odisha-751030, India.
[†]Authors equally contributed
Corresponding author email id: tapashrautray@soa.ac.in

The increasing prevalence of drug resistance poses a significant burden on patients and society, particularly related to bone diseases. To address this issue, a novel microsphere has been developed having both antibacterial and osteogenic properties, which is achieved by incorporating nano-silver into hydroxyapatite-xanthan gum composite. Chemical modifications have been employed to improve the applicability of xanthan gum for biological applications. Although it has several limitations, such as vulnerability to microbiological contamination, unsuitable viscosity, poor thermal and mechanical stability, and insufficient water solubility. The coating of silver (Ag) nanoparticles was applied to microspheres which significantly enhanced their antibacterial effectiveness. The morphology and structure of the composite material, consisting of nano-silver coated hydroxyapatite and xanthan gum (nano Ag-HA-XG), were characterized using x-ray diffraction and scanning electron microscopy techniques. Antibacterial assays showed that Ag-coated HA-XG material had specific antibacterial action against Gram-negative *S. aureus* bacteria. The elevated concentration of intracellular reactive oxygen species (ROS) in silver leads to the death of significant proportion of *S. aureus* cells. However, the microspheres exhibited an increased swelling ratio during prolonged exposure to simulated bodily fluid (SBF). The nonimmunogenic properties of HA-XG microspheres in MG-63 cells were validated by *in vitro* examination using the MTT assay. The synthesized microspheres have potential application as a drug delivery system for bone regeneration.

Keywords: Xanthan gum, Microsphere, nano Ag-HA-XG, drug delivery, antibacterial.

Reference:

[1] Shakeel, S., Talpur, F. N., Sirajuddin, Anwar, N., Iqbal, M. A., Ibrahim, A., ...& Bashir, M. S. (2023). Xanthan gum-mediated silver nanoparticles for ultrasensitive electrochemical detection of Hg2+ ions from water. *Catalysts*, *13*(1), 208.

[2] Mishra, S., &Rautray, T. R. (2020). Fabrication of Xanthan gum-assisted hydroxyapatite microspheres for bone regeneration. *Materials Technology*, *35*(6), 364-371.

Effect of Nano-mechanical Vibration on a Quantum Heat Engine in the Electromagnetically Induced Transparency Regime

Rejjak Laskar*, Aparajita Das, Samim Akhtar, Md. Mabud Hossain, Jayanta K. Saha
Department of Physics, Aliah University, Action Area IIA/27, Newtown, Kolkata-160, India
Corresponding author email id: laskarrejjak786@gmail.com

The present work is devoted to understand the efficiency of a model three-level quantum heat engine [1] in the regime of electromagnetically induced transparency (EIT) [2] that uses an ultra-cold atomic gas and a vibrating nano-mechanical mirror as a perturbation. The novelty of the said model lies in the fact that the opto-mechanical effect on the response properties is studied without considering any external cavity confinement, rather than exploiting the vibration of the mirror. Three different types of heat engine configurations are proposed: a vibration-free heat engine, a vibration-aided heat engine, and a mirror damping-induced heat engine. As the control field strength increases, the entropy flow rate decreases in the proposed heat engines. The decrease in the entropy flow rate is more significant in vibration-aided and mirror-damping-induced heat engines, while vibration-free heat engine shows a similar pattern but less affected by the strength of the control field. The emission rates of the proposed three types of models are compared and discussed in details. Comparisons between the proposed model and an ideal quantum heat engine are made in terms of the entropy balance condition, adhering to the constraints of the second law of thermodynamics.

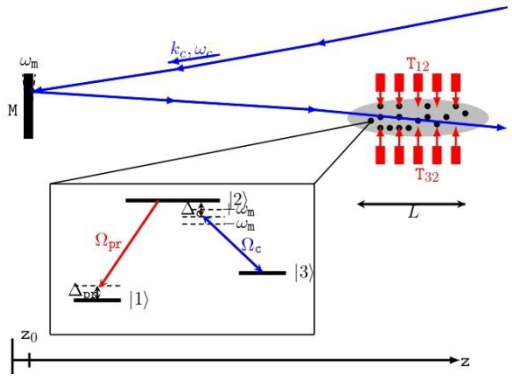

Figure:*The three-level heat engine is coupled with a mirror via the control field and two blackbody reservoirs at temperatures T_{12} and T_{32}. The control field (with wave no. k_c, frequency ω_c) couples the transition between the level |3> and level |2> with detuning Δ_c, Rabi frequency Ω_c. The Rabi frequency and detuning of the emitted probe field are denoted by Ω_{pr} and Δ_{pr}, respectively.*

Keywords: Mirror Vibration, Electromagnetically induced transparency (EIT), Entropy Balance, Heat Engine, Emission Rate.

References:

[1] Harris, S. E. (2016). Electromagnetically induced transparency and quantum heat engines. *Physical Review A*, *94*(5), 053859.
[2] Boller, K. J., Imamoğlu, A., & Harris, S. E. (1991). Observation of electromagnetically induced transparency. *Physical Review Letters*, *66*(20), 2593.

Reduced Driving voltage of Nanoparticles Doped Polymer Dispersed liquid Crystal

Nidhi Pandey*, Rama Shanker Gupta, Sudhanshu Pandey
Department of Physics, United University, Rawatpur, Jhalwa, Prayagraj-211012, India
**Corresponding author email id: nidhipandey.phdph21@uniteduniversity.edu.in*

Polymer dispersed liquid crystal (PDLC) materials have garnered significant attention for their versatile applications in display technologies. The polymer is chosen for its excellent optical transparency and compatibility with liquid crystal molecules. The nematic liquid crystal, with its anisotropic optical properties, contributes to the unique electro-optical characteristics of the PDLC material. The PDLC was synthesised by mixing 40% of polymer NOA-65 and 60% nematic liquid crystal preceded by sonication, stirring polymerization processes. Fig. 1 shows an optical texture of PDLC without and with (50 Volt) applying electric field. The threshold and operating voltage, transmission of PDLC were estimated with the help of Voltage Transmittance curve. The 0.1 wt. % of ferroelectric nanoparticles $BatiO_3$ was doped in PDLC. The operating voltage in case of nanoparticles doped in PDLC was 4.5 V smaller than that of PDLC.

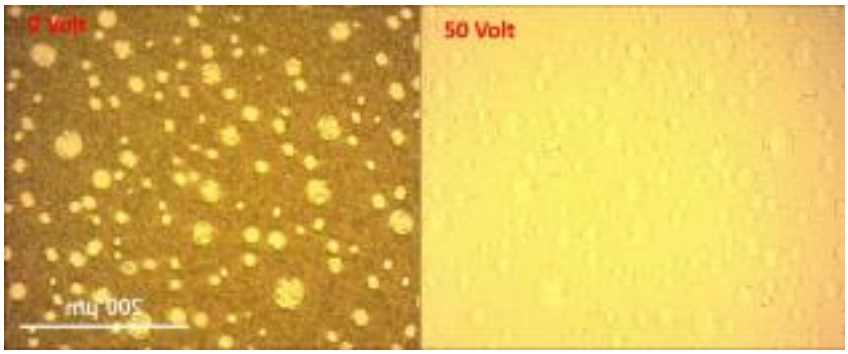

Fig. 1 optical textures of PDLC at 0 Volt and 50 Volt

Keywords- Polymer dispersed liquid crystal (PDLC), NOA 65, Nematic liquid crystals, Eectro optical characteristics

2D Ti_3C_2 MXene: A potential material for photoelectrochemical water splitting application

Mohit Khosya, Mohd. Faraz, and Neeraj Khare*
Department of Physics, Indian Institute of Technology Delhi, New Delhi-110016, India
**Corresponding author email id: mohitkhosyaiitd@gmail.com*

Two-dimensional (2D) materials have attracted significant attention in the field of renewable energy due to their unique electronic properties and high potential for improving the efficiency of energy conversion devices. Among 2D materials, titanium carbide (Ti_3C_2) MXene has emerged as a promising candidate for photoelectrochemical (PEC) water splitting due to its unique layered structure, high electrical conductivity, and excellent PEC activity [1-2]. In this study, we synthesized Ti_3C_2 MXene by etching Ti_3AlC_2 MAX phase with hydrofluoric (HF) acid [3]. The synthesized Ti_3C_2 MXene was then characterized using X-ray diffraction (XRD) and field emission scanning electron microscopy (FESEM). To demonstrate its PEC performance, a Ti_3C_2 MXene photoelectrode was fabricated on a fluorine-doped tin oxide (FTO) substrate. Under light illumination, the photoelectrode exhibited a significantly enhanced photocurrent density of ~2.6 mA/cm^2at 1 V vs. Ag/AgCl. Furthermore, to study the flat band potential and charge transfer behavior of the Ti_3C_2 MXene photoelectrode, Mott-Schottky (M-S) measurements and electrochemical impedance spectroscopy (EIS) have been performed, respectively. The results of these characterizations suggest that Ti_3C_2 MXene is a promising material for the development of high-performance and cost-effective PEC catalysts for water splitting.

Keywords: MXene, Ti_3C_2, 2D material, PEC water splitting

References:

[1] Wei, L., Deng, W., Li, S., Wu, Z., Cai, J., & Luo, J. (2022). Sandwich-like chitosan porous carbon Spheres/MXene composite with high specific capacitance and rate performance for supercapacitors. *Journal of Bioresources and Bioproducts, 7(1)*, 63-72.

[2] Nguyen, V. H., Nguyen, T. P., Le, T. H., Vo, D. V. N., Nguyen, D. L., Trinh, Q. T., Kim, I. T., & Le, Q. V. (2020). Recent advances in two-dimensional transition metal dichalcogenides as photoelectrocatalyst for hydrogen evolution reaction. *Journal of Chemical Technology & Biotechnology, 95(10)*, 2597-2607.

[3] Zhang, S., Zhuo, H., Li, S., Bao, Z., Deng, S., Zhuang, G., Zhong, X., Wei, Z., Yao, Z., & Wang, J. G. (2021). Effects of surface functionalization of MXene-based nanocatalysts on hydrogen evolution reaction performance. *Catalysis Today, 368*, 187-195.

Design low power consumptions CMOS amplifier using Darlington amplifier at nano technology

K.K. Shukla[2], Arvind Tiwari[1], Arunendra Nath Tripathi[3], Vaibhav Srivastava[4]
[1,2]Department of Physics, Maharishi University of Information Technology, Lucknow U.P. India
[4,3]Department of Physics and Electronics, Dr. Ram Manohar Lohiya Awadh University Ayodhya U.P. India
Corresponding author mail id: arvind7800rudra@gmail.com, tripathiarun37@gmail.com

In the presented article, CMOS op-amp has been designed using Darlington pair. The salient features of presented op-amp low power consumptions, high speed, excellent temperature stability, high phase margin, larger bandwidth with high gain, high noise immunity. To design this op-amp gain boosting technology with Darlington pair has been used along with capacitor companions' technique,180 nm technology has been used to design this circuit and its simulation has been done on Cadence Virtuoso software. The detailed result obtained after simulation are as fallows, bandwidth range 6.89 GHz with voltage gain 89db along with power consumptions 36 microwatt with slew rate 996.6V/us and phase margin 65^0 and it can be operated at less than $\pm$ 900 milliwatt. The applications areas of proposed amplifier in the field of wireless communication will prove to be very beneficial because its power consumptions is much less than the amplifier used till now, due to which communication devices can be use long time.

Keywords - Low power consumptions, high speed, Darlington pair, op-amp, temperature stability large bandwidth and high gain**.**

Advances in Synthesis of Novel Magnetic Nanohybrids for Photocatalytic Degradation Applications

Gulfam Ansari[1], Sachin Kumar[2] and Kavita Sharma[1*]
[1]Department of Physics, C.C.S. University, Meerut
[2]Department of Applied Science, SCRIET, C.C.S. University, Meerut
**Corresponding author email id:Sharmak29@gmail.com*

Environmental pollution has become a grave global concern that needs to be embarked upon expeditiously. Industrial developments, urbanization, population growth, agriculture developments, economic growth and deforestation are the leading factors contributed to present environmental crisis. Nowadays the growth of organic contaminants in water sources has been a universal problem. The application of novel technologies for removing water contaminants is constantly being investigated by the researchers. Among various techniques, photocatalytic degradation is a benign solution for purifying water from organic dyes using photocatalysts and light. The widely used metal oxide semiconductor-based nanomaterials are easy to reuse. However to recycle photocatalysts is difficult because of its recovery from aqueous media. In fact, the reusability of photocatalysts is a major concern of industrial applications. The use of magnetic Nanohybrid based photocatalyst can be a promising alternative as they both allow easy recovery by an external magnetic field and demonstrate high degradation efficiency. Magnetic Nanohybrids have magnetic properties which make them easy to recover. The present study provides an extensive snapshot on some of the most recent advancements in the synthetic methods of magnetic nanocomposites. In addition, it outlines the underlying causes in the enhancement of materials performance.

Keywords: Magnetic Nanohybrids, environment pollution, photocatalytic degradation, wastewater treatment

Fundamentals of Microstrip Antennas

Yashashwani K[1] and Sandhya Mann[2]
Dept. of Physics, Agra College, Dr. Bhimrao Ambedkar University, Agra
e-mail: yashibaghel@gmail.com, ssmvinayakvihar@gmail.com

Antennas have undergone many changes depending on their applications over the years. Microstrip Antennas came into use in early 1970s with different features for wireless portable devices. Easy integration and small sized design of microstrip antenna influenced its performance. Microstrip antennas perform in the frequency of > 1 GHz. Microstrip antenna is metallic patch placed on a dielectric material (ε_r) and is supported by ground plane which is placed just below the dielectric plane. Thus they are also called microstrip patch antennas. It can be easily fabricated on a printed circuit board making it most widely used antenna nowadays. The installation of microstrip antenna is very easy due to its small size, low weight and effective cost. Microstrip antennas are low-profile antennas with a two-dimensional flat structure and they offer low-radiation antenna characteristics.

The purpose of this paper is to put together all the basic knowledge of microstrip antennas. The compilation of fundamentals is provided to revise the elementary knowledge of microstrip antennas along with the recent models used till today. The study in this paper carries the reader through the journey of microstrip antenna and it's advancement to the present era thus, catering for new application in the evolving technology. Also the analysis talks about the structure, types of microstrip antennas and feeding methods. The structure of microstrip antenna with the antenna parameters and different shapes of microstrip patch antenna for different applications and function are discussed here. Applications of microstrip patch antenna in various fields are also discussed.

Structural and electrochemical study of Polyethylene Glycol assisted nanostructured ZnO

Jay N. Mishra[1], Uma Sharma[1], Manisha Chauhan[2], Priyanka A. Jha[1], Pardeep K. Jha[1], Prabhakar Singh[1*]
[1]Department of Physics, Indian Institute of Technology (Banaras Hindu University), Varanasi 221005
[2]Department of Chemical Engineering, Ariel University, Ariel, 40700, Israel
**Corresponding author email id: psingh.app@itbhu.ac.in*

ZnO is well known wideband material with a band gap of 3.2 eV, which is being investigated for its wide scale applications in last two decades. The nanostructures varieties give its proper landscape of applications. Earlier, it is observed that the properties of ZnO are texture and thickness dependent. There are various methods to synthesize the nanomaterials using various precursors. In the present work nanostructured Zinc oxide is synthesized by hydrothermal process by using Zinc Nitrate hexa-Hydrate, Ammonium carbonate and Polyethylene Glycol of different molecular weight. We have characterized the structural and electrical properties of Nano powders obtained via hydrothermal process and compared them with the bulk ZnO. The X ray diffractograms confirmed the hexagonal phase formation of the nanoparticles. The structural broadening is visible as compared to the bulk. Thus an increase in stress and strain parameters is anticipated. The band gap and urbach energy were estimated using UV-VIS spectra for the nano powders and bulk sample. From electrochemical studies we have recorded several voltammograms with different scan rates and compared their stability and electrochemical reversibility in order to make a comparative of bulk and nano particles.

Keywords: Hydrothermal process; electrochemical reversibility; voltammograms; Urbach energy; Nanostructure

DNA Guardians: Topoisomerase IA Cleavage Mechanism Explored

Muralidhar, Rakesh Kumar Tiwari*
Department of Physics, DDU Gorakhpur University, Gorakhpur
**Corresponding author email id: drrkt@yahoo.com*

Topoisomerase IA (Topo IA), a mesmerizing enigma in the realm of molecular biology, orchestrates a captivating ballet with DNA. Employing the artistry of molecular dynamics (MD) simulations, we embark on an enchanting journey deep into the heart of Topo IA's conformational landscape, where its mastery of artificial DNA strand cleavage takes center stage. In this study, we employ molecular dynamics (MD) simulations to elucidate the pivotal role of Topoisomerase IA (Topo IA) in artificial DNA strand cleavage. Our findings provide critical insights into the enzyme's function in maintaining genomic stability by strategically managing DNA topology without causing double-strand breaks. This research not only enhances our understanding of Topo IA mechanism but also holds promise for potential therapeutic applications, especially in cancer research.

Keywords: Topoisomerase IA, MD simulations, DNA cleavage, genomic stability.

References:

[1] Tan,K.;Cao, N.;Cheng, B.; Joachimiak, A.; Tse-Dinh, Y.-C. Insights from the structure of Mycobacterium tuberculosis Topoisomerase I with the Novel Protein Fold.J.Mol.Biol.2016,428,182-193.
[2] Pommier Y (2013). "Drugging topoisomerases: lessons and challenges". *ACS Chem. Biol*. 8 (1): 82-95.
[3] Wang JC (June 2002). "Cellular roles of DNA topoisomerases: a molecular perspective". *Nat. Rev. Mol. Cell Biol*. 3 (6):
[4] Dutta Dubey, K.; Dutta Dubey,K.; Kumar Tiwari, R., & Prasad Ojha, R. (2013) 'Recent Advances in Protein−Ligand Interactions: Molecular Dynamics Simulations and Binding Free Energy Current Computer-Aided Drug Design, 9(4), 518-531. Bentham Science Publishers.
[5] Dubey, K. D., & Ojha, R. P. (2012). Conformational flexibility, binding energy, role of salt bridge and alanine-mutagenesis for c-Abl kinase complex. Journal of Molecular Modeling, 18, 1679–1689.

In silico investigation on interaction of small Ag_6 nano-particle cluster with tyramine neurotransmitter

T. Yadav[1*], R. Mishra[1], E. Shakerzadeh[2], F. P. Pandey[3]
[1]Department of Basic Sciences, IES Institute of Technology and Management, IES University, Bhopal (M. P.)
[2]Chemistry Department, Faculty of Science, Shahid Chamran University of Ahvaz, Ahvaz, Iran
[3]Scitechesy Research and Technology Private Limited, Central Discovery Center, Banaras Hindu University, Varanasi (U.P.), India
**Corresponding author email id: tarunyadavbly@gmail.com*

The interaction of tyramine neurotransmitter with silver nano-particle (Ag_6) cluster is explored in terms of the molecular structure, electronic properties and NBO analysis of tyramine AgNPs bio-molecular conjugate. The adsorption mechanism of tyramine onto the Ag_6 cluster has been investigated through computing of the electronic and geometrical properties in addition to the adsorption energies in various possible configurations. The magnitude of adsorption energy corresponding to the most favorable tyramine-Ag_6 bio-molecular conjugate has been computed to be -14.36 kcal/mol in the gas phase, which infers a good adsorption of tyramine with AgNPs cluster suggesting the practical applications of tyramine-AgNPs bio-molecular conjugates in bio-sensing, drug delivery, bio-imaging and other applications. Different electronic properties such as the energy gap of HOMO-LUMO, Fermi level and work function have been investigated in detail. Moreover, the effect of aqueous media on adsorption energy and electronic properties of the most favorable tyramine-AgNPs bio-molecular conjugate is investigated in order to understand the impact of the real biological situation.

Keywords: DFT, Tyramine, AgNPs, NBO, Adsorption mechanism.

Synthetization and Characterization of g-C_3N_4:ZnO:CdO nanocomposite for gas sensing applications

Akash Rawat, Shailesh Kumar Pandey, L. P. Purohit*
Semiconductor Research Laboratory, Department of Physics, Gurukula Kangri (Deemed to be University), Haridwar, India
**Corresponding author email id: proflppurohitphys@gmail.com*

The g-C_3N_4-TiO_2-Co_3O_4nanocomposite was successfully synthesized via the sol-gel hydrothermal method. The sample was then characterized by employing XRD, FE-SEM, EDX, and UV visible spectroscopy for their structural, morphological, surface, and optical properties. On the formation of the nanocomposite, the absorption edge increased, and the blue shift in the band gap was observed. The XRD results show that the nanocomposite is highly crystalline. The UV-vis spectroscopy results show that the nanocomposite has a broad absorption spectrum, which makes it potent for absorbing a wide range of wavelengths in the visible region. The FESEM results show that the nanocomposite has a high surface area with metal oxide nanoparticles embedded in g-C_3N_4 nanosheets with rough surfaces.The EDX results show that the nanocomposite is composed of C, N, O, Ti, and Co elements. The g-C_3N_4 -TiO_2-Co_3O_4 nanocomposite is a promising new material with the potential to be a valuable tool for environmental remediation as it degrades 99 % of pollutants in 80 minutes under visible light.

Keywords: Hydrothermal; g-C_3N_4; Photocatalysis; ZnO; Nanocomposite.

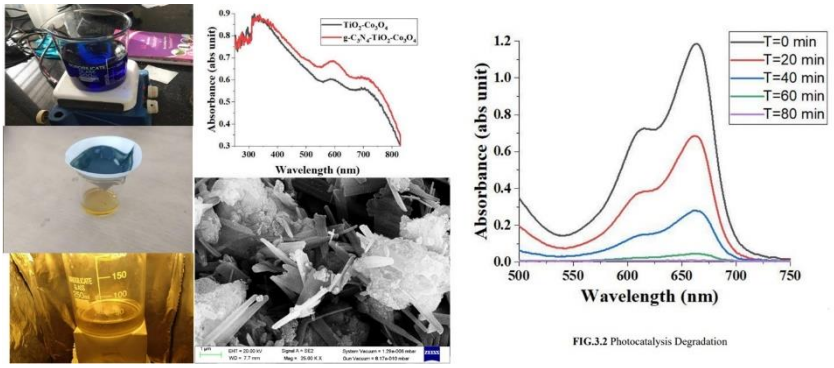

Graphical Abstract

Hierarchical α-MoO_3: A versatile eco-friendly material for humidity assisted ammonia sensing and efficient catalytic activity in wastewater treatment

Atul Kumar*, Pratima Chauhan
Advanced Nanomaterials Research Laboratory, U.G.C. Centre of advanced studies, Department of Physics, University of Allahabad, Prayagraj-211002, India
*Corresponding author email id: atulkumar@allduniv.ac.in

In this work, a facial synthesis of α-MoO_3 nanoparticles was done by chemical co precipitation method. The synthesized α-MoO_3 nanomaterials have been reported for sensing and photocatalysis applications together. For sensing, the α-MoO_3 was coated on FTO based interdigitated electrodes, and the prepared sensor was tested for numerous concentrations of ammonia (100-600 ppm) under different relative humidity levels (11% - 33% - 56% - 75% - 95% RH). The response and recovery time of α-MoO_3 based sensor for 500 ppm of NH_3 were 8 s and 11 s under 95% RH, respectively. The prepared α-MoO_3 based sensor exhibits high selectivity and stability towards ammonia. To analyze the photocatalytic activity of prepared α-MoO_3 nanoparticles, the photodegradation of methylene blue (MB) and methyl orange (MO) under visible light irradiation was studied. The first-order reaction rate constant for MB dye is 0.02434 min^{-1}, and for MO dye is 0.01111 min^{-1}. Finally, the maximum degradation efficiency for MB and MO dyes was calculated to be 95% and 73%, respectively. The given data conclude that the synthesized α-MoO_3 nanoparticles can be used as an effective NH_3 sensor as well as an efficient photocatalyst in organic dye degradation.

Keywords: α-MoO_3, Co-precipitation, NH_3 Sensing, Photocatalyst, Nanoparticles.

Composition dependent variation in structural, morphological, optical and magnetic properties of biogenic CuO/NiO bimetallic nanoparticles

Shalu Yadav*, Ankit Singh, Abhay Kumar Choubey
Department of Sciences and Humanities, Rajiv Gandhi Institute of Petroleum Technology, Jais, Amethi-229304, India
**Corresponding author email id:20bs0009@rgipt.ac.in*

A series of CuO/NiO nanoparticles with different Cu and Ni precursor concentrations represented as N12 (1:2), N22 (1:1) and N21 (2:1) (Cu:Ni) were produced by modified green solution combustion route using Moringa oleifera leaves extract as an organic fuel for the first time. The prepared CuO/NiO nanoparticles were analytically characterized using UV-Vis diffuse reflectance spectroscopy (UV-DRS), X-ray diffractometry (XRD), X-ray photoelectron spectroscopy (XPS), Brunauer-Emmett-Teller analysis (BET), field-emission scanning electron microscopy (FE-SEM), high-resolution transmission electron microscopy (HR-TEM), and vibrating sample magnetometry(VSM). Morphological studies showed uniform and monodisperse nanoparticles having average grain size of 34 nm for N22 nanoparticles while the N12 and N21 compositions showed uniform nanoparticles with the grain size of 12 nm and22 nm respectively. The existence of CuO and NiO phases in nanoparticles was verified by XPS analysis. N12, N22 and N21 had band gaps in the range of 2.19-2.49 eV and specific surface area in the range of 4.92-11.2 m2/g. The magnetization vs applied magnetic field plots for bimetallic nanoparticles showed unusual feeble ferromagnetic behaviour. The coercivity (Hc) and saturation magnetization (Ms) reached a maximum value for N22 (130 Oe and 0.133 emu/g). These biogenic nanoparticles could be a strong choice for biological applications due to their soft ferromagnetic behaviour and biocompatibility.

Keywords: CuO/NiO nanoparticles, Green solution combustion, XRD analysis, Weak ferromagnetism

References:

[1] Hassanpour, M., Safardoust, H., Ghanbari, D., Salavati-Niasari, M., (2016). Microwave synthesis of CuO/NiO magnetic nanocomposites and its application in photo-degradation of methyl orange. Journal of Materials Science: Materials in Electronics, 27, 2718—2727.

[2] Sankaranarayanan, S., Hariram, M., Vivekanandhan, S. and Ngamcharussrivichai, C., (2022). Biosynthesized transition metal oxide nanostructures for photocatalytic degradation of organic dyes. In Micro and Nano Technologies, Green Functionalized Nanomaterials for Environmental Applications, Elsevier. pp. 417-460.

Antibiofilm activity of Lemongrass extract against *Staphylococcus aureus* bacterial biofilm

Reema Singh[1], Manish Gaur[1], Awadh Bihari Yadav[1]*
[1]Centre of Biotechnology, University of Allahabad, Prayagraj-211002, U.P., India
**Corresponding author email id: awadhyadav@allduniv.ac.in*

Background: Antimicrobial resistance (AMR) developed by a pathogen to help it to survive in an unfavourable environment or developed resistance against antibiotics.AMR due to many factors such as mutation, overuse of antibiotics, gene transfer and biofilm formation by bacteria. The biofilm are defensive coverings formed by bacteria to shield themselves from hostile environments. These communities adhere to surfaces and are enclosed in protective substances. Lemongrass (*Cymbopogon citratus*) was investigated for its antimicrobial and antibiofilm properties in vitro. The study aimed to determine if lemongrass could be a potential alternative therapy for reducing biofilm formation and countering antimicrobial effects.

Methods: Lemongrass was dried and crushed to form a powder and dissolved in different solvents (methanol, ethanol, ethyl acetate, and water) to extract different components using a Soxhlet apparatus. The samples were dried under reduced pressure using a rotary evaporator. The antimicrobial and antibiofilm activities of these extracts were assessed using an agar diffusion assay and the crystal violet staining method.

Results: The extract collected by the Soxhlet apparatus using different solvents showed biofilm inhibition and disruption both activity against *S. aureus* biofilm. The biofilm inhibition by methanolic extract 95%, ethanolic extract 91%,ethyl acetate 86%, and aqueous extract 86%. The biofilm disruption by methanolic extract 97%, ethanolic extract 95%, and aqueous extract 83%.

Conclusion: The present study concluded that the lemongrass extract was showing biofilm inhibition as well as biofilm disruption activity against *S. aureus* biofilm.

Keywords: Biofilm, *Cymbopogon citratus*, Crystal violet staining.

References:

[1] Sánchez, E., Morales, C. R., Castillo, S., Leos-Rivas, C., García-Becerra, L., & Martínez, D. M. O. (2016). Antibacterial and antibiofilm activity of methanolic plant extracts against nosocomial microorganisms. *Evidence-based complementary and alternative medicine: eCAM, 2016*.

[2] Balducci, E., Papi, F., Capialbi, D. E., & Del Bino, L.(2023). Polysaccharides' Structures and Functions in Biofilm Architecture of Antimicrobial-Resistant (AMR) Pathogens. *InternationalJournal of Molecular Sciences, 24*(4), 4030.

Black Tea mediated Green Synthesis of Copper Nanoparticles and their Photo Catalytic and Antioxidant Properties

Sonam Mishra*, Ravindra Dhar
Centre of material sciences IIDS, University of Allahabad, Prayagraj
Corresponding author email id: sonam14989@gmail.com

The present work focuses on black tea-mediated green synthesis of copper nanoparticles (CuNPs). Biosynthesized CuNPs are characterized by X-ray diffraction, UV-visible absorption, Raman spectroscopy, and FTIR spectroscopy. X-ray diffraction patterns corroborate the non-crystalline nature of CuNPs, and FTIR spectra confirm the presence of different functional groups that are associated with CuNPs. Further photocatalytic activity of CuNPs was investigated against methylene blue in the presence of sun light at different times. Moreover, the antioxidant activity of CuNPs was analyzed and systematically compared with standard vitamin C. The results obtained are very encouraging.

Key words: CuNPs, green synthesis, Antioxidant, photo catalytic activity

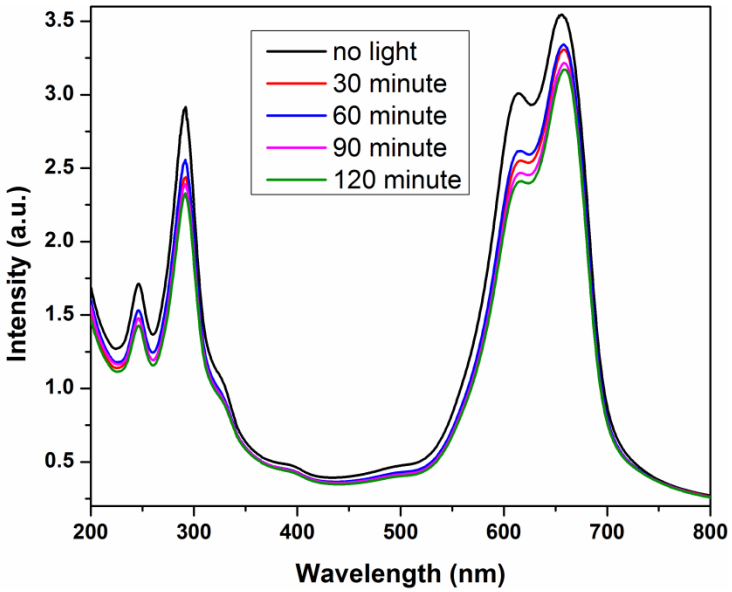

Fig. 1: Photo catalytic activity of CuNPs.

Hydrothermal production of irregular α-V_2O_5nanodiscs for extremely responsive and selective ethanol sensors

Surya Prakash Singh and Pratima Chauhan
Advanced Nanomaterials Research Laboratory, U.G.C. Centre of Advanced Studies, Department of Physics, University of Allahabad, Prayagraj-211002, India.
E-mail: *sps.phd2021@allduniv.ac.in**, *mangu167@yahoo.co.in*

The current study provides a straightforward and template-free hydrothermal method for the synthesis of nanodiscs like vanadium pentoxide (V_2O_5) nanostructures and their prospective usage as materials for ethanol gas detection. The orthorhombic phase of highly crystallized $V_2O_5$is confirmed by XRD investigation. The morphological characteristics of the V_2O_5 were studied using FESEM approaches. The chemical structure and bond analysis of V_2O_5have been analyzed using FTIR analysis. The chemical structure and bond analysis of V_2O_5 have been analyzed using FTIR analysis. EDX elemental spectroscopy has been used to explore the fundamental chemical constitution of V_2O_5. The sensing capacities of the V_2O_5 sensor have been evaluated at room temperature in an atmosphere of ethanol vapor. The prepared V_2O_5based sensor revealed impressive ethanol selectivity over other VOCs (including methanol, acetone, isopropanol, and toluene) with a sensing response of 74.88% toward 1000 ppm at room temperature (30 ^{0}C). The results reveal that the V_2O_5-based sensor works effectively in ethanol, with rapid response and recovery times of 36 and 12 seconds, respectively, at room temperature.

Sustainable Nanotechnology: Green Synthesis Strategies for Cost-Effective Aluminum Oxide Nanoparticles and Their Multifaceted Applications: A Comprehensive Review"

Sapna Chahar*, Neera Sharma
Department of Physics, Agra College, Agra
**Corresponding author email id: Chaharsam66@gmail.com*

Aluminum oxide nanoparticles (Al_2O_3 NPs) have gained popularity as adaptable materials with a variety of uses in numerous fields of science and technology. Within this comprehensive review article, we delve into the various techniques employed for the synthesis of Aluminum oxide nanoparticles. Our main goal is to find low-cost, environmental friendly ways to make these nanoparticles, with the final goal of making their commercial synthesis more accessible. Upon close examination, our review reveals that green synthesis methods for Aluminum oxide nanoparticles outshine traditional chemical approaches. This environmentally conscious synthesis route not only yields Aluminum oxide nanoparticles at a high rate but also does so at a significantly reduced cost, while also posing no harm to the environment.

Furthermore, this review article provides a comprehensive overview of the myriad applications of Aluminum oxide nanoparticles, offering insights into their diverse utility in various fields.

Key words: Aluminum oxide nanoparticles (Al_2O_3 NPs), green synthesis, applications

Study the structural, chemical and optical properties of Hydroxyapatite synthesized via Sol-Gel Method for Biomedical Applications

Ravi Kumar Pandey, R. K. Shukla*
Department of Physics, University of Lucknow, Lucknow – 226007
**Corresponding author email id: rajeshkumarshukla_100@yahoo.co.in*

The field of biomaterials has undergone remarkable advancements over recent decades, leading to the development of bioactive materials capable of triggering specific and predictable cellular and tissue responses. Among these bioactive materials, Hydroxyapatite (HA), a calcium phosphate compound renowned for its exceptional biocompatibility and bioactivity, stands out as a promising candidate for various biomedical applications. Utilizing the versatile and precise sol-gel method, we synthesized HA with customized properties, subjecting the material to three distinct temperature treatments at 700°C, 800°C and 900°C in an effort to enhance its crystallinity. In order to study the HA, morphological, structural, chemical and optical properties by using scanning electron microscopy (SEM), X-ray diffraction (XRD), Fourier transform infrared (FTIR) and UV-visible spectroscopic technique. More elaborative discussions on experimental techniques, findings and their implications will be presented.

Keywords: X-Ray Diffraction, SEM, FTIR, Bioactivity, Biocompatibility.

References:

[1] Weng W, Shen G, Han G, 2000. Low temperature preparation of hydroxyapatite coatings on titanium alloy by a sol-gel route, Materials Science Letters, Vol. 19, pp. 2187- 2188.
[2] Agrawal K, Singh G, Puri D and Prakash S (2011). Synthesis and Characterization of Hydroxyapatite Powder by Sol-Gel Method for Biomedical Application. Journal of Minerals & Materials Characterization & Engineering, Vol. 10, No.8, 727-734.
[3] Weng W, Zhang S,Cheng K,Qu H,Du P,Shen G,Yuan J,Han G, 2003. Sol– gel preparation of bioactive apatite films, Surface and Coatings Technology, Vol. 167, pp. 292-296.
[4] Choi D,Marra K,Kumta P.N., 2004. Chemical synthesis of hydroxyapatite/poly (caprolactone) composite, Materials Research Bulletin, Vol. 39, pp. 417-432.
[5] Haddow DB, James PF, Van Noort R, 1998.Sol-gel derived calcium phosphate coatings for biomedical applications, Journal of Sol-Gel Science and Technology, Vol. 13, pp. 261-265.
[6] Chai CS, Ben-Nissan B, Pyke S, Evans L, 1995. Sol-gel derived hydroxyapatite coatings for biomedical applications, Materials and Manufacturing Processes, Vol. 10, pp. 205-216.

The effect of ceramic nanofillers on conductivity and ion-transport behaviour in potato starch based solid bio-polymer electrolyte

Jyoti Rai*, Manindra Kumar
Department of Physics, D.D.U. Gorakhpur University, Gorakhpur- 273014, Uttar- Pradesh, INDIA
*Corresponding author email id: *jyoti.deoria1008@gmail.com*

A solution casting technique was used to synthesize nanocomposite solid polymer electrolytes, which consist of potato starch (PS) as the host polymer, sodium iodide (NaI) as an ion source, and cobalt ferrite ($CoFe_2O_4$) nanoparticles as ceramic nanofillers. Techniques such as electrical impedance spectroscopy (EIS)(Kumar et al., 2012),FTIR deconvolution technique(Arof et al., 2014),linear sweep voltammetry (LSV) and cyclic voltammetry (CV)(Abdulwahid et al., 2023;Yadav et al., 2018) were employed to characterize the nanocomposite solid polymer electrolyte. With the help of EIS, the highest conductivity is achieved $8.13x10^{-3}$ S/cm for the system containing 1.0 wt.% of $CoFe_2O_4$ceramic nanofillers. Ceramic nanofillers enhance ion motion within the polymer matrix, thereby increasing the conductivity of the electrolyte.In order to determine the parameters of ion transport, such as mobility (μ), carrier density (n), and the diffusion coefficient (D), deconvoluted FTIR spectra were used to compute the free ions, and contact ion pairs. The results of LSV and CV suggest that the current material has the potential to be utilized in electrochemical devices. The specific capacitance (C_{sp}) of the electrode using CV at a scan rate of 5V/s is found to be 2.09F/g.

Keywords: Potato starch, EIS, Linear sweep voltammetry, Cyclic voltammetry.

References:

[1] Abdulwahid, R. T., Aziz, S. B., & Kadir, M. F. Z. (2023). Environmentally friendly plasticized electrolyte based on chitosan (CS): Potato starch (PS) polymers for EDLC application: Steps toward the greener energy storage devices derived from biopolymers. Journal of Energy Storage, 67(February), 107636. https://doi.org/10.1016/j.est.2023.107636

[2] Arof, A. K., Amirudin, S., Yusof, S. Z., & Noor, I. M. (2014). A method based on impedance spectroscopy to determine transport properties of polymer electrolytes. Physical Chemistry Chemical Physics, 16(5), 1856–1867. https://doi.org/10.1039/c3cp53830c

[3] Kumar, M., Tiwari, T., & Srivastava, N. (2012). Electrical transport behaviour of bio-polymer electrolyte system: Potato starch + ammonium iodide. Carbohydrate Polymers, 88(1), 54–60. https://doi.org/10.1016/j.carbpol.2011.11.059

[4] Yadav, M., Kumar, M., & Srivastava, N. (2018). Supercapacitive performance analysis of low cost and environment friendly potato starch based electrolyte system with anodized aluminium and teflon coated carbon cloth as electrode. Electrochimica Acta, 283, 1551–1559. https://doi.org/10.1016/j.electacta.2018.07.060

Effect of oxygen partial pressure on PLD deposited $Hf_{0.95}Y_{0.05}O_2$ oriented thin films

Mangla Nand[1,2,*], S. N. Jha[2], Shilpa Tripathi[1], Yogesh Kumar[1], Himal Bhatt[3], Satish K Mandal[4,5], Mukul Gupta[6]
[1]Beamline Development and application section, Bhabha Atomic Research Centre, Mumbai, 400085, India
[2]Homi Bhabha National Institute, Anushaktinagar, Mumbai 400094, India
[3]High Pressure & Synchrotron Radiation Physics Division, Bhabha Atomic Research Centre, Mumbai 400085, India
[4]Surface Physics and Material Science Division, Saha Institute of Nuclear Physics Kolkata, 1/AF Bidhannagar, Sector 1, Kolkata 700064, India
[5]Solid State Physics Division, Bhabha Atomic Research Centre, Mumbai 400085, India
[6]UGC-DAE Consortium for Scientific Research, University Campus, Khandwa Road, Indore 452017, India.
[*]*Corresponding author email id: kappu001@gmail.com*

Oriented thin films of$Hf_{0.95}Y_{0.05}O_2$ on YSZ(100) substrate were prepared at different oxygen (O_2) partial pressures (100, 70, 30, and 10 sccm) using pulsed laser deposition(PLD) technique. The Fourier Transform Infrared (FTIR) spectroscopy, X-ray diffraction (XRD), and Soft X-ray Absorption Spectroscopy (SXAS) characterization techniques were utilized to investigate the effect of oxygen partial pressure on crystalline and local electronic structure of thin films. The out of plane XRD results show that the thin films are in monoclinic phase and all the films are oriented in (002) direction. The FTIR results also confirm the monoclinic phase with a small change in vibrational properties with change in oxygen partial pressure. The elemental composition of all the thin films was determined by the X-ray photoelectron spectroscopy (XPS). The XPS results confirm the 4^+ oxidation states of Hf in all the thin films. The composition changes with larger incorporation of Y as the O_2 partial pressure changes from 100 sccm. The SXAS O K-edge analysis show that the hybridization of O 2*p* orbitals with metal 5*d* orbitals changes with change in deposition pressure. The intensity of crystal field split e_g and t_{2g} peaks varies with oxygen partial pressure. The results enlighten a deeper understanding of crystalline and local electronic structure of technologically important Y doped HfO_2 films used for dielectric applications in microelectronic industry.

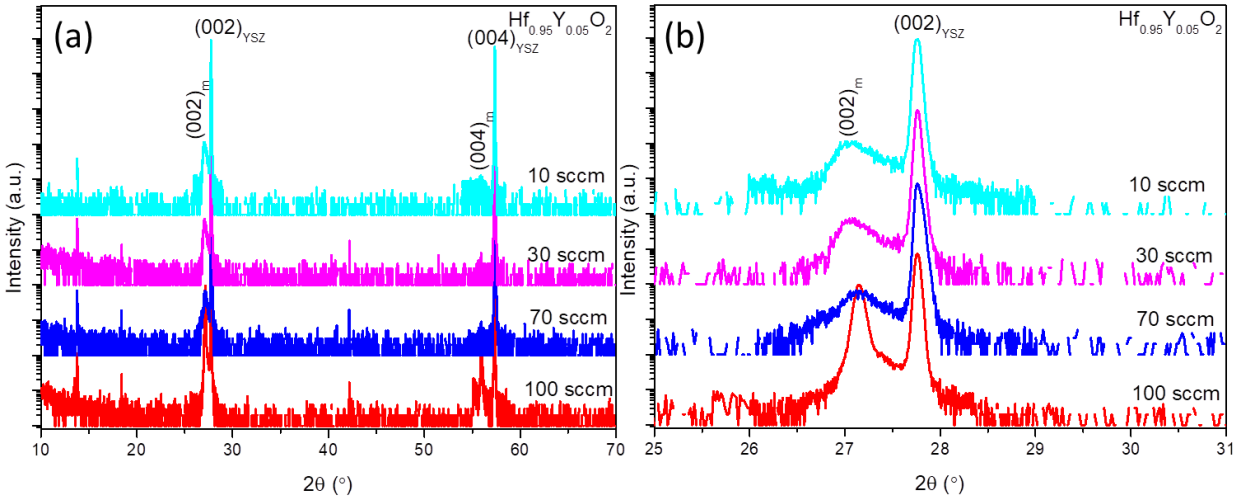

Figure-1: *(a) The out of plane ω-2θ XRD pattern of all the thin films. (b) The zoomed graph showing the enlarge view of (002) film peak close to substrate peak.The plots at different oxygen partial pressure are vertically shifted for the clarity.*

A Eu^{3+}doped functional core-shell nanophosphor as fluorescent biosensor for sensitive detection of dsDNA

Arpita Dwivedi[1*], S. K. Srivastava[1]*

[1] Department of Physics, Institute of Science, Banaras Hindu University, Varanasi-221005, India

**Corresponding author email id: joinarpit@gmail.com,sanjay, itbhu@yahoo.com*

The revealing aspect of qualitative and quantitative presence of biological markers alongside other analytes, including DNA, proteins, and carbohydrates, can indicate disease states and physiological progressions. Sensitive and accurate detection of these at low levels has the unique advantage of potentially being used for identifying the earliest sign of cancer, TB, HIV, malaria, and other disorders [1,2, 3]. Lanthanide-doped core-shell nanomaterials have illustrated budding potential as luminescent materials, but their biological applications have still been very limited due to their aqueous solubility and biocompatibility. Hence, in present work we have reported a simple method for the synthesis of chitosan functionalized lanthanoid based core shell (Ca-Eu:Y2O3@SiO2) phosphor. The chitosan functionalized Ca Eu:Y2O3@SiO2 phosphor contains hydroxyl, and amino groups which coordinate with the dsDNA and causes fluorescence enhancement and act as "turn on" sensor Fig. 1(a). The ratio of fluorescence intensity enhancement of phosphor is proportional to the concentration of dsDNA. The range 0.1–90 nM, with the limit of detection at ~16.1 pM under optimal experimental conditions Fig. 1(b). The enhancement in fluorescence response of functionalized core-shell phosphor with dsDNA is due to the antenna effect. Additionally, response of probe has been studied for the real samples.

Keywords: Core-shell, Fluorescence, dsDNA detection

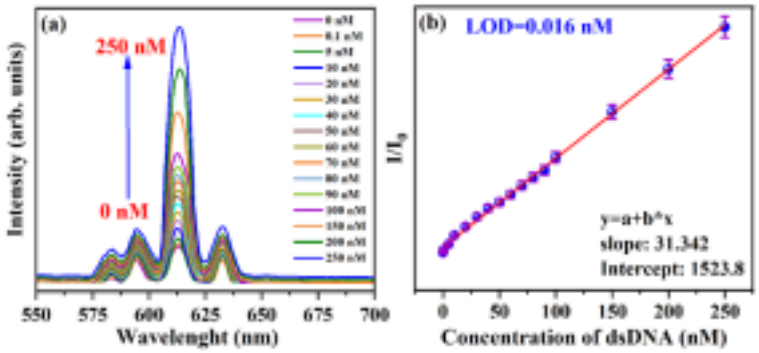

Fig. 1(a) *Photoluminescence spectra of CEY@SiO_2-chitosan functionalized core-shell phosphors in the presence of different concentrations of dsDNA* ***(b)*** *curve is the characteristic peak emission intensity at different concentrations.*

References:

[1] S. Godavarthi, K. Mohan Kumar, E. Vázquez Vélez, A. Hernandez-Eligio, M. Mahendhiran, N. Hernandez Como, M. Aleman, L. Martinez Gomez, Nitrogen doped carbon dots derived from Sargassum fluitans as fluorophore for DNA detection, Journal of Photochemistry and Photobiology B: Biology, 172 (2017) 36-41.

[2] T. Arslan, O. Güney, Ratiometric sensor based on imprinted quantum dots-cationic dye nanohybrids for selective sensing of dsDNA, Analytical biochemistry, 591 (2020) 113540.

[3] B.T. Murti, A.D. Putri, S. Kanchi, M.I. Sabela, K. Bisetty, Inamuddin, A.M. Asiri, Light induced DNA functionalized TiO2 nanocrystalline interface: Theoretical and experimental insights towards DNA damage detection, Journal of Photochemistry and Photobiology B: Biology, 188 (2018) 159-176.

Structural, optical and electrical properties of $CaSnO_3$ and $Ca_{0.98}Nd_{0.02}Sn_{0.98}Ti_{0.02}O_3$ synthesized using Sol-Gel method

Gulab Singh[1*], Aditya Kumar[2], Ajaj Hussain[3], P.P. Singh[2], Upendra Kumar[3], Manoj K Singh[4]
[1]Department of Physics, Feroze Gandhi College, Raebareli,229001 U.P, India
[2]Department of Applied Sciences and Humanities Inverits University, Bareilly, 243123, U.P., India
[3]Department of Physics, University of Lucknow, Lucknow, 226007, U.P, India
[3]Advanced Functional Materials Laboratory, Department of Applied Sciences, IIIT Allahabad, Prayagraj, 211015, U. P., India
[4]Center of Material Science, University of Allahabad, Prayagraj, U. P 211002, India
[*]*Corresponding author email id: gulabau08@gmail.com*

Due to its dielectric, semiconducting, and optical characteristics, the perovskite type structure of alkaline earth stannates materials ($XSnO_3$, X= Sr^{2+}, Ca^{2+}, and Ba^{2+}) has drawn attention from around the globe [1, 2]. The sol-gel method was used to create the single phase samples of $CaSnO_3$ and $Ca_{0.98}Nd_{0.02}Sn_{0.98}Ti_{0.02}O_3$, which were then calcined at 800°C. At ambient temperature, the samples were discovered to have a single phase polycrystalline orthorhombic perovskite structure with space group Pbnm (D_{2h}^{16}). Furthermore, when the temperature rises, these perovskites materials experience a number of structural phase changes, including the rotation of BO_6 octahedra around the three O-B-O crystallographic axes [3]. The X-ray diffraction pattern of both samples show it crystallized into similar crystal structure. The dielectric loss (tan-δ) and dielectric constant (ε') of the $CaSnO_3$ nanomaterial were measured at room temperature in the frequency range of 100 Hz to 1 MHz. In the frequency range of 100 Hz to 1 MHz, the dielectric constant (ε') value was determined to be around 31 to 24. In the same frequency range, samples' tangent losses (tan-δ) were likewise discovered to be between 0.2 and 0.005 at the same moment. The findings showed that when frequency increases, the dielectric constant and tangent loss decrease. The Maxwell-Wanger mechanism for the contributing polarisation may be used to explain this fluctuation in ε' and tan-δ. The room temperature reflection spectra of the $CaSnO_3$ and $Ca_{0.98}Nd_{0.02}Sn_{0.98}Ti_{0.02}O_3$ nanoparticles recorded in the wavelength range of 200–800 nm. For $CaSnO_3$ and $Ca_{0.98}Nd_{0.02}Sn_{0.98}Ti_{0.02}O_3$ nanoparticles, respectively, the band gap (Eg) values were 4.17 eV and 4.07 eV. The UV Vis. Studies of samples show minimum reflectance in UV-range and higher in visible to NIR range, which makes it suitable for UV-filter and sensor application.

Keywords: $CaSnO_3$, sol-gel, dielectric constant, band gap.

Study on Sm^{3+} modified $0.60Bi_{1-x}Sm_xFeO_3–0.40PbTiO_3$ multiferroic solid solutions

Anand Kumar Maurya[1] and Anar Singh[1]*
Department of Physics, Faculty of Science, University of Lucknow, Lucknow-226007, India
**Corresponding author email id: manand0174gmail.com*

The system (1-y)$BiFeO_3$–y$PbTiO_3$exhibits a very large tetragonal spontaneous lattice strain (c/a -1) of 0.18, hence it can be a suitable system for increase piezoelectric properties[1,2].In the literature it is reported that in BF-yPT, doping of rare earth Smat Bi site increases the piezoelectric properties than La because as compared with La^{3+}, Sm^{3+} has a smaller ionic radius than Bi^{3+}.In this work, we have studied of $0.6Bi_{(1-x)}Sm_xFeO_3$-0.4$PbTiO_3$system(were x= 0, 0.03, 0.05, 0.07, 0.10, 0.20). The used method of preparation of sample was solid state reaction method. We have taken precursors in the stochiometric amount and mixed them properly in the mixing media. We have calcined mixed powders at 760°Cfor 6 hours which has been optimized for this solid solutions. Polyvinyl alcohol (PVA) has been added as binder to make pellets which has been evaporated after heating at 500^0C for 10 hours. The sintering was carried out at 850°C for 4 hours in the closed environment to minimize the loss of Bi and Pb. The phase formation and purity of the samples were checked by employing X-ray diffraction technique. Rietveld refinement was carried out with the help of Full prof software to analyze the crystal structure of these modified solutions. For x=0, we observed the occurrence of tetragonal phase with space group P4mm. As we increased doping, crystal structure changes from tetragonal to cubic phase. For x= 0.03, 0.05, 0.07, we found mixed phases of tetragonal (P4mm) and cubic (Pm-3m) where the phase fraction of tetragonal phase decreases with increasing x. On further increasing x beyond 0.70, we found single cubic phase (Pm-3m) at x≥0.10.The ferroelectric, piezoelectric and magnetic properties of the Sm doped 0.60BF-0.40PT will be carried out to understand the role of rare earth doping on these properties in this solid solutions.

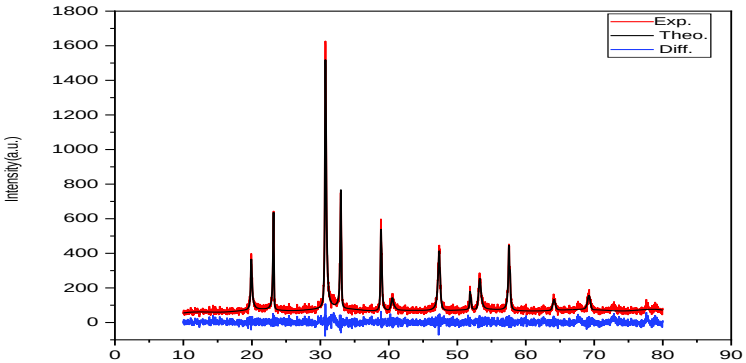

Figure 1.Rietveld refined XRD diffraction pattern of undoped 0.6BF-0.4PT.

Keywords: Rietveld refinement, piezoelectricity.

References:

[1] Fedulov, S. A., Ladyzhinskii, P. B., Pyatigorskaya, I. L. &Venevetsev, Yu. N. Complete phase diagram of the PbTiO3-BiFeO3 system. Sov. *Phys. Solid State***6**, 375–378 (1964).

[2] Comyn, T. P. et al. Phase-specific magnetic ordering in BiFeO3− PbTiO3. *Appl. Phys. Lett.* **93**, 232901 (2008).

Fabrication of sputtered deposited copper-doped ZnO thin filmsforphotodetector application

Manohar Singh*, Beer Pal Singh
Nano Laboratory, Department of Physics, CCS University, Meerut -250004, India.
**Corresponding author email id: manoharvimalrajpoot@gmail.com*

The reactive co-sputtering process was employed in this work to create pureand copper-doped zinc oxide (CZO) thin films with varying copper (Cu) concentrations. The influence of Cu doping on the structural, optical, hydrophobicity, and electrical properties of ZnO thin films was investigated using X-ray diffraction (XRD), Field emission scanning electron microscope (FESEM), energy-dispersive X-ray spectroscopy (EDX), UV-Vis spectroscopy, spectroscopic ellipsometry (SE), contact angle, and current-voltage graph measurements. XRD and SEM confirmed the increase in crystallite and grain size of ZnO with increasing concentrations of Cu. UV-Vis spectroscopy revealed a red shift in the band gap for CZO thin films as Cu concentrations increased.I-V measurements revealed that Cu doping decreasedthe electrical resistance or resistivity of the ZnO thin film.Thesedeposited thin films were used to createaphotodetector(PD) basedon CZO/n-SiandUZO/n-Si junctions by establishing silver (Ag) contact on both sides of the device. Various visible light intensities examined the photosensitivity of UZO/n-Si and CZO/n-Si-based PD.

Keywords: Zinc Oxide,Ellipsometry, Reactive-co-sputtering, Electric-resistivity, Photodetector.

Systematics Study for Tidal Waves in ^{102}Pd

A. Choudhary[1,*] V. Kumar[1], Y. P. Singh[1], Gobind Ram[1], A. Shukla[1], Manoj Kumar Sharma[1], P. Jain[2], and Y. Kumar[3]

[1]Department of Physics, University of Lucknow, Lucknow-226007, India

[2]Department of Physics, Sri Aurobindo College,
University of Delhi, Malviya Nagar, New Delhi-110017, India

[3]Department of Physics, Hansraj College, University of Delhi, Malka Ganj, New Delhi-110007, India

**Corresponding author email id:* annu9602881091@gmail.com

Theoretically predicted the tidal wave in mass A ~ 100, based on the calculations with shell correction version of the Tilted Axis Cranking model [1]. One of the experimental features of tidal wave is the B(E2) value decreasing with increasing spin. The B(E2) values of the yrast states of ^{102}Pd were measured in two lifetime experiments, both are contradictory results. Firstly showed that B(E2) values increasing with spin and claim tidal wave behaviour [2]. Another one showed that B(E2) values decreasing with spin and rule out the tidal behaviour [3]. Also a similar contradiction was observed in B(E2) values theoretically calculated by various model [4]. Recently, Deo and Sharma measures the B(E2) value of a decoupled band, $\nu h_{11/2}$ of ^{103}Pd which is also shows B(E2) is decreasing with spins and claim the antimagnetic rotation [5,6].

One can expect that if the B(E2) values are decreasing with spins of a decoupled band, the B(E2) values must be decreasing with spins for the corresponding even-even core and vice verse. Moreover, the experimental B(E2) values of ^{102}Pd, agree with the theoretical B(E2) values determined by Interacting Boson Model (IBM). The systematics suggest that the B(E2) values of yrast sequence of ^{102}Pd, are decreasing with spins and agree with the experimental results given by Konstantinopoulos (2016), and consistent with the theoretically IBM calculation.

Key words: Tidal wave, cranked shell model, Interacting boson model, reduced transition probability B(E2)

References:

[1] Frauendorf, S., Gu, Y., & Sun, J. (2011). Tidal Waves: A non-adiabatic microscopic description of the yrast states in near-spherical nuclei. Int. J. Mod. Phys. E, 20(2), 465-473.

[2] Ayangeakaa, A. D., Garg, U., Caprio, M. A., Carpenter, M. P., Ghugre, S. S., Janssens, R. V. F., Kondev, F. G., Matta, J. T., Mukhopadhyay, S., Patel, D., Seweryniak, D., Sun, J., Zhu, S., & Frauendorf, S. (2013). Tidal Waves in ^{102}Pd: A Rotating Condensate of Multiple d Bosons. Phys. Rev. Lett., 110, 102501.

[3] Konstantinopoulos, T., Ashley, S. F., Axiotis, M., Spyrou, A., Harissopulos, S., Dewald, A., Litzinger, J., Möller, O., Müller-Gatterman, C., Petkov, P., Napoli, D. R., Marginean, N., Angelis, G. D., Ur, C. A., Bazzacco, D., Farnea, E., Lenzi, S. M., Vlastou, R., & Balabanski, D. (2016). Lifetime measurements in ^{102}Pd: Searching for empirical proof of the E(5) critical-point symmetry in nuclear structure. Phys. Rev. C, 93, 014320.

[4] Frauendorf, S. (2015). The low-energy quadrupole mode of nuclei. Int. J. Mod. Phys. E, 24(9), 1541001.

[5] Deo, A. Y., Yadav, K., Madhu, Tandel, S. K., & Kumar, R. (2021). Antimagnetic rotation and role of gradual neutron alignment in ^{103}Pd. Eur. Phys. J. A, 57, 126.

[6] Sharma, A., Raut, R., Muralithar, S., Singh, R. P., Bhattacharjee, S. S., Das, S., Samanta, S., Ghugre, S. S., Palit, R., Jehangir, S., Rather, N., Bhat, G. H., Sheikh, J. A., Tiwary, S. S., Neelam, Madhusudhana Rao, P. V., Garg, U., & Dhiman, S. K. (2021). Evidence of antimagnetic rotational motion in ^{103}Pd. Phys. Rev. C, 103, 024324.

One Pot Synthesis of Highly Luminescent CsPbBr3 Nanocrystals using Ultrafast Thermodynamic Control

Sultan Ahmad, Mohd. Bilal Khan, Mohd. Salman Khan, Asim Khan, Ankur Mishra, Reeba Marry Thomas, Zishan Husain Khan*
Organic Electronics & Nanotechnology Research Laboratory (OENRL), Department of Applied Sciences & Humanities, Faculty of Engineering & Technology, Jamia Millia Islamia, New Delhi, India
**Corresponding author email id: zishanhk@jmi.ac.in*

$CsPbBr_3$ perovskite nanocrystals (PNCs) of superior quality have been successfully synthesized employing a one-pot method, leveraging ultrafast thermodynamic control in the presence of organic capping molecules, all achieved without resorting to polar solvents. This streamlined approach, characterized by its simplicity, scalability, and single-step accomplishment, represents a noteworthy advance in perovskite nanocrystal synthesis.Transmission electron microscopy (TEM) analysis reveals the cubic morphology of $CsPbBr_3$ perovskite nanocrystals (PNCs), showcasing an average crystal size ranging between 6to 13 nm. The elemental composition of $CsPbBr_3$ PNCs, including the presence of Cs, Pb and Brhas been confirmed through Energy Dispersive X-ray Spectroscopy (EDAX). Furthermore, X-ray diffraction (XRD) studies affirm the cubic nature of $CsPbBr_3$ PNCs.In-depth UV-Vis spectroscopy investigations of $CsPbBr_3$ PNCs demonstrate notable optical absorption within the visible range, featuring an optical bandgap of 2.3 eV. The emission profile of $CsPbBr_3$PNCs is characterized by a broad peak at approximately 539 nm. This innovative synthesis method not only facilitates the production of highly luminescent $CsPbBr_3$ PNCs but also presents an economically viable route, conducted in ambient atmosphere conditions, thereby contributing to the advancement of perovskite nanocrystal synthesis techniques. These synthesized $CsPbBr_3$ perovskite nanocrystals (PNCs) have found versatile applications in both solar cells and light-emitting diodes (LEDs).

Keywords: Perovskite, Inorganic perovskite, Nanocrystals, Perovskite solar cells, Perovskitelight emitting diodes

Optical and electrical properties of P3HT/MWCNT thin films for Sensors application

C.K. Singh, A. Vishwakarma, P. Shukla, R. Walia and L. Kumar*
Molecular Electronics Research Laboratory(MERL),
Physics Department, University of Allahabad, Prayagraj-211002, UP, India
*Corresponding author email id: lokendrakr@allduniv.ac.in

Multi-walled Carbon Nanotubes and conjugated polymers have broad applications in charge storage, sensing, and photovoltaic technology due to their impressive mechanical, electrical, and optical properties. Herein, we have investigated the optical and electrical properties of Poly(3-hexylthiophene) (P3HT) and P3HT/MWCNT composites. The aggregation in P3HT was observed by introducing MWCNT in a polymer matrix followed by ultrasonication in chloroform. Thin films of P3HT and its composite with 0.5wt% and 1wt% MWCNT concentrations were deposited on quartz and Indium Tin Oxide (ITO) substrates to study their optical and electrical properties. Blue shift in absorbance edge observed from UV-Vis absorption spectra for P3HT/MWCNT composites. The Schottky diodes with configuration Al/P3HT-MWCNT composite/ITO were fabricated to explore the electrical characteristics. The ideality factor (η) changes from 1.93 to 1.23 compared to pristine P3HT, and barrier height decreases with increasing MWCNT concentration, respectively. However, the reverses saturation current density (J_0) increases with an increase in MWCNT concentration. The results show that the electrical and optical properties of the conjugated polymer-MWCNTs composites can be tailored by varying concentrations of MWCNT and can be promising materials for organic photovoltaic technology with improved device performance.

Keywords: MWCNT, Nanotubes, Schottky diodes, thin films, Ideality factor.

References:

[1] E. Kymakis and G. A. J. Amaratunga, (2002), Single-wall carbon nanotube/conjugated polymer photovoltaic devices, Appl. Phys. Lett. 80, 112–114.
[2] Vivek Chaudhary, Rajiv K. Pandey, Rajiv Prakash, and Arun Kumar Singh, (2017), Self-assembled H aggregation induced high performance poly(3-hexylthiophene) Schottky diode, Journal of applied Physics 122, 225501.
[3] S. Gantayat1, D. Rout1 and S. K. Swain, (2016) Structural and electrical properties of functionalized multi-walled carbon nanotube/epoxy composite, American Institute of Physics 1731, 050113.
[4] Y. Du, S.Z. Shen, W.D. Yang, K.F. Cai, P.S. Casey, (2012), Preparation and characterization of multi-walled carbon nanotube/poly(3-hexylthiophene) thermoelectric composite materials, 162, 375–380.

Enhanced thermoelectric performance of flexible n-type Ag_2Te-nylon composite film for thermoelectric generator

Amish Kumar Gautam* and Neeraj Khare
Department of Physics, Indian Institute of Technology Delhi, NewDelhi-110016, India
**Corresponding author email id:amish.iitd@gmail.com*

Due to the rapid advancement of flexible electronics, flexible thermoelectric materials that capture waste thermal energy have attracted much interest in recent years (Gautametal.,2023). In this study, utilizing a vacuum filtering technique, we created a flexible Ag_2Te film on a nylon membrane and investigated its thermoelectric properties. Metal chalcogenide silver telluride (Ag_2Te) is selected as a thermoelectric material because of its distinctive characteristics, including low thermal conductivity, adjustable carrier density, and high electron mobility (Gautam & Khare, 2022). The fabricated film exhibited a high Seebeck coefficient(-135.5μV/K) and simultaneous lower thermal conductivity (0.29W/mK) resulting in an enhanced power factor of about 450 $\mu W/mK^2$ and a figure of merit (zT) of about 0.48 at 313K. The high thermoelectric performance is due to the high value of the Seebeck coefficient and simultaneous low thermal conductivity associated with the composite film. The developed composite film demonstrates good flexibility in the bending test by retaining about 87% of the electrical conductivity even after 500 times bending. A single TEG strip of the prepare dflexible Ag_2Te-nylon film can generate the maximum power density (PD_{max}) of ~ 466 $\mu W/cm^2$ at a temperature difference (ΔT) of ~36.8K. The obtained thermo electric performance in this study is higher in comparis onto the previously reported *n*-type flexible Ag_2Te-based film. This work illustrates an effective way of preparing flexible thermoelectric devices that can be used for converting low-grade heat into useful electrical energy.

Keywords: thermoelectrics; flexible film; silver telluride; nanoparticles; energy harvesting.

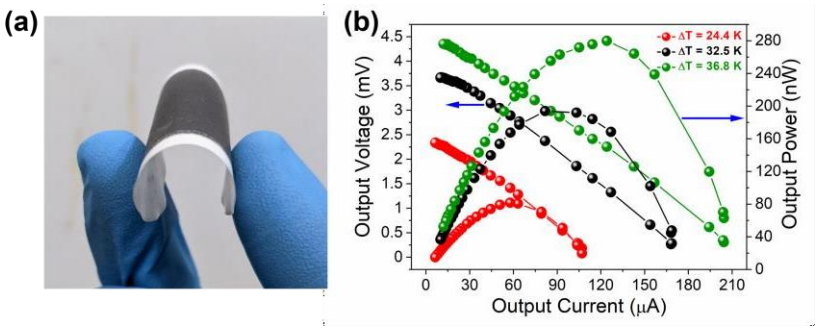

Figure: (a) Pictorial image of the fabricated Ag2 Te-nylon film (b) Output voltage vs. Output current vs. Output power of Ag2Te-nylon film.

References:

[1] Gautam, A. K., & Khare, N. (2023). Enhancedthermoelectric figureof merit atnear roomtemperature in n-type binary silver telluride nanoparticles. *Journal of Materiomics*. *9*, 310-317. https://doi.org/10.1016/J.JMAT.2022.10.003

[2] Gautam, A. K., Singh, H. H., & Khare, N. (2023). Multifunctional flexible Ag2Te-nylon nanocomposite freestanding film for harvesting thermal and mechanical energy. *Nano Energy*, *107*, 108125. https://doi.org/10.1016/J.NANOEN.2022.108125

Tailored Mesoporous γ-WO3 nanoplates: Unraveling their potential for highly sensitive NH3 detection and Efficient Photocatalysis

Shubham Tripathi*, Pratima Chauhan
Advanced Nanomaterials Research Laboratory, Department of Physics, University of Allahabad, Prayagraj, Uttar Pradesh, India-211002
*Corresponding author email id:shubhamtripathi@allduniv.ac.in

Herein, the monoclinic phase of tungsten oxide (γ-WO_3) was successfully obtained after annealing hydro thermally synthesised WO_3powder at 500°C. As per the result obtained from the N_2adsorption-desorption isotherm, the material has been identified as mesoporous with a specific surface area of 3.71 m^2/g from BET (Brunauer-Emmett-Teller) analysis. Moreover, the average pore size (49.52 nm) and volume (0.050 cm^3/g) were also determined by the BJH (Barrett-Joyner-Halenda) method. FE-SEM (Field Emission Scanning Electron Microscopy) and HR-TEM (High Resolution Transmission Electron Microscopy) have confirmed the formation of nanoplates with an average diameter of approximately 274 nm. The Raman spectroscopy has shown the peaks at the lower wavenumber region (270 $cm^{-1}$and 326 cm^{-1}) and the higher wavenumber region (713 $cm^{-1}$and 806 cm^{-1}) for O-W-O bending modes and stretching modes, respectively. The combined effect of relative humidity (RH-11% — RH-95% — RH-11%) and NH_3(150 ppm, 300 ppm, 450 ppm, 600 ppm, 700 ppm, and 800 ppm) was carried out in this reported work. The synthesised γ-WO_3has shown highly responsive behaviour for humidity as 96.5% (RH-11%—95%) and NH_3sensing (under humidity) as 97.4%(RH-11%—95% with 800 ppm NH_3).The response and recovery time were calculated as 15s and 52s, 16s and 54s for humidity, and NH_3under humidity, respectively. The experimental findings demonstrated that the resistance of the sensor depends on the concentrations of $NH_3$and humidity. Moreover, γ-WO_3has been investigated as a promising catalyst for the dye degradation of methylene blue (MB) with a degradation efficiency of 72.82% and methyl orange (MO) with a degradation efficiency of 53.84% under visible light exposure. This dye degradation occurred within 160 min. in the presence of a catalyst under visible light irradiation.

Keywords: Tungsten Oxide(γ-WO_3), Ammonia Sensing, Photocatalytic, MB and MO dye.

Interfacial Engineering Enables Organic-Inorganic Nanohybrid of Polyaniline Decorated Bi_2S_3 Nanorods Towards Ultrafast Metal-Semiconductor-Metal Photodetector

Anshika Singh[a], Pratima Chauhan[a], Arpit Verma[b], Bal Chandra Yadav[b]
[a]Advanced Nanomaterials Research Laboratory, U.G.C. Centre of Advanced Studies, Department of Physics, University of Allahabad, Prayagraj-211002, India
[b]Nanomaterials and Sensors Research Laboratory, Babasaheb Bhimrao Ambedkar University, Lucknow-226025, U.P., India
Corresponding author email id: mangu167@yahoo.co.in; anshikasingh@allduniv.ac.in

Herein, we reported photoelectric measurements of the Bi_2S_3/PANI nanohybrid of the metal-semiconductor-metal (MSM) device in the broad electromagnetic (EM) spectrum from ultraviolet (UV) to visible range. Bi_2S_3 nanorods decorated with polyaniline were utilized for the photodetection. In such a novel structure, the fast electron transfer at the interface of Bi_2S_3 and polyaniline occurs, which enhances the overall performance of the photodetection process. Current-voltage (I-V) characteristics of the MSM photodetector device of Bi_2S_3/PANI nanohybrid show good ohmic nature. The photodetector device offers the highest external quantum efficiency of 10^4 in the UV and visible regions.It also shows the greatest detectivity of the order of 10^{14} Jones. The photoresponsivity of the Bi_2S_3/PANI nanohybrid photodetector device shows 270 $mAW^{-1}$and 1270 mAW^{-1}at only 1 V with the minimum optical signal of 50 μWcm^{-2}. The highest photoresponsivity of the Bi_2S_3/PANI nanohybrid photodetector offers 26760 mAW^{-1} and 13250 $mAW^{-1}$for the UV and visible spectrum. The higher value of the LDR is 64.31 dB and 58.21 dB in UV and visible regions, respectively, at 100 V with the lowest illumination intensity. And the minimum value of NEP found in the order of $10^{-9,}$ which is the lowest value, suggests that the nanohybrid material is perfect for low-intensity photon signals.The current MSM photodetector technology exhibits a high response in the visible to UV region.

Keywords: Conducting Polymers, Nanohybrids, Polyaniline, Bismuth Sulfide, Metal Semiconductor Photodetectors.

References:

[1] Huo N, Figueroba A, Yang Y, Christodoulou S, Stavrinadis A, Magén C, et al. Engineering Vacancies in Bi2S3 yielding Sub-Bandgap Photoresponse and Highly Sensitive Short-Wave Infrared Photodetectors. Advanced Optical Materials. 2019;7:1900258.
[2] Ahmed AA, Devarajan M, Afzal N. Fabrication and characterization of high performance MSM UV photodetector based on NiO film. Sensors and Actuators A: Physical. 2017;262:78-86.
[3] Badhulika S. A flexible, rapid response, hybrid inorganic-organic SnSe2-PEDOT: PSS bulk heterojunction based high-performance broadband photodetector. 2022.
[4] Yang X, Bao D, Zhang Y, Li B. Single crossed heterojunction assembled with quantum-dot-embedded polyaniline nanowires. ACS Photonics. 2016;3:1256-64.
[5] O'Brien GA, Quinn AJ, Tanner DA, Redmond G. A single polymer nanowire photodetector. Advanced Materials. 2006;18:2379-83.
[6] Rawal I, Tripathi RK, Panwar O. Easy synthesis of organic–inorganic hybrid nanomaterials: study of DC conduction mechanism for light dependent resistors. RSC advances. 2016;6:31540-50.
[7] Zheng L, Yu P, Hu K, Teng F, Chen H, Fang X. Scalable-production, self-powered TiO2 nanowell–organic hybrid UV photodetectors with tunable performances. ACS Applied Materials & Interfaces. 2016;8:33924-32.

In silico investigation on sensing of tyramine by Boron and Silicon doped C_{60} Fullerenes

A.K.Vishwkarma[1*], T. Yadav[2], A. Pathak[1]
[1]Department of Physics, Institute of Science, Banaras Hindu University, Varanasi, India
[2]Department of Basic Sciences, IES College of Technology, IES University, Bhopal (M. P.), India.
**Corresponding author email id: akv1993.au@gmail.com*

The present communication deals with the adsorption of tyramine neurotransmitter over the surface of pristine, Boron (B) and Silicon (Si) fullerenes. Density functional theory (DFT) calculations have been used to investigate tyramine adsorption on the surface of fullerenes in terms of stability, shape, work function, electronic characteristics, and density of state spectra[1, 2].The most favourable adsorption configurations for tyramine have been computed to have adsorption energies of -1.486, -30.889, and -31.166 kcal/mol, respectively. The band gap of pristine, B- and Si- doped fullerenes shows changes in their band gaps after adsorption of tyramine neurotransmitters. However, the change in band gaps reveals more in Boron doped fullerene rather than pristine and Si- doped fullerenes. The change in band gaps of B and Si-doped fullerenes lead a change in the electrical conductivity which helps to expose tyramine. Furthermore, NBO computations demonstrated a net charge transfer of 0.006, 0.394, and 0.257*e* from tynamine to pristine, Boron (B) and Silicon (Si) fullerenes.

Keywords: DFT, C_{60}Fullerene, NBO, Tyramine.

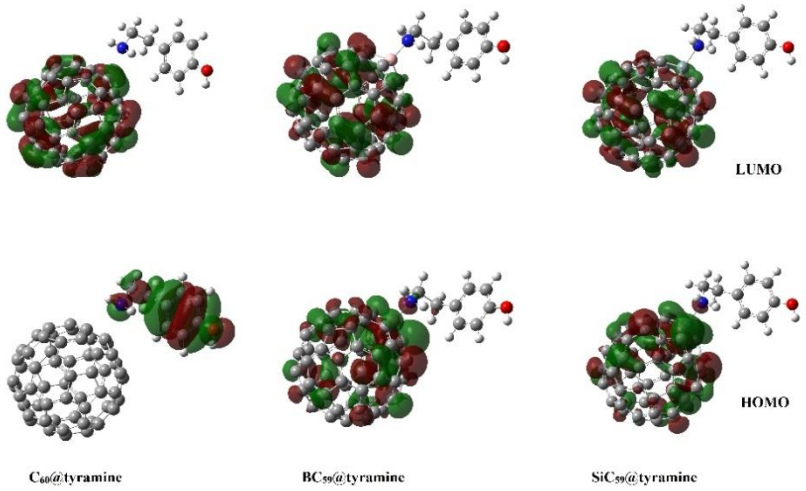

***Figure**: HOMO-LUMO plot of the most stable C_{60}@tyramine, BC_{59}@tyramineand SiC_{59}@tyramine complexes.*

References:

[1] I. Urdaneta, A. Keller, O. Atabek, J. L. Palma, D. F. Shapiro, P. Tarakeshwar, V. Mujica, M. Calatayud, J. Phys. Chem. C, 118, (2014), 20688-20693.
[2] A. L. Pereira Silva, A. C. A. Silva, J. de J. G. V.Júnior, Comp.Theo.Chem.,1215, (2022), 113836.

Synthesis and characterization of Copper doped Zirconia (Cu-ZrO_2)-based nanomaterial for Potential antimicrobial application

Surya Pratap[1*], Horesh Kumar[2]
[1,2]*Department of Physics, Institute of Science, Banaras Hindu University, Varanasi, 221005*
[1]*Department of Physics, Harishchandra Post Graduate College, Varanasi, 221001*
**Corresponding author email id: suryakvpy2012@gmail.com*

Copper doped Zirconium oxide (Cu-ZrO_2) is a ceramic bioactive material with unique mechanical and chemical properties. Cu-ZrO_2 nanomaterials have prospective uses in the production of biomedical devices, including dental crowns, cement for bone fractures, and antibacterial properties. The current work investigates the hydrothermal approach for the synthesis of Cu-ZrO_2 nanomaterials, employing copper chloride ($CuCl_2$.H2O), zirconium oxychloride ($ZrOCl_2$.8H2O), and sodium hydroxide (NaOH) as starting agents. The monoclinic Cu-ZrO_2 (JCPDS: 89-9066) has a distinctive peak at an angle of 30^o that corresponds to reflection from plane (111), and the XRD findings showed that this peak had a higher intensity than the other peaks. This is because the sample is highly crystalline. Moreover, the shape of XRD peaks observed around ~30.21°, ~35.02°, ~50.31°, ~59.2°, ~62.2° indicates nano level size of crystalline entities. Further, the Raman characterisation spectrum revealed several characteristic peaks at ~ 65cm^{-1}, ~ 139 cm^{-1}, ~ 181 cm^{-1},~251 cm^{-1}, ~ 461cm^{-1} corresponds to the monoclinic ZrO_2. FTIR characterisation shows the presence of various functional groups over zriconia surface such as –OH, and =OH. The synthesised nanomaterial exhibits antimicrobial activity against different bacterial species such as E-coli and Salmonella Enterica. Hence, it could be successfully used for various biomedical industrial applications.

Key Words: Bioactive material, Zirconium Oxide, Nanomaterial, Antimicrobial activity.

References:

[1] A.P. Ayanwale, A.D.J. Ruíz-Baltazar, L. Espinoza-Cristóbal, S.Y. Reyes-López, Bactericidal Activity Study of ZrO_2-Ag_2O Nanoparticles, Dose-Response. 18 (2020) 1–13.
[2] J.B. Fathima, A. Pugazhendhi, R. Venis, Synthesis and characterization of ZrO_2 nanoparticles-antimicrobial activity and their prospective role in dental care, Microb. Pathog. 110 (2017) 245–251.

$CaTiO_3$ coated Sr-HA scaffold by Low Temperature High Speed Collison techniques showed multifunctional properties

Samapika Bhuyan[†], Sangita Mangaraj[†], Subhasmita Swain, Tapash R. Rautray*
Biomaterials and Tissue Regeneration Lab, Centre of Excellence, Siksha 'O' Anusandhan (Deemed to be University), Bhubaneswar- 751030, Odisha, India
[†]Authors contributed equally.
Corresponding author email id: tapashrautray@soa.ac.in

In the context of clinical advancements in bone tissue engineering, the integration of biomaterials and mesenchymal stem cells (MSCs) involves the use of an ideal bone scaffold that exhibits certain vital properties. These properties encompass biodegradability, biocompatibility, bioactivity, porosity, and the capacity to offer adequate mechanical support for the effective regeneration of bone defects. However, the process of developing such a structure is an enormous challenge. Hydroxyapatite (HA), a bioceramic that exhibits exceptional biocompatibility, bioactivity, and structural resemblance to the inorganic component of bone, is extensively used as a biomaterial. Despite the remarkable biocompatible and biological qualities shown by HA, it is lacking in antibacterial action. In order to enhance its antibacterial efficacy, we used a novel approach of surface polarization on biomaterials. Furthermore, to promote HA's bioactive and biomimetic properties in bone microenvironment, Sr substituted HA (SrHA) composite was taken for synthesis of scaffold. Where Sr not only enhance osteoblast cell proliferation but also helps in osteoclast cell resorption. SrHA scaffolds were prepared and fabricated with calcium titanate using a novel coating method called low-temperature high-speed collision (LTHSC) followed by negative surface polarization. However, coating of calcium titanate on SrHA scaffold using the LTHSC method gives rise to more hydrophilicity with less delamination. The samples were characterized by X-ray diffraction, and scanning electron microscopy to investigate the phase composition and microstructure of the scaffold. The thermally stimulated depolarization current (TSDC) was employed to measure the maximum stored charge. The antibacterial activity of the fabricated scaffold revealed polarized samples showed inhibition of bacterial growth against methicillin-sensitive *S. aureus* with poor bacterial growth compared to their unpolarized counterparts. The osteogenic MG 63 cell proliferation showed increased gene expression on polarized samples. These results deduced that a negatively surface-polarized SrHA scaffold fabricated with $CaTiO_3$ could induce greater bioactivity, improved differentiation of BMSCs as well as enhanced antibacterial activity.

Keywords: Strontium, Hydroxyapatite, LTHSC, Antibacterial activity, Osteogenic activity

References:

[1] Lee, K. W., Bae, C. M., Jung, J. Y., Sim, G. B., Rautray, T. R., Lee, H. J., ... & Kim, K. H. (2011). Surface characteristics and biological studies of hydroxyapatite coating by a new method. *Journal of Biomedical Materials Research Part B: Applied Biomaterials*, *98*(2), 395-407.

[2] Hu, B., Meng, Z. D., Zhang, Y. Q., Ye, L. Y., Wang, C. J., &Guo, W. C. (2020). Sr-HA scaffolds fabricated by SPS technology promote the repair of segmental bone defects. *Tissue and Cell*, *66*, 101386.

An ultrasensitive, humidity assisted and room temperature operable ammonia gas sensor based on RGO@SnO_2 nanocomposite

Divya Tripathi*, Pratima Chauhan
U.G.C. Centre of Advanced Studies, Department of Physics, University of Allahabad, Prayagraj-211002, Uttar Pradesh, India
**Corresponding author email id: divyatripathi@allduniv.ac.in*

In this work, the fabrication of an ultrahigh selective NH_3 gas sensor based on RGO/SnO_2 nanocomposite has been proposed. The hydrothermal method was employed to synthesize the RGO/SnO_2 nanocomposite and their structural, optical and morphological properties were analyzed through XRD, Raman and FE-SEM. For gas sensing applications, RGO/SnO_2 have effectively spin-coated onto the interdigitated electrodes (IDE's) based on fluorine-doped tin oxide (FTO) respectively, and their sensitivity towards NH_3 was tested. Gas sensing characteristics of RGO/SnO_2 were analyzed at room temperature (25ºC) under different relative humidity (RH) levels. The developed RGO/SnO_2 demonstrated a high sensing response of 97% towards 300 ppm NH_3 under 11%—97%—11%RH conditions. Notably, the sensor exhibited rapid response and recovery times of 39and105 s, respectively under the specified RH conditions. The high sensitivity and rapid response/recovery times of NH_3 suggest its good selectivity over other tested volatile organic compounds. This superior performance can be attributed to the abundant active sites and the excellent electron transport properties inherent to the RGO component. Importantly, the RGO/SnO_2 sensor displayed high reproducibility and consistent responses. The sensor displayed extremely low power consumption, outperforming a commercially available metal oxide sensor when operating at ambient temperature, establishing it as a promising material for next-generation gas sensing technologies.

Keywords: NH_3 gas sensor, hydrothermal method, reduced graphene oxide, SnO_2 nanosphere

References:

[1] Tripathi, D., & Chauhan, P.(2022).Highly Responsive Room-Temperature Operable Ethanol Gas Sensor Based on Thermally Reduced Graphene Oxide. ECS J. Solid State Sci. Technol., 11, 087002.
[2] Xing, T., Wang,Y., Shang, Y., Zhao, R., Du, J.,& Asefa, T. (2023), Heterojunction-Engineered Reduced Graphene Oxide/SnO_2 with Mesoporous Structures for Gas Chemo sensors. ACS Appl. Nano Mater., 6(15), 13984-13993.
[3] Chen, Y., Zheng, W., & Wu, Q. (2017), A highly sensitive room-temperature sensing material for NH_3: SnO_2-nanorods couple by rGO. Sensors and Actuators B: Chemical, 242 1216-1226.

Understanding of charge carrier dynamics in $CsPbBr_3$ perovskite quantum dots for optoelectronics devices

Preeti Shukla[1], Rajveer Singh[2], Mahesh Kumar[3], Anand Pandey[1] and Lokendra Kumar[1†]
[1]Physics Department, University of Allahabad, Prayagraj-211002, India
[2]Department of Physics, D.J. (P.G.) College, Baraut.
[3]CSIR-National Physical Laboratory, Dr. K. S. Krishnan Marg, New Delhi-110012, India
†Corresponding Author (lkumarau@gmail.com)

Abstract

We successfully synthesized and characterized the $CsPbBr_3$ QDs via the hot injection method. The uniformly distributed cubic structure of $CsPbBr_3$ QDs with an average particle size of ~13 nm was observed with transmission electron microscopy (TEM). UV-Vis absorption and photoluminescence (PL) spectra show the band edge at 500 nm and 513 nm, respectively. To understand the carrier kinetics of $CsPbBr_3$ QDs, ultrafast transient absorption spectroscopy (UTAS) at pump fluence 1 mW with an excitation wavelength of 450 nm was performed. The TA spectra of as-synthesized $CsPbBr_3$ QDs show ground state bleaching (GSB) for various time delays. The GSB signal grew up to 5 ps and then diminished with time. The peak position of the GSB signal at ~502 nm is in close agreement with the steady-state UV-Vis absorption peak, suggesting that GSB generates due to band edge absorption. The time constant τ_1 (48.1 ps), τ_2 (205 ps), and τ_3 (1660 ps) from kinetic fit at 500 nm were calculated using the tri-exponential decay function. This study gives insight into the charge carrier dynamics of $CsPbBr_3$ QDs, which would improve the manufacturing of quantum dot-based optoelectronic devices.

Keywords: All-inorganic perovskite, $CsPbBr_3$ QDs, ultrafast transient absorption, photoluminescence, optoelectronics

References:

[1] Qin, Chaochao, Yujie Geng, Zhongpo Zhou, Jian Song, Shuhong Ma, Guangrui Jia, Zhaoyong Jiao, Zunlue Zhu, and Yuhai Jiang. "Observation of carrier transfer in a vertical 0D-CsPbBr 3/2D-MoS_2 mixed-dimensional van der Waals heterojunction." *Optics Express* 31, no. 2 (2023): 2593-2601.

[2] Protesescu, Loredana, Sergii Yakunin, Maryna I. Bodnarchuk, Franziska Krieg, Riccarda Caputo, Christopher H. Hendon, Ruo Xi Yang, Aron Walsh, and Maksym V. Kovalenko. "Nanocrystals of cesium lead halide perovskites ($CsPbX_3$, X= Cl, Br, and I): novel optoelectronic materials showing bright emission with wide color gamut." *Nano letters* 15, no. 6 (2015): 3692-3696.

[3] Anand Pandey, A Vishwakarma, A Saini, M Kumar, L Kumar. "Light-induced micro-strain regulation and charge carrier dynamics of $(FA_{0.83}MA_{0.17})_{0.95}Cs_{0.05}Pb(I_{0.83}Br_{0.17})_3$ hybrid perovskite films." *Optical Materials*, 147 (2024), 114564.

Unraveling Morphological Changes in $CsBi_3I_{10}$ Perovskite via Composition Mediation

Anil K. Sharma[1], Ambreesh Kumar[1], Jitendra Yadav[1], Bharti[2], Savita[1,4], H. P. Bhasker[3], Punit K. Dhawan[4], Shiv P. Patel[2], Dhirendra K. Chaudhary[1*]

[1]Centre for Renewable Energy, Prof. Rajendra Singh (Rajju Bhaiya) Institute of Physical Sciences for Study and Research, V. B. S. Purvanchal University, Jaunpur-222003, India.

[2]Department of Pure and Applied Physics, Guru Ghasidas Vishwavidyalaya, Bilaspur, 495009, India

[3]Department of Physics, C.M.P. Degree College, University of Allahabad, Allahabad-211002, India.

[4]Department of Physics, Prof. Rajendra Singh (Rajju Bhaiya) Institute of Physical Sciences for Study and Research, V. B. S. Purvanchal University, Jaunpur-222003, India.

* *Corresponding author email id: phydhiren@gmail.com*

Bismuth-based perovskite materials have emerged as a key component in the development of lead-free perovskite solar cells. This study explored the morphological evolution within $CsBi_3I_{10}$ perovskite solar cell devices. Through a systematic investigation, we have taken the different ratios of the CsI and BiI_3 such as 1:3 1.1:3, 1.2:3, 1.3:3, and 1.4:3 in which the optimized ratio found 1.3:3. The physico-chemical characteristic of the film has been investigated using different characterization tools. Our study delved into essential factors influencing device morphology, including fabrication conditions, interfacial layers, and environmental stresses. Through careful analysis, we successfully fabricated a lead free Perovskite solar cell with efficiency ~3.1%.

References:

[1].Jang, W.J., H.W. Jang, and S.Y. Kim, *Recent Advances in Wide Bandgap Perovskite Solar Cells: Focus on Lead-Free Materials for Tandem Structures.* Small Methods, 2023: p. 2300207.

[2].Karim, M.A., et al., *Bathocuproine interfacial layer leads to solid improvement of reproducibility and stability of Pb-free CsBi3I10 based perovskite solar cells.* Journal of Materials Science: Materials in Electronics, 2022. **33**(10): p. 8114-8126.

[3].Kang, J., et al., *Fabrication of High-Quality CsBi3I10 Films via a Gas-Assisted Approach for Efficient Lead-Free Perovskite Solar Cells.* Energy Technology, 2022. **10**(7): p. 2200318.

[4].Ahmad, K., et al., *Improved Stability of CsBi3I10 Based Pb-Free Perovskite Solar Cells.* ChemistrySelect, 2023. **8**(16): p. e202300520.

Fabrication of Novel 3-D Nanocomposites of HAp-TiC-hBN-ZrO_2: Enhanced Mechanical Performances and *In Vivo* Toxicity Study for Biomedical Applications

Sarvesh Kumar Avinashi,[1] Shweta,[1] Bhavna Bohra,[2] Rajat Kumar Mishra,[1] Savita Kumari[1], Zaireen Fatima,[1,3] Ajaz Hussain,[1] Bhagawati Saxena,[2] Chandkiram Gautam[1]*

[1]Advanced Glass and Glass Ceramics Research Laboratory, Department of Physics, University of Lucknow, Lucknow, 226007, India

[2]Department of Pharmacology, Institute of Pharmacy, Nirma University, S.G. Highway, Ahmedabad, 382481, India

[3]Department of Physics, Integral University, Lucknow, 226026, India

**Corresponding author email id: gautam_ceramic@yahoo.com (C.R. Gautam).*

Hydroxyapatite (HAp) is one of the most suitable biomaterials for numerous biomedical applications due to its outstanding biocompatibility, bioactivities, and osteoconductivity [1,2]. In this study, HAp was fabricated using a bottom-up approach i.e. wet chemical method and its composites with TiC, h-BN, and ZrO_2 were fabricated by solid state reaction method with enhanced mechanical and biological performances [3,4]. The structural, surface morphology, and mechanical behaviour of the fabricated composites were characterized by employing various characterization techniques. Furthermore, TEM micrographs show randomly oriented rod-like morphology, with the length and width of these nanorods ranging from 78-122 nm and from 9-13 nm. Moreover, the mechanical characterizations of the composite HZBT4 (80HAp-10TiC-5hBN-5ZrO_2) reveal very high compressive strength (246 MPa), which is comparable to the steel (250 MPa), fracture toughness (14.78 MPa $m^{1/2}$), and Young's modulus (1.02 GPa). In order to check the biocompatibility of the composites, numerous biological tests on different body organs of healthy adult Sprague Dawley rats were also performed. This study shows that the composite HZBT4 could not reveal any significant influence on the hematological, serum biochemical and histopathological parameters. Hence, the fabricated composite can be used for several biological applications, such as bone implants, bone grafting, and bone regeneration [5].

Keywords: Hydroxyapatite; Composites; Morphology; Mechanical performances; *In Vivo*-study

References:

[1] Kantharia, N., Naik, S., Apte, S., Kheur, M., Kheur, S. and Kale, B. (2014) Nano-hydroxyapatite and its contemporary applications. *Bone*, 34, 1-71.

[2] Giacomini, D., Torricelli, P., Gentilomi, G. A., Boanini, E., Gazzano, M., Bonvicini, F., Benetti, E., Soldati, R., Martelli, G., Rubini, K. and Bigi, A. (2017) Monocyclic β-lactams loaded on hydroxyapatite: new biomaterials with enhanced antibacterial activity against resistant strains. *Sci. Rep.* 7(1), 2712.

[3] Avinashi, S. K., Singh, P., Sharma, K., Hussain, A., Singh, D. and Gautam, C. R. (2022) Morphological, mechanical, and biological evolution of pure hydroxyapatite and its composites with titanium carbide for biomedical applications. Ceram. Int. 48(13), 18475-18489.

[4] Gautam, A., Gautam, C. R., Mishra, M., Sahu, S., Nanda, R., Kisan, B., Gautam, R. K., Prakash, R., Sharma, K., Singh, D. and Gautam, S.S. (2021) Synthesis, structural, mechanical, and biological properties of HAp-ZrO2-hBN biocomposites for bone regeneration applications. Ceram. Int. 47(21), 30203-30220.

[5] Bal, Z., Kaito, T., Korkusuz, F. and Yoshikawa, H. (2020) Bone regeneration with hydroxyapatite-based biomaterials. Emergent Mater. 3(4), 521-544.

We gratefully acknowledge the financial support from

SERB

NASI

BRNS

INSA

CSIR

DRDO